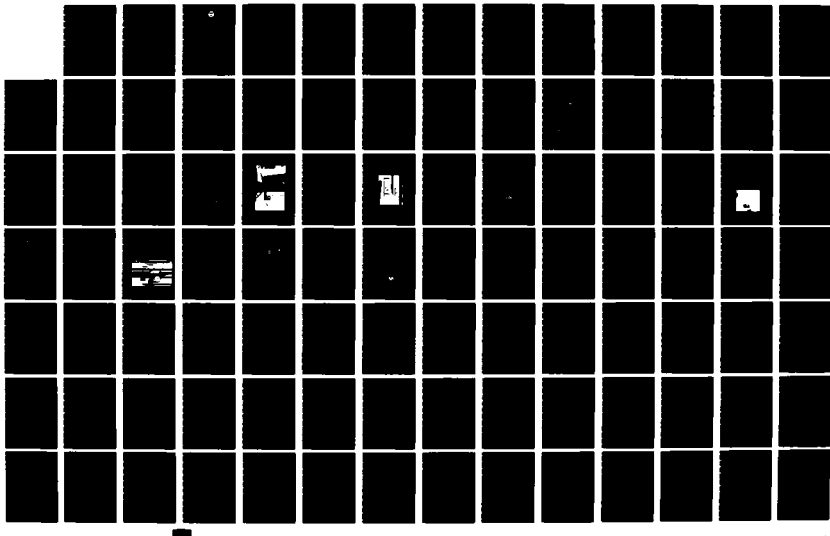
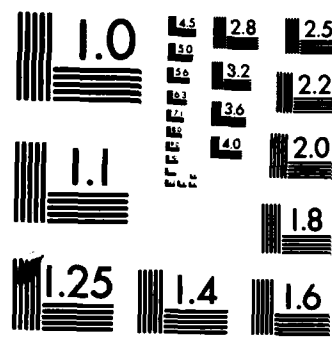


HD-A138 206 AN EXPERIMENTAL STUDY OF CYLINDRICAL ANTENNAS RADIATING 1/2
IN OR NEAR A LOSS. (U) MISSISSIPPI UNIV UNIVERSITY DEPT
OF ELECTRICAL ENGINEERING C M BUTLER ET AL. DEC 83
UNCLASSIFIED NOSC-CR-218 N66001-82-C-0045 F/G 9/1 NL





MICROCOPY RESOLUTION TEST CHART
NATIONAL BUREAU OF STANDARDS-1963-A

ADA138206

NOSC CR 218

Contractor Report 218

AN EXPERIMENTAL STUDY OF CYLINDRICAL ANTENNAS RADIATING IN OR NEAR A LOSSY HALF SPACE

C. M. Butler
C. A. Harrison
University of Mississippi

December 1983
Final Report
March 1982 — June 1983

Prepared for
Naval Ocean Systems Center
Code 811

Sponsored by
Naval Electronic Systems Command
PME 117

Approved for public release; distribution unlimited.

DTIC FILE COPY

DTIC
FEB 24 1984

A

NOSC
NAVAL OCEAN SYSTEMS CENTER
San Diego, California 92152

84 02 24 006



NAVAL OCEAN SYSTEMS CENTER SAN DIEGO, CA 92152

AN ACTIVITY OF THE NAVAL MATERIAL COMMAND

J.M. PATTON, CAPT, USN

Commander

R.M. HILLYER

Technical Director

ADMINISTRATIVE INFORMATION

Administrative information pertaining to Naval Ocean Systems Center Contractor Report 218 is listed below.

Item	Data
Performing Organization	Department of Electrical Engineering University of Mississippi University, MS 38677
Contract Number	N66001-82-C-0045
Controlling Office	Naval Ocean Systems Center Code 8112 San Diego, CA 92152
Sponsor	Naval Electronic Systems Command(PME 117), Washington, DC 20360 in conjunction with U.S. Army Headquarters Communications Electronic Engineering Installation Agency, 1900 Half St. SW, Washington, DC 20324
Program Element	OMN

The contracting officers' technical representative was James C. Logan, NOSC Code 8112.

Released by
M. S. Kvigne, Head
Communications Research and
Technology Division

Under authority of
H. F. Wong, Head
Communications Systems and
Technology Department

TJ

UNCLASSIFIED

SECURITY CLASSIFICATION OF THIS PAGE (When Data Entered)

REPORT DOCUMENTATION PAGE		READ INSTRUCTIONS BEFORE COMPLETING FORM
1. REPORT NUMBER NOSC CR 218	2. GOVT ACCESSION NO. <i>NDS-A1132206</i>	3. RECIPIENT'S CATALOG NUMBER
4. TITLE (and Subtitle) AN EXPERIMENTAL STUDY OF CYLINDRICAL ANTENNAS RADIATING IN OR NEAR A LOSSY HALF SPACE	5. TYPE OF REPORT & PERIOD COVERED Final March 15, 1982-June 20, 1983	
7. AUTHOR(s) C.M. Butler C.A. Harrison	6. PERFORMING ORG. REPORT NUMBER N66001-82-C-0045	
9. PERFORMING ORGANIZATION NAME AND ADDRESS Department of Electrical Engineering University of Mississippi University, MS 38677	10. PROGRAM ELEMENT, PROJECT, TASK AREA & WORK UNIT NUMBERS OMN	
11. CONTROLLING OFFICE NAME AND ADDRESS Naval Ocean Systems Center Code 8112 San Diego, CA 92152	12. REPORT DATE June 20, 1983	
14. MONITORING AGENCY NAME & ADDRESS (if different from Controlling Office) Naval Electronic Systems Command (PME 117) Washington, DC 20360 with US Army Headquarters Communications Electronic Eng. Installation Agency Washington, DC 20324	13. NUMBER OF PAGES 180	
16. DISTRIBUTION STATEMENT (of this Report) Approved for public release; distribution unlimited	15. SECURITY CLASS. (of this report) Unclassified	
17. DISTRIBUTION STATEMENT (of the abstract entered in Block 20, if different from Report)	15a. DECLASSIFICATION/DOWNGRADING SCHEDULE	
18. SUPPLEMENTARY NOTES		
19. KEY WORDS (Continue on reverse side if necessary and identify by block number) Electromagnetic fields and waves Microwave measurements Monopole antenna Antenna above water Antenna in two-media space		
20. ABSTRACT (Continue on reverse side if necessary and identify by block number) Conducting structures residing near, within and partially within a lossy half space are investigated experimentally. The conducting structures are modeled by monopole antennas, and the lossy half space is modeled by the water within a non-metallic tank. Antenna aperture admittances are obtained using swept-frequency network analysis techniques with automated data collection and reduction. Results are compared to results of numerical analysis conducted as a related project.	(Continued on reverse side)	

UNCLASSIFIED

SECURITY CLASSIFICATION OF THIS PAGE (When Data Entered)

20. Continued

A sleeve monopole is oriented normal to the water surface with driving point near the bottom of the tank and source gap (aperture) in air. Gap height above the water surface, antenna radius and monopole length are varied. Electromagnetic properties of the water are varied by addition of NaCl. Coax-fed wire antennas are mounted perpendicular to a ground plane which is normal to and intersects the water surface. The antennas used are a straight-wire antenna in which the monopole is parallel to the water surface and a bent-wire antenna in which the wire is partially immersed in water. Height of the aperture above the water is varied. A coax-fed cylindrical monopole antenna is mounted perpendicular to a ground plane which is in contact with the water surface so that monopole and aperture are immersed in water. Reflection coefficient at the driving point is measured and antenna aperture admittance is derived for the 0.5 - 1.0 GHz octave for the sleeve and straight-wire monopoles, the 0.5 - 1.1 GHz band for the bent-wire antenna and the 0.25 - 0.75 GHz band for the fully immersed cylindrical antenna. Aperture heights are varied from approximately 0.02λ - 1.0λ for all cases in which the aperture is above the water. Good agreement is obtained in all cases between the aperture admittance determined experimentally and that derived from numerical analysis of current distribution on the structure.

For the sleeve monopole normal to the water surface, the water surface is shown to act as an effective reflector with aperture admittance differing only slightly from that measured for the same antenna geometry above a ground plane. For the coax-fed antennas with aperture in air above the water, the presence of the water is shown to have little effect on aperture admittance as long as the structure does not make contact with the water; at heights of approximately 1.0λ , the effect is negligible.

The electromagnetic constitutive properties of the water used in each experiment are measured by guided wave techniques using specially constructed coaxial and rectangular waveguide apparatus. Good agreement with available data from other sources is shown.

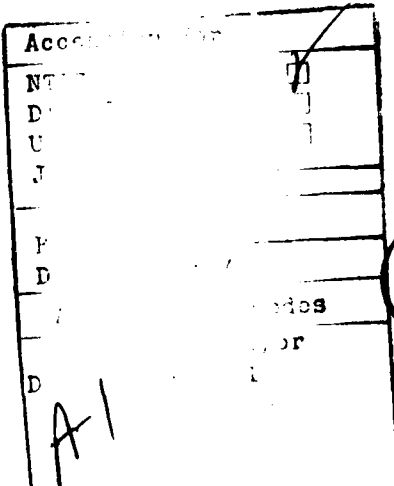
S/N 0102-LF-014-6601

UNCLASSIFIED

SECURITY CLASSIFICATION OF THIS PAGE (When Data Entered)

TABLE OF CONTENTS

	Page
LIST OF TABLES.....	vii
LIST OF FIGURES.....	viii
CHAPTER	
1. INTRODUCTION.....	1
EXPERIMENTAL MODELS.....	2
Operating Environment.....	3
Scaling.....	3
Conducting Structures.....	4
Model Configurations.....	4
Electromagnetic Constitutive Properties.....	8
DATA COLLECTION AND INSTRUMENTATION.....	9
2. DESIGN AND CONSTRUCTION OF APPARATUS.....	11
WATER TANKS.....	11
Large Water Tank.....	11
Small Water Tank.....	19
ANTENNAS.....	19
Configuration I Experiments.....	19
Configuration II Experiments.....	23
Configuration III Experiments.....	23



SLOTTED WAVEGUIDES.....	25
Rectangular Waveguide Apparatus.....	25
Coaxial Waveguide Apparatus.....	27
3. EXPERIMENTAL PROCEDURES.....	34
SERIES I PROCEDURES.....	35
Water Tank Configuration.....	35
Antenna Installation.....	35
Water Level Determination.....	36
Data Collection.....	37
SERIES II PROCEDURES.....	39
Water Tank Configuration.....	39
Antenna Installation.....	40
Water Level Determination.....	40
Data Collection.....	40
SERIES III PROCEDURES.....	41
Water Tank Configuration.....	41
Antenna Installation.....	41
Data Collection.....	41
WATER PROPERTIES MEASUREMENT PROCEDURES.....	42
Preparation of the Rectangular Waveguide Apparatus.	42
Preparation of the Coaxial Waveguide Apparatus.....	42
Instrumentation Connections.....	43
Data Collection.....	43
SEMI-AUTOMATIC FREQUENCY DOMAIN NETWORK ANALYZER (ANWA) SYSTEM.....	44
Reflection Measurements.....	45
Attenuation and Phase Shift Measurements.....	45

	iii
4. ANALYSIS AND RESULTS.....	48
CONFIGURATION I EXPERIMENTS.....	48
Preliminary Testing and Analysis.....	49
Summary of Results.....	55
CONFIGURATION II EXPERIMENTS.....	63
Comparison of Numerical and Experimental Results for the Straight-Wire Monopole.....	66
Comparison of Numerical and Experimental Results for the Bent-Wire Monopole.....	69
CONFIGURATION III EXPERIMENT.....	71
Numerical Analysis.....	71
Comparison of Experimental and Numerical Results...	71
EXPERIMENTS TO MEASURE THE CONSTITUTIVE PROPERTIES OF WATER.....	73
Analysis of Measured Values of σ and ϵ_r	76
COMPENDIUM OF RESULTS.....	76
COMMENTS AND SUGGESTIONS FOR FUTURE INVESTIGATIONS...	83
Configuration I Experiments.....	83
Configuration II Experiments.....	84
Water Properties Measurements.....	85
APPENDICES.....	145
A. MEASUREMENT OF THE ELECTROMAGNETIC CONSTITUTIVE PROPERTIES OF WATER.....	146
B. DERIVATION OF ANTENNA APERTURE ADMITTANCE.....	149
C. COMPUTATIONS RELATED TO THE DESIGN OF THE SLOTTED COAXIAL WAVEGUIDE.....	157

LIST OF TABLES

Table		Page
	Chapter 2	
2-1	Dimensions of Configuration I Experiments.....	21
	Chapter 4	
4-1	Key to Compendium of Results.....	79

LIST OF FIGURES

Figure	Page
 <u>Chapter 1</u> 	
1. Sleeve Monopole Antenna in Water Tank (Experimental Model Configuration I).....	5
2. Coax-Fed Monopole Antennas with Aperture Above Water (Experimental Model Configuration II).....	5
3. Coax-fed Monopole Antenna Immersed in Water (Experimental Model Configuration III).....	7
4. Two-port Model for Water Properties Measurements.....	7
 <u>Chapter 2</u> 	
1a. Details of Base of Large Water Tank.....	13
1b. Details of Walls of Large Water Tank.....	15
2. Large Water Tank.....	14
3. Filling the Large Water Tank.....	14
4. Water Level Gauge.....	16
5. Ground Plane for Large Water Tank.....	18
6. Small Water Tank and Ground Plane.....	18

7.	Details of Antennas for Configuration I Experiments....	21
8.	Brass Shorting Collar for "Sleeve" Monopole Antennas....	22
9.	Antenna Mounting Pedestal.....	22
10.	Details of Antennas for Configuration II Experiments....	24
11.	Details of Antenna for Configuration III Experiment....	24
12a.	Schematic of Slotted Rectangular Waveguide Apparatus....	26
12b.	Slotted Rectangular Waveguide Apparatus.....	26
13a.	Schematic of Slotted Coaxial Waveguide Apparatus.....	28
13b.	Details of Slotted Coaxial Waveguide Excitation Section.	28
14.	Details of Slotted Coaxial Waveguide Slotted Section....	30
15a.	Details of Slotted Coaxial Waveguide Probe and Probe Carriage.....	33
15b.	Slotted Coaxial Waveguide Apparatus with Reservoir and Stand.....	33

Chapter 3

1.	Schematic of Water Level Calibration Procedure.....	38
2.	ANWA Configuration for Series I, II and III Experiments.	38
3.	ANWA Configuration for Water Properties Measurement....	46

Chapter 4

1.	Aperture Admittance of Sleeve Monopole Antenna Above Ground Plane.....	51
2.	Aperture Admittance of Sleeve Monopole Antenna Above Ground Plane.....	53

3.	Aperture Admittance of Sleeve Monopole Antenna Above Ground Plane.....	54
4.	Aperture Admittance of Sleeve Monopole Antenna Above Tap Water ($T = 17.4^\circ\text{C}$).....	56
5.	Aperture Admittance of Sleeve Monopole Antenna Above Salt Water ($T = 15.7^\circ\text{C}$; $S = 9.08 \text{ g/kg}$).....	57
6.	Aperture Admittance of Sleeve Monopole Antenna Above Tap Water ($T = 17.4^\circ\text{C}$).....	58
7.	Aperture Admittance of Sleeve Monopole Antenna Above Salt Water ($T = 15.7^\circ\text{C}$; $S = 9.08 \text{ g NaCl per kg H}_2\text{O}$)....	59
8.	Aperture Admittance of Sleeve Monopole Antennas Above Water.....	61
9.	Aperture Admittance of Sleeve Monopole Antennas Above Water.....	62
10.	Aperture Admittance of Sleeve Monopole Antenna Above Water.....	64
11.	Aperture Admittance of Sleeve Monopole Antenna Above Water.....	65
12.	Aperture Admittance of Coax-Fed Monopole Antenna (Straight-wire) Above Ground Plane and Parallel to Water Surface.....	67
13.	Aperture Admittance of Coax-Fed Monopole Antenna (Straight-wire) Above Ground Plane and Parallel to Water Surface.....	68
14.	Aperture Admittance of Coax-Fed Monopole Antenna (Bent-wire) Above Ground Plane and Parallel to Water Surface.....	70

15.	Aperture Admittance of Coax-Fed Monopole Antenna Above Ground Plane and Immersed in Water.....	72
16.	Electromagnetic Constitutive Properties of Water Measured with Waveguide Apparatus.....	75
17.	Electromagnetic Constitutive Properties of Salt Water Used in Experiments I-G-1 through I-G-4.....	77
18.	Electromagnetic Constitutive Properties of Salt Water Used in Experiments I-F-1 through I-F-4.....	78
19.	Aperture Admittance of Sleeve Monopole Antenna Above Tap Water (I-A-1).....	86
20.	Aperture Admittance of Sleeve Monopole Antenna Above Tap Water (I-A-2).....	87
21.	Aperture Admittance of Sleeve Monopole Antenna Above Tap Water (I-A-3).....	88
22.	Aperture Admittance of Sleeve Monopole Antenna Above Tap Water (I-A-4).....	89
23.	Aperture Admittance of Sleeve Monopole Antenna Above Tap Water (I-A-5).....	90
24.	Aperture Admittance of Sleeve Monopole Antenna Above Ground Plane (I-B-1).....	91
25.	Aperture Admittance of Sleeve Monopole Antenna Above Ground Plane (I-B-2).....	92
26.	Aperture Admittance of Sleeve Monopole Antenna Above Ground Plane (I-B-3).....	93
27.	Aperture Admittance of Sleeve Monopole Antenna Above Ground Plane (I-B-4).....	94
28.	Aperture Admittance of Sleeve Monopole Antenna Above Ground Plane (I-B-5).....	95

29.	Aperture Admittance of Sleeve Monopole Antenna Above Salt Water (I-C-1).....	96
30.	Aperture Admittance of Sleeve Monopole Antenna Above Salt Water (I-C-2).....	97
31.	Aperture Admittance of Sleeve Monopole Antenna Above Salt Water (I-C-3).....	98
32.	Aperture Admittance of Sleeve Monopole Antenna Above Salt Water (I-C-4).....	99
33.	Aperture Admittance of Sleeve Monopole Antenna Above Salt Water (I-C-6).....	100
34.	Aperture Admittance of Sleeve Monopole Antenna Above Salt Water (I-D-1).....	101
35.	Aperture Admittance of Sleeve Monopole Antenna Above Salt Water (I-D-2).....	102
36.	Aperture Admittance of Sleeve Monopole Antenna Above Salt Water (I-D-3).....	103
37.	Aperture Admittance of Sleeve Monopole Antenna Above Salt Water (I-D-4).....	104
38.	Aperture Admittance of Sleeve Monopole Antenna Above Salt Water (I-D-5).....	105
39.	Aperture Admittance of Sleeve Monopole Antenna Above Salt Water (I-E-1).....	106
40.	Aperture Admittance of Sleeve Monopole Antenna Above Salt Water (I-E-2).....	107
41.	Aperture Admittance of Sleeve Monopole Antenna Above Salt Water (I-E-3).....	108
42.	Aperture Admittance of Sleeve Monopole Antenna Above Salt Water (I-E-4).....	109

43.	Aperture Admittance of Sleeve Monopole Antenna Above Salt Water (I-F-1).....	110
44.	Aperture Admittance of Sleeve Monopole Antenna Above Salt Water (I-F-2).....	111
45.	Aperture Admittance of Sleeve Monopole Antenna Above Salt Water (I-F-3).....	112
46.	Aperture Admittance of Sleeve Monopole Antenna Above Salt Water (I-F-4).....	113
47.	Aperture Admittance of Sleeve Monopole Antenna Above Salt Water (I-G-1).....	114
48.	Aperture Admittance of Sleeve Monopole Antenna Above Salt Water (I-G-2).....	115
49.	Aperture Admittance of Sleeve Monopole Antenna Above Salt Water (I-G-3).....	116
50.	Aperture Admittance of Sleeve Monopole Antenna Above Salt Water (I-G-4).....	117
51.	Aperture Admittance of Sleeve Monopole Antenna Above Tap Water (I-H-1).....	118
52.	Aperture Admittance of Sleeve Monopole Antenna Above Tap Water (I-H-2).....	119
53.	Aperture Admittance of Sleeve Monopole Antenna Above Tap Water (I-H-3).....	120
54.	Aperture Admittance of Sleeve Monopole Antenna Above Tap Water (I-H-4).....	121
55.	Aperture Admittance of Sleeve Monopole Antenna Above Tap Water (I-I-1).....	122
56.	Aperture Admittance of Sleeve Monopole Antenna Above Tap Water (I-I-2).....	123

57.	Aperture Admittance of Sleeve Monopole Antenna Above Tap Water (I-I-3).....	124
58.	Aperture Admittance of Sleeve Monopole Antenna Above Tap Water (I-I-4).....	125
59.	Aperture Admittance of Sleeve Monopole Antenna Above Tap Water (I-I-5).....	126
60.	Aperture Admittance of Sleeve Monopole Antenna Above Tap Water (I-I-6).....	127
61.	Aperture Admittance of Coax-Fed Wire Monopole Antenna Above Tap Water (II-A-1).....	128
62.	Aperture Admittance of Coax-Fed Wire Monopole Antenna Above Tap Water (II-A-2).....	129
63.	Aperture Admittance of Coax-Fed Wire Monopole Antenna Above Tap Water (II-A-3).....	130
64.	Aperture Admittance of Coax-Fed Wire Monopole Antenna Above Tap Water (II-A-4).....	131
65.	Aperture Admittance of Coax-Fed Wire Antenna With Open End Immersed in Tap Water (II-B-1).....	132
66.	Aperture Admittance of Coax-Fed Bent Wire Antenna With Open End Immersed in Tap Water (II-B-2).....	133
67.	Aperture Admittance of Coax-Fed Bent Wire Antenna With Open End Immersed in Tap Water (II-B-3).....	134
68.	Aperture Admittance of Coax-Fed Bent Wire Antenna Above Tap Water (II-B-4).....	135
69.	Aperture Admittance of Cylindrical Coax-Fed Monopole Antenna Immersed in Water (III-A-1).....	136
70.	Effective Conductivity and Relative Permittivity of Tap Water Used in Configuration I, Series A Experiments....	137

71.	Effective Conductivity and Relative Permittivity of Salt Water Used in Configuration I, Series C Experiments.....	138
72.	Effective Conductivity and Relative Permittivity of Salt Water Used in Configuration I, Series D Experiments.....	139
73.	Effective Conductivity and Relative Permittivity of Salt Water Used in Configuration I, Series E Experiments.....	140
74.	Effective Conductivity and Relative Permittivity of Salt Water Used in Configuration I, Series F Experiments.....	141
75.	Effective Conductivity and Relative Permittivity of Salt Water Used in Configuration I, Series G Experiments.....	142
76.	Effective Conductivity and Relative Permittivity of Tap Water Used in Configuration I, Series H Experiments.....	143
77.	Effective Conductivity and Relative Permittivity of Tap Water Used in Configuration I, Series I Experiments.....	144

Appendix B

B1.	Model for Deriving Aperture Admittance from Reflection Coefficient.....	151
B2.	Model for Deriving Aperture Admittance from Reflection Coefficient with Dielectric Bead in Feed Line.....	153

Appendix C

C1. Cross-Section of Coaxial Waveguide..... 159

Chapter 1

INTRODUCTION

In the study of antennas in or near a lossy medium, three distinct practical cases are evident: (1) the antenna which resides completely in air above the lossy medium, (2) the antenna which resides completely within the lossy medium, and (3) the antenna which resides partially in both media. An examination of the usual sources of information regarding antenna research indicates that many investigators have considered the first case, fewer have considered the second case, and only a very few have considered the third case. Most of the work has been analytical in nature, and only a small number of investigators offer experimental substantiation of the analysis. None of the experimental results noted in a search of the literature was obtained using swept frequency techniques with automated data collection. The book by Banos [1] appears to be a touchstone for investigators studying the case of the antenna above a lossy medium, while those investigators concerned with the antenna immersed in the lossy medium most frequently cite work by King and Smith [2] or by other investigators associated with King [4], [5].

The experiments described in this report were undertaken to provide measured data in support of analytical and numerical methods developed to determine current distribution on cylindrical structures which reside near the interface between media of different electromagnetic constitutive properties or which reside partially in both media. The results of

these experiments should be useful as a touchstone for other analytical and numerical methods and for experiments involving more complex models. It is evident that these experiments are closely associated with problems involving current distribution on the ground stake antenna; further association may be made with problems involving current distribution on antenna structures installed on ships and buoys. The actual structures involved in the investigation are not representative of any specific application.

This report describes the experimental models and apparatus, presents details of the experimental procedures and provides a compendium of the results. Configuration, construction and assembly of apparatus is described in Chapter 2. Chapter 3 contains details related to operation of the apparatus and to measurement and data reduction procedures. Chapter 4 presents a complete collection of measured results after reduction and attempts to validate selected results by comparison to theory, numerical analysis or the results of other measurements. Design computations, analytical techniques and data reduction methods have, for the most part, been relegated to appendices.

EXPERIMENTAL MODELS

Details of construction and assembly of all apparatus used in these experiments may be found in Chapter 2. Details of the model configurations and experimental procedures may be found in Chapter 3.

Operating Environment

The first consideration in designing the experiment was to model the desired operating environment by providing two adjacent regions with measurably different electromagnetic constitutive properties. Air was chosen for one region and water was chosen for the other region because of availability, ease of handling and homogeneity. In order to define a region of water of sufficient extent to be treated as a half space, a 16-foot by 16-foot by 4-foot (deep) tank was constructed; anechoic materials were positioned around and 10 feet above the tank to cause the half space in air to appear infinite in extent. A related experiment was performed in a smaller (3-foot by 3-foot by 3-foot) tank in which a metal screen was placed in contact with the water surface. The screen served to confine the operating environment to the water in the tank.

Scaling

The scale of the models was influenced by several factors--laboratory space, availability of materials and availability of instrumentation--all of which ultimately translated into cost and time constraints. Selection of 0.6 GHz as a design center frequency was, in the end, largely judgemental. The wavelength of a 0.6 GHz signal is approximately 50 cm in air and 5.6 cm in water. Therefore, from a position at the center of the large tank the minimum extent of the air-water interface is approximately 4.7λ in air and 42λ in water, and the maximum water depth is approximately 20λ . From a position in the center of the metal screen at the surface of the small tank, the minimum extent of the water is approximately 16λ .

Conducting Structures

Monopole antennas in various configurations were used to model the conducting structures. The monopole was chosen because it is simple to construct and because its free-space properties are well known. Further, any analytical or numerical model designed for use with more complex structures can likely be specialized for use with the monopole. The monopole antennas used in these experiments were constructed from copper semi-rigid coaxial cable stock.

Model Configurations

Three configurations of the experimental model were used (Figures 1-1 through 1-3). Variations of each of the principal configurations are outlined below.

Configuration I. This configuration was intended as a model for the ground stake antenna. A thin, hollow, right-circular conducting cylinder was placed normal to, and allowed to extend through, the interface between the two regions of the model. This was achieved by mounting a sleeve monopole antenna with driving point submerged, the sleeve emerging through the water surface, and the source gap in air. Variations in the model were achieved by:

- (1) using antennas of different radii;
- (2) using antennas with different lengths of extension above the source gap;
- (3) changing the water level, thereby changing the height of the source gap above the water surface;

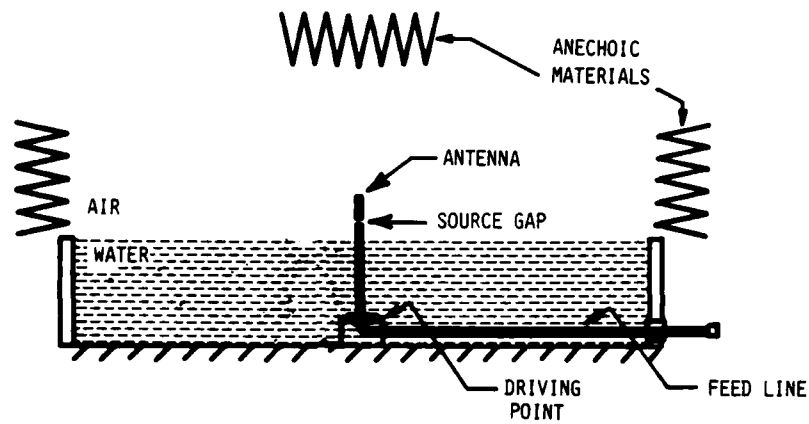


FIGURE 1-1

Sleeve Monopole Antenna in Water Tank
(Experimental Model Configuration I)

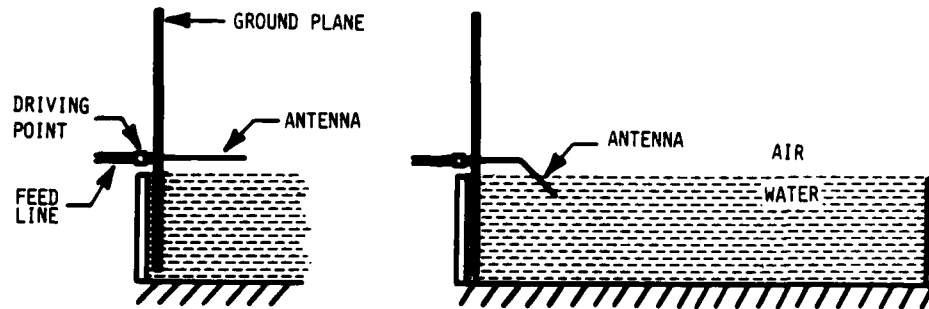


FIGURE 1-2

Coax-Fed Monopole Antennas with Aperture Above Water
(Experimental Model Configuration II)

(4) altering the electromagnetic constitutive properties of the water half space by dissolving common salt (NaCl) in the water.

Configuration II. This configuration was intended to model the thin, right-circular conducting cylinder (wire) near and/or extending through the interface between the two regions. This was achieved by mounting a monopole antenna perpendicular to a conducting screen (ground plane) erected along one wall of the tank. The ground plane was normal to the water surface and extended below the surface to the bottom of the tank and above the surface to the top of the air half space. This configuration essentially established the water as a "quarter space" and the air above as another "quarter space." The ground plane served to image the two "quarter spaces" into half spaces, and the monopole into a dipole. Variations of the configurations were achieved by:

- (1) using "straight" and "bent" wires;
- (2) changing the water level, thereby changing the separation between the conducting structure and the water surface and the length of wire immersed in water.

Configuration III. This configuration was intended as a model for a thin-walled, right-circular conducting cylinder in lossy space. This was achieved by mounting a monopole antenna perpendicular to a ground plane and placing the ground plane in contact with the surface of the water with the monopole fully submerged. The ground plane served to define the water as a lossy half space and to image the water as lossy space. The monopole was hollow and open at the end. When imaged by the ground plane, the monopole appeared to be a

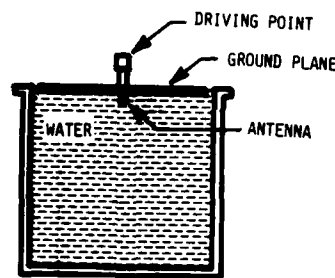


FIGURE 1-3

Coax-Fed Monopole Antenna Immersed in Water
(Experimental Model Configuration III)

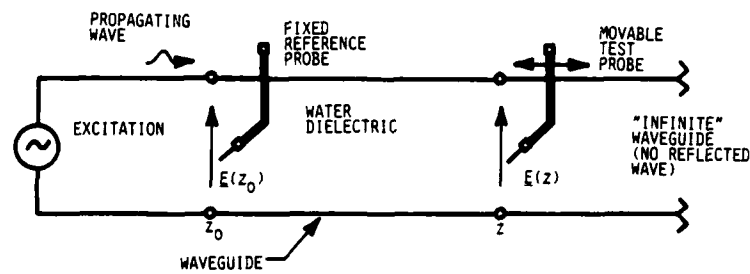


FIGURE 1-4

Two-Port Model for Water Properties Measurements

cylinder open at both ends. The particular monopole used in the model had a low aspect ratio (length to diameter) of 2.65.

Electromagnetic Constitutive Properties

The well-known electromagnetic constitutive properties of free space were used to characterize the air half space, while for the water half space it was necessary to measure the constitutive properties of a sample of the water used in each experiment. The constitutive properties of water vary with source i.e., underground, lake, stream, rain, etc., temperature and ion concentration. In some variations of these experiments, the constitutive properties were intentionally altered by introduction of NaCl ions.

The technique used to measure constitutive properties of the water samples was adapted from reference [5] and employed a waveguide which incorporated the water sample as a dielectric. The waveguide, equipped with a fixed (reference) E-field probe and a movable (test) E-field probe, was excited in its dominant mode. The waveguide was sufficiently long that, in the presence of the lossy dielectric, the transmitted energy was dissipated within the waveguide. Under these conditions of no reflected energy, the waveguide was treated as a simple passive two-port transmission model (Figure 1-4) in which the ratio of the voltage developed by the reference probe to that developed by the test probe is a function of the phase shift and the attenuation of the field by the dielectric. The electromagnetic constitutive properties, relative permittivity (ϵ_r) and effective conductivity (σ), were calculated from observations of this voltage ratio made for several positions of the

test probe along the waveguide (Appendix A). A rectangular waveguide and a coaxial waveguide were constructed to provide corroborating measurements of the electromagnetic constitutive properties of the water samples.

DATA COLLECTION AND INSTRUMENTATION

In all configurations of the experimental model, the fundamental measurement was of driving point reflection coefficient for the antenna under test. In this report the term driving point refers to the connection between the antenna structure and the instrumentation used in the experiment. The term antenna aperture refers to the source region on the antenna structure. For the sleeve monopole antenna, the aperture is the delta-gap between the sleeve and the monopole. For the coax-fed monopole antennas, the aperture is the annular region at the base of the monopole and the outer conductor of the coaxial cable. Antenna aperture admittance can be derived from driving point reflection coefficient by means of the techniques outlined in Appendix B. When a unity source voltage is assumed, admittance is equivalent to current at the position of the gap (sleeve monopole) or at the base (coax-fed antennas).

In determining the constitutive properties of water, the fundamental measurement was of transmission coefficient of the waveguide section between the reference probe and the test probe. The required E-field ratio was derived from transmission coefficient by means of the techniques outlined in Appendix A.

Measurements of transmission and reflection coefficients were accomplished with a semi-automatic frequency domain network analyzer

operated in a swept frequency mode. A major portion of the data reduction and graphical display was accomplished "on board" with the computer-controller of the network analyzer.

Chapter 2

DESIGN AND CONSTRUCTION OF APPARATUS

Design and construction of apparatus used in this project is described in this chapter under the headings of (1) water tanks, (2) antennas, and (3) slotted waveguides.

WATER TANKS

Large Water Tank

The central item of test apparatus, and the one that required the greatest effort to design and fabricate, is the large water tank. Electromagnetic considerations dictated that the tank have non-metallic containing surfaces and that it be assembled using a minimum amount of metal for fasteners and reinforcement. The necessity that this relatively large tank be free-standing and without extensive metal reinforcement, and an assessment of the construction capabilities of this organization, led to the decision to construct the tank from 2-inch by 4-inch (2x4) pine lumber covered with exterior-grade plywood. The dimensions, 16 feet by 16 feet along the exterior perimeter and 4 feet interior depth, were a compromise based on the required water surface

range, the 4-foot by 8-foot dimensions of standard plywood sheets, and the amount of available laboratory space.

Each wall frame was constructed separately from 2x4 studs on 16-inch centers, with 2x4 cross-braces at approximately 16-inch intervals. The 2x4 lumber was doubled, glued and nailed to provide additional strength and rigidity for the end and central studs and for the cap of each wall. The base was constructed in four 8-foot by 8-foot sections from 2x4 joists on 16-inch centers with 2x4 cross braces at 16-inch intervals. The four sections were fastened together with 0.5-in steel cap screws, nuts and fender washers to form the 16-foot by 16-foot base. Details of the framework can be seen in Figure 2-1.

The entire base was covered with 0.75-inch plywood and each wall section was covered with 0.50-inch plywood. All plywood edges were sealed with polyester resin, and the sheets were glued and nailed to the framework. The wall sections were then fastened to the base, and to each other, by means of 0.5-inch steel cap screws, nuts and fender washers. Buttresses of 2x4 lumber were attached to the base on the outside of the tank at the center of each wall. The assembled tank rests on a concrete basement-level floor (Figure 2-2); wooden shims were placed under the floor joists where necessary to compensate for irregularities in the concrete floor.

An attempt was made to seal the tank by fastening wooden laths over the wall and floor seams and wooden fillets in all corners and then applying three liberal coats of polyester resin to all exposed interior surfaces. When filled with water, there was some cracking of the resin coating, resulting in water seepage into the plywood and through seams and corners. Several attempts were made to eliminate the seepage by

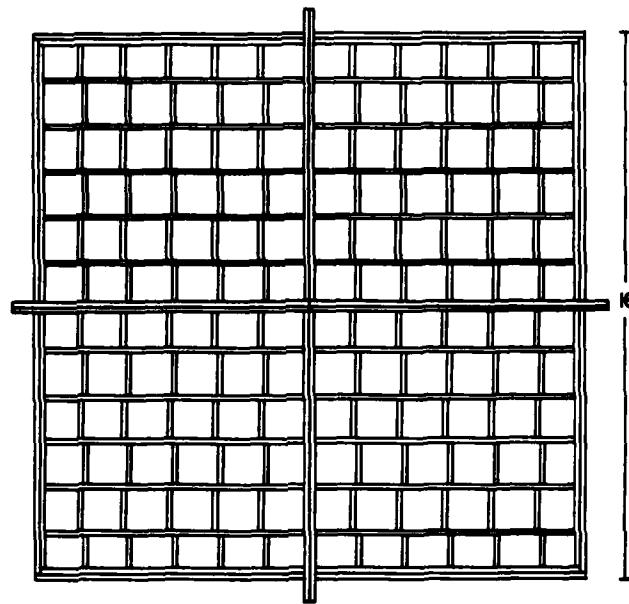


FIGURE 2-1a
Details of Base of Large Water Tank

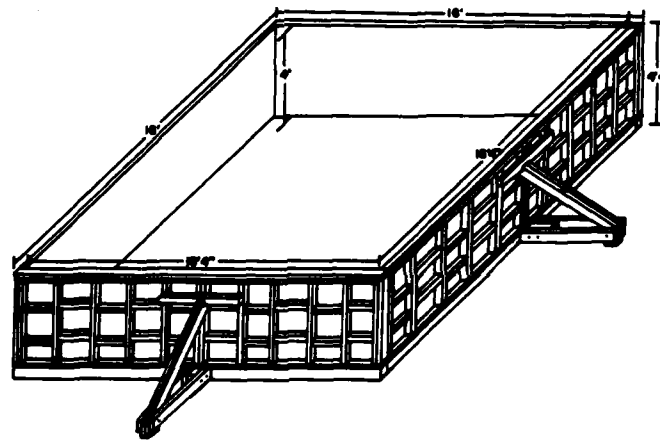


FIGURE 2-1b
Details of Walls of Large Water Tank



FIGURE 2-2
Large Water Tank

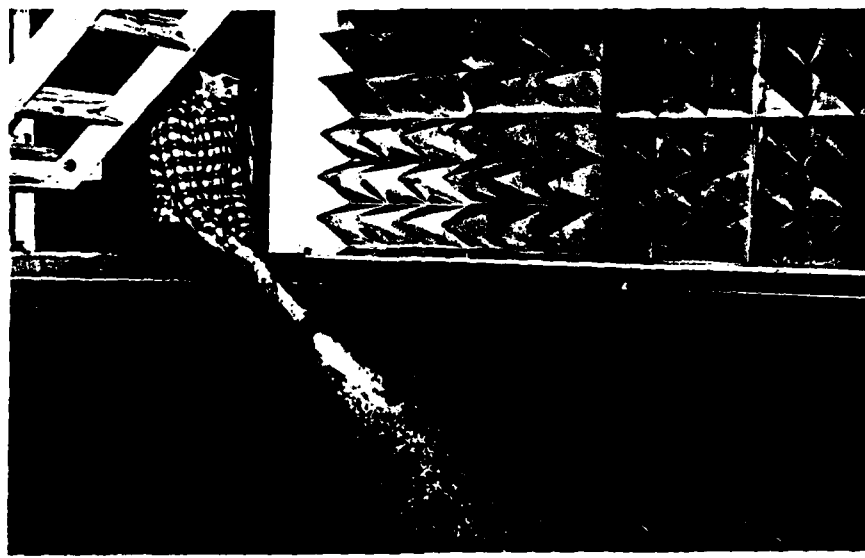


FIGURE 2-3
Filling the Large Water Tank

reinforcing seams and corners with fiberglass strips and additional resin. When the seepage persisted, the decision was made to install a specially fabricated 22-mil vinyl liner of the type used in swimming pools. The liner was installed over a 125-mil plastic foam pad and clamped along the top edge of the tank by a 1-inch by 2-inch wooden coping. Performance of the liner has been entirely satisfactory, and a great deal of labor and materials could have been saved by incorporating the liner into the original design.

Since the basement laboratory in which the tank is located formerly housed the campus laundry, adequate water supply and drainage were available. Filling is accomplished through a 1.5-inch firehose adapted to a 2-inch, 90 pounds-per-square-inch water supply line (Figure 2-3); the rate of filling is approximately 1 inch per minute. A 1.5-inch swimming pool inlet fitting was installed in the floor of the tank and adapted to a 2-inch gate valve located outside the tank; the rate of drainage is approximately 0.5 inch per hour when the tank is full, but slows to less than half that rate as the head pressure decreases. The tank filling scheme could be improved by installing another inlet valve in the wall of the tank and adapting the fire hose to the inlet fitting. Since the liner was an addition to the original design, the drain fitting flange stands approximately 0.5 inch above the floor and traps 50-75 gallons of water in the tank; the drainage scheme could be improved by recessing the drain fitting into the floor. A sight gauge for monitoring water level was assembled by attaching a copper tube to a 1-inch (ID) by 36-inch pyrex glass tube and inserting the copper tube into the throat of the drain line (Figure 2-4). While this is a simple and convenient arrangement, gauge readings are inaccurate when the drain



FIGURE 2-4
Water Level Gauge

valve is open because of the Venturi effect created by water flow in the throat of the valve. Since the experimental procedures require that precise water levels be achieved by draining water from the tank, an improved design would provide a separate inlet fitting for attachment of the sight gauge so that water level could be monitored more accurately when the drain valve is open.

Another swimming pool inlet fitting was installed in one wall just above floor level. This fitting serves as an entry for the coaxial cable (coax) which is used to connect the bottom-mounted antenna to instrumentation outside the tank.

For the Configuration I experiments, the tank is surrounded by anechoic panels of carbon-impregnated latex foam and styrofoam pyramids for the Configuration II experiments a 13-foot (high) by 14-foot, 4-inch, (wide) aluminum ground plane was erected inside of one wall of the tank (Figure 2-5). The ground plane was constructed from two 125-mil aluminum sheets, seamed together by bolting them to a 6-inch, 125-mil aluminum backing plate. Vertical stiffeners of 3-inch aluminum channel stock were bolted to the sheets. Countersunk screws were used throughout, and all screwheads and seams were covered with aluminum foil tape. An inverted-U framework of 2x4 (upright) and 2x6 (horizontal beam) pine lumber, doubled, glued and nailed, was attached and braced to the exterior walls of the tank. A system of four double-hung pulleys were installed to be used to erect the ground plane and to raise it from the water when necessary. A 3-inch diameter hole was cut into the ground plane, centered at a point 42 inches above the bottom of the plane; an aluminum collar, machined to accomodate a 2-inch diameter antenna base, was pressed into the hole. The plane, when erect, intersects the water

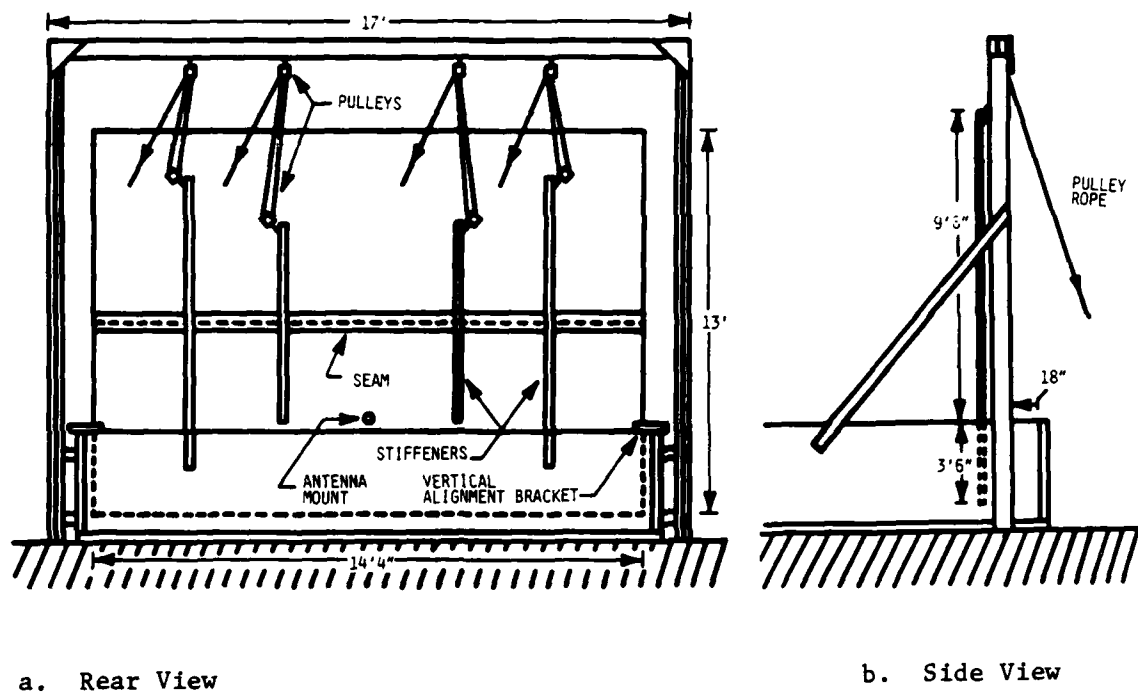


FIGURE 2-5
Ground Plane for Large Water Tank

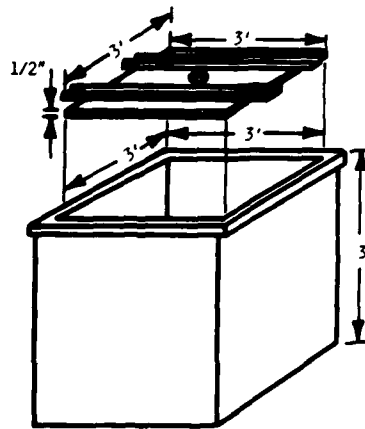


FIGURE 2-6
Small Water Tank and Ground Plane

surface along a line 18 inches from the wall, and the edges of the plane are approximately 6 inches from either side wall.

Small Water Tank

The small water tank was salvaged from a previous research project. This tank is made of pre-formed fiberglass and measures 3 feet by 3 feet by 3 feet. A ground plane constructed from 0.375-inch thick aluminum, 35 inches square, was also salvaged from a previous project. Aluminum channel stock was attached to the aluminum ground plane and served to suspend the sheet from the edge of the tank (Figure 2-6). A 1.5-inch diameter hole was cut into the center of the ground plane to accomodate an antenna mounting base.

ANTENNAS

Configuration I Experiments

Three sleeve monopole antennas, all fabricated from copper semi-rigid (SR) coax, were used in these experiments. One monopole was constructed from 0.085-inch OD coax, a second from 0.141-inch OD coax, and a third from 0.250-inch OD coax. Each monopole was assembled from two sections of coax, a sleeve section and an extension section. A male SMA connector was fitted to one end of each sleeve section, and approximately 0.25-inch of center conductor was exposed at the other end; a rectangular mounting bracket was soldered to the outer conductor of each sleeve section 1.5 inches above the SMA connector. The center conductor and dielectric were removed from each extension section leaving only an

open-ended tube; one end of each resulting tube was plugged with brass soldered to a depth of approximately 0.25 inch. For the 0.085-inch and 0.141-inch OD antennas, the brass plug was bored to accept the exposed center conductor of the sleeve section (see Figure 2-7). The two sections were joined by soldering the center conductor from the sleeve section to the brass plug of the extension section. A 0.5-mm stainless steel shim was used during soldering to maintain the gap between sleeve and extension. For the 0.250-inch OD antenna, a solid brass cylinder, also 0.250-inch in diameter, and approximately 1 inch in length, was bored and soldered to the center conductor of the sleeve section (see Figure 2-7). The opposite end of the brass cylinder was bored and tapped to accommodate a screw; the brass plug in the 0.250-inch extension section was allowed to protrude, and that protrusion was threaded to mate with the brass cylinder. Four such extensions were constructed for the 0.250-inch antenna. The details and dimensions of all three antennas can be found in Table 2-1.

Brass collars, suitable for electrically shorting the source gap, were constructed for use with each antenna (Figure 2-8). These devices were used in the data reduction procedures described in Appendix B.

A wooden mounting pedestal was anchored by concrete blocks near the center of the water tank and used to support the antenna under test. A 0.5-inch OD Spirafil coax, also anchored to the floor by concrete blocks, was used to connect the antenna to the instrumentation outside the tank. The coax penetrated the tank wall through the inlet fitting described above in this chapter and was clamped to the pedestal below the antenna connector. An adapter, fabricated from PVC plastic, was sealed to the coax by O-rings and threaded to mate with the inlet

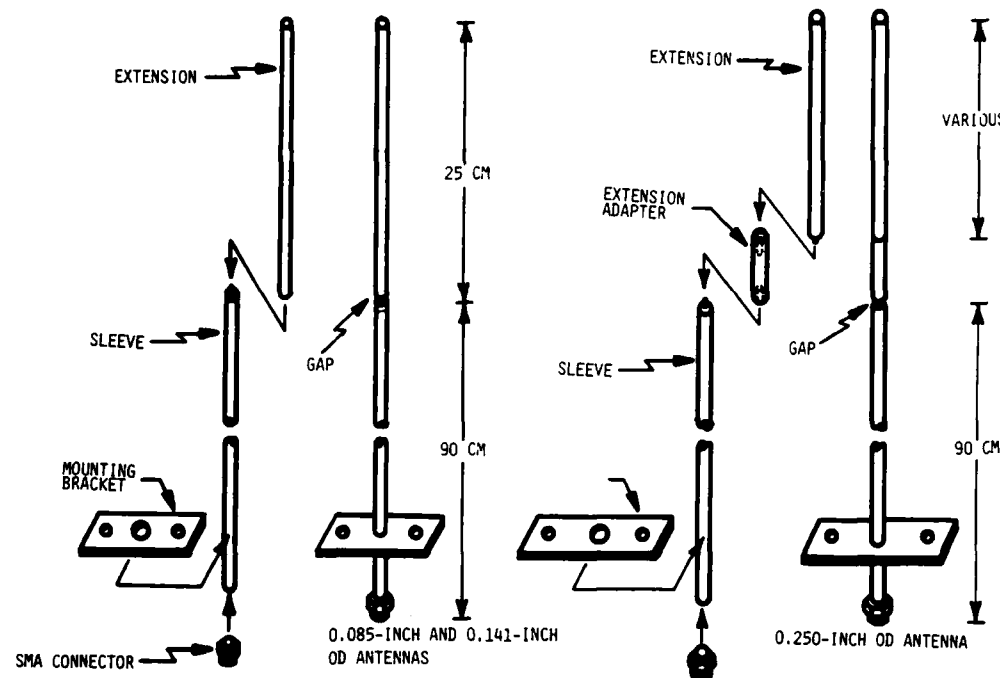
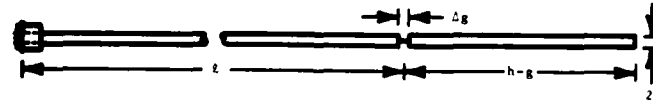


FIGURE 2-7

Details of Antennas for Configuration I Experiments

TABLE 2-1

Dimensions of Configuration I Antennas



Nominal Radius	l (cm)	$h-g$ (cm)	$2a$ (cm)	Δg (cm)
0.085-inch OD	90.545	25.427	0.216	0.054
0.141-inch OD	90.645	25.504	0.358	0.060
0.250-inch OD	90.624	(1) 6.042 (2) 25.395	0.635	0.070

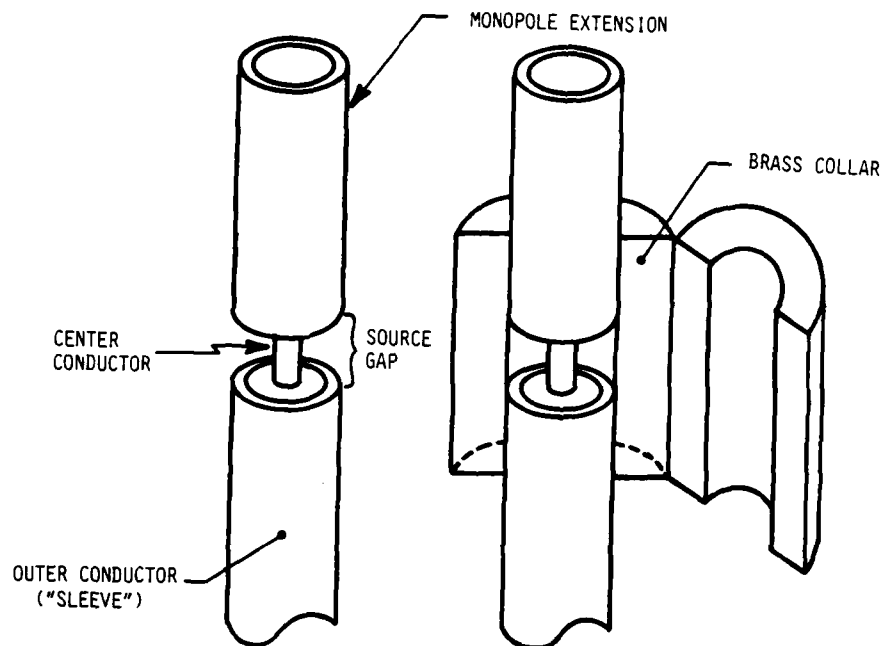


FIGURE 2-8

Brass Shorting Collar for Sleeve Monopole Antennas

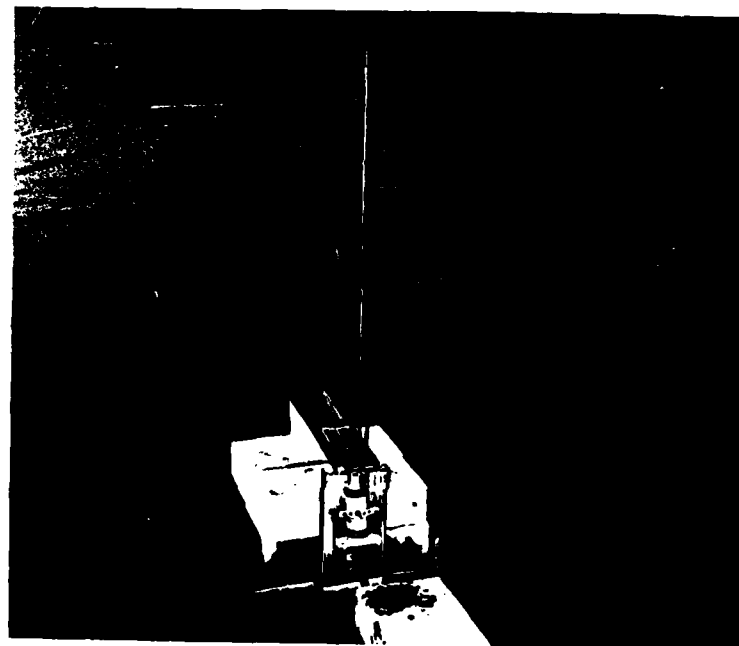


FIGURE 2-9

Antenna Mounting Pedestal

fitting in the tank wall. The connection between coax and antenna was encased in a PVC plastic shell, and the shell was filled with paraffin to prevent water from entering the connection. The details of the pedestal and the antenna connection may be seen in Figure 2-9.

Configuration II Experiments

Two wire antennas, each fabricated from a single section of 0.250-inch OD copper SR coax, were used in these experiments. As can be seen in Figure 2-10, one antenna is a straight wire and the other is a bent wire. A male SMA connector was fitted to one end of the coax section, and a length of center conductor equal to the required antenna height was exposed at the other end. A 2-inch diameter brass mounting base, 0.250-inch thick, was soldered to the outer conductor at the point where the center conductor emerges from the coax. An aperture reference section was also constructed by shorting center conductor to outer conductor at one end of a section of coax equal in length to the distance from driving point to aperture of the monopole. This reference section was used in data reduction procedures described in Appendix B.

Configuration III Experiments

A monopole antenna was constructed from a 3-inch section of 50-ohm General Radio (GR) coaxial air line. A GR connector was fitted to one end of the section, and the outer conductor was cut away to expose 1.65 cm of center conductor at the other end (Figure 2-11). A 1-cm Teflon bead was placed into the open end of the air line; the bead served to seal the air line and to support and center the center conductor. The

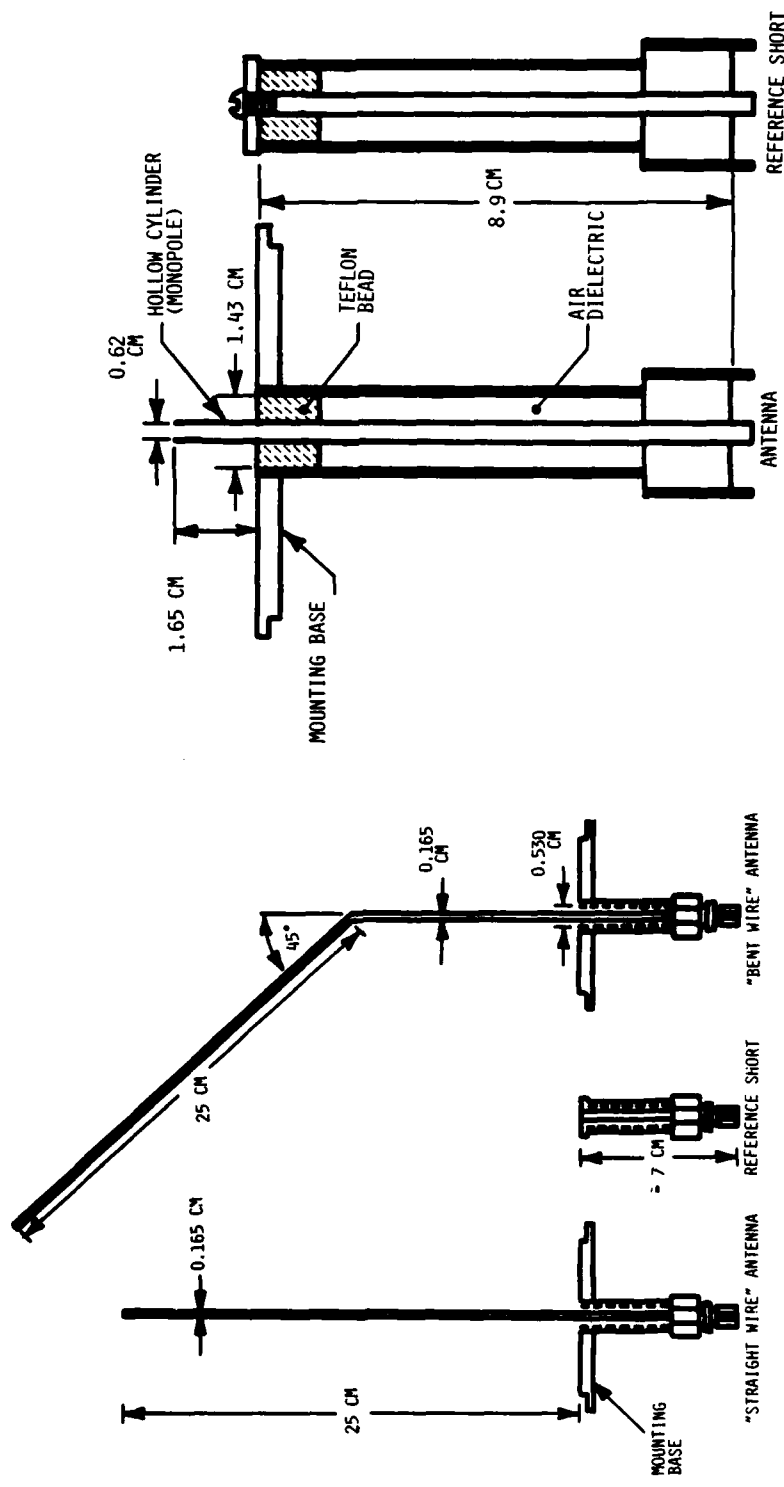


FIGURE 2-10
Details of Antennas for Configuration II Experiments

FIGURE 2-11

Details of Antenna for Configuration III Experiment

exposed center conductor was bored to achieve a wall thickness of 0.5 mm. A vent hole of 0.032-inch diameter was drilled through the connector center conductor to allow water to enter the hollow section of the center conductor when the apparatus is submerged. A 1.5-inch diameter base was constructed from 0.250-inch thick brass and soldered to the outer conductor at the position where the center conductor emerges from the coax. Another 3-inch section of GR coax was fitted with a GR connector at one end and electrically shorted by a brass disk at the other end (Figure 2-11) for use as an aperture reference section. This device was used in the data reduction procedures described in Appendix B.

SLOTTED WAVEGUIDES

Two slotted waveguides were constructed to provide corroborating measurements of the electromagnetic constitutive properties of water. One is a rectangular waveguide fabricated from WR-137 (RG-50/U) waveguide accessories; the other is a coaxial waveguide fabricated from brass tubing (outer conductor) and rod (center conductor).

Rectangular Waveguide Apparatus

The rectangular waveguide apparatus consists of five sections: excitation, reference, slotted, "infinite" line and termination (Figure 2-12a). The excitation section is a Narda 612A Type N - to - WR-137 adapter with cover butt flange. The reference section was fabricated by attaching brass choke butt flanges to a 6.35-cm section of copper WR-137 waveguide stock. The reference probe is the exposed center conductor

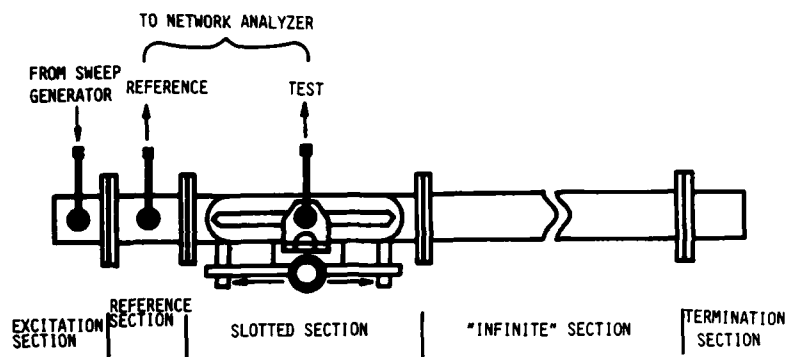


FIGURE 2-12a

Schematic of Slotted Rectangular Waveguide Apparatus

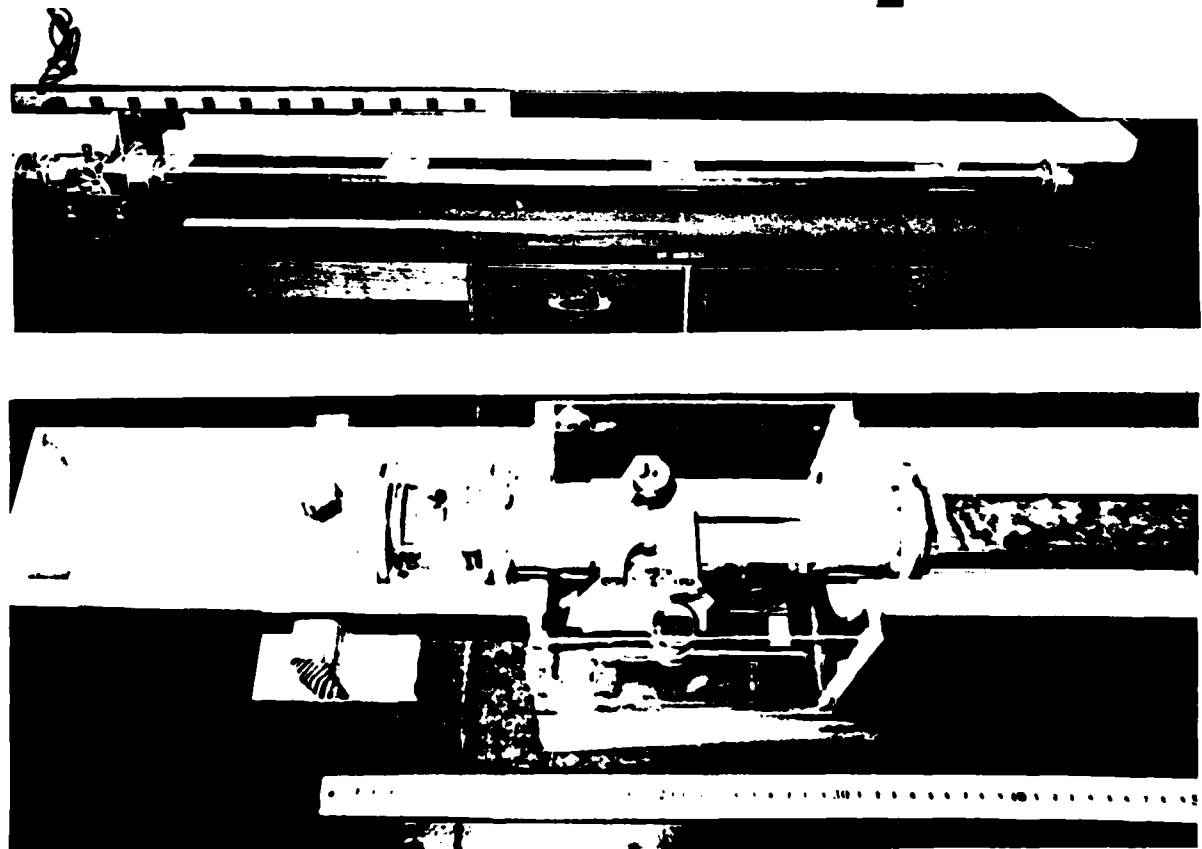


FIGURE 2-12b

Slotted Rectangular Waveguide Apparatus

(approximately 0.8 cm) from a section of 0.085-inch OD SR coax. A female SMA connector was attached to one end of the coax, and the other end was soldered into a hole in the broadwall of the waveguide so that only the exposed center conductor penetrated the interior of the waveguide. A brass collar was soldered around the SR coax and to the waveguide to provide coax-to-waveguide connection with sufficient rigidity to withstand the weight of connecting cables. The slotted section is an IM-45/U (military version of Narda 222) with cover butt flanges and a moveable probe carriage with vernier position indicator. The test probe, fabricated from 0.085-inch OD SR coax in the same manner as the reference probe, was soldered to a brass housing which was constructed to fit the IM-45/U probe carriage. The "infinite" section was assembled by attaching brass choke butt flanges to a 183-cm section of WR-137 copper waveguide stock. The termination section was fabricated by removing the Type N connector from a Narda 612A Type N - to - WR-137 adapter and replacing the connector with a brass plug; the modified adapter was filled with carbon-impregnated latex foam.

The assembled waveguide apparatus, which may seen in Figure 2-12b, is 210-cm in length and, when in operation, is submerged in a 240-cm trough constructed of plexiglas and PVC plastic sewer pipe. The trough, with waveguide apparatus in place, has a liquid capacity of approximately 12 liters.

Coaxial Waveguide Apparatus

The coaxial waveguide apparatus consists of three parts: excitation section, slotted section and probe carriage (Figure 2-13a). The outer

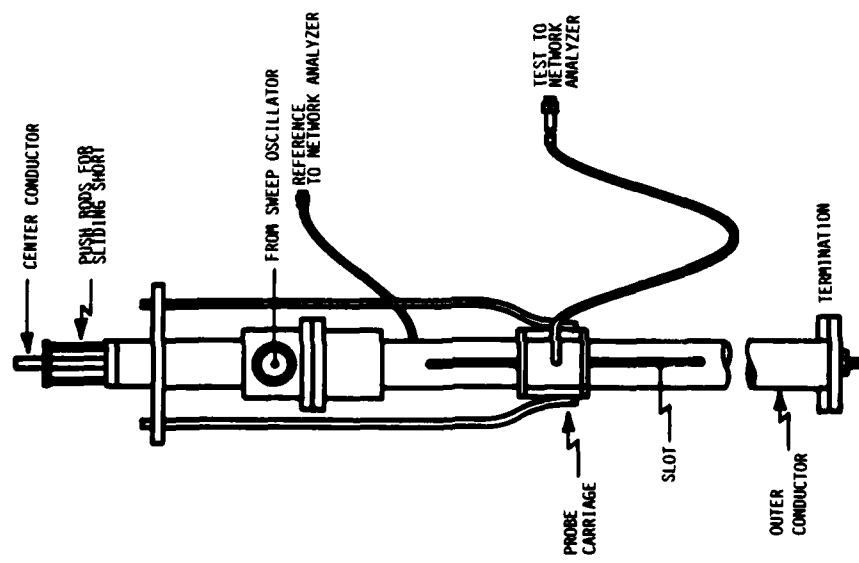


FIGURE 2-13a
Schematic of Slotted Coaxial
Waveguide Apparatus

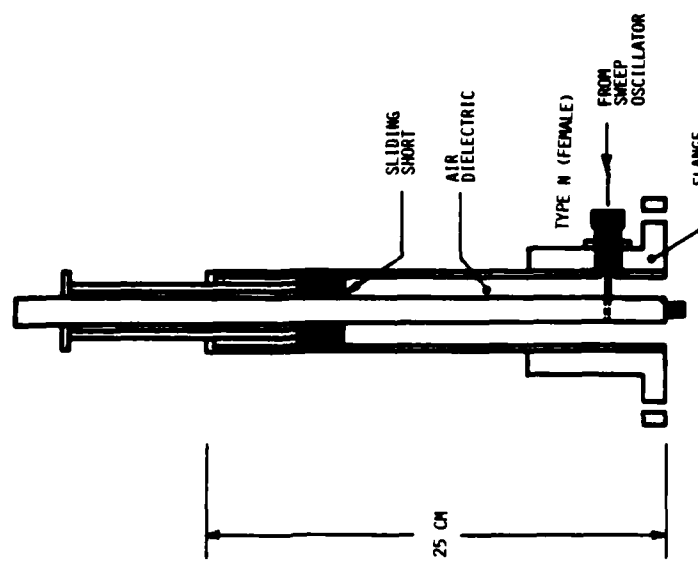


FIGURE 2-13b
Details of Slotted Coaxial
Waveguide Excitation Section

conductor of the coaxial line was constructed of 0.650-inch ID (0.750-inch OD) extruded brass tubing and the center conductor was constructed of 0.250-inch brass rod. The excitation section is 30-cm long and the slotted section is 180-cm long. The outer conductors of the two sections were joined by brass flanges, and the center conductors were screwed together. Since the waveguide must be filled with water, there can be no internal structure to maintain uniform separation between center and outer conductors. To overcome the sagging of the center conductor due to absence of internal support, the coaxial line is mounted vertically, and the center conductor rod is centered at either end of the assembled apparatus and placed in tension.

The excitation section (Figure 2-13b) includes a sliding short constructed from a brass piston, bored to accomodate the center conductor and attached to 0.125-inch brass push rods; the sliding short has approximately 25-cm of travel. Sliding contact is maintained by brass spring "finger" stock which was soldered around the outer perimeter and around the bore of the piston. A Type N bulkhead connector was mounted to a flat area on the flange shoulder 3.175 cm from the flange face; the center conductor of the connector was tapered and pressed into a lateral hole in the 0.250-inch brass center conductor rod. A centering disk was fitted over the end of the outer conductor; the centering disk is drilled to accomodate the push rods for the sliding short and the center conductor. When assembled, the center conductor is pinned outside of the waveguide, with the pin resting against the centering disk, and tension is applied at the termination of the slotted section.

A 28-cm slot, approximately 0.0625 inch wide, was cut into the brass tubing of the slotted section (Figure 2-14) beginning at a point 25-cm

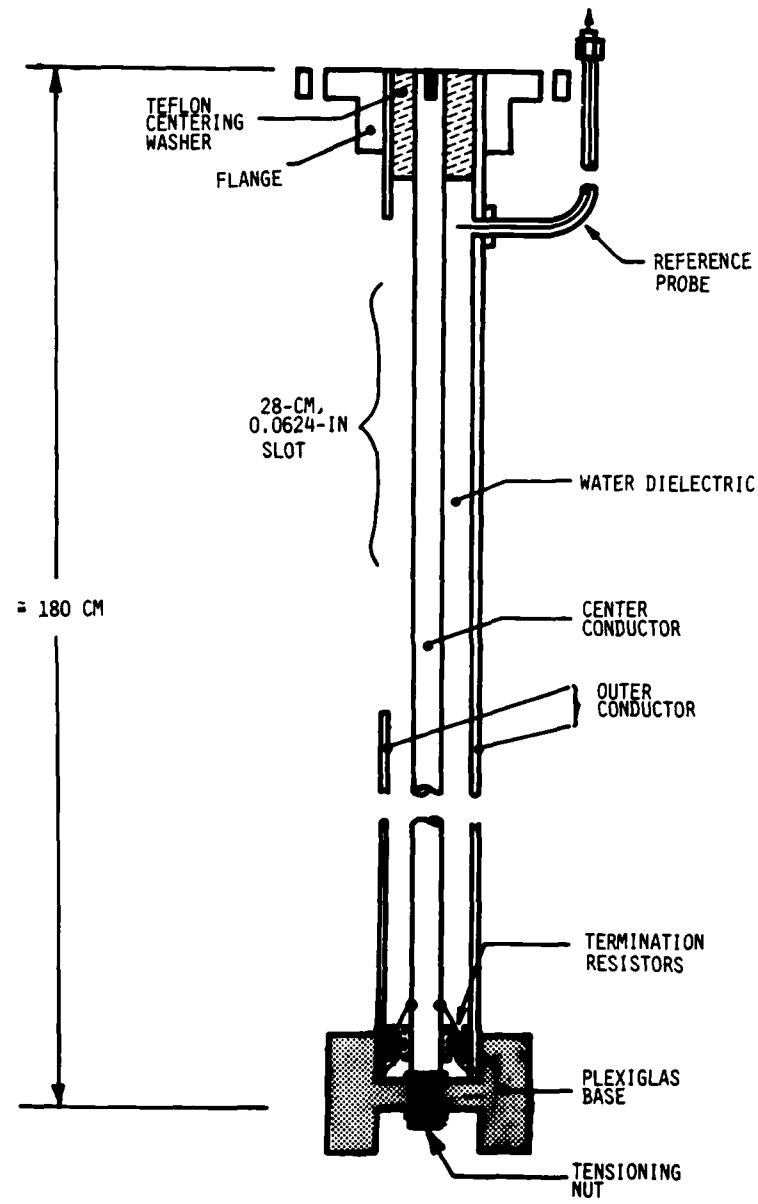


FIGURE 2-14

Details of Slotted Coaxial Waveguide Slotted Section

from the flange face. The slot was made by repeatedly scoring the tubing with a 0.0625-inch end mill. After milling, the tube was clamped and heated to eliminate spreading of the slot which occurred when stresses in the extruded tubing were released during milling. A reference probe, constructed by exposing approximately 0.05 inch of the center conductor of a section of 0.034-inch OD SR coax at one end and attaching an SMA connector at the other, was inserted through the brass tubing at a point diametrically opposite the end of the slot nearest the flange; only the exposed center conductor was allowed to penetrate the interior of the waveguide.

A 5.35-cm long Teflon cylinder, machined to fit within the brass tubing, and bored to accomodate the center conductor rod, was positioned approximately 2.5 cm from the reference probe. This Teflon cylinder serves to center and support the center conductor and to reduce reflections.

The slotted section is terminated by a plexiglas cylinder approximately 2.5-cm in length; this cylinder was bored to accomodate the center conductor rod, and three holes were drilled parallel to the bore and at 120° spacing around the bore. A 0.125-watt carbon resistor was sealed with silicon rubber caulk into each of the three holes; one end of each resistor was soldered to the center conductor within the waveguide, and the other end was soldered to the outer conductor outside the waveguide. The entire termination assembly of plexiglas cylinder and resistors was sealed into the brass tubing with silicon rubber caulk.

A plexiglas base, recessed to accomodate the brass tubing and bored to accomodate the center conductor rod, was constructed. The center conductor which protrudes into another recess in the plexiglas base, was

threaded to accomodate a tensioning nut. When assembled, this nut is used to place the center conductor rod in tension by working against the pin in the opposite end of the rod.

The test probe carriage (Figure 2-15a), which was fabricated from a 1.5-inch brass cube, bored to accomodate Teflon bushings, is designed to slide along the outer surface of the brass tubing. A portion of the brass cube was cut away to permit attachment of the test probe. The test probe was constructed from 0.034-inch OD SR coax in the same manner as the reference probe, and was soldered to a brass key machined to fit the waveguide slot. The key was attached to 20-mil brass shim stock, which was then shaped to the curvature of the tubing and attached to the probe carriage with screws. The curved shim stock with the slot key serves to maintain sliding contact. The probe carriage was fitted with steel push rods and a push rod guide.

A wooden stand was constructed to maintain the apparatus upright and to support a plexiglas reservoir which surrounds the slot and contains the water which floods the waveguide. The reservoir has a liquid capacity of approximately 5 liters. Figure 2-15b shows the assembled waveguide with stand and reservoir.

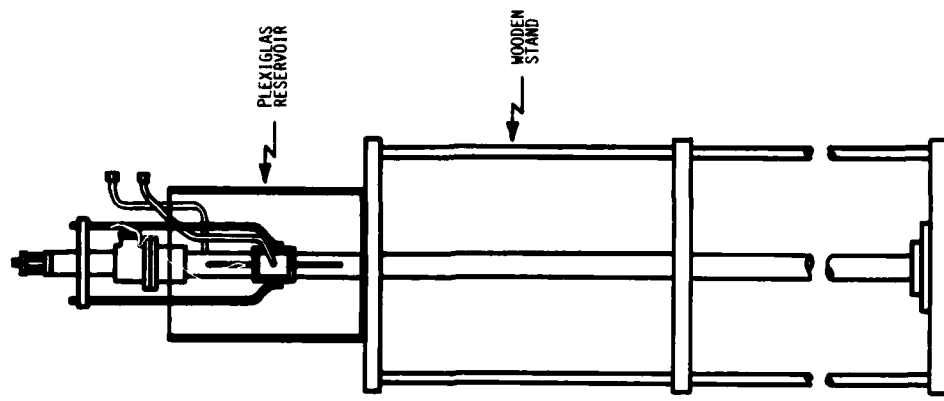


FIGURE 2-15b

Slotted Coaxial Waveguide Apparatus
with Reservoir and Stand

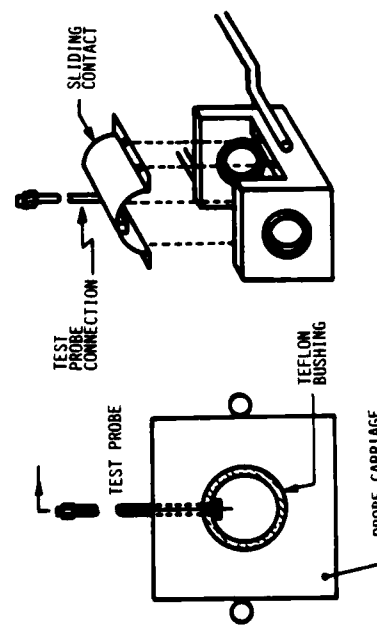


FIGURE 2-15a

Details of Slotted Coaxial Waveguide
Probe and Probe Carriage

Chapter 3

EXPERIMENTAL PROCEDURES

The experiments of this project were divided into four categories according to the configuration of the experimental model and the type of measurements and observations to be made.

The Series I experiments are associated with Configuration I of the experimental model. The objective was to obtain source gap admittance for a sleeve monopole antenna with driving point connection submerged near the center of the tank and the source gap in air. The general configuration of the apparatus may be seen in Figure 1-1. The source gap admittance was derived from reflection coefficient measured at the driving point connection.

The Series II experiments are associated with Configuration II of the experimental model. The objective was to obtain aperture admittance for a wire antenna with aperture in air above the water surface. The wire antenna was mounted on a ground plane which extended through the air-water interface at a right angle. The general configuration of the apparatus may be seen in Figure 1-2. The aperture admittance was derived from reflection coefficient measured at the driving point connection.

The Series III experiments are associated with Configuration III of the experiment model. The objective was to obtain aperture admittance

for a monopole antenna mounted perpendicular to a ground plane and fully immersed in water. The general configuration of the apparatus may be seen in Figure 1-3. The aperture admittance was derived from reflection coefficient measured at the driving point connector.

The objective of the water properties measurements was to determine the electromagnetic constitutive properties (ϵ_r and σ) for a sample of the water used in each of the Series I and Series II procedures. A slotted waveguide was filled with water from the test sample, and attenuation and phase shift were measured for a section of the waveguide between a fixed reference probe and a movable test probe for several positions of the test probe. ϵ_r and σ were derived from this series of attenuation and phase shift measurements.

SERIES I EXPERIMENTS

Water Tank Configuration

During experiments with the Configuration I model, the water tank was surrounded by anechoic material consisting of pyramids of carbon-impregnated latex foam or styrofoam. Panels of this material were positioned along all four tank walls, extending to a height of approximately 10 feet; additional panels of the material were suspended above the tank to create an anechoic chamber above the water surface.

Antenna Installation

The sleeve monopole antenna was attached by a mounting bracket (Figure 2-7) to a pedestal located near the center of the water tank

(Figure 2-9). Care was taken to ensure that the antennas were mounted in a true vertical position so that the sleeve axis would be normal to the water surface. The 0.250-inch OD antenna was sufficiently rigid that no support other than the mounting bracket was required, but the 0.141-inch OD and 0.085-inch OD antennas required additional support to maintain verticality. This support was provided by a network of monofilament threads attached between the sides of the tank and a styrofoam shell cemented to the antenna so that the source gap was in the center of the shell. Connection of the antenna to the instrumentation system outside the tank was by means of the bottom-lying 0.5-inch OD Spirafil coaxial cable described in Chapter 2.

Water Level Determination

One method of varying the Configuration I model was to change the water level, thereby changing the height of the source gap above the water surface. Water level was monitored with a sight gauge (Figure 2-4) located outside the tank; gap height was determined indirectly by calibrating the sight gauge to a marked position on the antenna sleeve. White tape was wrapped around the sleeve of the 0.250-inch OD antenna at an accurately measured distance (g') from the lower edge of the source gap. The antenna was then installed, and a surveyor's transit was positioned just outside one wall of the tank. As the tank was slowly filled, the white band was observed through the transit. When the water level was precisely aligned with the edge of the white band, the scale on the sight gauge was repositioned to establish a convenient reference level (L') as shown in Figure 3-1. Operating level (L_o) for each experi-

ment was then read from the sight gauge scale and converted to gap height by means of the formula

$$g_0 = g' + (L_o - L') .$$

When the 0.141-inch OD or 0.085-inch OD antenna was installed, the gap height was corrected to reflect the difference in position of the mounting bracket on the sleeve. The final value of gap height in all cases was adjusted to the center of the source gap so that

$$g = g_0 + \Delta g/2 .$$

Surface tension created a meniscus around the antenna sleeve and within the glass tube of the sight gauge, and it produced a capillary rise within the glass tube. According to reference [6], the capillary rise of water near room temperature within a 1-inch ID glass tube is on the order of 10^{-1} mm, a value considered to introduce negligible error into these experiments. The presence of the meniscus, while apparent in all water level observations, did not introduce error into the experiments because all observations, including those made to establish a reference level, were referred to the same point in the meniscus.

Data Collection

The general plan for data collection was to measure reflection coefficient at 0.01 GHz intervals over the 0.5 - 1.0 GHz octave and repeat this for several gap heights with each antenna. Prior to installing the

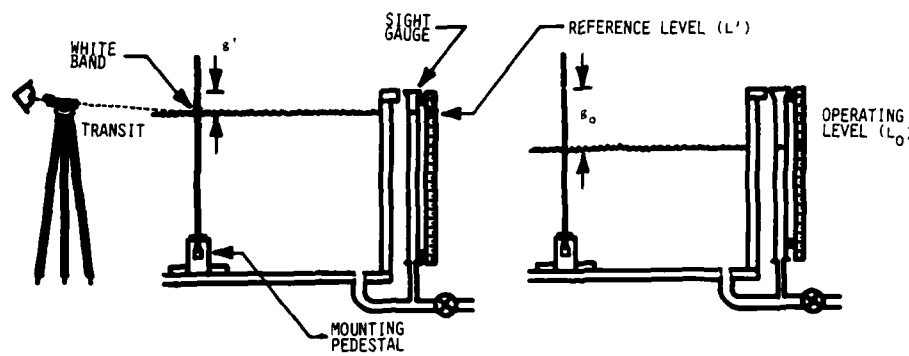


FIGURE 3-1

Schematic of Water Level Calibration Procedure

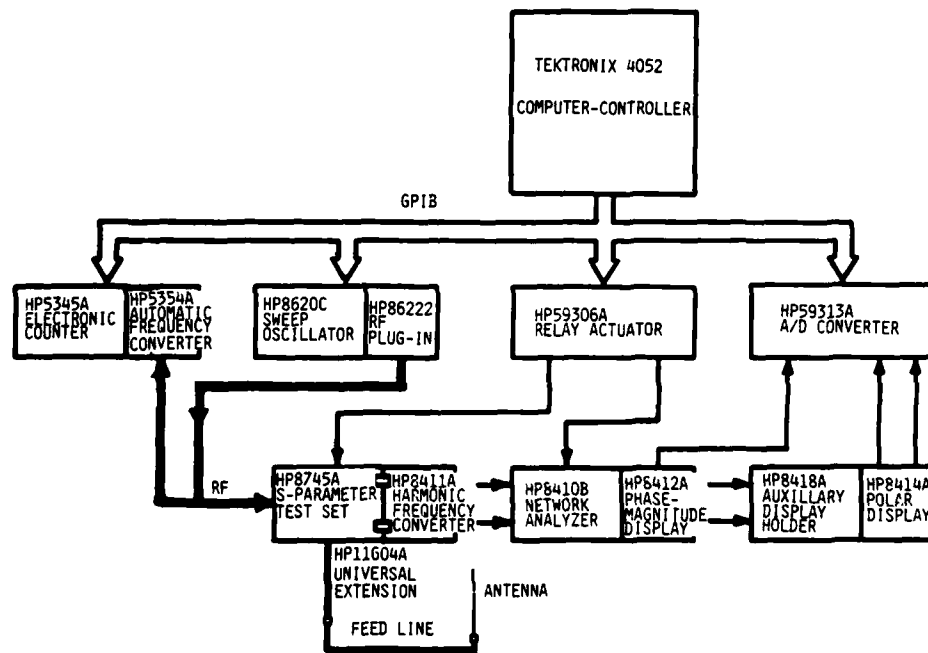


FIGURE 3-2

ANWA Configuration for Series I, II and III Experiments

antenna, it was necessary to establish a reference plane at the antenna driving point connector, as described later in this chapter. The antenna was then installed, and a brass collar was clamped around the source gap effectively shorting the antenna aperture. Reflection coefficient was measured and recorded for each frequency with the gap shorted. The reflection coefficient data recorded with the gap shorted were used in deriving antenna aperture admittance from antenna driving point reflection coefficient (see Appendix B). The driving point connector was then sealed in paraffin to prevent entry of water into the connector, and the tank was filled with water.

Four antenna configurations were used in models in which the tank contained ordinary tap water; two of the antenna configurations were also used in models in which salt (NaCl) was dissolved in the water. Table 4-1 contains a detailed description of the configurations for which data was collected.

SERIES II EXPERIMENTS

Water Tank Configuration

During experiments with the Configuration II model, an aluminum ground plane was erected 18 inches inside and parallel to one wall of the tank. The remaining three sides of the tank were surrounded with anechoic material as in Series I procedures.

Antenna Installation

The wire antennas were mounted into a circular opening in the ground plane at a position just below the lip of the tank wall (Figure 2-5). Connection of the antenna to the instrumentation system was by means of an HP11605A Flexible Arm.

Water Level Determination

As in the Series I experiments, height of the antenna above the water surface was varied by changing the water level. Again, water level was monitored with a sight gauge which, in these experiments, was calibrated to the center of the antenna mount. A pointed brass rod, 0.250-inch in diameter, was placed in a mounting base identical to those used to construct the antennas. The base with the pointed rod was installed in the ground plane with the point to the rear of the ground plane, and the tank was then filled to cover the brass rod. When the surface was calm, water was slowly drained until the point of the brass rod was aligned with the surface. The scale on the sight gauge was then repositioned to establish a convenient reference level. Operating levels, and hence height of the antenna above the water surface, were then read from the sight gauge.

Data Collection

The general plan for data collection was to measure reflection coefficient at intervals of 0.01 GHz over the 0.5 - 1.0 GHz octave for a straight wire antenna, and at the same intervals over a 0.5 - 1.1 GHz

band for a bent wire, and to repeat this for several heights above the water surface for each antenna. As in the Series I procedures, it was necessary to establish a reference plane at the antenna driving point connector before making reflection coefficient measurements. It was also necessary to measure reflection coefficients for a shorted section of coaxial cable of the same stock as the antenna. Table 4-1(d) contains a detailed description of the configurations for which data was collected.

SERIES III EXPERIMENTS

Water Tank Configuration

The small tank was filled with water and the ground plane was suspended from the edge of the tank such that the water surface and ground plane were coplanar.

Antenna Installation

The monopole antenna was mounted onto the circular opening in the center of the ground plane. Connection of the antenna to the instrumentation was by means of a HP11605A Flexible Arm and a precision GR-SMA adapter.

Data Collection

The general plan for data collection was to measure reflection coefficients at intervals of 0.01 GHz over the 0.25-0.75 GHz band. As in the Series I and II experiments, it was necessary to establish a refer-

ence plane at the antenna driving point before making reflection coefficient measurements. It was also necessary to measure reflection coefficient of the shorted section of coax for use in data reduction procedures.

WATER PROPERTIES MEASUREMENTS

Preparation of the Rectangular Waveguide Apparatus

The water sample to be tested was cooled to approximately 5° Celcius and then poured into the PVC trough described in Chapter 2. One end of the "infinite" section (Figure 2-12) was submerged and the other end was lowered slowly to drive out air bubbles which tended to form on the inner side of the top wall of the waveguide. The remaining components were submerged, and after allowing time for percolation of trapped air, the assembly was completed with all components submerged. The necessary instrumentation connections were made, and the apparatus was allowed to warm at room temperature until the water sample reached approximately 1° Celcius below the temperature at which it had been collected. At this time, data collection was commenced; the sample continued to warm during data collection such that the median temperature during data collection was approximately that at which the sample had been used in the experimental model.

Preparation of the Coaxial Waveguide Apparatus

The water sample to be tested was again cooled to approximately 5° Celcius and then allowed to flow slowly into the reservoir (Figure 2-

15b); from the reservoir the water flowed through the slot into the coaxial waveguide. The necessary instrumentation connections were made, and the apparatus was allowed to warm at room temperature. During the warming period, the waveguide was tapped lightly to encourage percolation of trapped air. The procedures described for the rectangular waveguide were followed for the coaxial waveguide in order to collect water properties data at median sample temperature equal to that at which the sample had been used in the experimental model.

Instrumentation Connections

The excitation section for each waveguide was connected through a 1-watt broadband amplifier to the output of the sweep oscillator of the network analyzer. The reference probe for each waveguide was connected through an 8-inch section of 0.141-inch OD semi-rigid coaxial cable to the reference channel of the network analyzer. The test probe was connected through an 18-inch section of flexible RG-196/U coaxial cable to the test channel of the network analyzer. Further details of the instrumentation may be seen in Figure 3-3 and are discussed in this chapter.

Data Collection

The original plan was to determine constitutive properties for each water sample from transmission coefficient data measured with each waveguide in anticipation that the results would be corroborative. This plan was modified due to shortcomings of the rectangular waveguide apparatus, an assessment of which is presented in a subsequent chapter.

Measured data obtained with the coaxial waveguide are presented in Figure 4-70 through 4-77.

SEMI-AUTOMATIC FREQUENCY DOMAIN NETWORK ANALYZER (ANWA) SYSTEM

All measurements of transmission and reflection coefficients described above were made with a semi-automatic frequency domain network analyzer (ANWA) system. Data reduction and graphical analysis were accomplished with the computer-controller of the ANWA system. The ANWA system was adapted from the system described in reference [7]. This system provides for collection and storage of reflection and transmission measurements of microwave devices during swept frequency operation. The limits of the band to be swept and the frequency interval at which measurements are to be made are programmed by the user. The system implements a program-directed calibration procedure which computes and stores corrections for source match, frequency tracking error and directivity for each frequency at which measurements are to be made. These corrections are then applied to measurements of the device under test, and the corrected measurements are stored for later analysis. Initial translation of the software listing in [7] was made by the University of Kentucky and published in reference [8]; the University of Mississippi has further adapted the system described in [7] and the University of Kentucky software to include closed-loop frequency control of the sweep oscillator and immediate graphical display of the corrected measurements.

Reflection Measurements

For the purpose of the reflection measurements required by the Series I, II and III procedures, the ANWA system is configured as shown in Figure 3-2. The program-directed calibration procedure requires that reflection coefficient be measured at each programmed frequency with a precision matched load connected to the S-parameter test set in place of the device under test. This procedure is then repeated with a high quality short connected, and repeated again with a compensated open connected (manufacturer's compensation data for the capacitance of the open is entered into the error model by the user). These three sequences of measurements are then entered into an error model, as described in reference [7], and used to generate corrections for any subsequent reflection measurements. This calibration procedure effectively establishes a reference plane at the input port to the device under test and includes all errors associated with the S-parameter test set and the external cables and connectors in the error model. In all cases, the reference plane was established at the driving point connector.

Attenuation and Phase Shift Measurements

For the purpose of the attenuation and phase shift measurements required in the water properties measurement procedures, the ANWA system was configured as shown in Figure 3-3. In most applications of the ANWA, the device under test is excited through one port of the S-parameter test set, and the reference and test channels are selected from the directional couplers within the S-parameter test set. In this application, the reference signal had to be taken from the fixed probe and

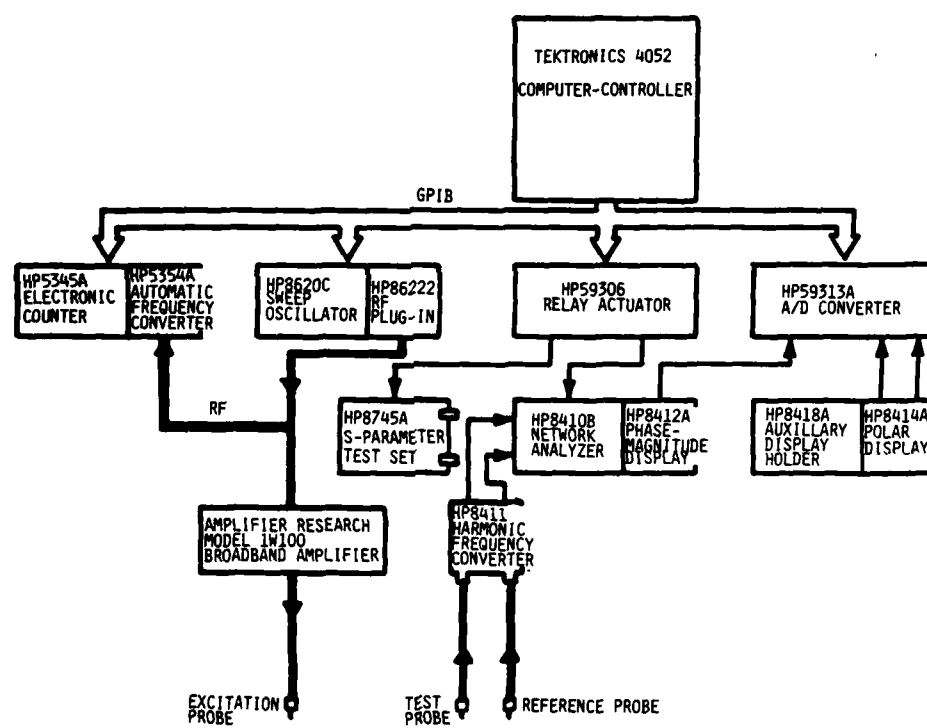


FIGURE 3-3
ANWA Configuration for Water Properties Measurements

the test signal from the movable probe, both of which were excited by transmitted energy within the waveguide. It was necessary, therefore, to bypass the radio frequency section of the S-parameter test set and connect the harmonic frequency converter (HFC) directly to the probes. The S-parameter test set connections to the ANWA were maintained in order to satisfy GPIB protocol. The program-directed calibration procedure for transmission measurements requires that transmission coefficient be measured at each programmed frequency with a "thru" connection installed between the ports of the S-parameter test set; this "thru" connection is normally a short circuit, unless there is some reason to refer the transmission coefficient to a level other than 0 db. These calibration measurements are entered into the error model and used to generate error corrections for subsequent transmission measurements. When the "thru" connection is replaced with the device under test, errors associated with the S-parameter test set and the external cables and connectors are included in the error model. In this application, the usual calibration procedure could not be followed since the S-parameter test set was not in use; therefore, to obtain error corrections, the "thru" was established, and calibration procedures conducted, with the test probe positioned as near as possible to the reference probe. All subsequent transmission measurements were referred to the attenuation and phase delay realized between reference and test probes rather than to 0 db; however, since all attenuation and phase delay measurements were used in ratios during data reduction (see Appendix A), this does not effect the results of the procedure.

Chapter 4

ANALYSIS AND SUMMARY OF RESULTS

This chapter is organized so that the three principal experimental configurations and the water properties measurements are each discussed separately. A compendium of the results for all experiments is included. The stated purpose of substantiating numerical codes is carried out in this chapter for the Configuration I and III experiments. No accurate numerical model was available for the Configuration II experiments, so the results of these experiments are presented and an attempt is made to demonstrate the plausibility of the results.

CONFIGURATION I EXPERIMENTS

In the Configuration I experiments a sleeve monopole antenna was operated with its driving point connector immersed in water and its source gap in air above the water (Figure 1-1) to simulate a ground stake antenna. Antenna aperture admittance was derived from driving point reflection coefficient measurements made at 0.01 GHz intervals over the 0.5 - 1.0 GHz octave for thirty-seven geometric variations of the configuration. Five additional experiments were conducted as part of a preliminary testing procedure. The antenna aperture admittances for all forty-two experiments are presented in Figures 4-19 to 4-60.

Preliminary Testing and Analysis

In order to verify proper operation of the sleeve monopole antennas and to validate data collection and data reduction schemes, preliminary experiments were conducted with the antenna operating above a 6-m by 8-m ground plane. The current distribution, and hence source gap admittance, was obtained by moment method analysis and compared to the experimentally determined values of source gap admittance.

Moment Method Analysis. When image theory is applied to the monopole perpendicular to a ground plane, and the current is assumed to exist only in an axially-directed sheet on the surface of the structure, then the magnetic vector potential may be expressed as

$$A_z = \frac{\mu}{4\pi} \int_{-h}^h I_z(z') K(z-z') dz' , \quad (1)$$

where z is the axial direction, $I_z(z')$ represents the surface current and h is the height of the antenna above the ground plane. The kernel of the integrand is

$$K(z-z') = \frac{1}{2\pi} \int_{-\pi}^{\pi} \frac{e^{-jkR}}{R} d\phi' . \quad (2)$$

where $R = [(z-z')^2 + 4a^2 \sin^2(\phi'/2)]^{1/2}$, ϕ' is the azimuth angle in cylindrical coordinates and a is the radius of the antenna wire. From Maxwell's equations and the definition of magnetic vector potential,

$$j \frac{\eta}{4\pi k} \left[\frac{d^2}{dz^2} + k^2 \right] \int_{-h}^h I_z(z') K(z-z') dz' = -E_z(z) , \quad (3)$$

where η is the intrinsic impedance and k is the wavenumber of the medium above the ground plane. Equation (3) is recognized as a Pocklington-type integral equation.

A moment method code incorporating pulse expansion and triangle testing was developed to solve (3). Construction of the impedance matrix was adapted from [9]. Gap admittances computed with this code are identical to those reported in [10] which were obtained by a moment method solution to Hallen's integral equation, and substantiated by experiment, for a sleeve monopole antenna. This same code was used for preliminary analysis and for substantiation of results in several phases of this project. Because the code is a straightforward application of the moment method for solving integral equations, a listing of the code is not included in this report.

Comparison of Numerical and Experimental Results. When the source gap of the sleeve monopole antenna is located near the ground plane, the equivalent (imaged) structure is approximately a thin-wire, center-fed, 50-cm dipole in free space. Within the 0.5 - 1.0 GHz octave, this equivalent structure is resonant at 0.9 GHz ($3\lambda/2$ current distribution). From thin-wire theory [11], the radiation resistance for a $3\lambda/2$ center-fed dipole is approximately 105.5 ohms. The radiation resistance of the actual monopole (with zero gap height) is one-half of the radiation resistance of the free-space dipole, or 52.7 ohms, which gives a normalized (to 50 ohms) admittance of 0.95 Si. Numerical and experimental results for the 0.250-inch OD antenna with the height of the source gap (g) equal to 1.77 cm above the ground plane are shown in Figure 4-1. The equivalent structure in this case is slightly longer than the

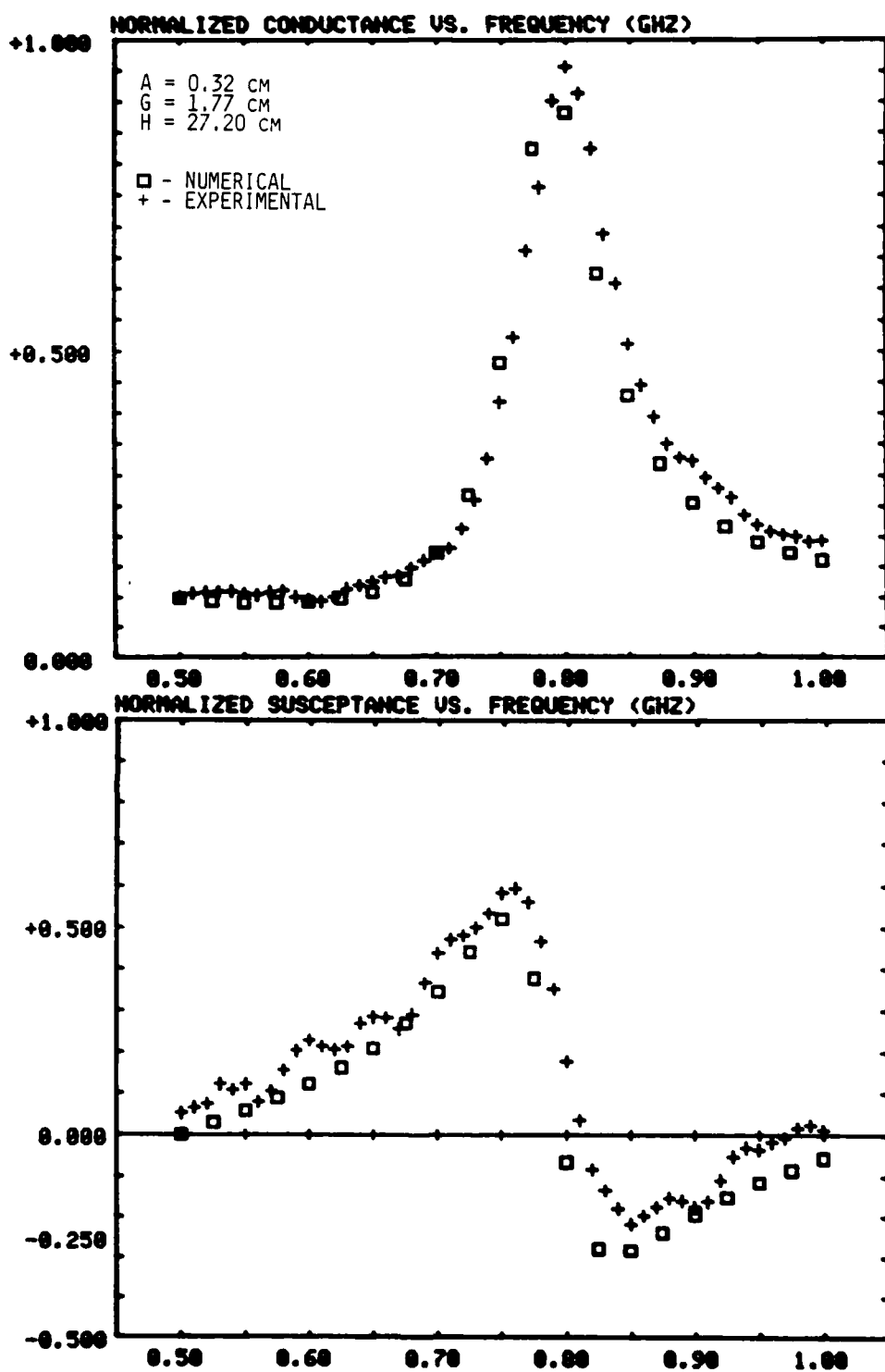


FIGURE 4-1

Aperture Admittance for Sleeve Monopole
Antenna Above Ground Plane

equivalent structure when $g = 0$; hence, the resonance occurs below 0.9 GHz. Further, the gap is not at the center of the equivalent structure, so radiation resistance is increased, which accounts for a peak conductance somewhat lower than 0.95 Si. The agreement between numerical and experimental results is excellent for this case, and the results are also quite plausible when the structure is approximated as a thin-wire dipole.

When g is changed to 8.22 cm, the agreement between numerical and experimental results is not as good (Figure 4-2). In this case, the gap is located near a current null at the resonant frequency (0.65 GHz). The small current at the gap indicates that conductance is correspondingly small and reflection coefficient at the driving point is low. Changing g to 23.22 cm places the gap closer to a peak of current at resonant frequency (0.75 Ghz). At this position, gap conductance is greater, and the agreement between numerical and experimental results is again quite good (Figure 4-3). Two additional cases were investigated ($g = 13.87$ cm and $g = 43.47$ cm) and agreement between experimental and numerical data was good in both cases. The measured admittances for these two cases are given in Figures 4-21 and 4-23. The agreement between measured and calculated data for this relatively simple experimental model lends credence to the measurement techniques and procedures. The fluctuations noted in the experimental data were traced to the used of a mismatched coaxial feed line between the ANWA and the antenna driving point connector. This cable was not used in subsequent experiments.

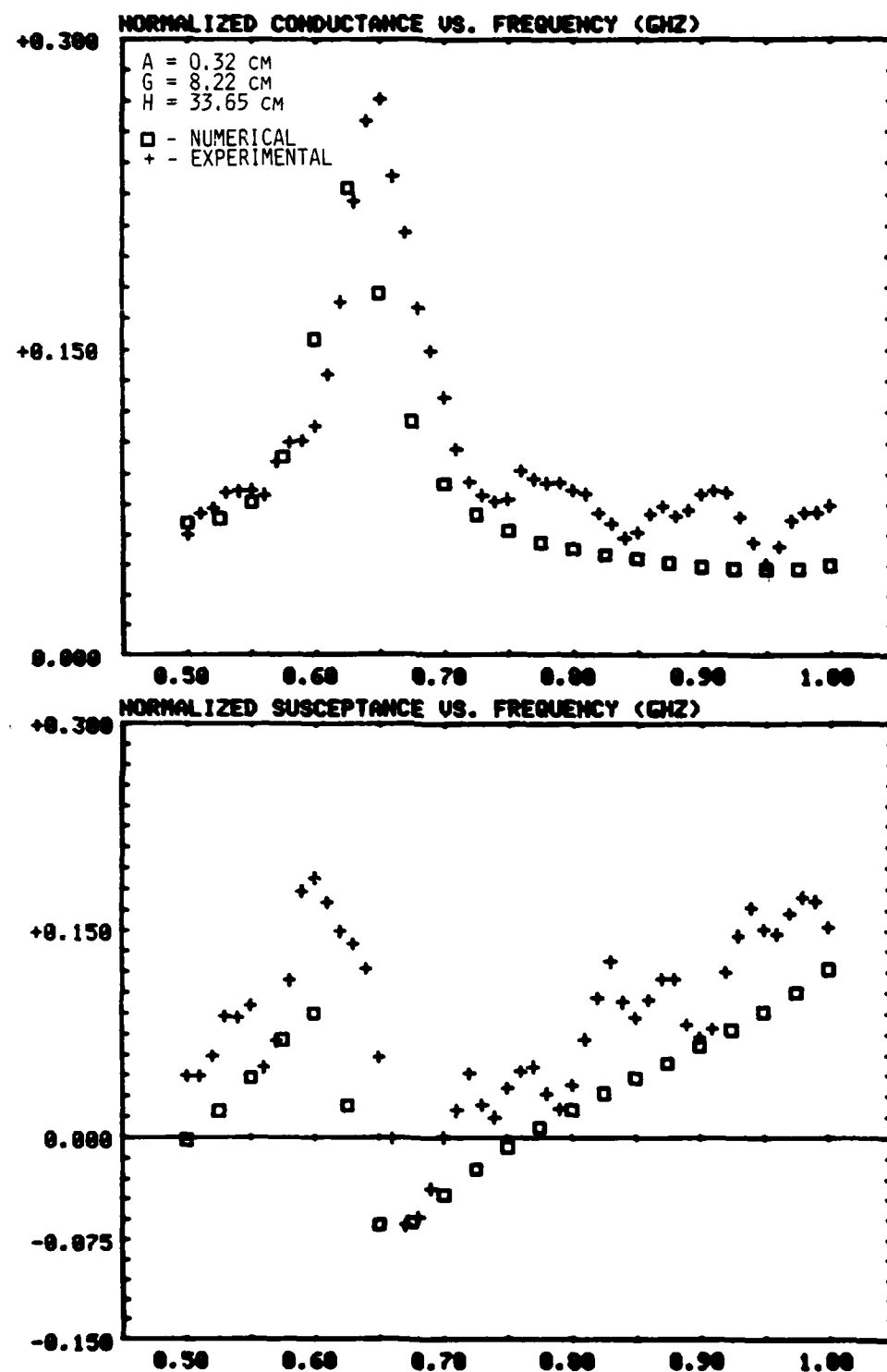


FIGURE 4-2

Aperture Admittance of Sleeve Monopole
Antenna Above Ground Plane

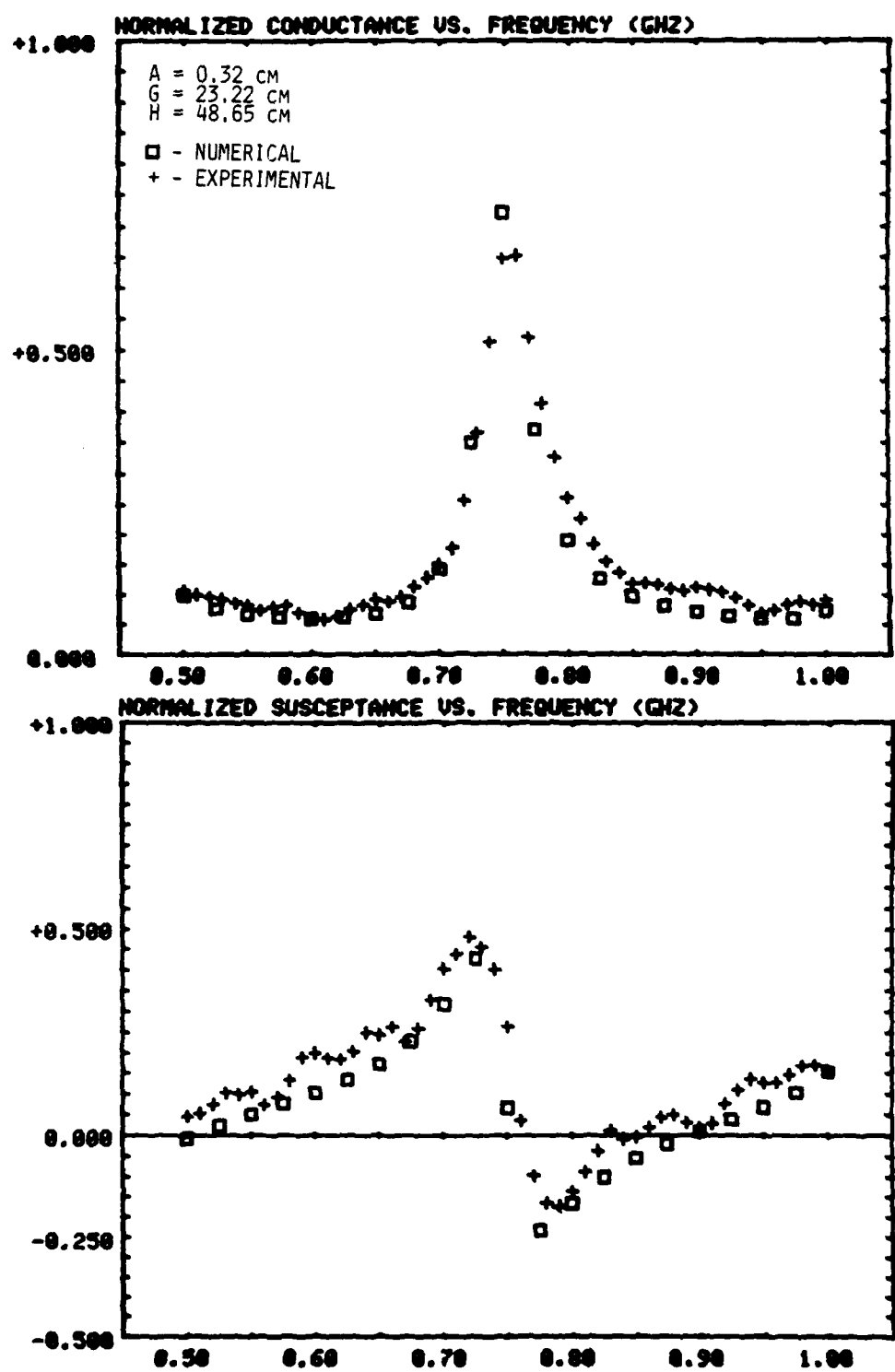


FIGURE 4-3

Aperture Admittance of Sleeve Monopole
Antenna Above Ground Plane

Summary of Results

Numerical Analysis. A numerical code for analysis of a right-circular cylinder residing in contiguous half spaces of different electromagnetic constitutive properties was developed by other investigators [12] as a related part of this project. Briefly, integral equations incorporating the exact kernel and the so-called Sommerfeld integrals were formulated to describe current distribution on the cylinder. The code was used to solve these integral equations for current distributions. The code was executed for several frequencies for each of several geometric variations of the Configurations I experiments. The long execution time (approximately 2 hours per data point) for this code precluded its execution for more than a limited number of cases.

Comparison of Numerical and Experimental Results. There is excellent agreement between the numerical and experimental results for the cases where the source gap is near the water surface (Figures 4-4 and 4-5). Figure 4-4 refers to an experiment in which $g = 1.455$ cm and the water is ordinary tap water; Figure 4-5 refers to an experiment in which $g = 1.505$ cm and the water is a saline solution (9.09 g NaCl per 1 kg H₂O). The numerical code could not accomodate this small gap height, so during execution of the code, g was set to zero for both cases. There is a less agreement between numerical and experimental results for cases in which the gap is near a current null at resonant frequency (Figure 4-6 and 4-7). This is consistent with the results noted during preliminary testing and discussed above in this chapter. Figure 4-5 refers to the case in which $g = 7.905$ cm above tap water, and Figure 4-6 refers to the

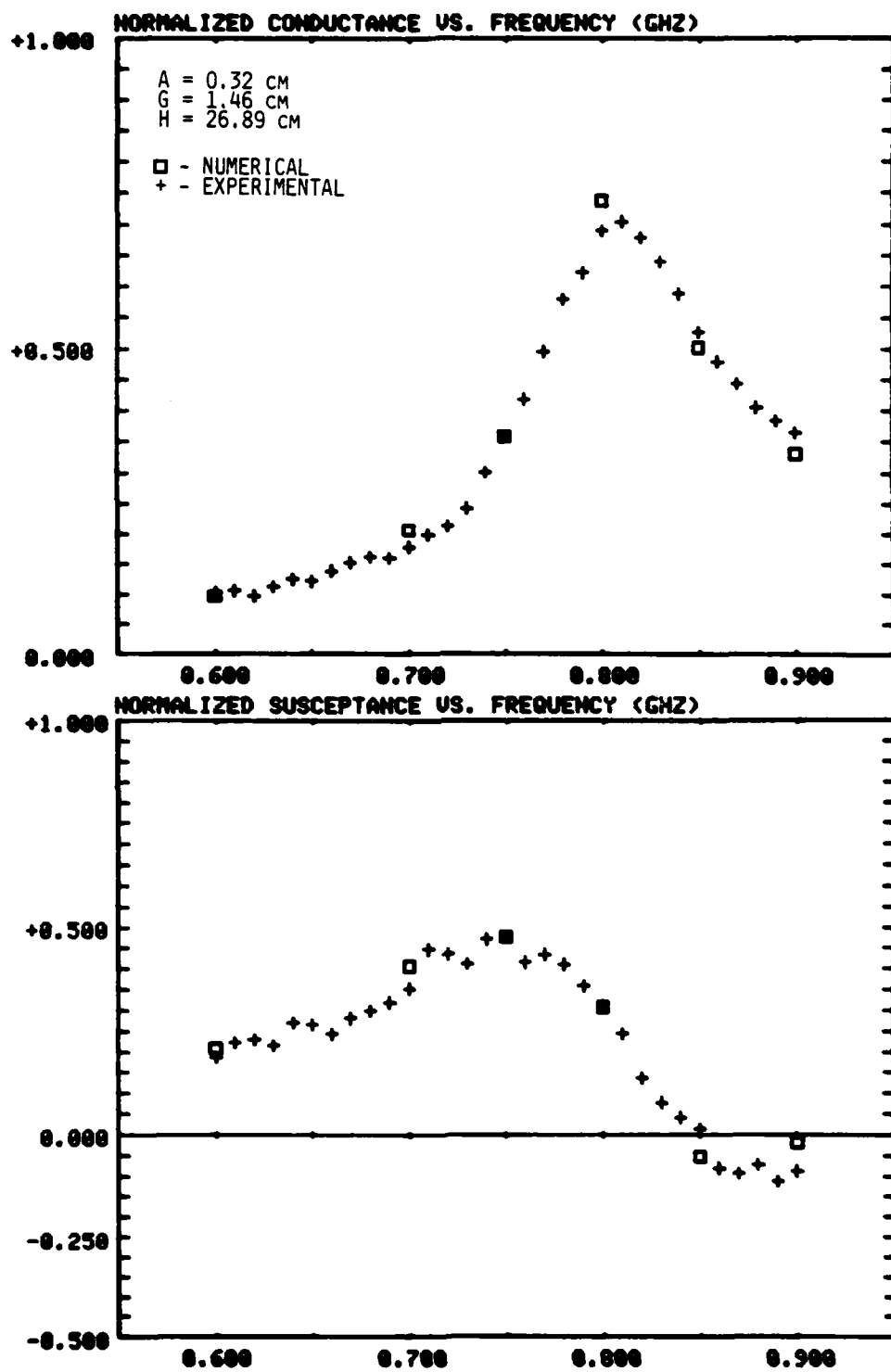


FIGURE 4-4

Aperture Admittance of Sleeve Monopole
Antenna Above Tap Water ($T = 17.4^\circ\text{C}$)

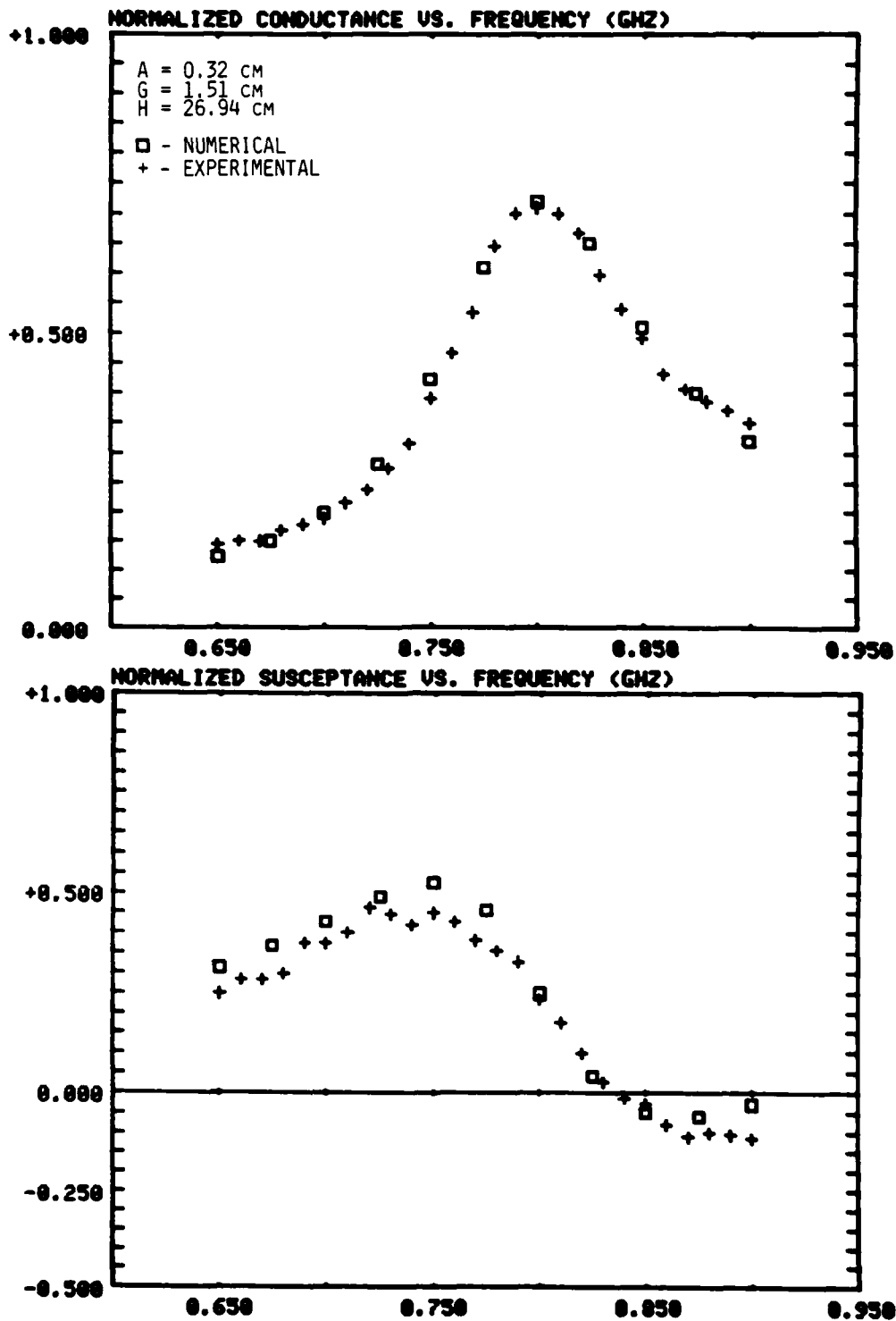


FIGURE 4-5

Aperture Admittance of Sleeve Monopole
Antenna Above Salt Water ($T = 15.7^\circ\text{C}$; $S = 9.08 \text{ g/kg}$)

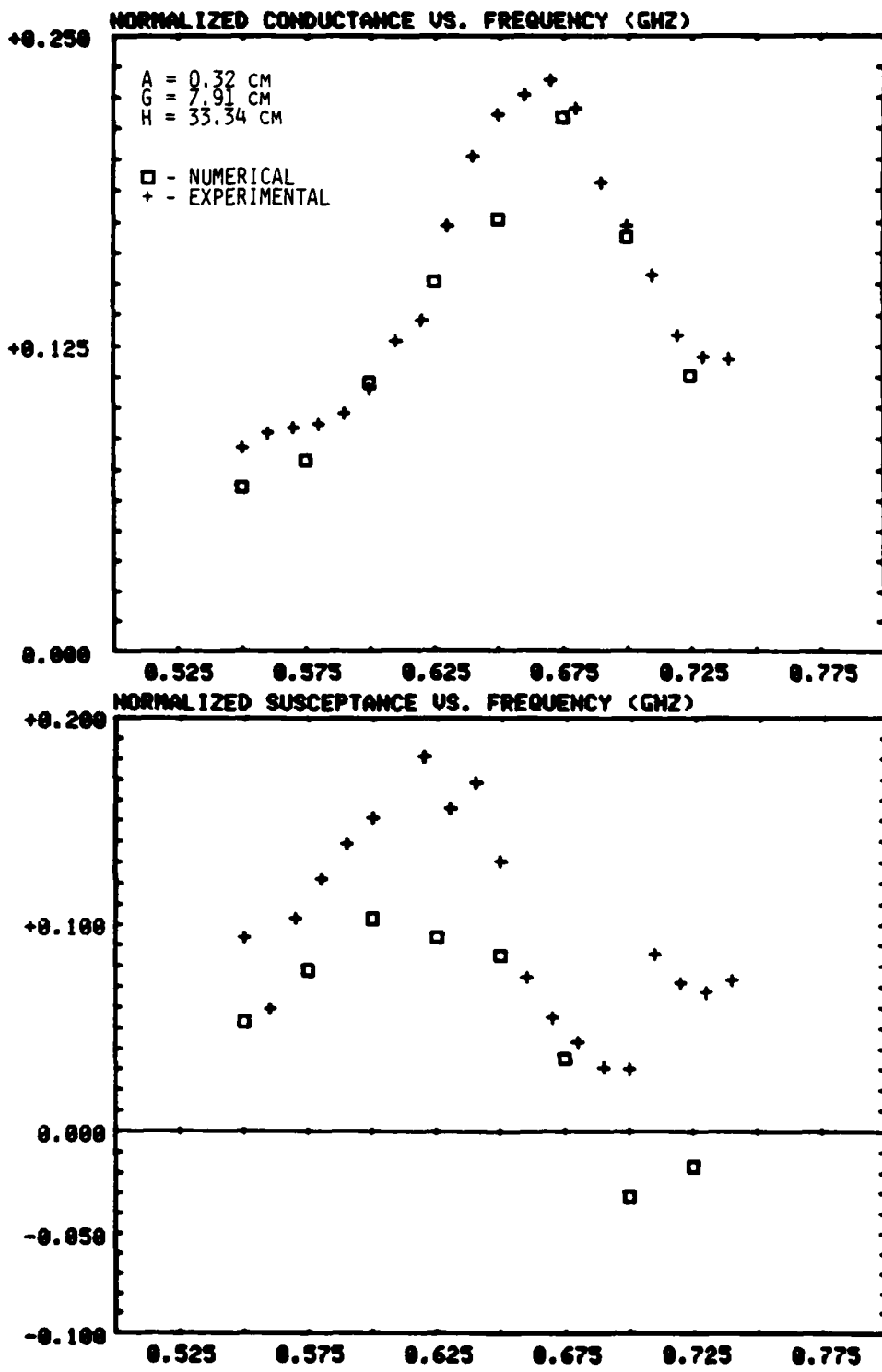


FIGURE 4-6

Aperture Admittance of Sleeve Monopole
Antenna Above Tap Water ($T = 17.4^\circ\text{C}$)

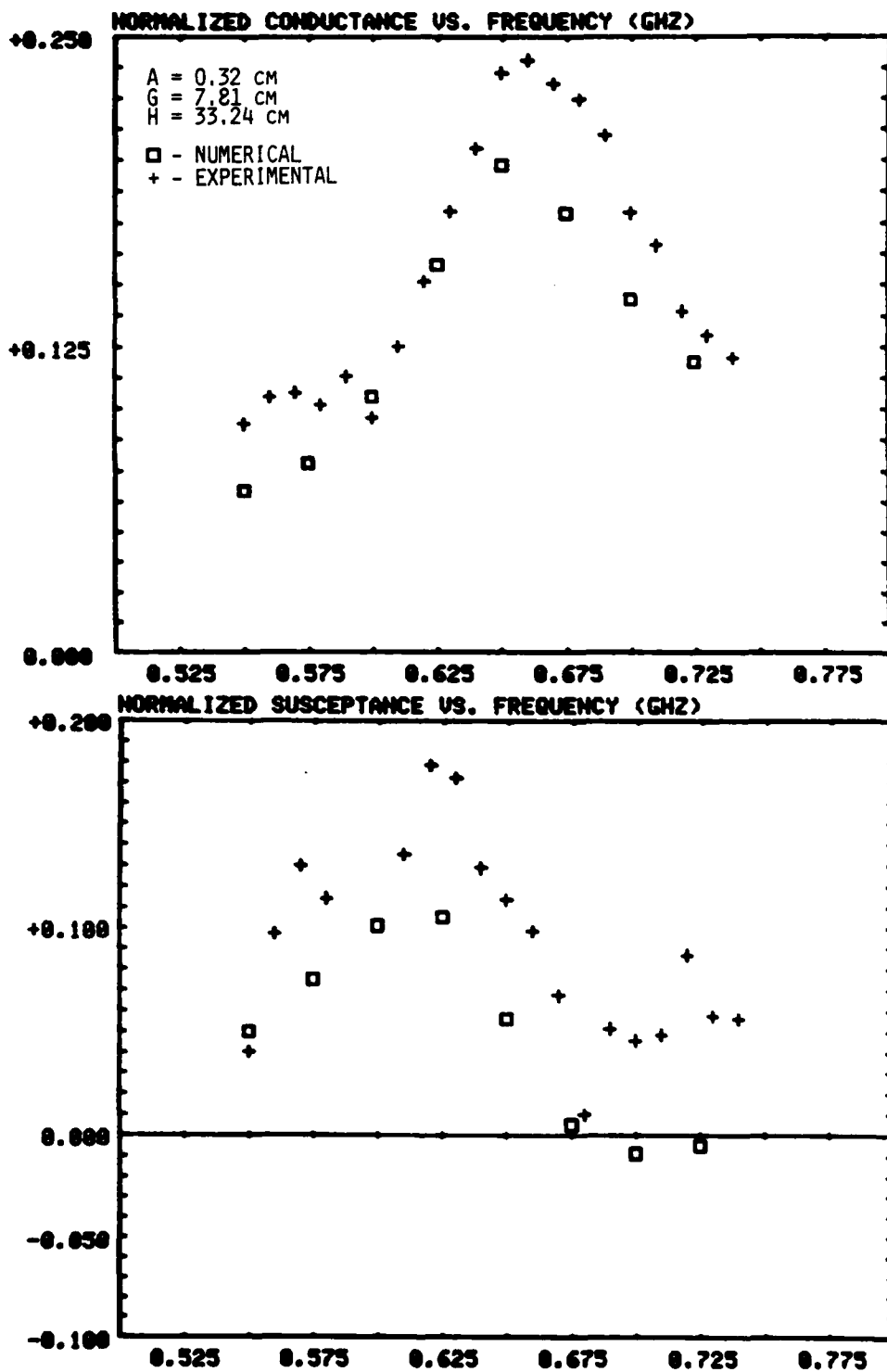


FIGURE 4-7

Aperture Admittance of Sleeve Monopole Antenna
Antenna Above Salt Water ($T = 15.7^\circ\text{C}$; $S = 9.08 \text{ g NaCl per kg H}_2\text{O}$)

case in which $g = 7.805$ cm above salt water. The conductance determined numerically indicates that there should be significant difference in the conductance at resonance and in the frequency of resonance for the two cases. The experimental results do not substantiate this, since the conductance response of the antennas was virtually the same in both experiments. Further, the susceptance determined numerically appears to be displaced consistently in a negative direction from the susceptance determined experimentally. This displacement can also be noted in the preliminary testing (Figure 4-2) for a similar geometry.

Effect of Cylinder Radius. The admittance of all three antennas is depicted in Figure 4-8. Geometry, except for the antenna radius, is essentially the same in all three cases, and the source gap is close to the water surface. As expected, the response is nearly the same for all antennas. Conductance is highest for the 0.250 inch OD antenna because radiation resistance increases with cylinder diameter [13]. Similar results were obtained for two of the antennas when the source gap is much farther from the water surface (Figure 4-9).

Effect of Conductivity of the Lossy Medium. Numerical analysis of the ground stake antenna indicated that the conductivity of the lossy half space and the length of the sleeve immersed in the lossy medium has little effect on the current distribution along that portion of the structure which resides in air above the lossy medium. Despite the numerical analysis, there was concern that the presence of the metallic antenna feed system and the discontinuity that exists between the water and the materials at the tank bottom would influence performance of that

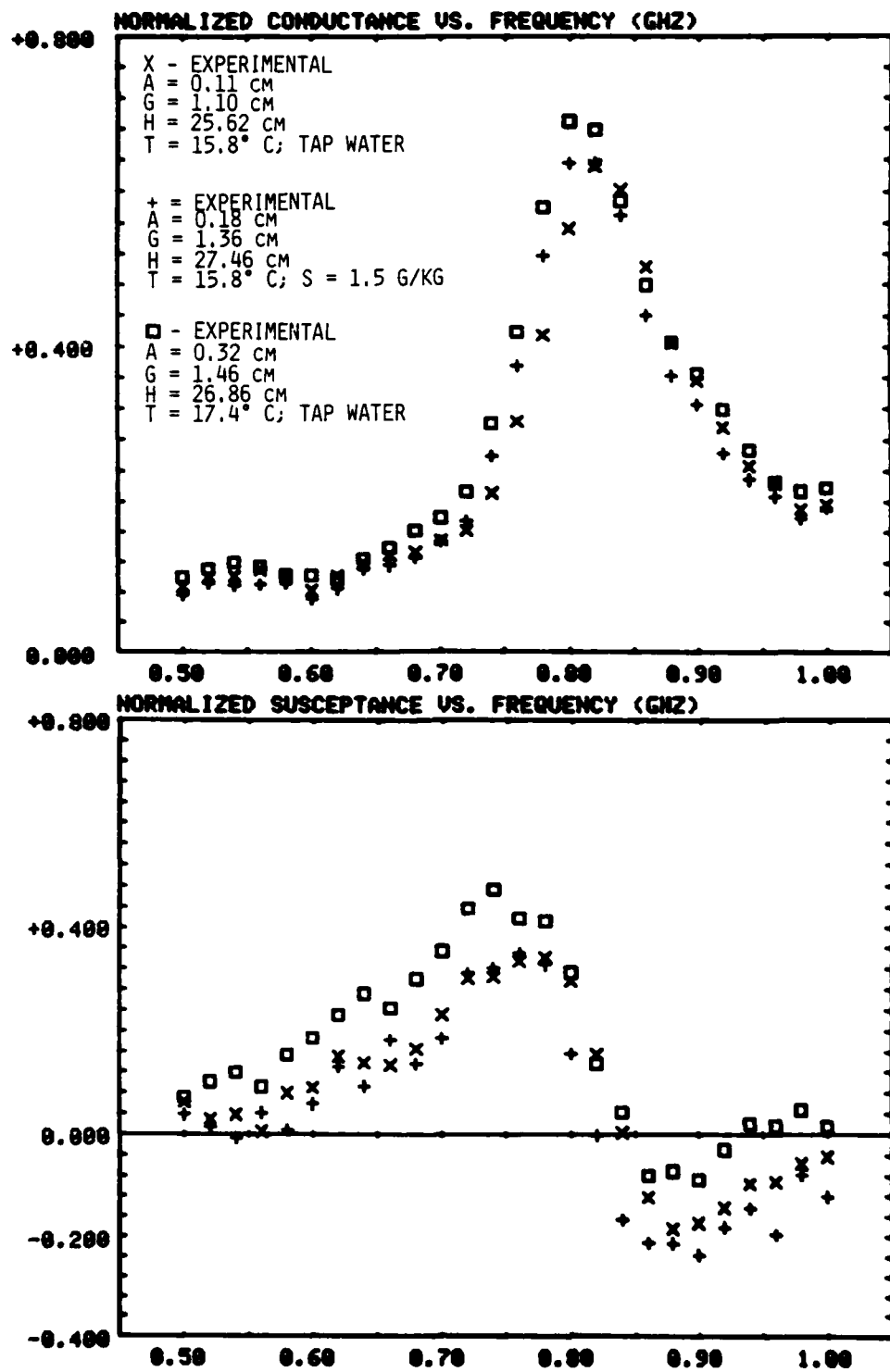


FIGURE 4-8

Aperture Admittance of Sleeve Monopole
Antennas Above Water

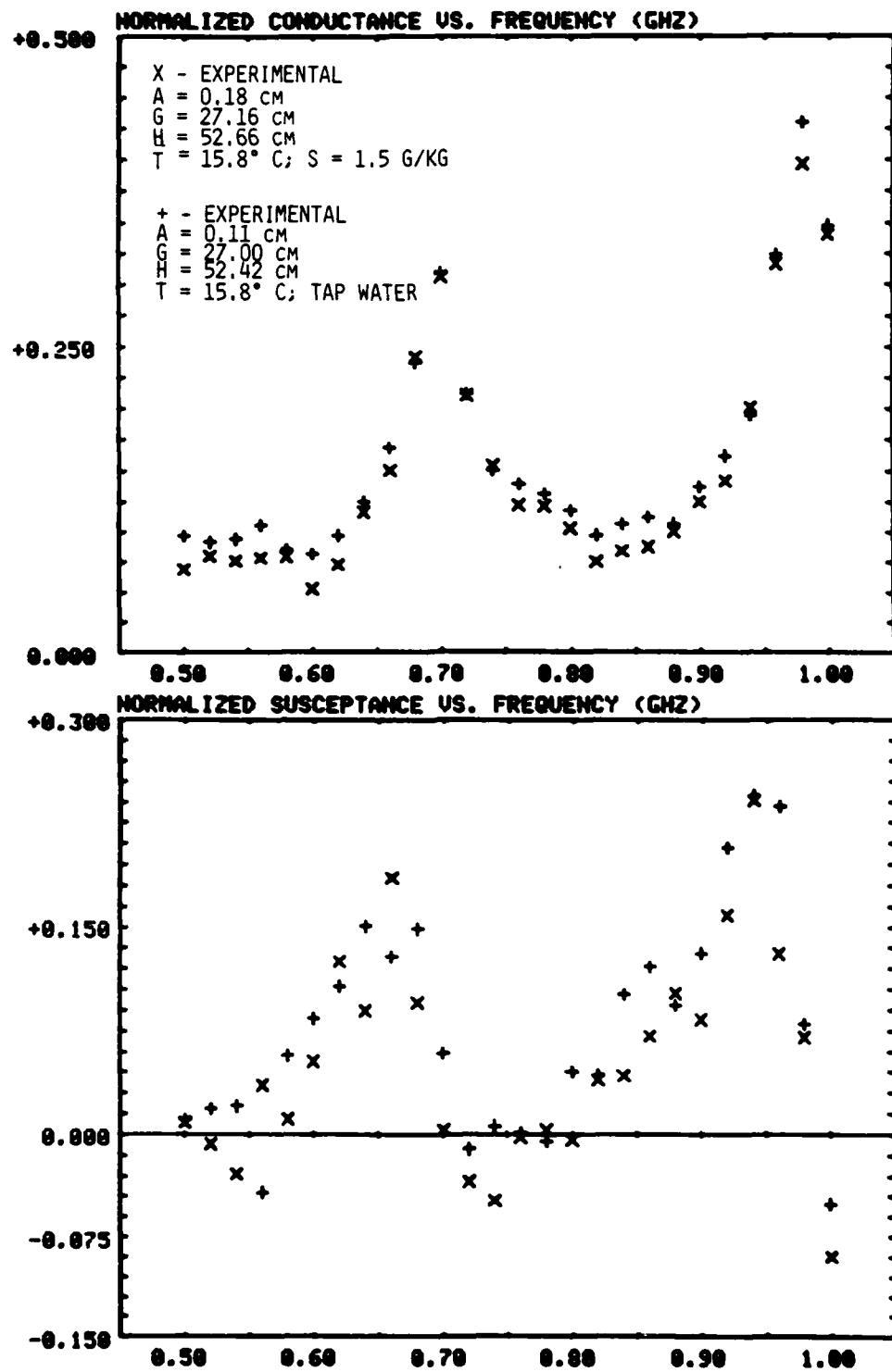


FIGURE 4-9

Aperture Admittance of Sleeve Monopole
Antennas Above Water

portion of the antenna in air above the water, particularly when tap water with relatively low losses was used. The results shown in Figures 4-10 and 4-11 indicate that the conductivity of the water has little effect on antenna aperture admittance. The measured constitutive properties of the water used in these three experiments can be found in Figures 4-73, 4-74, and 4-75. Briefly, conductivity varied by one order of magnitude and permittivity varied by 5% for the three cases depicted in Figures 4-10 and 4-11. These results lead to the conclusion that tap water is acceptable for simulating a lossy half space when evaluating the performance of that portion of the conducting structure which is in air above the water even though attenuation of energy by the water is relatively low. In this case, the depth of the water is slightly more than 1 m and the conductivity of the tap water is approximately 0.2 S/m, which leads to an attenuation of only 20% through the distance from surface to bottom in the tank of tap water. Apparently the discontinuity in constitutive properties between air and water is sufficiently large that coupling between the above-water portion of the antenna and below-surface objects or discontinuities is effectively marked.

CONFIGURATION II EXPERIMENTS

In the Configuration II experiments, a conducting structure above a lossy half space was simulated by a coax-fed wire antenna mounted against a ground plane so that the antenna was above and parallel to the water surface (Figure 1-2). In a variation of the experiment, the wire was bent downward and partially immersed in the water. Antenna aperture

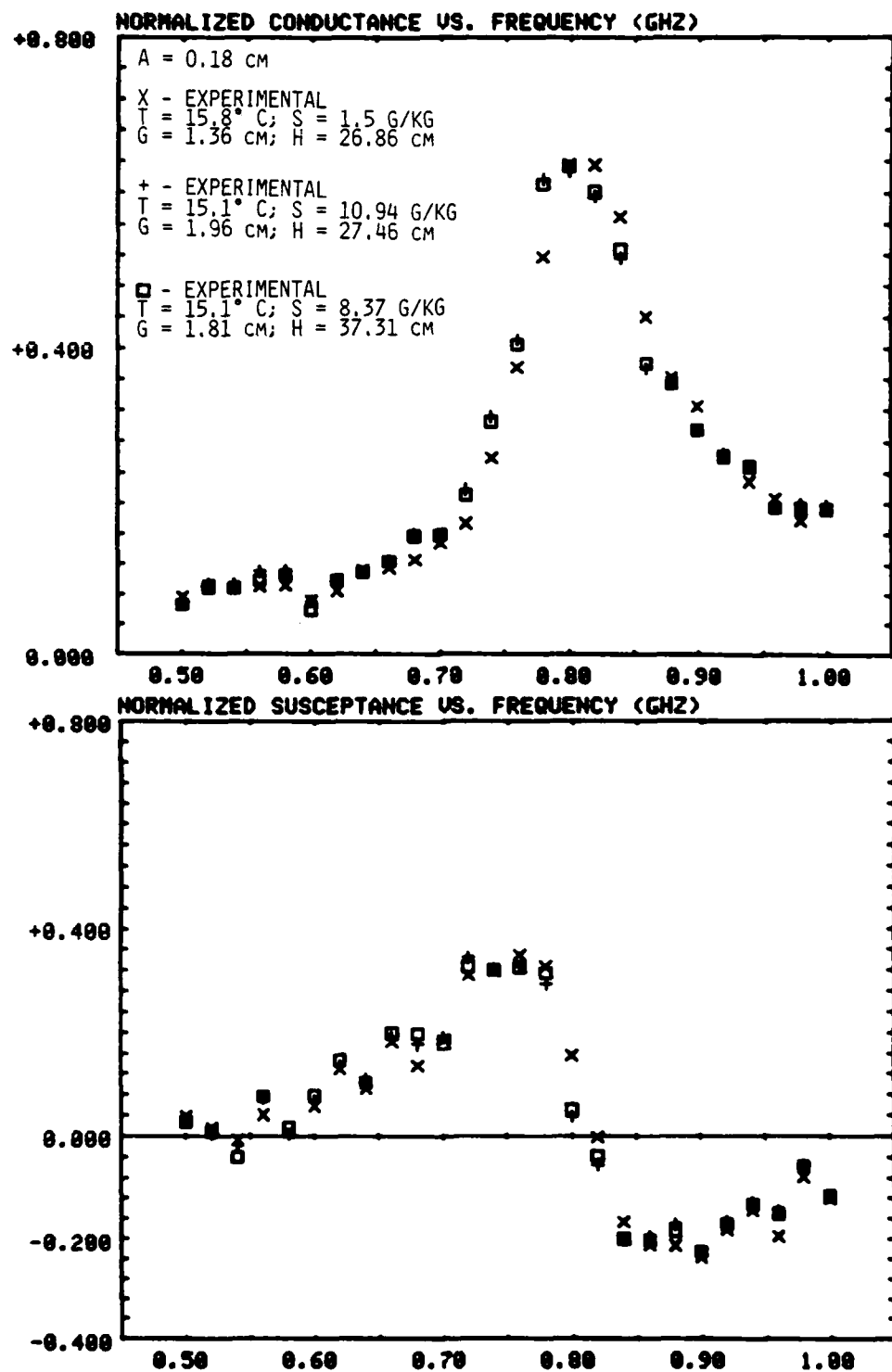


FIGURE 4-10

Aperture Admittance of Sleeve Monopole
 Antenna Above Water

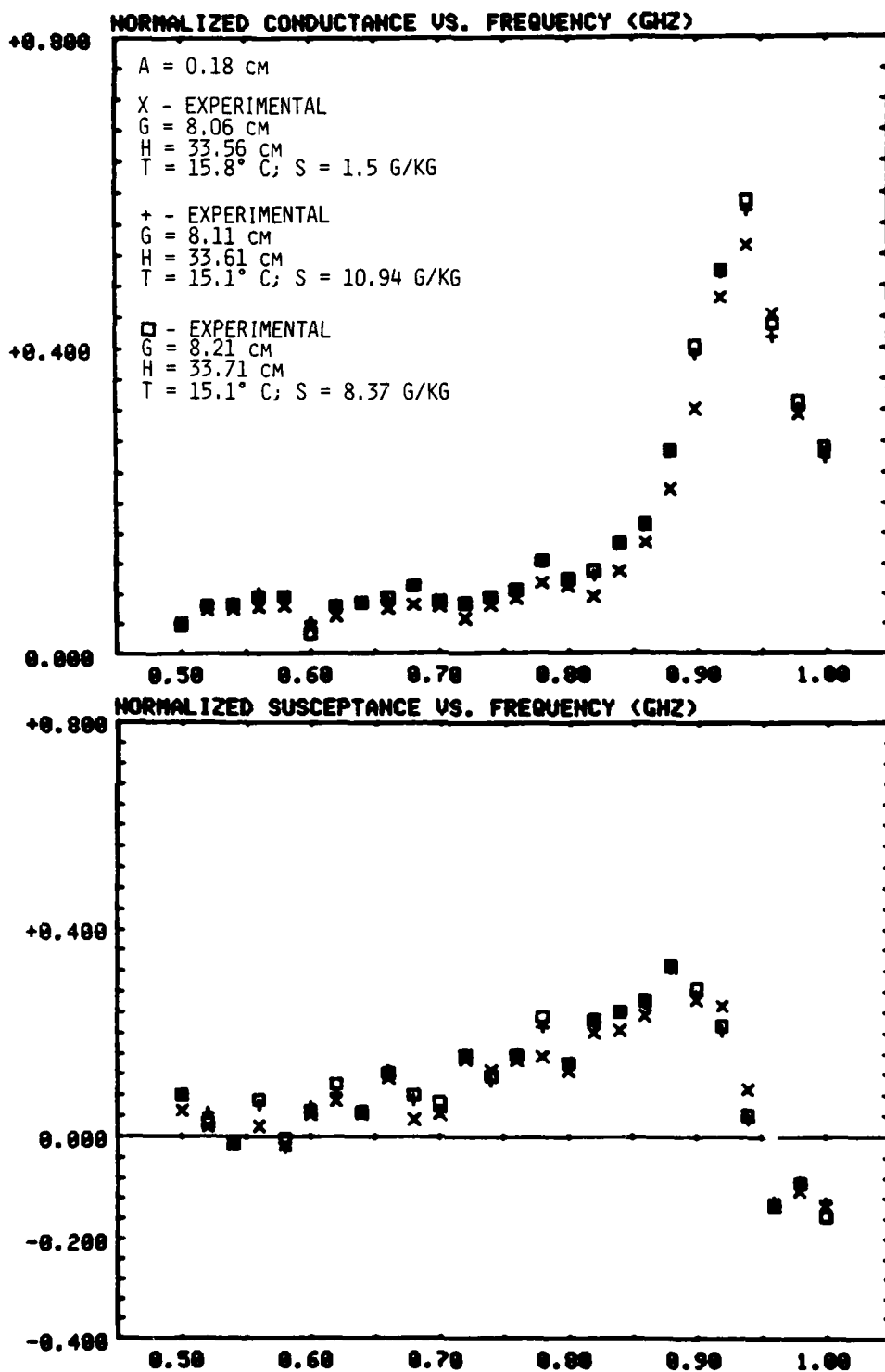


FIGURE 4-11

Aperture Admittance of Sleeve Monopole
Antenna Above Water

admittance was derived from driving point reflection coefficient measurements made at 0.01 GHz intervals over the 0.5 to 1.0 GHz octave for four geometric variations of the straight-wire antenna experiment and over the 0.5 to 1.1 GHz band for four geometric variations of the bent-wire antenna experiment. The antenna aperture admittances for all eight experiments are presented in Figures 4-61 to 4-68.

The intent of the Configuration II experiments was somewhat different from that of the Configuration I and III experiments in that substantiation of a particular numerical analysis code was not the goal. The results of the experiment are presented here as an impetus for further experimentation. Elementary numerical analyses of the structures used in the experiments were conducted to demonstrate plausibility of the results. In these elementary numerical models, the presence of the lossy half space was ignored.

Comparison of Numerical and Experimental Results for the Straight-Wire Monopole

The numerical code described earlier in this chapter for solution of the Pocklington integral equation was used to determine antenna aperture admittance for the monopole antenna operating above a ground plane. The presence of the water, the surface of which was parallel to the monopole in the experiment, was not considered in the analysis. The numerical data merely serve to confirm that measured data are plausible. The results shown in Figures 4-12 and 4-13 demonstrate that the presence of the water does not appreciably affect the admittance response of the antenna aperture. When the antenna is 0.07λ (referred to resonance frequency) above the water surface (Figure 4-12), experimental con-

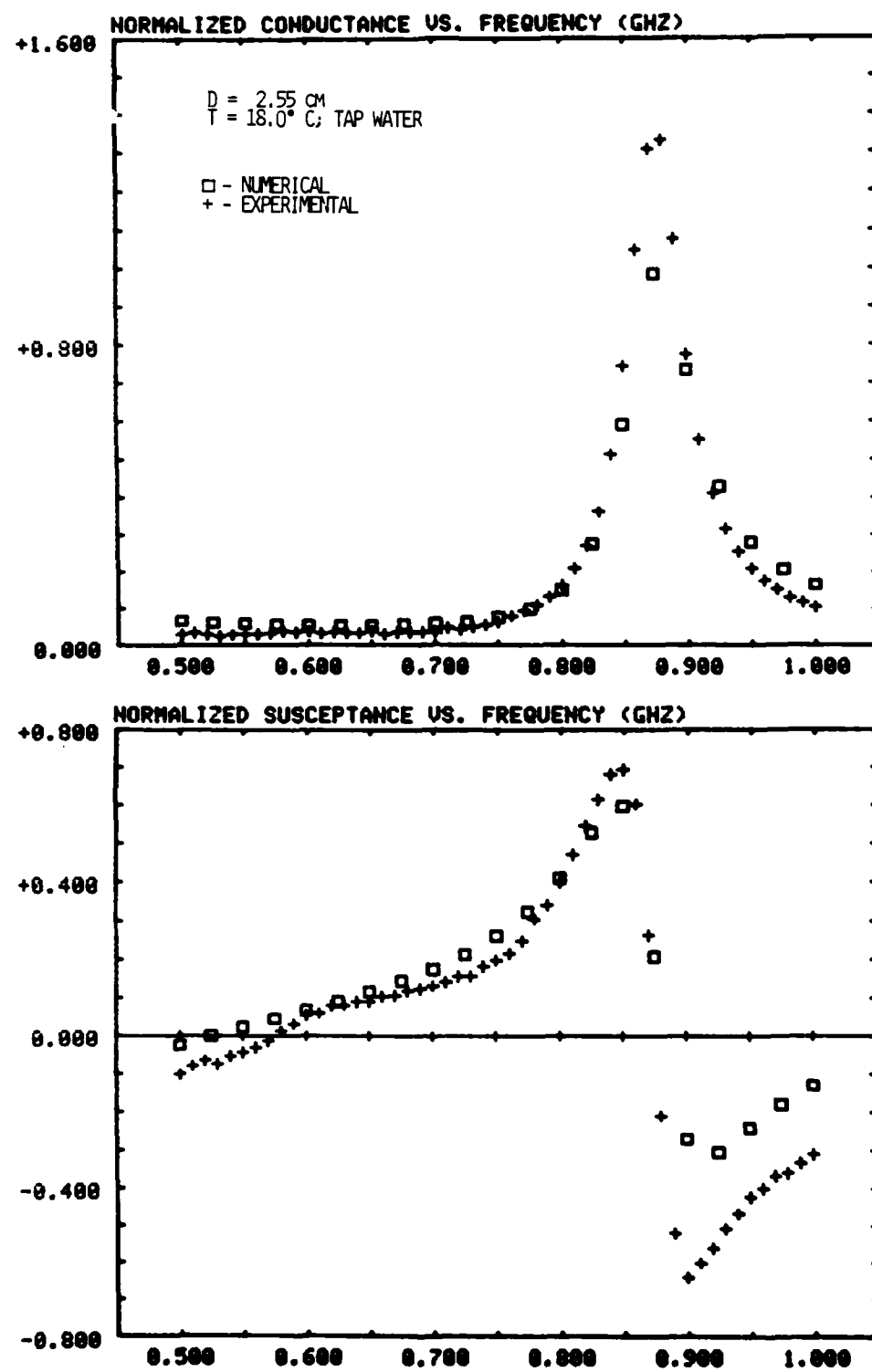


FIGURE 4-12

Aperture Admittance of Coax-Fed Monopole Antenna (Straight-Wire)
Above Ground Plane and Parallel to Water Surface

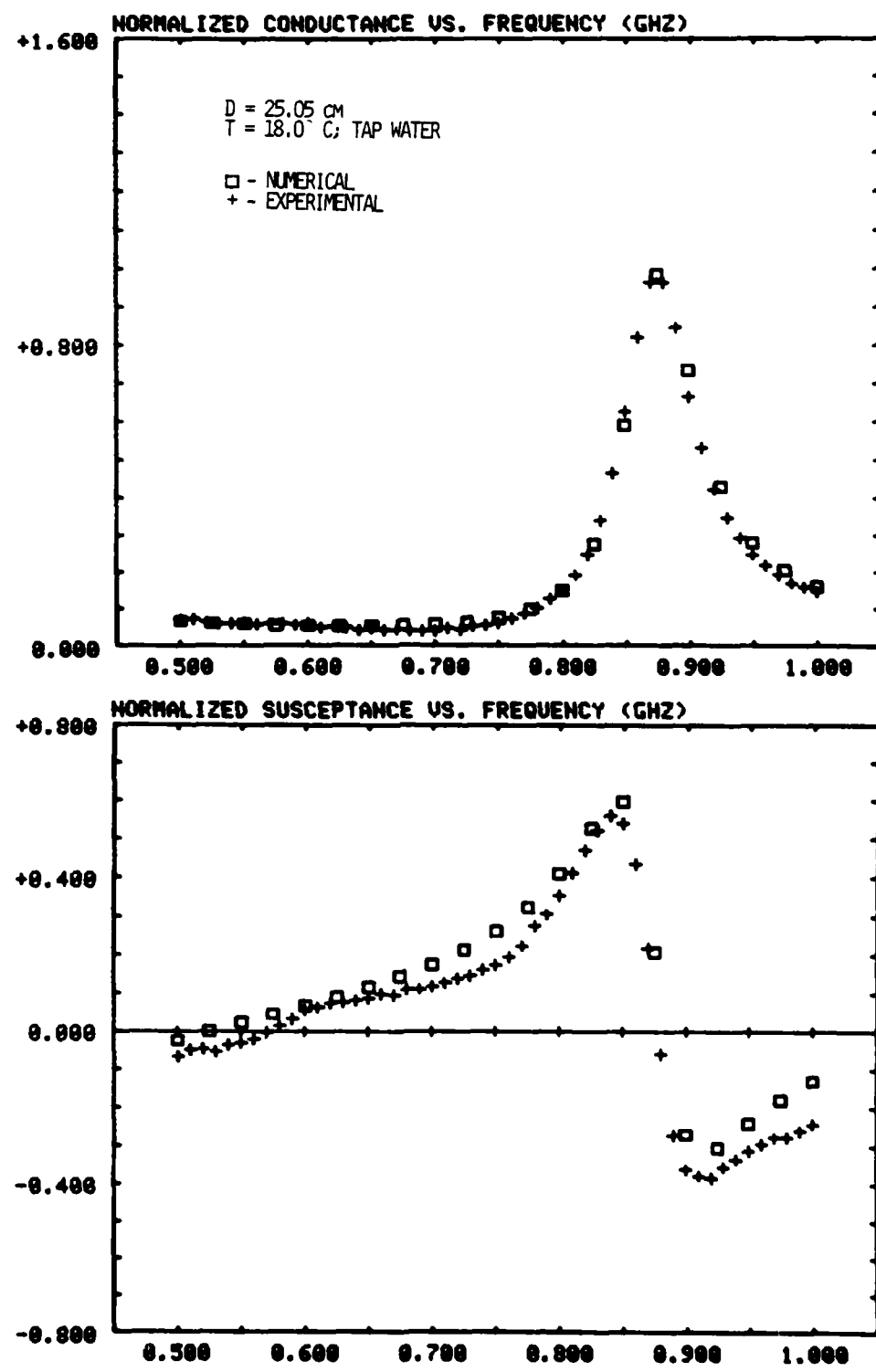


FIGURE 4-13

Aperture Admittance of Coax-Fed Monopole Antenna (Straight-Wire)
Above Ground Plane and Parallel to Water Surface

ductance has a peak values about 20% greater than computed for the free-space monopole. The difference in the conductance at resonance indicates that the nearby water has altered the radiation characteristics of the antenna. The experimental susceptance near resonant frequency, which is essentially symmetric about zero, differs significantly from the numerical susceptance. The symmetric behavior is characteristic of the normalized input admittance of an open-circuit, two-wire transmission line ($Y/Y_0 = -j \tan kl$). This result is plausible since, when the water surface is treated as a reflector, the antenna and its image do indeed appear as a two-wire transmission line. When the antenna is moved to 0.73λ (Figure 4-13) above the water surface, there is essentially no difference between experimental results and numerical results for the case in which the water is not present.

Comparison of Numerical and Experimental Results for the Bent-Wire Monopole

A numerical code called MININEC [14], designed for analysis of wire antennas with a personal computer, was used to determine aperture admittance for the bent-wire antenna operating above a ground plane. Again, the presence of the water was ignored in the analysis. MININEC results compare favorably with experimental results (Figure 4-14) for the case in which the open end of the monopole was visibly clear of the water. Clearly, the presence of the water has little effect on antenna aperture admittance. The results presented in this and in the foregoing paragraph should be interpreted only as a demonstration that the performance of the antennas was satisfactory and that measurement techniques were valid. No attempt was made to compare experimental results with a

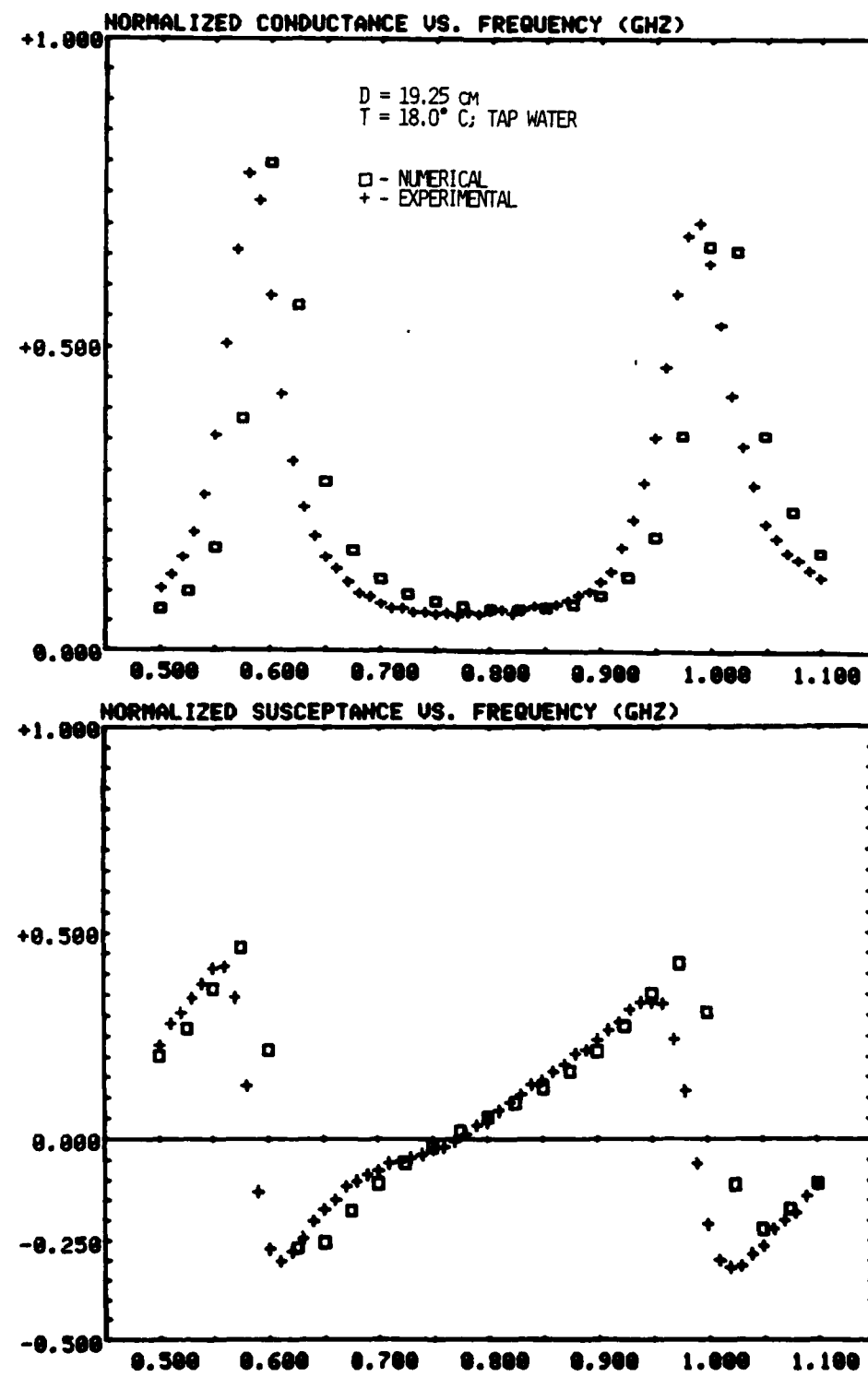


FIGURE 4-14

Aperture Admittance of Coax-Fed Monopole Antenna (Bent-Wire)
Above Ground Plane and Parallel to Water Surface

rigorous analysis. Further, no attempt has been made to validate the results obtained in the case of the bent-wire antenna when the open end was immersed in water.

CONFIGURATION III EXPERIMENT

In the Configuration III experiment, a conducting structure completely immersed in the lossy half space was simulated by a coax-fed monopole perpendicular to a ground plane which was in contact with the water surface (Figure 1-3). Antenna aperture admittance was derived from driving point reflection coefficient measurements made at 0.1 GHz intervals over the 0.25 - 0.75 GHz band. The antenna aperture admittances are presented in Figure 4-69.

Numerical Analysis

A numerical code for analysis of a coax-fed monopole was developed by other investigators [15] as a related part of this project. Briefly, this code evaluates the coupled integral equations for current distribution on the monopole antenna which result when the monopole (protruding center conductor of the coax) is viewed as a scatterer illuminated by the fields radiated from the annular aperture in the ground plane between center and outer conductors of the coaxial cable.

Comparison of Experimental and Numerical Results

There is good agreement between the experimentally and numerically determined values for antenna aperture admittance (Figure 4-15).

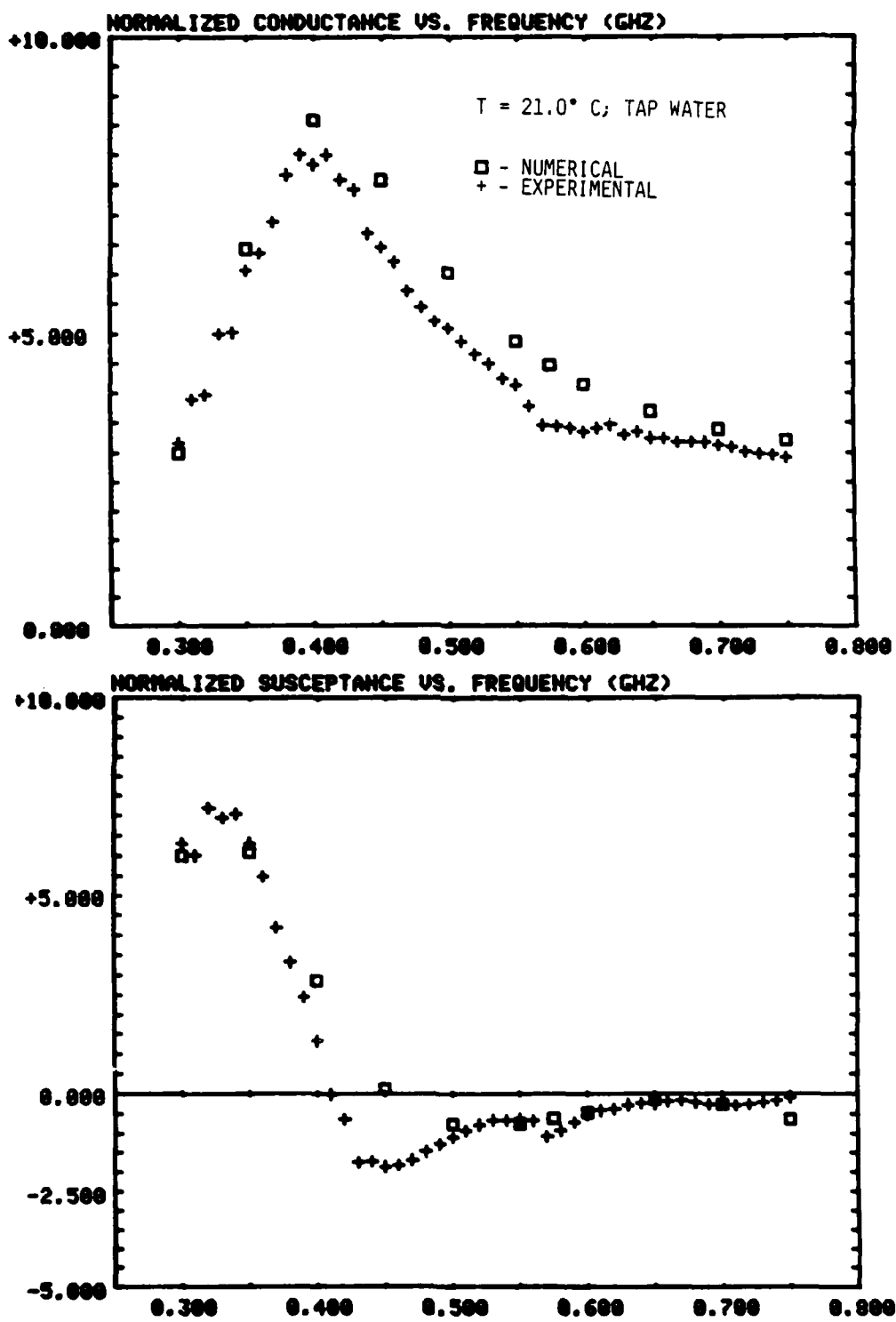


FIGURE 4-15

Aperture Admittance of Coax-Fed Monopole Antenna
Above Ground Plane and Immersed in Water

Although the computed conductance is generally larger than that determined experimentally, there is excellent agreement at peak values.

A major difference of some concern is that the computed frequency for zero phase angle does not coincide with the computed frequency for peak conductance. In the experiment, peak conductance and zero phase angle occurred at approximately the same frequency.

EXPERIMENT TO MEASURE THE CONSTITUTIVE PROPERTIES OF WATER

The conductivity (σ) and the relative permittivity (ϵ_r) of the water used in the Configuration I, II and III experiments was measured as part of this project so that the lossy half space could be properly characterized for numerical analysis of the antennas. Two slotted waveguides - one rectangular and one coaxial - were used for this purpose. The best choice of stock rectangular waveguide (WR-137), when filled with water, operated in the dominant mode only over the 0.6 to 1.0 GHz band. In order to measure σ and ϵ_r for the entire frequency band of these experiments and to have apparatus available for use at lower frequencies in future experiments, a coaxial waveguide apparatus was designed and constructed to operate in the TEM mode at all frequencies below approximately 1.0 GHz (see Appendix C), when filled with water. Since performance of the rectangular waveguide apparatus has been documented in reference [16], the measurements made with the rectangular waveguide were used to corroborate measurements made with the coaxial waveguide apparatus. Performance of both waveguides was generally very satisfactory. The termination sections described in Chapter 2 were included in each waveguide apparatus because there was concern that tap water was

not sufficiently lossy to dissipate the forward-travelling wave within the length of the waveguide. For the rectangular waveguide, the termination consisted only of a mass of absorbing material (carbon-imregnated latex foam). For the coaxial waveguide, the termination consisted of a resistive load matched to the characteristic impedance of the waveguide filled with tap water. This termination would not match the complex characteristic impedance of the waveguide fill with salt water (Appendix C); however, the salt water was considered to be sufficiently lossy to dissipate the forward-travelling wave within the length of the waveguide. The termination of the waveguides proved to be effective in all cases since during swept frequency network analysis there was no evidence of a measurable standing wave in the waveguides.

Even though there was general agreement between the results obtained with each apparatus (Figure 4-16), the coaxial waveguide measurements were more coherent and were smoother functions of frequency than were the rectangular waveguide measurements. (Note the expanded scale for permittivity.) Further, the signal level at the movable test probe of the rectangular waveguide apparatus was below noise threshold of the network analyzer when the waveguide was filled with salt water. Because of the limited bandwidth and the inability to measure constitutive properties of salt water with the rectangular waveguide apparatus and the apparent superior performance of the coaxial waveguide apparatus, the coaxial waveguide was used as the primary apparatus for measuring σ and ϵ_r . The results shown in Figures 4-70 to 4-77 were all obtained with the coaxial waveguide apparatus.

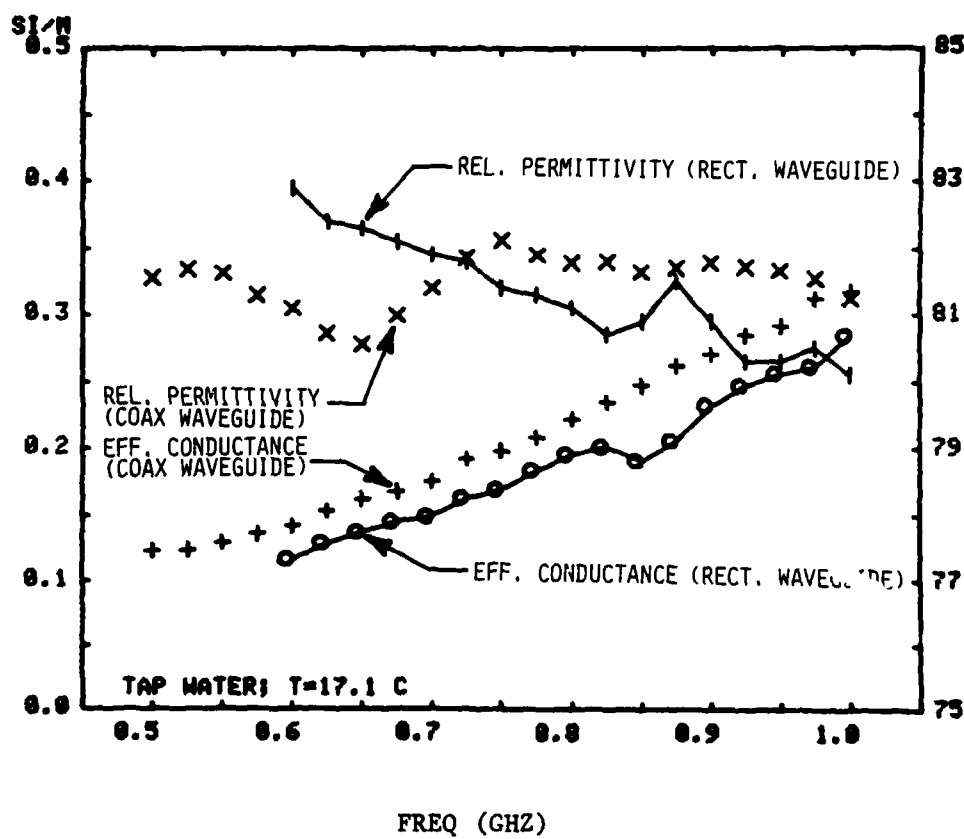


FIGURE 4-16

Electromagnetic Constitutive Properties of Water
Measured with Waveguide Apparatus

Analysis of Measured Values of σ and ϵ_r

The measured values of σ and ϵ_r for salt water agree very well (Figures 4-17 and 4-18) with the values obtained with an available computer code [17]. This code considers only the effect of the NaCl ion on pure water and cannot be used to evaluate the constitutive properties of tap water, which may contain any number of other impurities which may alter the constitutive properties. Since ordinary tap water varies from source to source with regard to its dissolved impurities, the measured constitutive properties for the tap water obtained at the location of these experiments cannot be meaningfully compared to the constitutive properties measured by other investigators at other locations. The values of σ and ϵ_r for "lake water" mentioned by other experimenters [2] and [3] agree in order of magnitude for σ and quite closely for ϵ_r .

COMPENDIUM OF RESULTS

A complete listing of all of the experiments conducted during this project is given in Table 4-1. Each experiment is assigned a serial number, and the geometric data and water characteristics (temperature and salinity) are given for each experiment. A compendium of results may be found in Figures 4-19 through 4-69. The results of each experiment are compiled on a single page in tabular and graphical format and identified by the serial number assigned in Tables 4-1 and 4-2. All data was normalized to the characteristic impedance of the antenna aperture, which was 50 ohms for all experiments of Configurations I and II and $50/\sqrt{2.1}$ ohms (or 34.5 ohms) for the Configuration III experi-

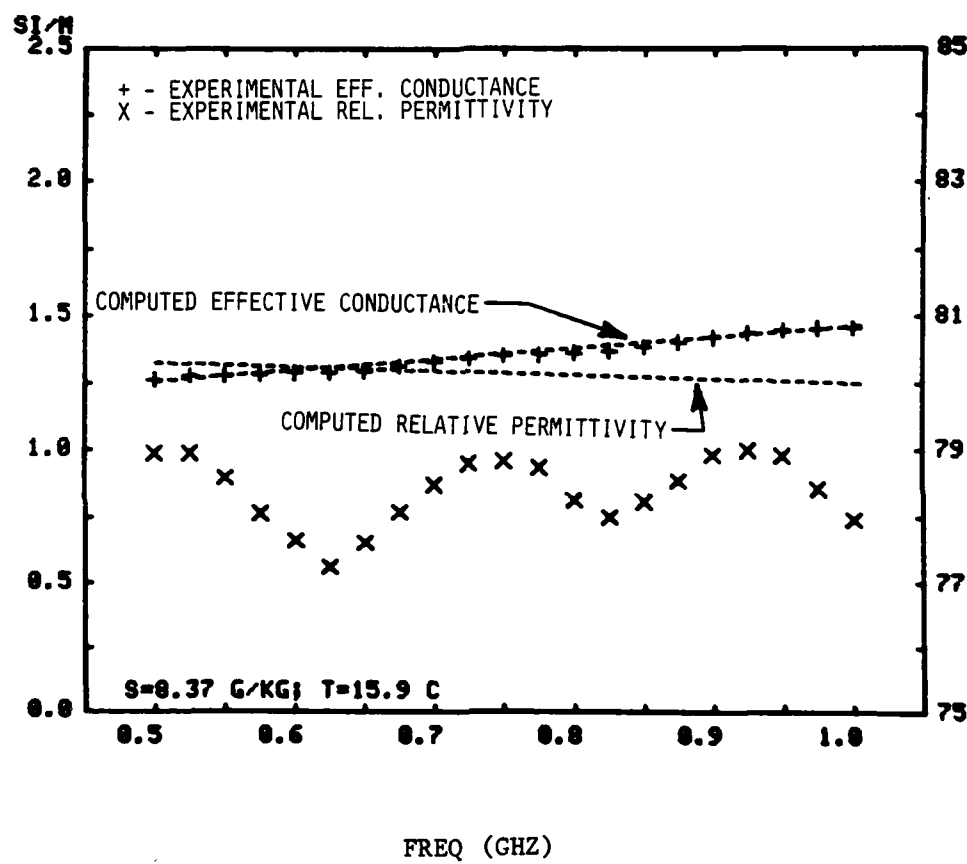


FIGURE 4-17

Electromagnetic Constitutive Properties of Salt Water
Used in Procedures I-G-1 through I-G-4

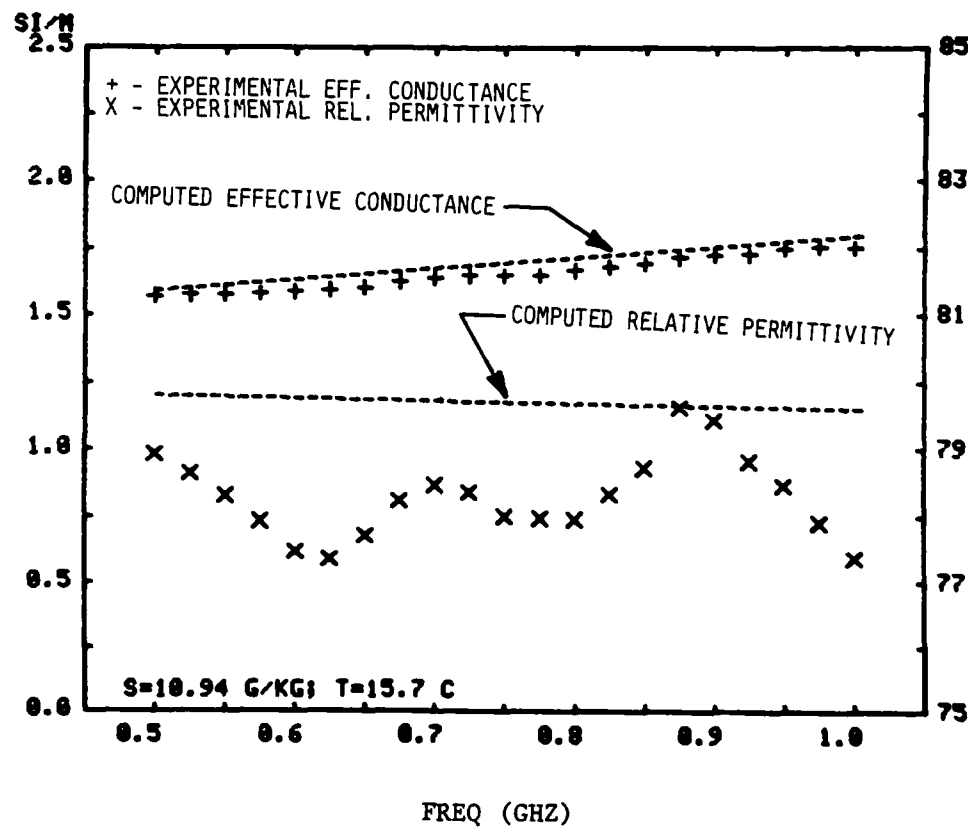


FIGURE 4-18

Electromagnetic Constitutive Properties of Salt Water
Used in Procedures I-F-1 through I-F-4

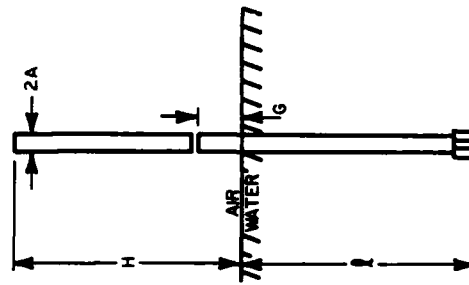


Table 4-1(a)

Key to Compendium of Results

Series I Experiments - 0.250-inch Antenna ($A=0.318\text{cm}$)

<u>Experiment</u>	<u>G(cm)</u>	<u>H(cm)</u>	<u>L(cm)</u>	<u>Remarks</u>
A-1	1.46	26.89	89.17	
A-2	7.91	33.34	82.72	Tap Water at 17.4°C
A-3	13.56	38.99	77.07	
A-4	22.91	48.34	67.72	
A-5	43.06	68.49	47.57	
B-1	1.77	27.20	N/A	Ground Plane
B-2	8.22	33.65	N/A	
B-3	13.87	39.30	N/A	
B-4	23.22	48.65	N/A	
B-5	43.37	68.80	N/A	
C-1	1.51	26.94	89.12	
C-2	7.81	33.24	82.82	Salt Water (9.08 g/kg)
C-3	14.21	39.64	76.42	
C-4	20.06	45.49	70.57	
C-5	27.31	52.74	63.32	
D-1	1.26	26.69	89.37	
D-2	6.86	32.29	83.77	Salt Water (6.95 g/kg)
D-3	13.56	38.99	77.07	
D-4	20.16	45.59	70.47	
D-5	26.70	52.13	63.92	

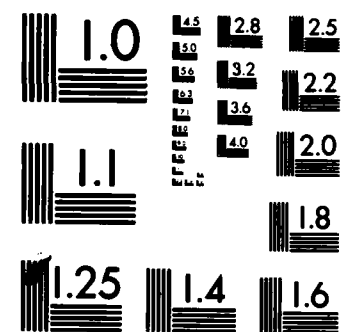
AD-A138 206 AN EXPERIMENTAL STUDY OF CYLINDRICAL ANTENNAS RADIATING 2/2
IN OR NEAR A LOSS. (U) MISSISSIPPI UNIV UNIVERSITY DEPT
OF ELECTRICAL ENGINEERING C M BUTLER ET AL. DEC 83

UNCLASSIFIED NO5C-CR-218 N66001-82-C-0045

F/G 9/1

NL

END



MICROCOPY RESOLUTION TEST CHART
NATIONAL BUREAU OF STANDARDS-1963-A

Table 4-1(b)
Key to Compendium of Results (cont'd)

Series I Experiments - 0.141-inch Antenna (A=0.179cm)				
<u>Experiment</u>	<u>G(cm)</u>	<u>H(cm)</u>	<u>l(cm)</u>	<u>Remarks</u>
E-1	1.36	26.86	89.29	Salt Water
E-2	8.06	33.56	82.59	(1.5 g/kg)
E-3	13.46	38.96	77.19	at 15.8°C
E-4	27.16	52.66	63.49	
F-1	1.96	27.46	88.69	Salt Water
F-2	8.11	33.61	82.54	(10.95 g/kg)
F-3	13.51	39.01	77.14	at 15.1°C
F-4	27.91	53.41	62.74	
G-1	1.81	27.31	88.84	Salt Water
G-2	8.21	33.71	82.44	(8.37 g/kg)
G-3	13.41	38.91	77.24	at 15.1°C
G-4	27.31	52.81	63.34	

Table 4-1(c)
Key to Compendium of Results (cont'd)

Series I Experiments - 0.085-inch Antenna ($A=0.110\text{cm}$)

<u>Experiment</u>	<u>G(cm)</u>	<u>H(cm)</u>	<u>l(cm)</u>	<u>Remarks</u>
H-1	1.10	26.52	89.45	
H-2	7.50	32.92	83.05	Tap Water at 15.8°C
H-3	13.15	38.57	77.40	
H-4	27.00	52.42	63.55	

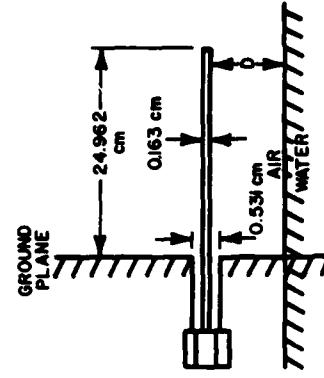
Series I Experiments - 0.250-inch Antenna ($A=0.318\text{cm}$)

<u>Experiment</u>	<u>G(cm)</u>	<u>H(cm)</u>	<u>l(cm)</u>	<u>Remarks</u>
I-1	1.39	7.43	89.24	
I-2	2.99	9.03	97.64	Tap Water at 15.8°C
I-3	4.64	10.68	85.99	
I-4	8.04	14.08	82.59	
I-5	21.17	27.12	69.45	
I-6	27.19	33.23	63.44	

Table 4-1(d)
Key to Compendium of Results

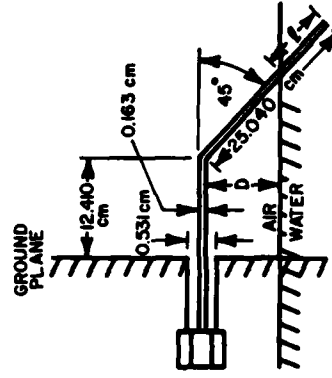
Series II Experiments - Straight Wire Antenna

<u>Experiment</u>	<u>D(cm)</u>	<u>Remarks</u>
A-1	2.55	Tap Water at 18.7°C
A-2	7.40	
A-3	12.40	
A-4	25.05	



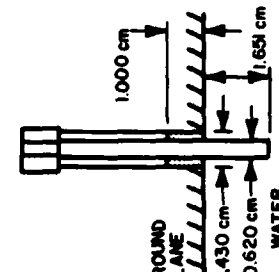
Series II Experiments - Bent Wire Antenna

<u>Experiment</u>	<u>D(cm)</u>	<u>λ(cm)</u>	<u>Remarks</u>
B-1	2.20	21.93	Tap Water at 18.7°C
B-2	7.15	14.93	
B-3	12.25	7.72	
B-4	19.25	0*	*Visibly clear of water



Series III Experiment

<u>Experiment</u>	<u>Remarks</u>
A-1	Tap Water at 21.0°C



ments. The measured constitutive properties of the water used in each procedure are given in Figures 4-70 through 4-77.

COMMENTS AND SUGGESTIONS FOR FUTURE INVESTIGATION

Configuration I Experiments

The most significant conclusion to be drawn from the results of the Configuration I experiments is that, for the vertical monopole antenna, the water surface serves as an effective ground plane. Current distribution on that part of the antenna above the water was essentially unaffected by the conductivity of the water or the length of the structure below the water surface, and it was not significantly different from the current distribution on the antenna above a ground plane. The foregoing was predicted by numerical analysis and well-substantiated by the experiments.

The results of the numerical analyses indicate that conductivity of the water has a pronounced effect on current distribution on that part of the antenna structure below the water surface. Clearly, complete substantiation of the numerical analyses can only be accomplished through current and charge distribution measurements. The construction of the water tank renders unacceptably difficult such measurements for the geometry of Configuration I. An alternate geometry is considered below.

Configuration II Experiments

Straight-Wire Antenna. The experiments with the straight wire antenna indicate that the aperture admittance of a horizontal monopole antenna radiating in air near the interface with a lossy half space can be reasonably well predicted by a free-space analysis of the antenna. The free-space admittance behavior of the antenna is significantly altered only when the antenna is very near (0.2λ or closer) to the interface. Again, current and charge distribution measurements are suggested to provide a fuller understanding of antenna performance. This configuration can be easily modified for current and charge distribution measurements by addition of a parallel conducting structure (parasite) capable of accomodating a current probe. Various geometries should be considered, namely, antenna and parasite in air and antenna in water with parasite in air. The plane containing the antenna and parasite need not be parallel to the air-water interface for all measurements.

Bent-Wire Antenna. The experimental results obtained for the bent wire clearly indicate a need for a sophisticated numerical model since no approximations can be derived from a free-space analysis of the structure. Performance of such a model should be substantiated by current distribution measurements on that portion of the structure which is in air and also on that portion which is in water. A somewhat complex, but very feasible modification to the apparatus would permit such measurements. A coax-fed antenna could be constructed to form three sides of a rectangular loop and mounted such that the antenna aperture is above the water surface and the end of the antenna is shorted to the

ground plane below the water surface. In this configuration, the ground plane images the structure as an apparent rectangular loop. Current and charge distribution measurements along the horizontal segment below the water would be relatively simple to accomplish and would complement the procedures suggested above for the straight wire antenna. Current and charge distribution measurements along the vertical segment which extends through the interface would be somewhat more difficult, but such measurements are feasible. Measurement of current along the vertical segment of the structure would provide the substantiation of current distribution below the water surface needed for the Configuration I experimental model.

Water Properties Measurements

The guided wave technique for measurement of constitutive properties was quite suitable for the purpose of this project and only minor changes in rendering this design could be suggested. One annoyance in using the apparatus was the requirement to employ alternate chilling and warming of the water sample in an effort to duplicate the temperature at which the sample was taken during the antenna experiment. A major re-design of the apparatus should provide the capability to submerge the apparatus in the test tank and measure water properties concurrent with the antenna experiment.

FREQ. (GHZ)	G1	B1	FREQ. (GHZ)	G1	B1
0.500	+0.899	+0.871	0.750	+0.359	+0.476
0.510	+0.110	+0.997	0.760	+0.419	+0.417
0.520	+0.111	+0.100	0.770	+0.495	+0.435
0.530	+0.106	+0.868	0.780	+0.580	+0.411
0.540	+0.120	+0.119	0.790	+0.622	+0.359
0.550	+0.111	+0.130	0.800	+0.690	+0.312
0.560	+0.114	+0.891	0.810	+0.705	+0.245
0.570	+0.110	+0.133	0.820	+0.679	+0.137
0.580	+0.102	+0.153	0.830	+0.641	+0.077
0.590	+0.098	+0.176	0.840	+0.588	+0.042
0.600	+0.102	+0.186	0.850	+0.526	+0.014
0.610	+0.105	+0.223	0.860	+0.479	-0.081
0.620	+0.097	+0.230	0.870	+0.444	-0.093
0.630	+0.113	+0.215	0.880	+0.406	-0.072
0.640	+0.125	+0.271	0.890	+0.384	-0.113
0.650	+0.121	+0.266	0.900	+0.365	-0.088
0.660	+0.139	+0.244	0.910	+0.349	-0.069
0.670	+0.153	+0.282	0.920	+0.319	-0.038
0.680	+0.162	+0.300	0.930	+0.294	-0.018
0.690	+0.161	+0.320	0.940	+0.267	+0.020
0.700	+0.179	+0.354	0.950	+0.242	+0.020
0.710	+0.199	+0.448	0.960	+0.225	+0.016
0.720	+0.213	+0.436	0.970	+0.220	+0.037
0.730	+0.243	+0.412	0.980	+0.214	+0.047
0.740	+0.381	+0.472	0.990	+0.210	+0.014
			1.000	+0.218	+0.016

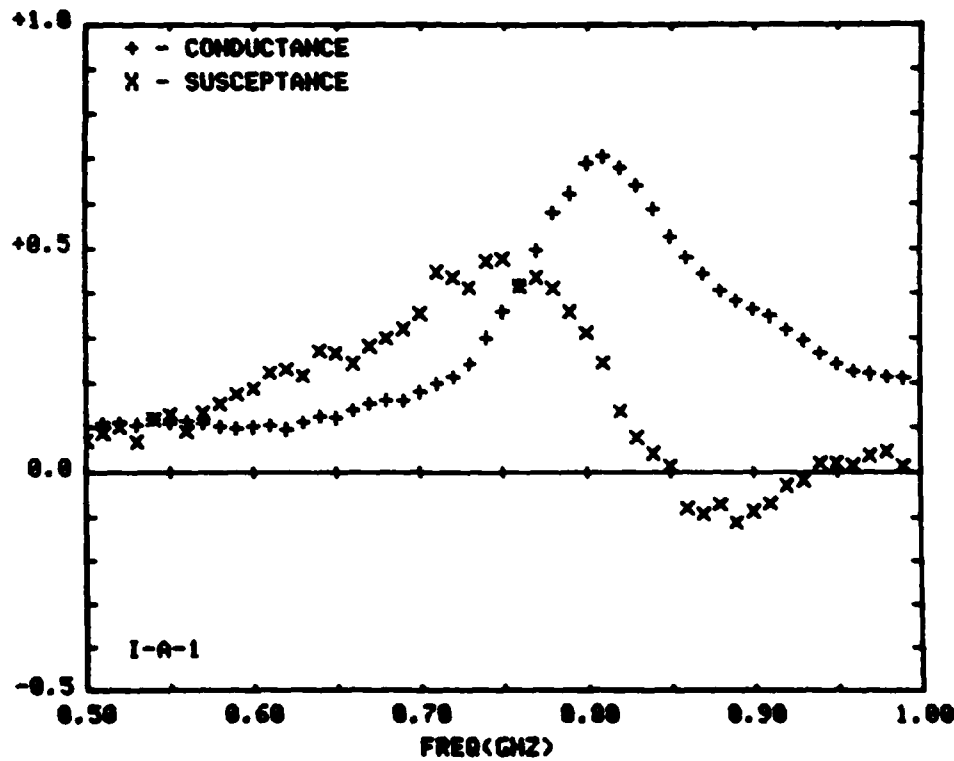


FIGURE 4-19

Aperture Admittance of Sleeve Monopole
Antenna Above Tap Water (I-A-1)

FREQ. (GHZ)	G1	B1	FREQ. (GHZ)	G1	B1
0.500	+0.064	+0.054	0.750	+0.113	+0.061
0.510	+0.077	+0.068	0.760	+0.126	+0.042
0.520	+0.077	+0.074	0.770	+0.132	+0.048
0.530	+0.078	+0.063	0.780	+0.127	+0.071
0.540	+0.096	+0.091	0.790	+0.107	+0.069
0.550	+0.084	+0.094	0.800	+0.122	+0.057
0.560	+0.090	+0.059	0.810	+0.108	+0.085
0.570	+0.092	+0.103	0.820	+0.100	+0.086
0.580	+0.093	+0.122	0.830	+0.097	+0.118
0.590	+0.098	+0.139	0.840	+0.104	+0.156
0.600	+0.108	+0.152	0.850	+0.083	+0.155
0.610	+0.127	+0.207	0.860	+0.090	+0.195
0.620	+0.135	+0.181	0.870	+0.097	+0.107
0.630	+0.174	+0.156	0.880	+0.097	+0.135
0.640	+0.201	+0.168	0.890	+0.094	+0.087
0.650	+0.218	+0.130	0.900	+0.111	+0.092
0.660	+0.226	+0.074	0.910	+0.113	+0.121
0.670	+0.232	+0.055	0.920	+0.099	+0.159
0.680	+0.221	+0.043	0.930	+0.093	+0.133
0.690	+0.191	+0.031	0.940	+0.083	+0.175
0.700	+0.174	+0.030	0.950	+0.071	+0.186
0.710	+0.154	+0.086	0.960	+0.076	+0.177
0.720	+0.129	+0.072	0.970	+0.083	+0.179
0.730	+0.121	+0.067	0.980	+0.090	+0.167
0.740	+0.120	+0.073	0.990	+0.093	+0.151
			1.000	+0.100	+0.151

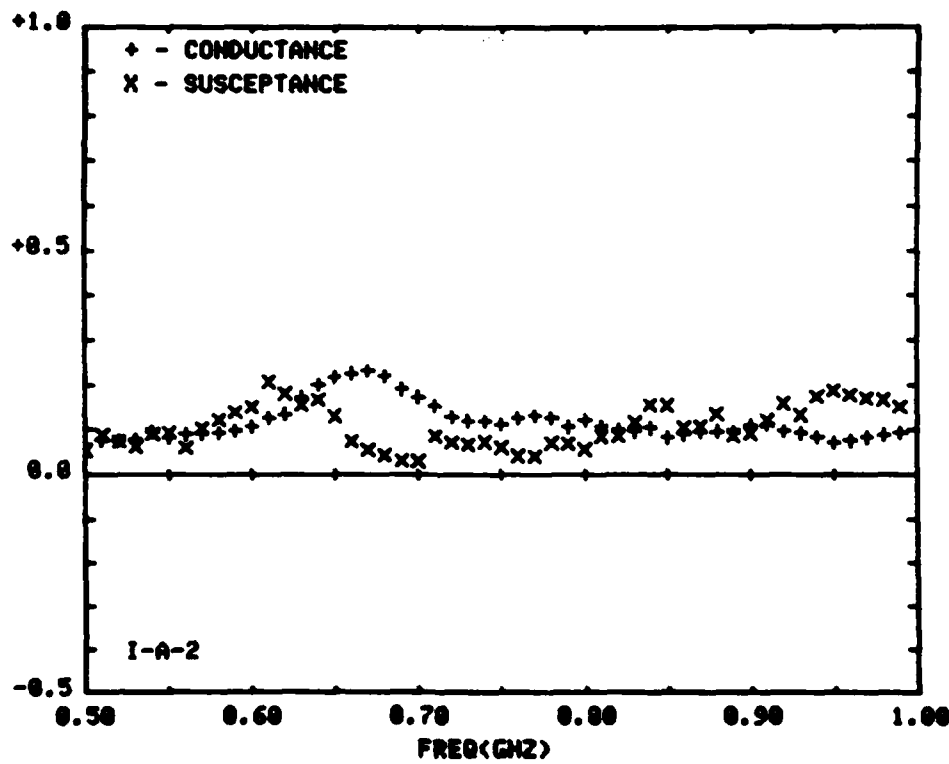


FIGURE 4-20

Aperture Admittance of Sleeve Monopole
Antenna Above Tap Water (I-A-2)

FREQ. (GHZ)	G1	B1	FREQ. (GHZ)	G1	B1
0.500	+0.846	+0.082	0.750	+0.871	+0.244
0.510	+0.866	+0.106	0.760	+0.885	+0.222
0.520	+0.861	+0.095	0.770	+0.891	+0.240
0.530	+0.867	+0.079	0.780	+0.891	+0.279
0.540	+0.880	+0.104	0.790	+0.877	+0.238
0.550	+0.867	+0.107	0.800	+0.894	+0.276
0.560	+0.866	+0.066	0.810	+0.897	+0.316
0.570	+0.869	+0.089	0.820	+0.885	+0.309
0.580	+0.862	+0.130	0.830	+0.898	+0.329
0.590	+0.853	+0.124	0.840	+0.118	+0.385
0.600	+0.860	+0.129	0.850	+0.124	+0.397
0.610	+0.859	+0.180	0.860	+0.146	+0.368
0.620	+0.849	+0.183	0.870	+0.182	+0.481
0.630	+0.863	+0.151	0.880	+0.204	+0.412
0.640	+0.866	+0.171	0.890	+0.240	+0.374
0.650	+0.857	+0.160	0.900	+0.302	+0.492
0.660	+0.869	+0.128	0.910	+0.368	+0.425
0.670	+0.877	+0.148	0.920	+0.428	+0.400
0.680	+0.879	+0.175	0.930	+0.468	+0.345
0.690	+0.862	+0.179	0.940	+0.487	+0.295
0.700	+0.864	+0.196	0.950	+0.464	+0.217
0.710	+0.856	+0.245	0.960	+0.419	+0.131
0.720	+0.845	+0.227	0.970	+0.375	+0.087
0.730	+0.859	+0.210	0.980	+0.334	+0.065
0.740	+0.867	+0.235	0.990	+0.303	+0.034
			1.000	+0.280	+0.034

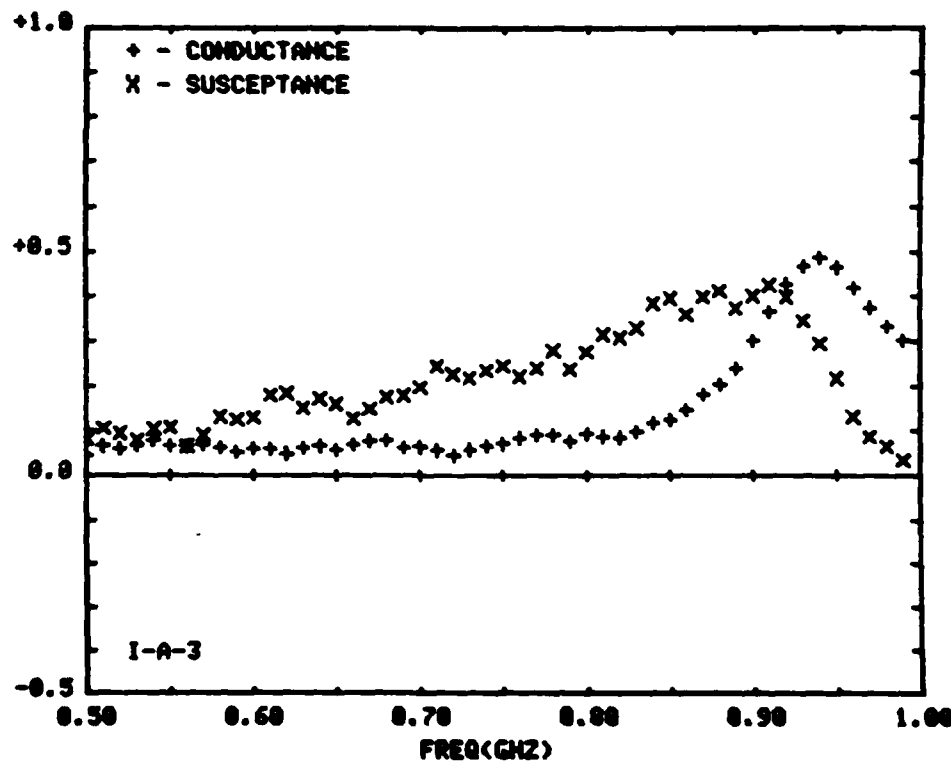
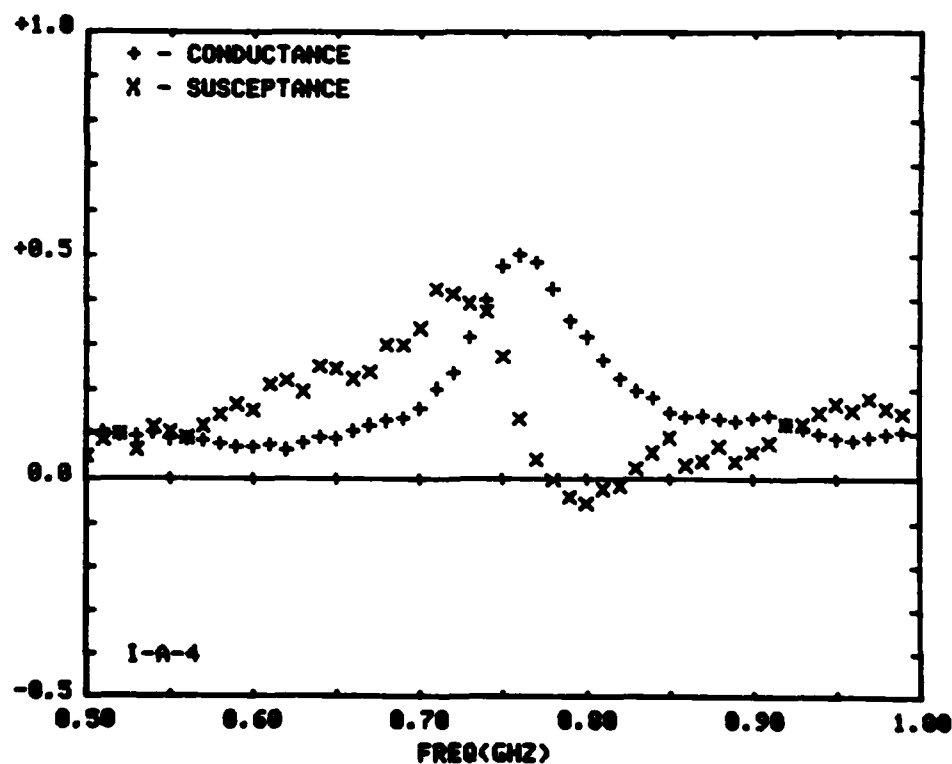


FIGURE 4-21

Aperture Admittance of Sleeve Monopole
Antenna Above Tap Water (I-A-3)

FREQ. (GHZ)	G1	B1	FREQ. (GHZ)	G1	B1
0.560	+0.105	+0.050	0.750	+0.476	+0.273
0.510	+0.103	+0.086	0.760	+0.500	+0.134
0.520	+0.100	+0.101	0.770	+0.484	+0.043
0.530	+0.095	+0.065	0.780	+0.426	-0.003
0.540	+0.103	+0.117	0.790	+0.354	-0.041
0.550	+0.090	+0.106	0.800	+0.318	-0.056
0.560	+0.090	+0.092	0.810	+0.267	-0.023
0.570	+0.087	+0.119	0.820	+0.224	-0.016
0.580	+0.079	+0.144	0.830	+0.197	+0.024
0.590	+0.072	+0.167	0.840	+0.182	+0.059
0.600	+0.072	+0.153	0.850	+0.149	+0.092
0.610	+0.077	+0.211	0.860	+0.139	+0.030
0.620	+0.066	+0.220	0.870	+0.142	+0.039
0.630	+0.082	+0.196	0.880	+0.135	+0.073
0.640	+0.094	+0.252	0.890	+0.129	+0.038
0.650	+0.099	+0.247	0.900	+0.136	+0.059
0.660	+0.107	+0.224	0.910	+0.142	+0.080
0.670	+0.121	+0.239	0.920	+0.123	+0.123
0.680	+0.131	+0.299	0.930	+0.113	+0.121
0.690	+0.137	+0.300	0.940	+0.101	+0.147
0.700	+0.158	+0.337	0.950	+0.090	+0.166
0.710	+0.203	+0.424	0.960	+0.087	+0.152
0.720	+0.237	+0.413	0.970	+0.094	+0.188
0.730	+0.316	+0.392	0.980	+0.101	+0.157
0.740	+0.401	+0.374	0.990	+0.104	+0.147
			1.000	+0.119	+0.153



FREQ. (GHZ)	G1	B1	FREQ. (GHZ)	G1	B1
0.500	+0.052	+0.000	0.750	+0.464	+0.246
0.510	+0.071	+0.104	0.760	+0.452	+0.075
0.520	+0.069	+0.097	0.770	+0.384	-0.003
0.530	+0.073	+0.097	0.780	+0.316	+0.004
0.540	+0.092	+0.131	0.790	+0.237	-0.007
0.550	+0.079	+0.114	0.800	+0.208	+0.001
0.560	+0.078	+0.098	0.810	+0.177	+0.050
0.570	+0.075	+0.102	0.820	+0.148	+0.063
0.580	+0.067	+0.146	0.830	+0.127	+0.110
0.590	+0.059	+0.142	0.840	+0.127	+0.135
0.600	+0.066	+0.149	0.850	+0.100	+0.164
0.610	+0.068	+0.204	0.860	+0.102	+0.130
0.620	+0.059	+0.213	0.870	+0.112	+0.150
0.630	+0.070	+0.188	0.880	+0.107	+0.191
0.640	+0.080	+0.216	0.890	+0.106	+0.137
0.650	+0.077	+0.209	0.900	+0.122	+0.170
0.660	+0.088	+0.187	0.910	+0.137	+0.229
0.670	+0.102	+0.221	0.920	+0.134	+0.290
0.680	+0.110	+0.256	0.930	+0.152	+0.284
0.690	+0.107	+0.281	0.940	+0.182	+0.352
0.700	+0.124	+0.316	0.950	+0.226	+0.370
0.710	+0.168	+0.411	0.960	+0.305	+0.316
0.720	+0.196	+0.410	0.970	+0.353	+0.248
0.730	+0.274	+0.376	0.980	+0.362	+0.148
0.740	+0.366	+0.350	0.990	+0.323	+0.067
			1.000	+0.291	+0.043

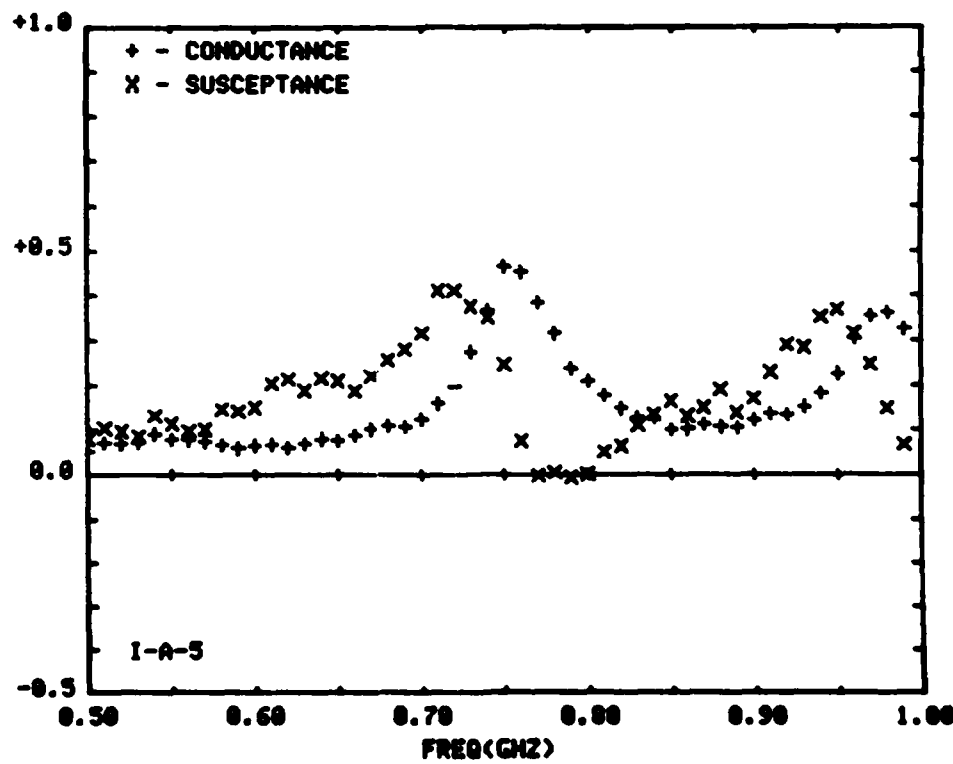


FIGURE 4-23

Aperture Admittance of Sleeve Monopole
Antenna Above Tap Water (I-A-5)

FREQ. (GHZ)	G1	B1	FREQ. (GHZ)	G1	B1
0.500	+0.101	+0.052	0.750	+0.417	+0.385
0.510	+0.107	+0.065	0.760	+0.522	+0.396
0.520	+0.108	+0.074	0.770	+0.661	+0.563
0.530	+0.110	+0.121	0.780	+0.763	+0.468
0.540	+0.110	+0.108	0.790	+0.902	+0.352
0.550	+0.106	+0.121	0.800	+0.957	+0.178
0.560	+0.104	+0.080	0.810	+0.913	+0.036
0.570	+0.108	+0.105	0.820	+0.825	-0.085
0.580	+0.111	+0.156	0.830	+0.688	-0.134
0.590	+0.109	+0.203	0.840	+0.608	-0.179
0.600	+0.096	+0.228	0.850	+0.510	-0.217
0.610	+0.093	+0.213	0.860	+0.444	-0.197
0.620	+0.100	+0.205	0.870	+0.393	-0.176
0.630	+0.113	+0.213	0.880	+0.350	-0.153
0.640	+0.119	+0.270	0.890	+0.328	-0.160
0.650	+0.124	+0.284	0.900	+0.323	-0.176
0.660	+0.133	+0.283	0.910	+0.296	-0.162
0.670	+0.134	+0.256	0.920	+0.279	-0.110
0.680	+0.147	+0.291	0.930	+0.264	-0.052
0.690	+0.159	+0.367	0.940	+0.235	-0.031
0.700	+0.175	+0.439	0.950	+0.220	-0.035
0.710	+0.181	+0.471	0.960	+0.208	-0.018
0.720	+0.213	+0.482	0.970	+0.203	-0.008
0.730	+0.260	+0.501	0.980	+0.200	+0.017
0.740	+0.327	+0.536	0.990	+0.192	+0.023
			1.000	+0.194	+0.011

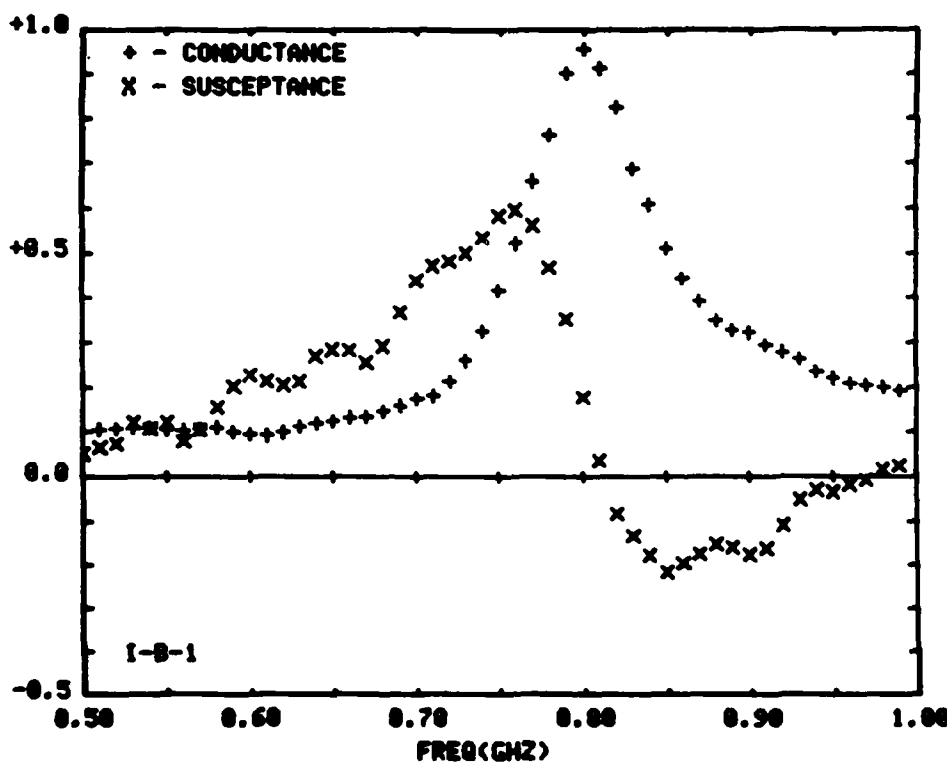


FIGURE 4-24

Aperture Admittance of Sleeve Monopole
Antenna Above Ground Plane (I-B-1)

FREQ. (GHZ)	G1	B1	FREQ. (GHZ)	G1	B1
0.500	+0.960	+0.944	0.750	+0.970	+0.936
0.510	+0.971	+0.945	0.760	+0.991	+0.948
0.520	+0.973	+0.959	0.770	+0.997	+0.951
0.530	+0.981	+0.988	0.780	+0.995	+0.932
0.540	+0.982	+0.987	0.790	+0.986	+0.921
0.550	+0.982	+0.986	0.800	+0.982	+0.938
0.560	+0.988	+0.951	0.810	+0.980	+0.972
0.570	+0.996	+0.970	0.820	+0.971	+0.101
0.580	+0.105	+0.114	0.830	+0.065	+0.128
0.590	+0.106	+0.179	0.840	+0.058	+0.098
0.600	+0.113	+0.188	0.850	+0.061	+0.087
0.610	+0.138	+0.171	0.860	+0.070	+0.100
0.620	+0.173	+0.149	0.870	+0.074	+0.115
0.630	+0.222	+0.141	0.880	+0.069	+0.115
0.640	+0.260	+0.122	0.890	+0.072	+0.082
0.650	+0.271	+0.058	0.900	+0.080	+0.073
0.660	+0.234	-0.001	0.910	+0.082	+0.079
0.670	+0.206	-0.064	0.920	+0.091	+0.120
0.680	+0.170	-0.058	0.930	+0.069	+0.146
0.690	+0.149	-0.037	0.940	+0.056	+0.167
0.700	+0.127	0.000	0.950	+0.046	+0.151
0.710	+0.102	+0.020	0.960	+0.054	+0.148
0.720	+0.086	+0.047	0.970	+0.067	+0.163
0.730	+0.079	+0.024	0.980	+0.071	+0.174
0.740	+0.076	+0.015	0.990	+0.071	+0.172
			1.000	+0.075	+0.152

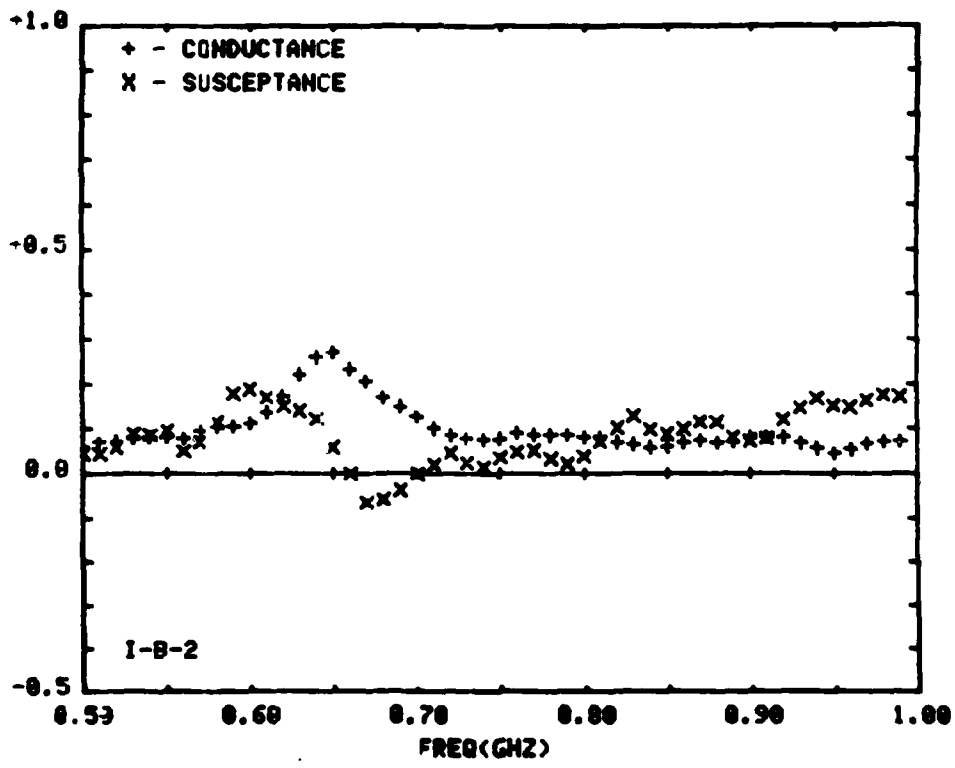


FIGURE 4-25

Aperture Admittance of Sleeve Monopole
Antenna Above Ground Plane (I-B-2)

FREQ. (GHZ)	G1	B1	FREQ. (GHZ)	G1	B1
0.500	+0.037	+0.074	0.750	+0.045	+0.239
0.510	+0.043	+0.072	0.760	+0.062	+0.253
0.520	+0.048	+0.088	0.770	+0.064	+0.252
0.530	+0.053	+0.107	0.780	+0.068	+0.218
0.540	+0.053	+0.094	0.790	+0.063	+0.224
0.550	+0.047	+0.096	0.800	+0.066	+0.264
0.560	+0.045	+0.062	0.810	+0.062	+0.323
0.570	+0.048	+0.074	0.820	+0.060	+0.353
0.580	+0.052	+0.109	0.830	+0.067	+0.394
0.590	+0.041	+0.158	0.840	+0.076	+0.361
0.600	+0.028	+0.163	0.850	+0.096	+0.372
0.610	+0.031	+0.146	0.860	+0.121	+0.429
0.620	+0.031	+0.137	0.870	+0.158	+0.471
0.630	+0.043	+0.144	0.880	+0.190	+0.493
0.640	+0.049	+0.182	0.890	+0.249	+0.476
0.650	+0.054	+0.164	0.900	+0.329	+0.491
0.660	+0.043	+0.174	0.910	+0.449	+0.523
0.670	+0.045	+0.123	0.920	+0.590	+0.490
0.680	+0.048	+0.131	0.930	+0.666	+0.376
0.690	+0.049	+0.166	0.940	+0.656	+0.287
0.700	+0.042	+0.212	0.950	+0.367	+0.877
0.710	+0.026	+0.221	0.960	+0.477	-0.091
0.720	+0.026	+0.244	0.970	+0.398	-0.021
0.730	+0.033	+0.208	0.980	+0.339	-0.006
0.740	+0.034	+0.204	0.990	+0.293	-0.001
			1.000	+0.263	-0.010

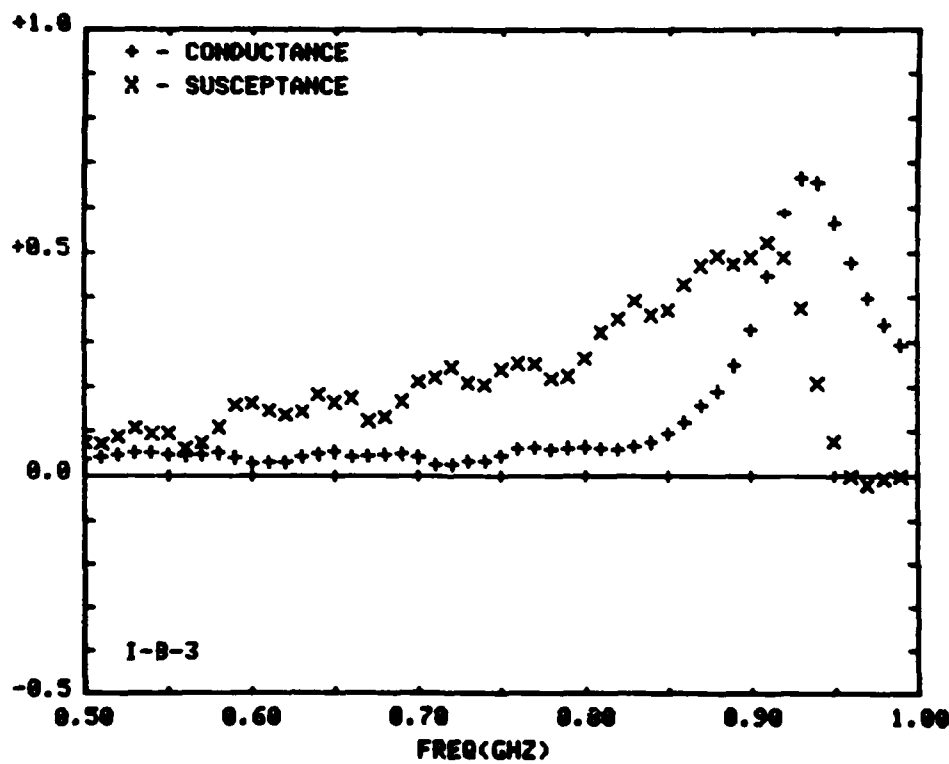


FIGURE 4-26

Aperture Admittance of Sleeve Monopole
Antenna Above Ground Plane (I-B-3)

FREQ. (GHZ)	G1	B1	FREQ. (GHZ)	G1	B1
0.500	+0.107	+0.045	0.750	+0.649	+0.263
0.510	+0.100	+0.054	0.760	+0.652	+0.036
0.520	+0.097	+0.075	0.770	+0.520	-0.099
0.530	+0.092	+0.103	0.780	+0.414	-0.166
0.540	+0.087	+0.100	0.790	+0.326	-0.174
0.550	+0.082	+0.105	0.800	+0.261	-0.136
0.560	+0.074	+0.074	0.810	+0.227	-0.089
0.570	+0.078	+0.092	0.820	+0.185	-0.037
0.580	+0.081	+0.133	0.830	+0.156	+0.011
0.590	+0.069	+0.190	0.840	+0.136	-0.009
0.600	+0.059	+0.200	0.850	+0.118	-0.004
0.610	+0.058	+0.187	0.860	+0.118	+0.018
0.620	+0.063	+0.185	0.870	+0.117	+0.043
0.630	+0.076	+0.203	0.880	+0.109	+0.050
0.640	+0.082	+0.250	0.890	+0.106	+0.030
0.650	+0.092	+0.244	0.900	+0.112	+0.019
0.660	+0.088	+0.263	0.910	+0.109	+0.038
0.670	+0.095	+0.227	0.920	+0.105	+0.077
0.680	+0.113	+0.258	0.930	+0.095	+0.110
0.690	+0.128	+0.329	0.940	+0.082	+0.135
0.700	+0.151	+0.404	0.950	+0.069	+0.127
0.710	+0.177	+0.438	0.960	+0.074	+0.127
0.720	+0.256	+0.480	0.970	+0.084	+0.147
0.730	+0.367	+0.456	0.980	+0.089	+0.167
0.740	+0.512	+0.402	0.990	+0.083	+0.178
			1.000	+0.092	+0.157

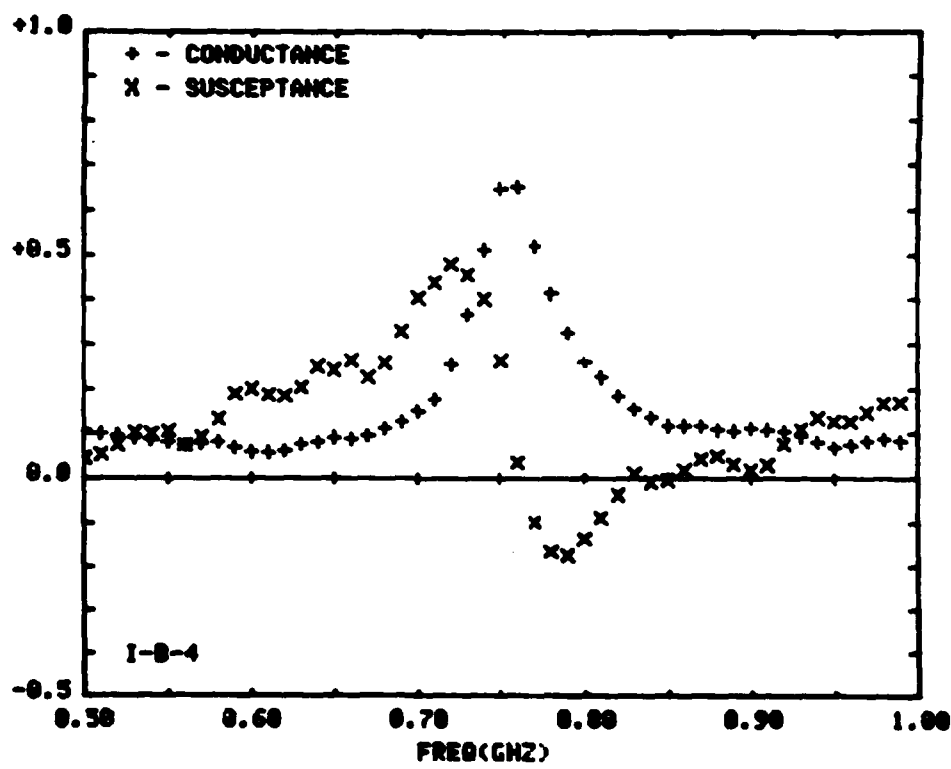


FIGURE 4-27

Aperture Admittance of Sleeve Monopole
Antenna Above Ground Plane (I-B-4)

FREQ. (GHZ)	G1	B1	FREQ. (GHZ)	G1	B1
0.500	+0.843	+0.072	0.750	+0.685	+0.182
0.510	+0.849	+0.079	0.760	+0.511	-0.038
0.520	+0.857	+0.100	0.770	+0.358	-0.094
0.530	+0.864	+0.129	0.780	+0.259	-0.114
0.540	+0.870	+0.117	0.790	+0.201	-0.088
0.550	+0.871	+0.111	0.800	+0.163	-0.046
0.560	+0.863	+0.077	0.810	+0.140	+0.011
0.570	+0.866	+0.098	0.820	+0.113	+0.068
0.580	+0.869	+0.129	0.830	+0.096	+0.112
0.590	+0.857	+0.182	0.840	+0.082	+0.095
0.600	+0.847	+0.198	0.850	+0.079	+0.099
0.610	+0.849	+0.175	0.860	+0.083	+0.126
0.620	+0.850	+0.171	0.870	+0.086	+0.154
0.630	+0.863	+0.185	0.880	+0.081	+0.169
0.640	+0.868	+0.217	0.890	+0.084	+0.157
0.650	+0.879	+0.223	0.900	+0.093	+0.162
0.660	+0.875	+0.239	0.910	+0.097	+0.194
0.670	+0.876	+0.199	0.920	+0.105	+0.274
0.680	+0.887	+0.227	0.930	+0.123	+0.337
0.690	+0.894	+0.291	0.940	+0.160	+0.403
0.700	+0.198	+0.363	0.950	+0.246	+0.417
0.710	+0.129	+0.492	0.960	+0.386	+0.358
0.720	+0.195	+0.456	0.970	+0.470	+0.219
0.730	+0.309	+0.445	0.980	+0.423	+0.093
0.740	+0.482	+0.398	0.990	+0.340	+0.029
			1.000	+0.283	0.000

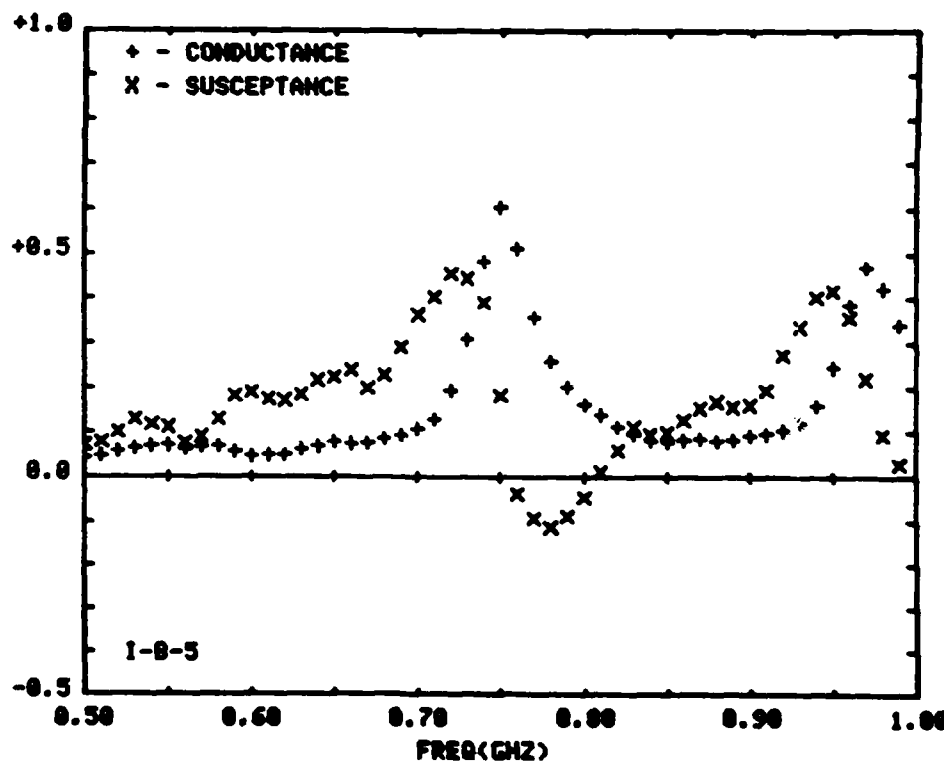


FIGURE 4-28

Aperture Admittance of Sleeve Monopole
Antenna Above Ground Plane (I-B-5)

FREQ. (GHZ)	G1	B1	FREQ. (GHZ)	G1	B1
0.500	+0.100	+0.100	0.750	+0.351	+0.448
0.510	+0.101	+0.062	0.760	+0.468	+0.427
0.520	+0.106	+0.075	0.770	+0.535	+0.381
0.530	+0.111	+0.099	0.780	+0.646	+0.355
0.540	+0.109	+0.075	0.790	+0.700	+0.327
0.550	+0.116	+0.067	0.800	+0.710	+0.233
0.560	+0.122	+0.130	0.810	+0.700	+0.175
0.570	+0.119	+0.159	0.820	+0.660	+0.099
0.580	+0.114	+0.148	0.830	+0.598	+0.027
0.590	+0.114	+0.227	0.840	+0.540	-0.015
0.600	+0.090	+0.213	0.850	+0.491	-0.029
0.610	+0.098	+0.176	0.860	+0.432	-0.081
0.620	+0.109	+0.233	0.870	+0.407	-0.111
0.630	+0.111	+0.237	0.880	+0.386	-0.101
0.640	+0.124	+0.212	0.890	+0.371	-0.107
0.650	+0.144	+0.248	0.900	+0.351	-0.115
0.660	+0.151	+0.283	0.910	+0.337	-0.073
0.670	+0.150	+0.283	0.920	+0.315	+0.010
0.680	+0.168	+0.298	0.930	+0.282	-0.016
0.690	+0.179	+0.375	0.940	+0.252	+0.023
0.700	+0.189	+0.373	0.950	+0.233	+0.048
0.710	+0.216	+0.401	0.960	+0.211	+0.005
0.720	+0.238	+0.462	0.970	+0.205	+0.012
0.730	+0.274	+0.446	0.980	+0.203	+0.022
0.740	+0.315	+0.420	0.990	+0.201	+0.007
			1.000	+0.210	+0.006

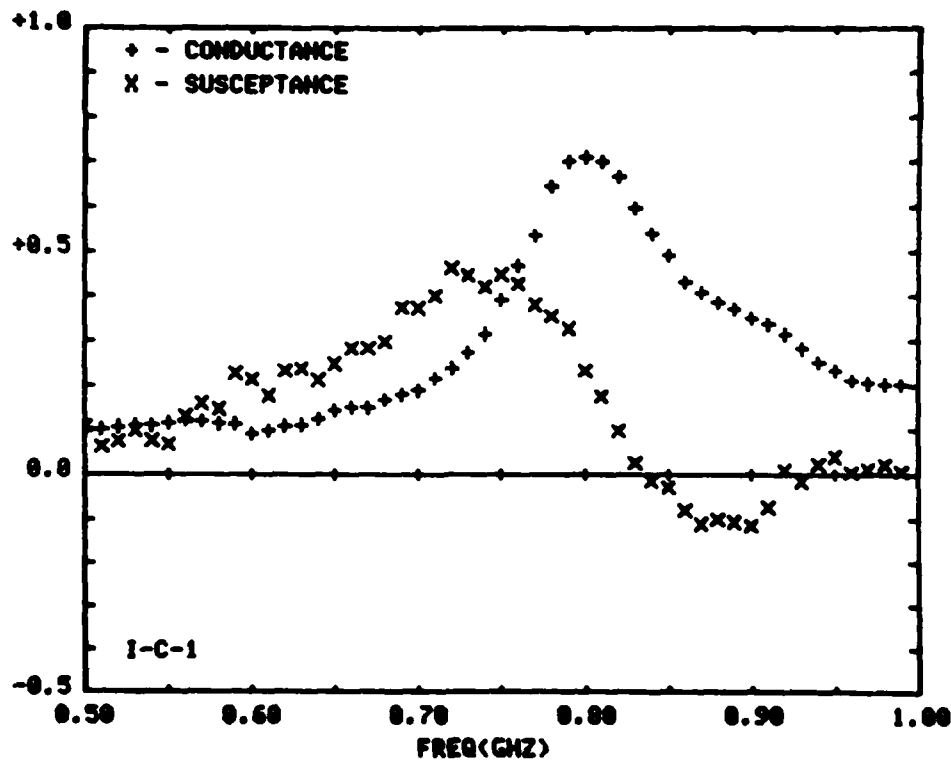


FIGURE 4-29

Aperture Admittance of Sleeve Monopole
Antenna Above Salt Water (I-C-1)

FREQ. (GHZ)	G1	B1	FREQ. (GHZ)	G1	B1
0.500	+0.967	+0.119	0.750	+0.126	+0.844
0.510	+0.970	+0.843	0.760	+0.124	+0.838
0.520	+0.980	+0.877	0.770	+0.124	+0.821
0.530	+0.982	+0.872	0.780	+0.142	+0.848
0.540	+0.985	+0.850	0.790	+0.127	+0.896
0.550	+0.994	+0.840	0.800	+0.115	+0.895
0.560	+0.105	+0.897	0.810	+0.111	+0.885
0.570	+0.107	+0.130	0.820	+0.101	+0.120
0.580	+0.102	+0.114	0.830	+0.091	+0.898
0.590	+0.113	+0.218	0.840	+0.893	+0.185
0.600	+0.997	+0.204	0.850	+0.095	+0.161
0.610	+0.125	+0.135	0.860	+0.084	+0.105
0.620	+0.151	+0.179	0.870	+0.094	+0.084
0.630	+0.180	+0.172	0.880	+0.099	+0.100
0.640	+0.205	+0.129	0.890	+0.102	+0.107
0.650	+0.235	+0.114	0.900	+0.107	+0.075
0.660	+0.241	+0.098	0.910	+0.115	+0.113
0.670	+0.231	+0.067	0.920	+0.109	+0.196
0.680	+0.225	+0.010	0.930	+0.103	+0.174
0.690	+0.210	+0.052	0.940	+0.086	+0.186
0.700	+0.179	+0.046	0.950	+0.074	+0.188
0.710	+0.166	+0.049	0.960	+0.068	+0.144
0.720	+0.139	+0.087	0.970	+0.063	+0.169
0.730	+0.130	+0.050	0.980	+0.091	+0.147
0.740	+0.121	+0.056	0.990	+0.096	+0.132
			1.000	+0.109	+0.126

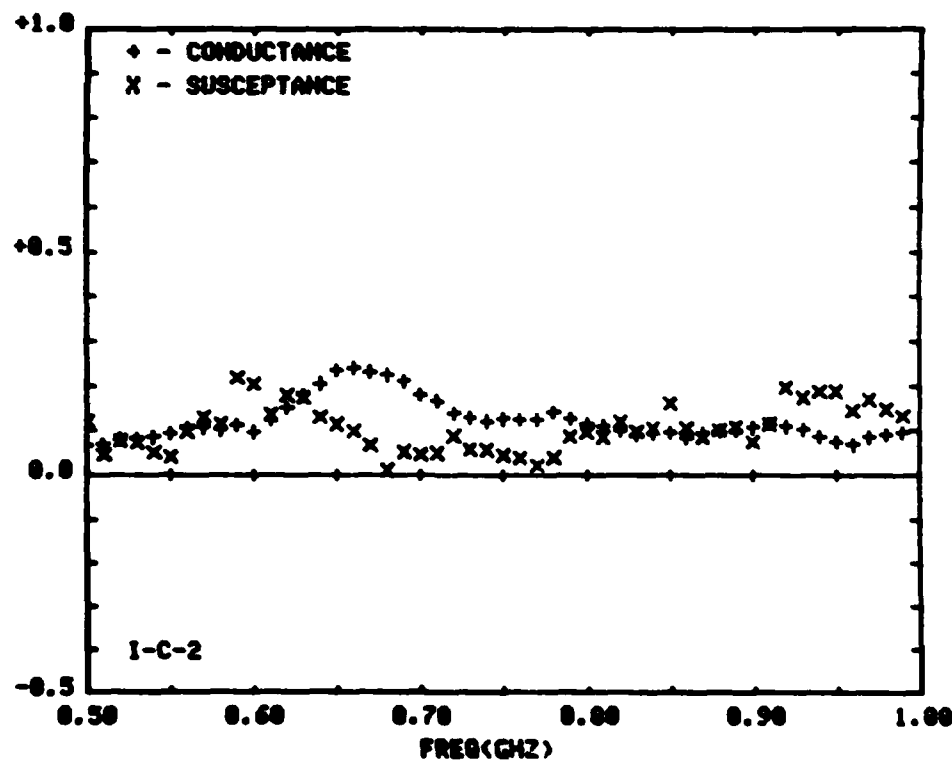


FIGURE 4-30

Aperture Admittance of Sleeve Monopole
Antenna Above Salt Water (I-C-2)

FREQ. (GHZ)	G1	B1	FREQ. (GHZ)	G1	B1
0.500	+0.050	+0.141	0.750	+0.071	+0.223
0.510	+0.050	+0.095	0.760	+0.091	+0.259
0.520	+0.064	+0.097	0.770	+0.099	+0.213
0.530	+0.062	+0.110	0.780	+0.103	+0.265
0.540	+0.068	+0.066	0.790	+0.106	+0.314
0.550	+0.067	+0.078	0.800	+0.101	+0.321
0.560	+0.075	+0.117	0.810	+0.101	+0.370
0.570	+0.073	+0.159	0.820	+0.093	+0.383
0.580	+0.062	+0.110	0.830	+0.110	+0.355
0.590	+0.061	+0.197	0.840	+0.130	+0.384
0.600	+0.049	+0.184	0.850	+0.172	+0.453
0.610	+0.047	+0.141	0.860	+0.194	+0.401
0.620	+0.054	+0.180	0.870	+0.238	+0.400
0.630	+0.053	+0.159	0.880	+0.308	+0.431
0.640	+0.067	+0.149	0.890	+0.390	+0.433
0.650	+0.072	+0.162	0.900	+0.452	+0.482
0.660	+0.071	+0.189	0.910	+0.517	+0.356
0.670	+0.069	+0.183	0.920	+0.572	+0.325
0.680	+0.069	+0.173	0.930	+0.540	+0.219
0.690	+0.076	+0.202	0.940	+0.477	+0.158
0.700	+0.061	+0.204	0.950	+0.418	+0.102
0.710	+0.066	+0.215	0.960	+0.357	+0.026
0.720	+0.049	+0.267	0.970	+0.307	+0.036
0.730	+0.036	+0.234	0.980	+0.273	+0.032
0.740	+0.058	+0.231	0.990	+0.292	-0.007
			1.000	+0.241	-0.001

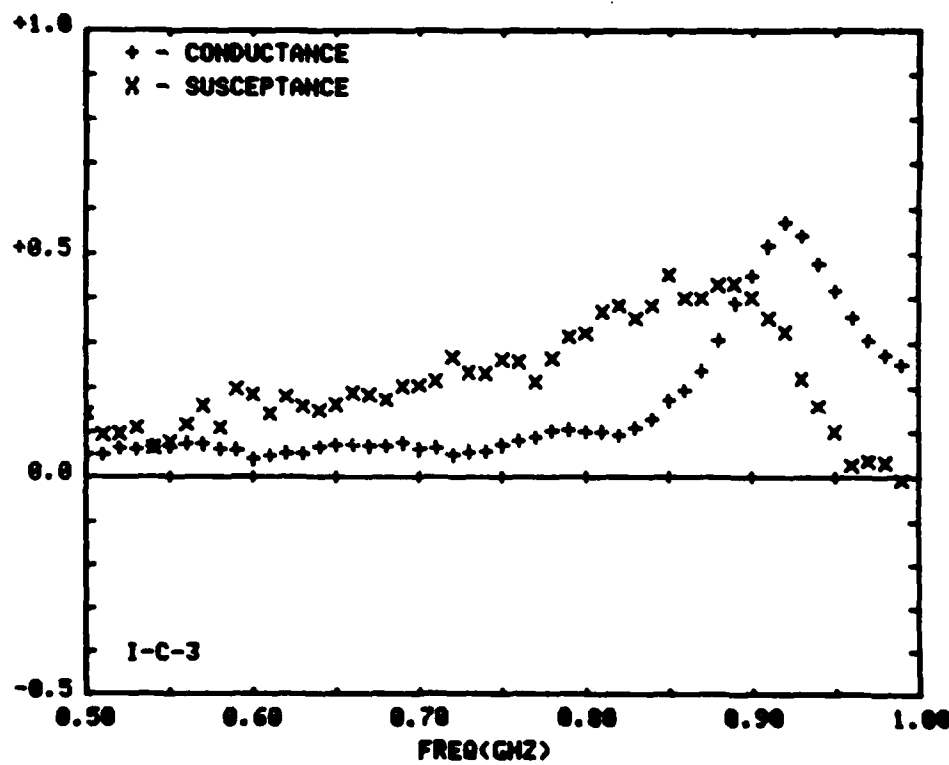


FIGURE 4-31

Aperture Admittance of Sleeve Monopole
Antenna Above Salt Water (I-C-3)

FREQ. (GHZ)	G1	B1	FREQ. (GHZ)	G1	B1
0.500	+0.122	+0.141	0.750	+0.228	+0.439
0.510	+0.107	+0.067	0.760	+0.291	+0.408
0.520	+0.102	+0.097	0.770	+0.362	+0.391
0.530	+0.094	+0.088	0.780	+0.484	+0.397
0.540	+0.092	+0.069	0.790	+0.584	+0.356
0.550	+0.089	+0.087	0.800	+0.623	+0.256
0.560	+0.093	+0.112	0.810	+0.593	+0.135
0.570	+0.091	+0.178	0.820	+0.539	+0.057
0.580	+0.079	+0.134	0.830	+0.458	-0.021
0.590	+0.075	+0.226	0.840	+0.365	-0.041
0.600	+0.053	+0.212	0.850	+0.305	-0.005
0.610	+0.061	+0.151	0.860	+0.262	-0.059
0.620	+0.066	+0.193	0.870	+0.236	-0.069
0.630	+0.072	+0.194	0.880	+0.217	-0.051
0.640	+0.080	+0.196	0.890	+0.214	-0.036
0.650	+0.085	+0.215	0.900	+0.205	-0.024
0.660	+0.092	+0.245	0.910	+0.193	-0.009
0.670	+0.089	+0.246	0.920	+0.179	+0.078
0.680	+0.096	+0.256	0.930	+0.164	+0.071
0.690	+0.102	+0.290	0.940	+0.137	+0.114
0.700	+0.100	+0.296	0.950	+0.117	+0.096
0.710	+0.113	+0.322	0.960	+0.116	+0.059
0.720	+0.113	+0.390	0.970	+0.111	+0.090
0.730	+0.138	+0.371	0.980	+0.111	+0.095
0.740	+0.172	+0.385	0.990	+0.121	+0.058
			1.000	+0.129	+0.058

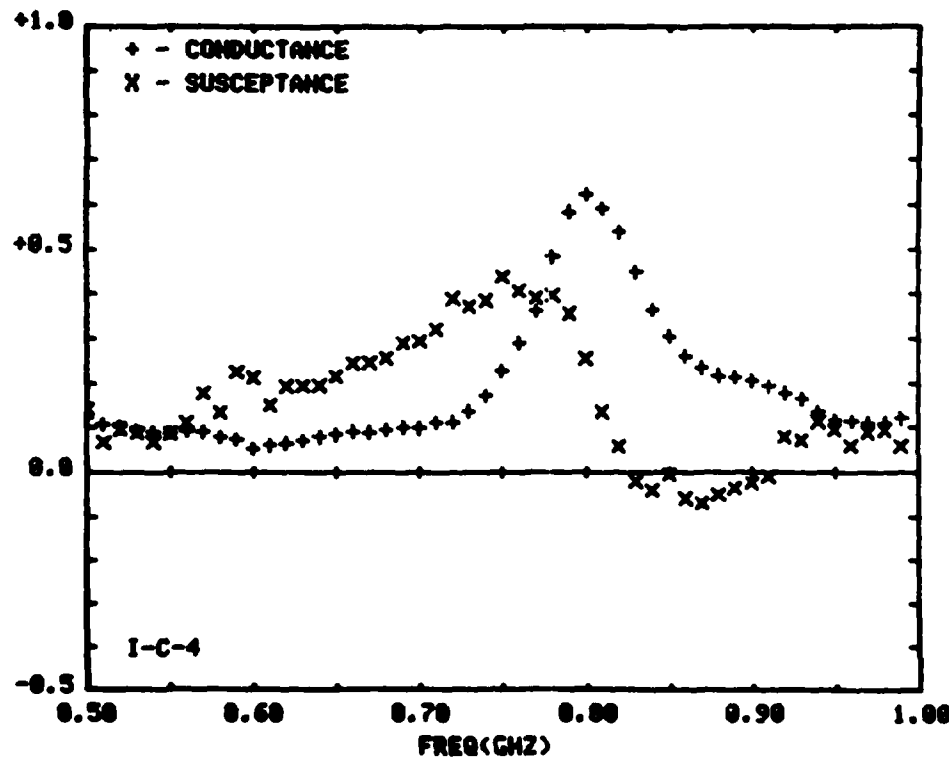


FIGURE 4-32

Aperture Admittance of Sleeve Monopole
Antenna Above Salt Water (I-C-4)

FREQ. (GHZ)	G1	B1	FREQ. (GHZ)	G1	B1
0.500	+0.891	+0.114	0.750	+0.145	+0.065
0.510	+0.884	+0.050	0.760	+0.141	+0.044
0.520	+0.891	+0.083	0.770	+0.131	+0.039
0.530	+0.890	+0.077	0.780	+0.137	+0.062
0.540	+0.891	+0.059	0.790	+0.127	+0.116
0.550	+0.894	+0.055	0.800	+0.117	+0.136
0.560	+0.899	+0.107	0.810	+0.100	+0.134
0.570	+0.897	+0.175	0.820	+0.088	+0.172
0.580	+0.891	+0.131	0.830	+0.094	+0.160
0.590	+0.891	+0.226	0.840	+0.092	+0.171
0.600	+0.872	+0.219	0.850	+0.086	+0.231
0.610	+0.881	+0.161	0.860	+0.085	+0.187
0.620	+0.896	+0.209	0.870	+0.096	+0.174
0.630	+0.110	+0.216	0.880	+0.090	+0.203
0.640	+0.133	+0.217	0.890	+0.112	+0.226
0.650	+0.161	+0.248	0.900	+0.126	+0.237
0.660	+0.208	+0.283	0.910	+0.139	+0.264
0.670	+0.249	+0.270	0.920	+0.155	+0.363
0.680	+0.303	+0.236	0.930	+0.175	+0.352
0.690	+0.341	+0.189	0.940	+0.190	+0.412
0.700	+0.331	+0.121	0.950	+0.227	+0.380
0.710	+0.282	+0.068	0.960	+0.279	+0.399
0.720	+0.229	+0.000	0.970	+0.332	+0.280
0.730	+0.188	+0.046	0.980	+0.366	+0.290
0.740	+0.155	+0.050	0.990	+0.356	+0.093
			1.000	+0.320	+0.052

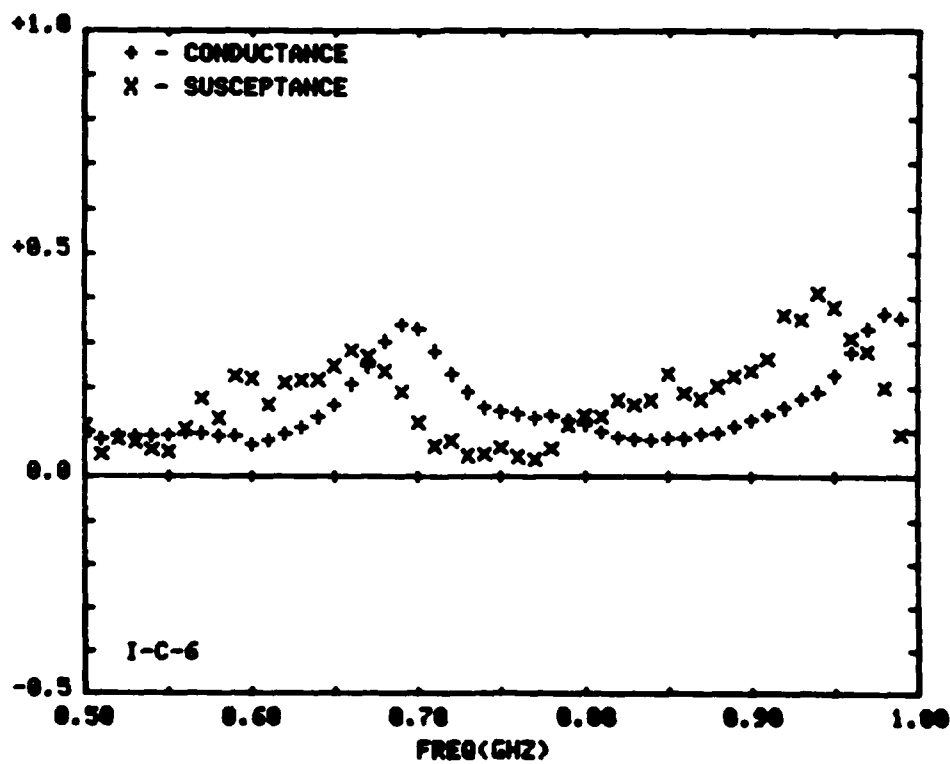


FIGURE 4-33

Aperture Admittance of Sleeve Monopole
Antenna Above Salt Water (I-C-6)

FREQ. (GHZ)	G1	B1	FREQ. (GHZ)	G1	B1
0.500	+0.103	+0.127	0.750	+0.334	+0.473
0.510	+0.101	+0.062	0.760	+0.405	+0.446
0.520	+0.107	+0.096	0.770	+0.459	+0.431
0.530	+0.111	+0.090	0.780	+0.560	+0.448
0.540	+0.115	+0.074	0.790	+0.637	+0.441
0.550	+0.116	+0.072	0.800	+0.689	+0.388
0.560	+0.122	+0.126	0.810	+0.703	+0.312
0.570	+0.121	+0.191	0.820	+0.708	+0.229
0.580	+0.114	+0.150	0.830	+0.668	+0.133
0.590	+0.108	+0.248	0.840	+0.607	+0.061
0.600	+0.091	+0.233	0.850	+0.532	+0.029
0.610	+0.098	+0.173	0.860	+0.519	-0.057
0.620	+0.103	+0.229	0.870	+0.476	-0.097
0.630	+0.111	+0.228	0.880	+0.438	-0.098
0.640	+0.123	+0.232	0.890	+0.420	-0.099
0.650	+0.134	+0.261	0.900	+0.397	-0.090
0.660	+0.146	+0.296	0.910	+0.376	-0.075
0.670	+0.149	+0.302	0.920	+0.348	+0.002
0.680	+0.158	+0.325	0.930	+0.320	+0.006
0.690	+0.164	+0.368	0.940	+0.272	+0.047
0.700	+0.173	+0.366	0.950	+0.245	+0.032
0.710	+0.189	+0.392	0.960	+0.235	+0.001
0.720	+0.204	+0.461	0.970	+0.220	+0.032
0.730	+0.236	+0.433	0.980	+0.214	+0.038
0.740	+0.276	+0.447	0.990	+0.210	+0.002
			1.000	+0.220	+0.000

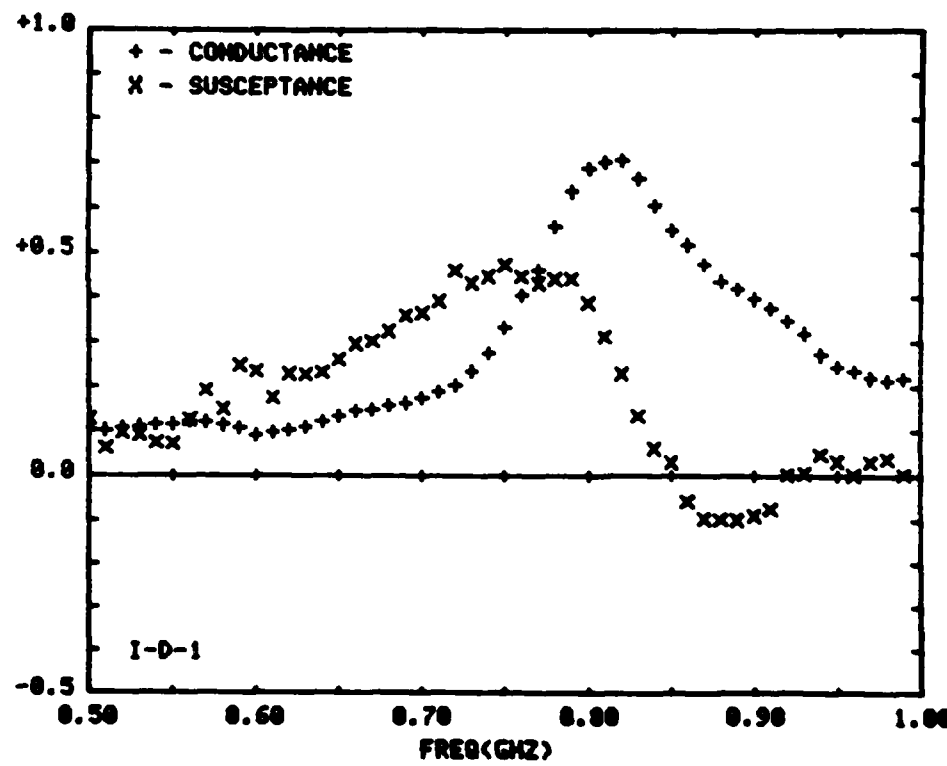


FIGURE 4-34

Aperture Admittance of Sleeve Monopole
Antenna Above Salt Water (I-D-1)

FREQ. (GHZ)	G1	B1	FREQ. (GHZ)	G1	B1
0.500	+0.067	+0.105	0.750	+0.162	+0.020
0.510	+0.072	+0.049	0.760	+0.162	+0.012
0.520	+0.079	+0.079	0.770	+0.156	+0.001
0.530	+0.082	+0.088	0.780	+0.163	+0.017
0.540	+0.091	+0.041	0.790	+0.155	+0.036
0.550	+0.094	+0.062	0.800	+0.143	+0.053
0.560	+0.105	+0.114	0.810	+0.128	+0.063
0.570	+0.108	+0.155	0.820	+0.119	+0.098
0.580	+0.102	+0.139	0.830	+0.109	+0.058
0.590	+0.106	+0.210	0.840	+0.104	+0.065
0.600	+0.096	+0.202	0.850	+0.100	+0.117
0.610	+0.115	+0.166	0.860	+0.095	+0.086
0.620	+0.137	+0.214	0.870	+0.104	+0.067
0.630	+0.163	+0.188	0.880	+0.102	+0.055
0.640	+0.202	+0.171	0.890	+0.112	+0.064
0.650	+0.241	+0.169	0.900	+0.123	+0.065
0.660	+0.280	+0.156	0.910	+0.122	+0.072
0.670	+0.300	+0.120	0.920	+0.114	+0.153
0.680	+0.304	+0.073	0.930	+0.108	+0.135
0.690	+0.293	+0.058	0.940	+0.086	+0.173
0.700	+0.264	+0.037	0.950	+0.074	+0.172
0.710	+0.232	+0.028	0.960	+0.066	+0.102
0.720	+0.201	+0.049	0.970	+0.085	+0.126
0.730	+0.182	+0.017	0.980	+0.084	+0.128
0.740	+0.166	+0.014	0.990	+0.095	+0.112
			1.000	+0.104	+0.109

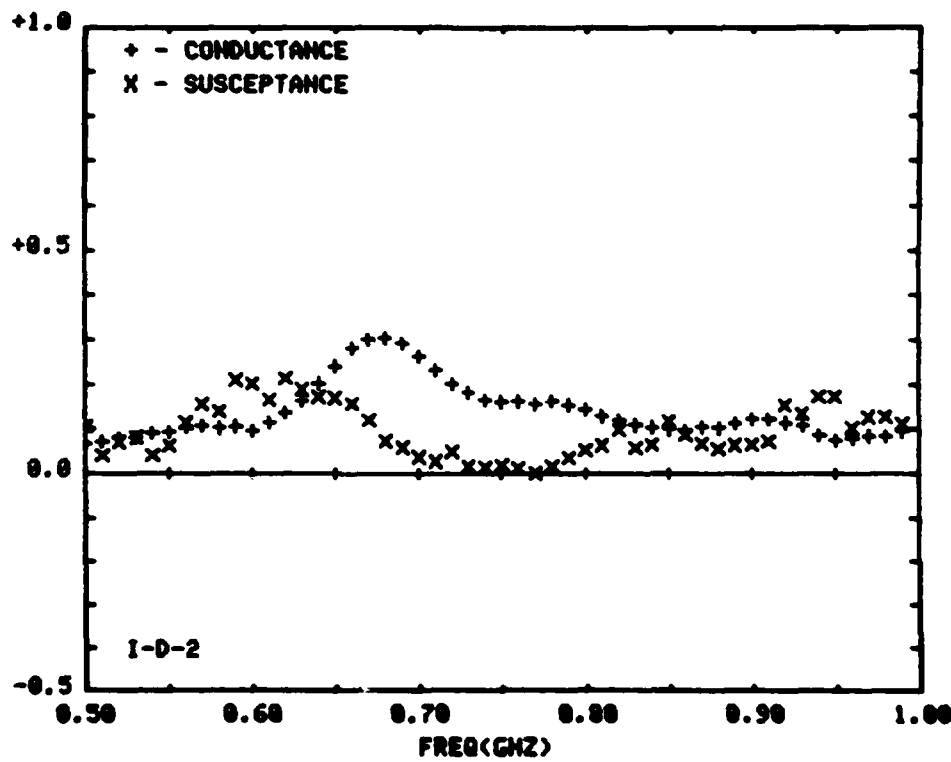


FIGURE 4-35

Aperture Admittance of Sleeve Monopole
Antenna Above Salt Water (I-D-2)

FREQ. (GHZ)	G1	B1	FREQ. (GHZ)	G1	B1
0.500	+0.950	+0.130	0.750	+0.970	+0.245
0.510	+0.956	+0.083	0.760	+0.979	+0.215
0.520	+0.964	+0.092	0.770	+0.986	+0.202
0.530	+0.962	+0.099	0.780	+0.102	+0.243
0.540	+0.968	+0.052	0.790	+0.999	+0.293
0.550	+0.972	+0.065	0.800	+0.100	+0.301
0.560	+0.976	+0.093	0.810	+0.089	+0.317
0.570	+0.973	+0.155	0.820	+0.078	+0.351
0.580	+0.968	+0.107	0.830	+0.095	+0.319
0.590	+0.961	+0.192	0.840	+0.108	+0.354
0.600	+0.940	+0.174	0.850	+0.126	+0.392
0.610	+0.950	+0.130	0.860	+0.149	+0.365
0.620	+0.953	+0.151	0.870	+0.176	+0.362
0.630	+0.959	+0.148	0.880	+0.219	+0.416
0.640	+0.964	+0.145	0.890	+0.273	+0.425
0.650	+0.972	+0.158	0.900	+0.315	+0.399
0.660	+0.971	+0.180	0.910	+0.386	+0.422
0.670	+0.968	+0.172	0.920	+0.466	+0.449
0.680	+0.975	+0.145	0.930	+0.482	+0.365
0.690	+0.970	+0.194	0.940	+0.484	+0.315
0.700	+0.964	+0.192	0.950	+0.456	+0.265
0.710	+0.965	+0.205	0.960	+0.409	+0.105
0.720	+0.949	+0.231	0.970	+0.358	+0.092
0.730	+0.956	+0.229	0.980	+0.320	+0.038
0.740	+0.957	+0.221	0.990	+0.297	+0.009
			1.000	+0.275	+0.010

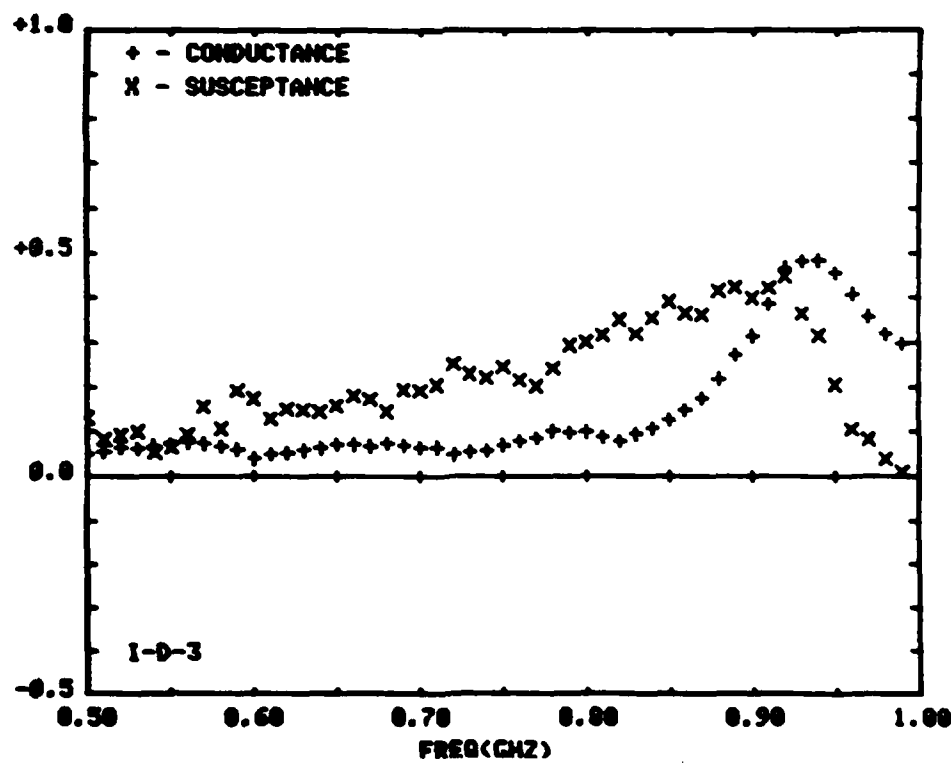


FIGURE 4-36

Aperture Admittance of Sleeve Monopole
Antenna Above Salt Water (I-D-3)

FREQ. (GHZ)	G1	B1	FREQ. (GHZ)	G1	B1
0.500	+0.121	+0.132	0.750	+0.226	+0.425
0.510	+0.108	+0.082	0.760	+0.300	+0.420
0.520	+0.102	+0.089	0.770	+0.367	+0.406
0.530	+0.094	+0.103	0.780	+0.490	+0.411
0.540	+0.091	+0.058	0.790	+0.576	+0.346
0.550	+0.089	+0.075	0.800	+0.623	+0.254
0.560	+0.093	+0.129	0.810	+0.596	+0.148
0.570	+0.091	+0.164	0.820	+0.536	+0.071
0.580	+0.088	+0.150	0.830	+0.450	-0.025
0.590	+0.074	+0.217	0.840	+0.365	-0.045
0.600	+0.053	+0.202	0.850	+0.305	-0.012
0.610	+0.058	+0.168	0.860	+0.262	-0.045
0.620	+0.066	+0.210	0.870	+0.236	-0.056
0.630	+0.073	+0.210	0.880	+0.217	-0.057
0.640	+0.080	+0.188	0.890	+0.214	-0.039
0.650	+0.085	+0.210	0.900	+0.205	-0.039
0.660	+0.092	+0.239	0.910	+0.193	+0.007
0.670	+0.089	+0.244	0.920	+0.178	+0.071
0.680	+0.099	+0.241	0.930	+0.164	+0.065
0.690	+0.102	+0.307	0.940	+0.137	+0.105
0.700	+0.100	+0.313	0.950	+0.118	+0.113
0.710	+0.112	+0.312	0.960	+0.110	+0.048
0.720	+0.112	+0.379	0.970	+0.111	+0.083
0.730	+0.136	+0.359	0.980	+0.111	+0.085
0.740	+0.170	+0.371	0.990	+0.122	+0.073
			1.000	+0.129	+0.072

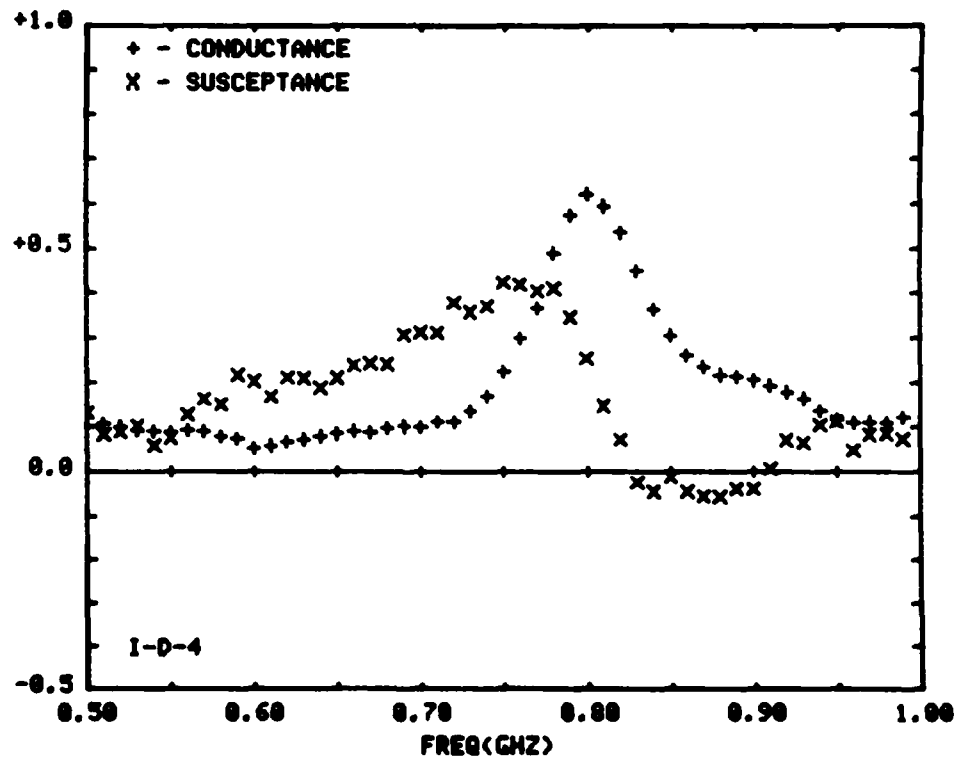


FIGURE 4-37

Aperture Admittance of Sleeve Monopole
Antenna Above Salt Water (I-D-4)

FREQ. (GHZ)	G1	B1	FREQ. (GHZ)	G1	B1
0.500	+0.891	+0.118	0.750	+0.178	+0.625
0.510	+0.884	+0.058	0.760	+0.162	+0.626
0.520	+0.891	+0.088	0.770	+0.156	+0.616
0.530	+0.888	+0.095	0.780	+0.153	+0.649
0.540	+0.892	+0.070	0.790	+0.139	+0.181
0.550	+0.894	+0.064	0.800	+0.121	+0.188
0.560	+0.899	+0.112	0.810	+0.112	+0.121
0.570	+0.897	+0.181	0.820	+0.095	+0.158
0.580	+0.891	+0.140	0.830	+0.091	+0.145
0.590	+0.888	+0.234	0.840	+0.088	+0.156
0.600	+0.865	+0.198	0.850	+0.091	+0.189
0.610	+0.881	+0.166	0.860	+0.087	+0.168
0.620	+0.890	+0.212	0.870	+0.094	+0.157
0.630	+0.898	+0.223	0.880	+0.097	+0.181
0.640	+0.122	+0.223	0.890	+0.111	+0.202
0.650	+0.150	+0.254	0.900	+0.119	+0.216
0.660	+0.181	+0.269	0.910	+0.127	+0.231
0.670	+0.213	+0.272	0.920	+0.135	+0.333
0.680	+0.270	+0.248	0.930	+0.141	+0.320
0.690	+0.335	+0.261	0.940	+0.139	+0.352
0.700	+0.360	+0.198	0.950	+0.154	+0.364
0.710	+0.339	+0.119	0.960	+0.199	+0.389
0.720	+0.290	+0.897	0.970	+0.245	+0.299
0.730	+0.240	+0.043	0.980	+0.305	+0.257
0.740	+0.194	+0.012	0.990	+0.338	+0.177
			1.000	+0.346	+0.120

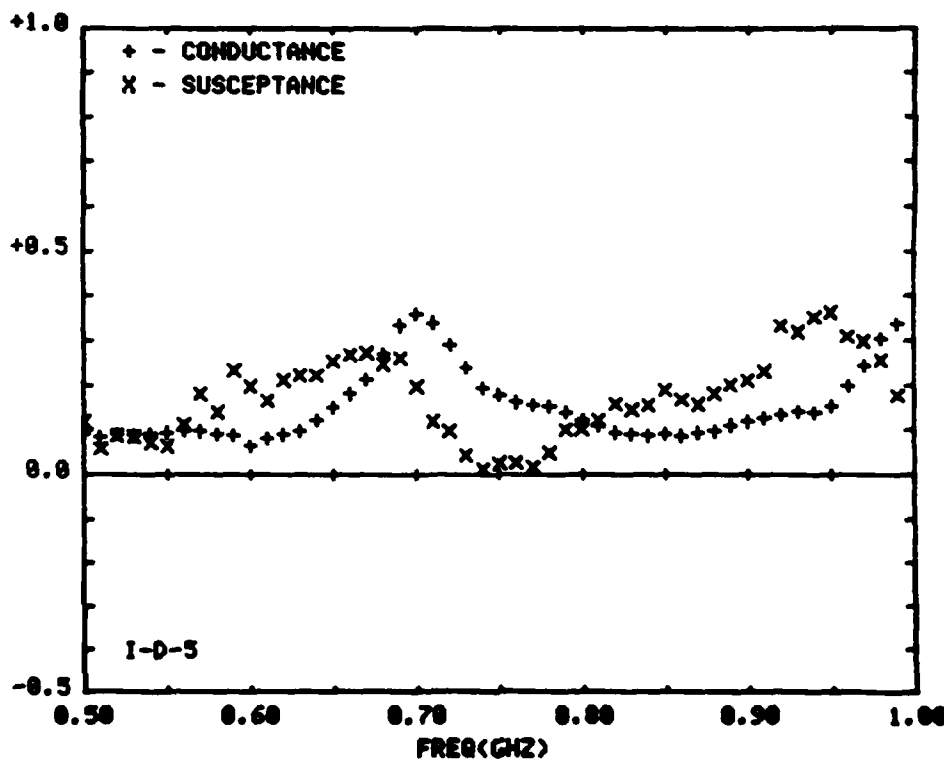


FIGURE 4-38

Aperture Admittance of Sleeve Monopole
Antenna Above Salt Water (I-D-5)

FREQ. (GHZ)	G1	B1	FREQ. (GHZ)	G1	B1
0.500	+0.076	+0.038	0.750	+0.306	+0.371
0.510	+0.094	-0.012	0.760	+0.375	+0.350
0.520	+0.091	+0.014	0.770	+0.448	+0.320
0.530	+0.091	+0.046	0.780	+0.517	+0.327
0.540	+0.098	-0.007	0.790	+0.573	+0.244
0.550	+0.093	-0.014	0.800	+0.637	+0.155
0.560	+0.090	+0.041	0.810	+0.652	+0.091
0.570	+0.096	+0.018	0.820	+0.636	-0.002
0.580	+0.091	+0.007	0.830	+0.616	-0.128
0.590	+0.077	+0.068	0.840	+0.579	-0.167
0.600	+0.071	+0.059	0.850	+0.481	-0.155
0.610	+0.091	+0.046	0.860	+0.440	-0.213
0.620	+0.084	+0.130	0.870	+0.411	-0.247
0.630	+0.098	+0.144	0.880	+0.363	-0.215
0.640	+0.111	+0.093	0.890	+0.330	-0.214
0.650	+0.111	+0.141	0.900	+0.326	-0.238
0.660	+0.115	+0.183	0.910	+0.302	-0.216
0.670	+0.120	+0.147	0.920	+0.263	-0.182
0.680	+0.126	+0.136	0.930	+0.253	-0.193
0.690	+0.134	+0.219	0.940	+0.229	-0.144
0.700	+0.147	+0.186	0.950	+0.198	-0.146
0.710	+0.171	+0.235	0.960	+0.207	-0.196
0.720	+0.174	+0.311	0.970	+0.263	-0.121
0.730	+0.221	+0.282	0.980	+0.178	-0.079
0.740	+0.259	+0.320	0.990	+0.179	-0.136
			1.000	+0.192	-0.120

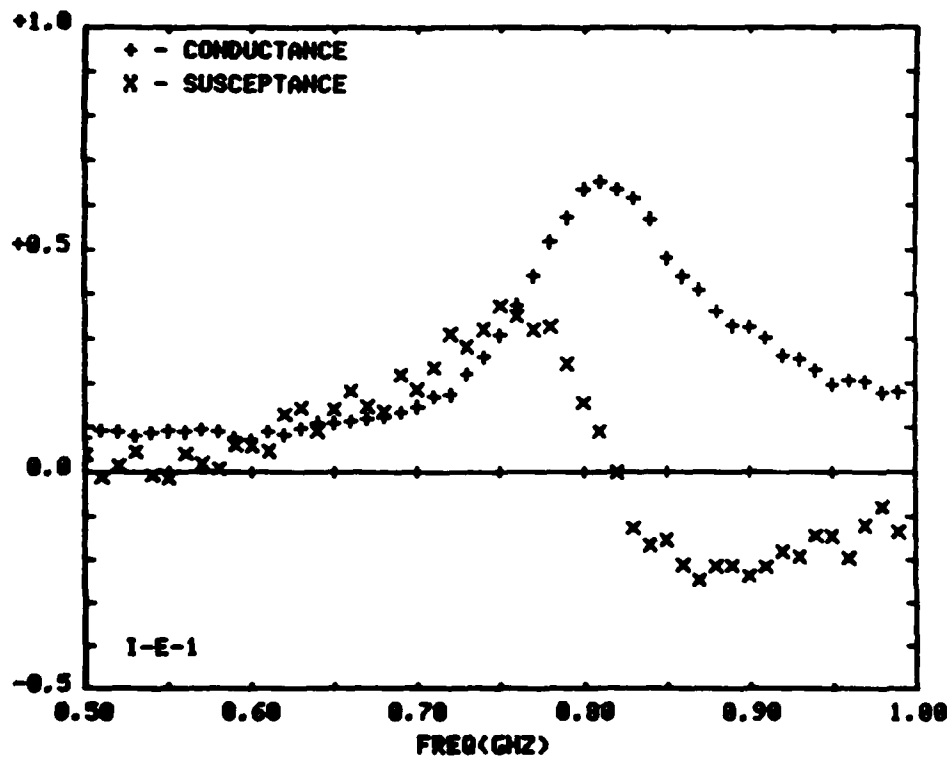


FIGURE 4-39

Aperture Admittance of Sleeve Monopole
Antenna Above Salt Water (I-E-1)

FREQ. (GHZ)	G1	B1	FREQ. (GHZ)	G1	B1
0.500	+0.846	-0.818	0.750	+0.892	+0.828
0.510	+0.865	-0.809	0.760	+0.896	+0.821
0.520	+0.864	-0.810	0.770	+0.104	-0.027
0.530	+0.858	+0.845	0.780	+0.105	+0.810
0.540	+0.865	-0.814	0.790	+0.107	+0.802
0.550	+0.876	-0.825	0.800	+0.097	-0.024
0.560	+0.876	+0.825	0.810	+0.085	-0.008
0.570	+0.884	-0.803	0.820	+0.073	+0.028
0.580	+0.886	-0.804	0.830	+0.061	-0.030
0.590	+0.874	+0.039	0.840	+0.082	-0.001
0.600	+0.877	+0.037	0.850	+0.074	+0.064
0.610	+0.114	+0.015	0.860	+0.080	+0.017
0.620	+0.123	+0.005	0.870	+0.084	+0.014
0.630	+0.148	+0.082	0.880	+0.084	+0.040
0.640	+0.172	+0.001	0.890	+0.085	+0.027
0.650	+0.172	+0.012	0.900	+0.100	-0.023
0.660	+0.161	+0.030	0.910	+0.100	+0.044
0.670	+0.164	-0.036	0.920	+0.089	+0.037
0.680	+0.153	-0.097	0.930	+0.089	+0.009
0.690	+0.134	-0.012	0.940	+0.083	+0.077
0.700	+0.128	-0.058	0.950	+0.070	+0.085
0.710	+0.121	-0.051	0.960	+0.067	+0.012
0.720	+0.092	+0.031	0.970	+0.099	+0.075
0.730	+0.097	-0.003	0.980	+0.094	+0.100
0.740	+0.095	-0.026	0.990	+0.110	+0.053
			1.000	+0.126	+0.072

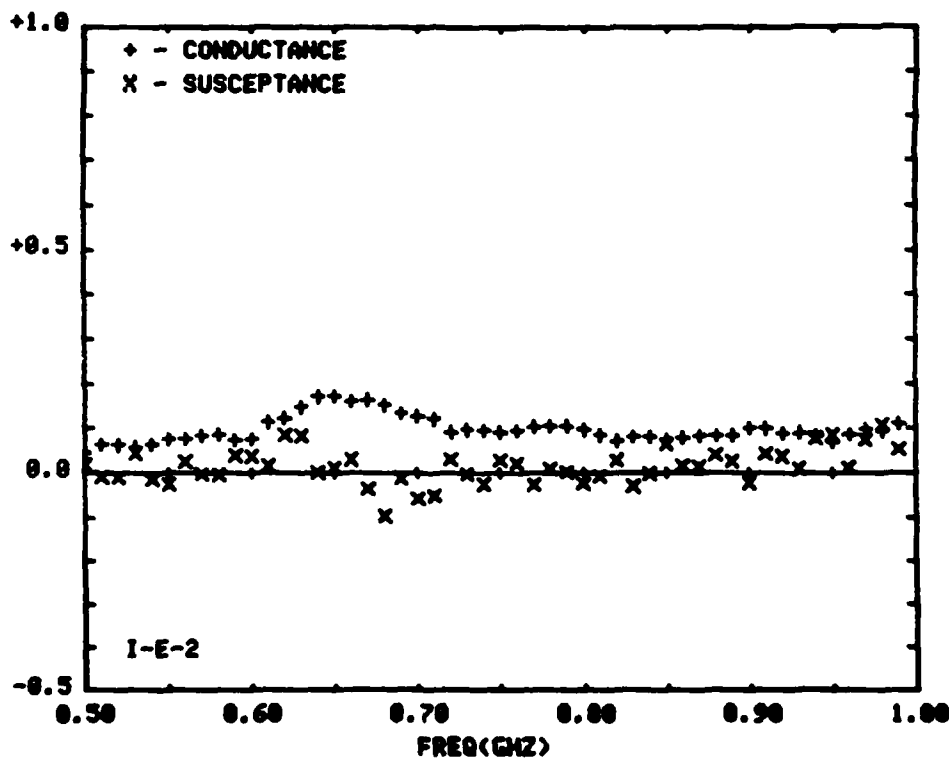


FIGURE 4-40

Aperture Admittance of Sleeve Monopole
Antenna Above Salt Water (I-E-2)

FREQ. (GHZ)	G1	B1	FREQ. (GHZ)	G1	B1
0.500	+0.041	+0.049	0.750	+0.057	+0.161
0.510	+0.060	+0.024	0.760	+0.073	+0.148
0.520	+0.059	+0.020	0.770	+0.082	+0.112
0.530	+0.053	+0.071	0.780	+0.094	+0.155
0.540	+0.059	-0.012	0.790	+0.092	+0.168
0.550	+0.065	-0.003	0.800	+0.088	+0.127
0.560	+0.062	+0.020	0.810	+0.082	+0.168
0.570	+0.068	+0.019	0.820	+0.075	+0.201
0.580	+0.063	-0.017	0.830	+0.096	+0.150
0.590	+0.046	+0.049	0.840	+0.109	+0.206
0.600	+0.034	+0.043	0.850	+0.119	+0.271
0.610	+0.053	+0.017	0.860	+0.148	+0.235
0.620	+0.058	+0.069	0.870	+0.178	+0.262
0.630	+0.054	+0.078	0.880	+0.217	+0.329
0.640	+0.067	+0.045	0.890	+0.261	+0.309
0.650	+0.066	+0.077	0.900	+0.321	+0.265
0.660	+0.059	+0.113	0.910	+0.394	+0.307
0.670	+0.065	+0.066	0.920	+0.465	+0.253
0.680	+0.063	+0.033	0.930	+0.525	+0.143
0.690	+0.062	+0.087	0.940	+0.532	+0.092
0.700	+0.063	+0.045	0.950	+0.490	-0.006
0.710	+0.067	+0.068	0.960	+0.444	-0.132
0.720	+0.046	+0.149	0.970	+0.388	-0.124
0.730	+0.056	+0.117	0.980	+0.315	-0.185
0.740	+0.064	+0.129	0.990	+0.292	-0.149
			1.000	+0.268	-0.134

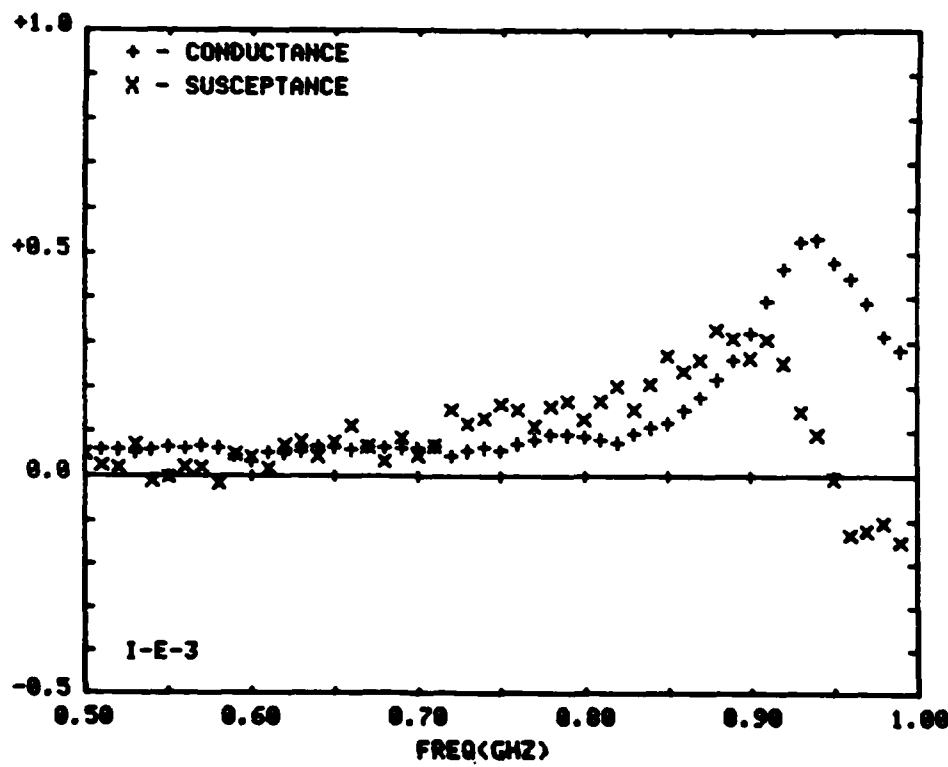


FIGURE 4-41

Aperture Admittance of Sleeve Monopole
Antenna Above Salt Water (I-E-3)

FREQ. (GHZ)	G1	B1	FREQ. (GHZ)	G1	B1
0.500	+0.069	+0.008	0.750	+0.131	-0.006
0.510	+0.088	-0.012	0.760	+0.122	-0.002
0.520	+0.086	-0.007	0.770	+0.125	-0.024
0.530	+0.078	+0.051	0.780	+0.121	+0.003
0.540	+0.076	-0.029	0.790	+0.118	-0.003
0.550	+0.082	-0.014	0.800	+0.103	-0.004
0.560	+0.079	+0.036	0.810	+0.098	+0.018
0.570	+0.085	+0.010	0.820	+0.075	+0.040
0.580	+0.088	+0.011	0.830	+0.084	+0.007
0.590	+0.061	+0.053	0.840	+0.084	+0.042
0.600	+0.053	+0.053	0.850	+0.080	+0.095
0.610	+0.080	+0.039	0.860	+0.088	+0.071
0.620	+0.073	+0.125	0.870	+0.093	+0.081
0.630	+0.092	+0.136	0.880	+0.101	+0.102
0.640	+0.116	+0.090	0.890	+0.104	+0.108
0.650	+0.128	+0.142	0.900	+0.125	+0.083
0.660	+0.151	+0.186	0.910	+0.136	+0.149
0.670	+0.196	+0.141	0.920	+0.142	+0.159
0.680	+0.242	+0.095	0.930	+0.165	+0.166
0.690	+0.290	+0.105	0.940	+0.201	+0.241
0.700	+0.306	+0.004	0.950	+0.241	+0.240
0.710	+0.274	-0.041	0.960	+0.317	+0.131
0.720	+0.211	-0.034	0.970	+0.393	+0.145
0.730	+0.179	-0.041	0.980	+0.397	+0.070
0.740	+0.154	-0.048	0.990	+0.376	-0.056
			1.000	+0.340	-0.090

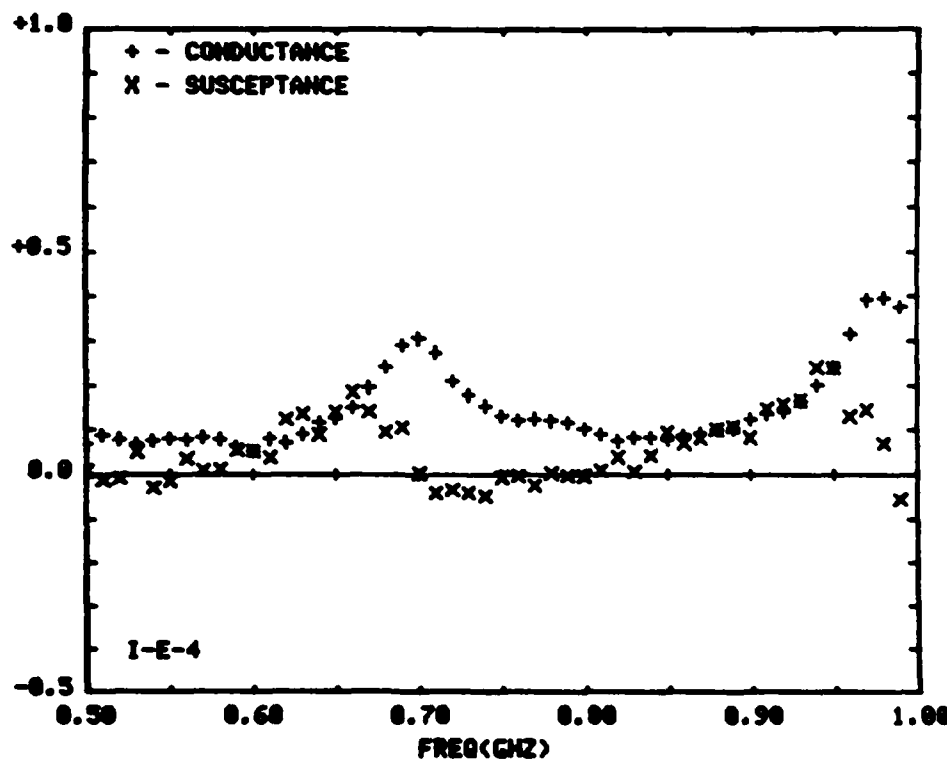


FIGURE 4-42

Aperture Admittance of Sleeve Monopole
Antenna Above Salt Water (I-E-4)

FREQ. (GHZ)	G1	B1	FREQ. (GHZ)	G1	B1
0.500	+0.071	+0.033	0.750	+0.370	+0.377
0.510	+0.097	-0.024	0.760	+0.411	+0.328
0.520	+0.093	+0.003	0.770	+0.500	+0.251
0.530	+0.084	+0.072	0.780	+0.618	+0.294
0.540	+0.093	-0.018	0.790	+0.596	+0.199
0.550	+0.104	-0.007	0.800	+0.628	+0.039
0.560	+0.118	+0.072	0.810	+0.668	-0.023
0.570	+0.079	+0.031	0.820	+0.596	-0.055
0.580	+0.111	+0.004	0.830	+0.534	-0.175
0.590	+0.093	+0.107	0.840	+0.517	-0.284
0.600	+0.078	+0.069	0.850	+0.452	-0.132
0.610	+0.108	+0.043	0.860	+0.374	-0.196
0.620	+0.099	+0.136	0.870	+0.371	-0.244
0.630	+0.098	+0.142	0.880	+0.356	-0.172
0.640	+0.109	+0.111	0.890	+0.304	-0.186
0.650	+0.135	+0.206	0.900	+0.295	-0.228
0.660	+0.123	+0.192	0.910	+0.308	-0.183
0.670	+0.125	+0.118	0.920	+0.263	-0.166
0.680	+0.168	+0.178	0.930	+0.239	-0.182
0.690	+0.149	+0.231	0.940	+0.247	-0.128
0.700	+0.168	+0.192	0.950	+0.221	-0.119
0.710	+0.212	+0.256	0.960	+0.198	-0.145
0.720	+0.218	+0.345	0.970	+0.214	-0.198
0.730	+0.243	+0.307	0.980	+0.199	-0.057
0.740	+0.312	+0.321	0.990	+0.181	-0.101
			1.000	+0.198	-0.113

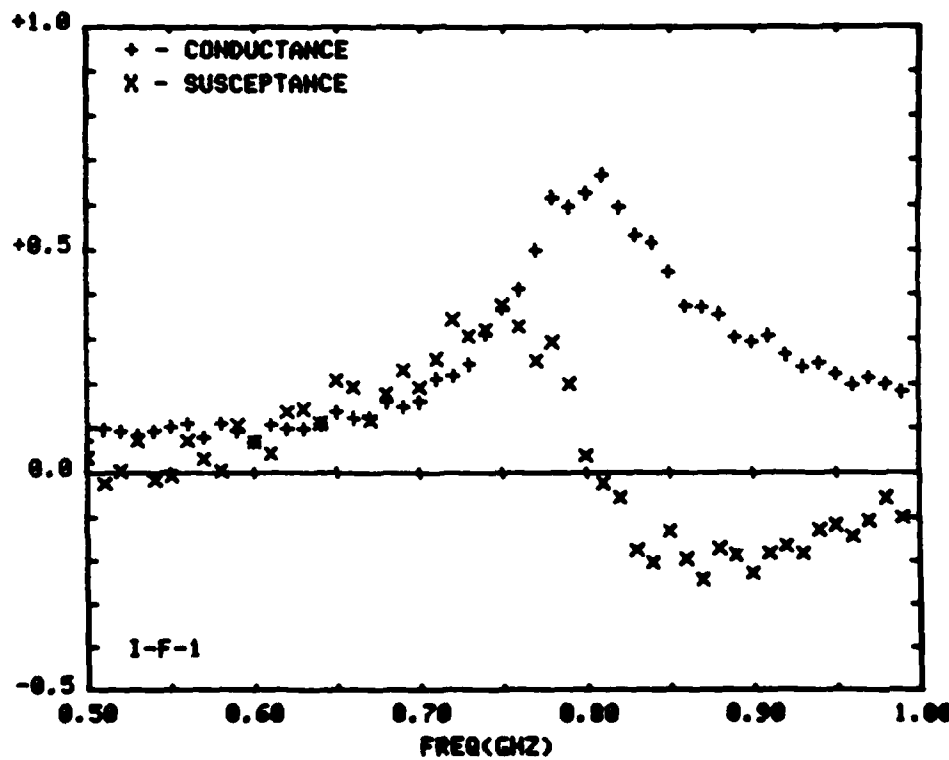


FIGURE 4-43

Aperture Admittance of Sleeve Monopole
Antenna Above Salt Water (I-F-1)

FREQ. (GHZ)	G1	B1	FREQ. (GHZ)	G1	B1
0.500	+0.049	+0.047	0.750	+0.116	+0.068
0.510	+0.070	-0.029	0.760	+0.107	+0.029
0.520	+0.070	+0.007	0.770	+0.114	-0.025
0.530	+0.061	+0.054	0.780	+0.133	+0.088
0.540	+0.076	-0.035	0.790	+0.103	+0.042
0.550	+0.086	-0.005	0.800	+0.098	-0.027
0.560	+0.093	+0.046	0.810	+0.122	+0.021
0.570	+0.067	+0.007	0.820	+0.108	+0.043
0.580	+0.099	-0.009	0.830	+0.091	-0.006
0.590	+0.087	+0.073	0.840	+0.106	+0.036
0.600	+0.075	+0.053	0.850	+0.188	+0.095
0.610	+0.124	+0.029	0.860	+0.090	+0.021
0.620	+0.134	+0.100	0.870	+0.110	+0.026
0.630	+0.144	+0.074	0.880	+0.118	+0.081
0.640	+0.157	+0.007	0.890	+0.098	+0.045
0.650	+0.180	+0.071	0.900	+0.120	+0.001
0.660	+0.157	+0.055	0.910	+0.139	+0.053
0.670	+0.148	-0.047	0.920	+0.189	+0.054
0.680	+0.164	-0.030	0.930	+0.114	+0.048
0.690	+0.138	+0.021	0.940	+0.125	+0.109
0.700	+0.124	-0.053	0.950	+0.108	+0.087
0.710	+0.135	-0.035	0.960	+0.108	+0.052
0.720	+0.115	+0.041	0.970	+0.138	+0.108
0.730	+0.103	+0.013	0.980	+0.134	+0.140
0.740	+0.106	-0.023	0.990	+0.136	+0.064
			1.000	+0.167	+0.002

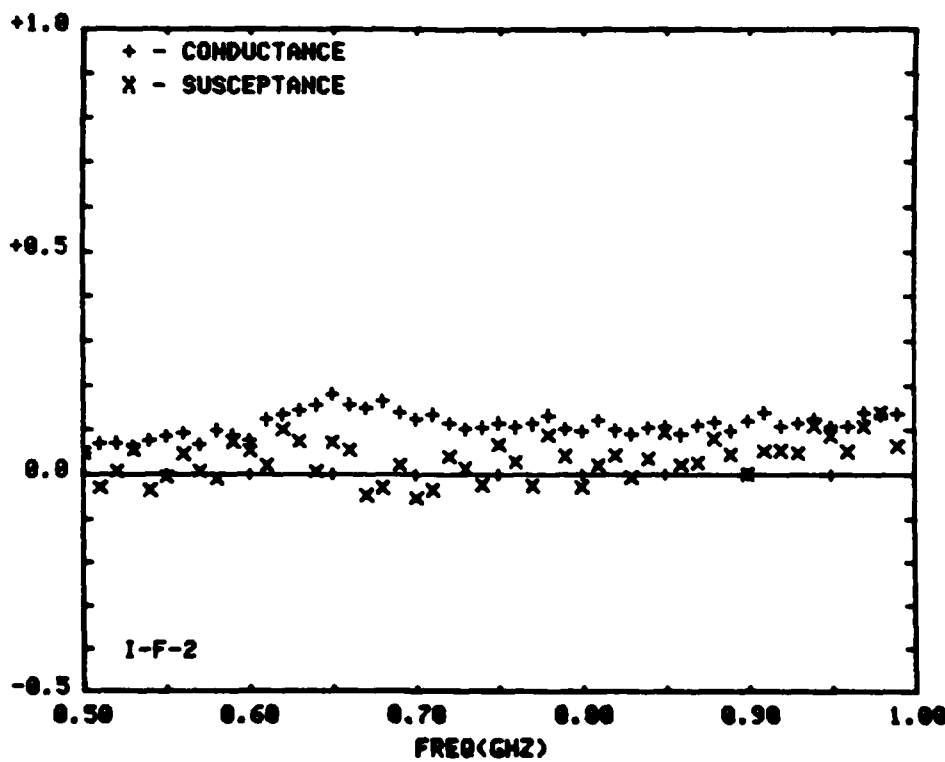


FIGURE 4-44

Aperture Admittance of Sleeve Monopole
Antenna Above Salt Water (I-F-2)

FREQ. (GHZ)	G1	B1	FREQ. (GHZ)	G1	B1
0.500	+0.841	+0.081	0.750	+0.887	+0.197
0.510	+0.871	-0.084	0.760	+0.884	+0.160
0.520	+0.864	+0.045	0.770	+0.894	+0.122
0.530	+0.856	+0.080	0.780	+0.122	+0.213
0.540	+0.866	-0.014	0.790	+0.094	+0.185
0.550	+0.880	+0.014	0.800	+0.898	+0.142
0.560	+0.881	+0.061	0.810	+0.122	+0.208
0.570	+0.851	+0.011	0.820	+0.104	+0.225
0.580	+0.876	-0.022	0.830	+0.116	+0.162
0.590	+0.855	+0.079	0.840	+0.147	+0.242
0.600	+0.841	+0.058	0.850	+0.158	+0.300
0.610	+0.874	+0.028	0.860	+0.170	+0.260
0.620	+0.863	+0.083	0.870	+0.235	+0.302
0.630	+0.862	+0.090	0.880	+0.267	+0.326
0.640	+0.867	+0.049	0.890	+0.287	+0.293
0.650	+0.888	+0.138	0.900	+0.392	+0.273
0.660	+0.869	+0.129	0.910	+0.486	+0.303
0.670	+0.866	+0.045	0.920	+0.497	+0.206
0.680	+0.890	+0.072	0.930	+0.561	+0.079
0.690	+0.872	+0.124	0.940	+0.578	+0.035
0.700	+0.868	+0.050	0.950	+0.484	-0.025
0.710	+0.866	+0.084	0.960	+0.414	-0.128
0.720	+0.866	+0.159	0.970	+0.391	-0.140
0.730	+0.867	+0.132	0.980	+0.320	-0.088
0.740	+0.873	+0.107	0.990	+0.265	-0.140
			1.000	+0.259	-0.129

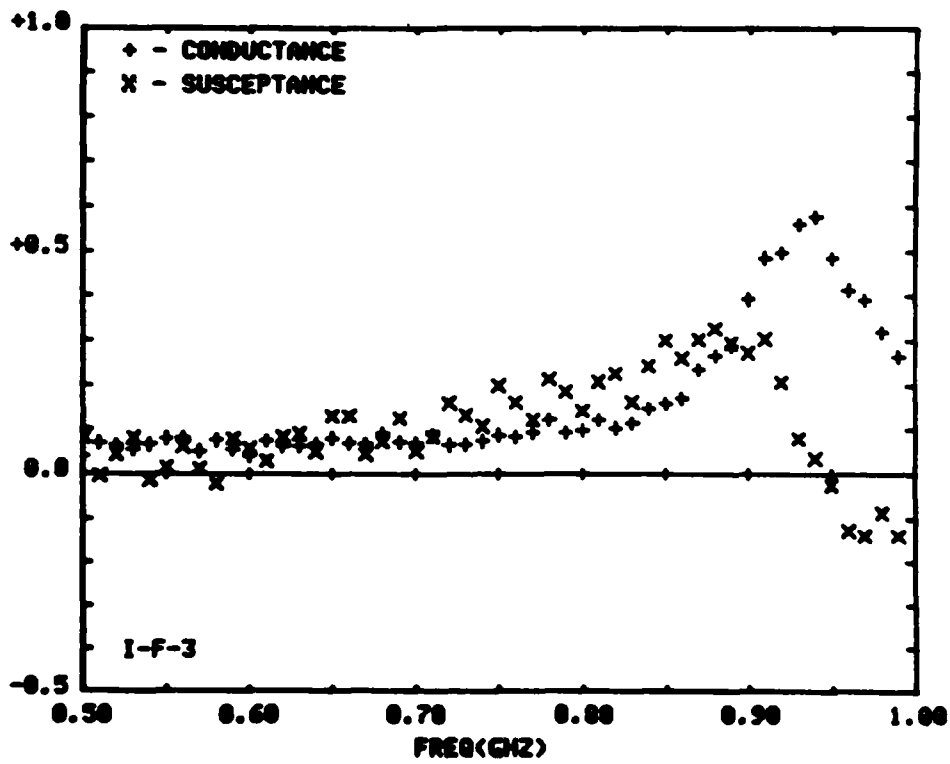


FIGURE 4-45

Aperture Admittance of Sleeve Monopole
Antenna Above Salt Water (I-F-3)

FREQ. (GHZ)	G1	B1	FREQ. (GHZ)	G1	B1
0.500	+0.065	+0.034	0.750	+0.133	+0.046
0.510	+0.088	-0.035	0.760	+0.112	+0.028
0.520	+0.082	+0.013	0.770	+0.114	-0.019
0.530	+0.067	+0.061	0.780	+0.136	+0.087
0.540	+0.076	-0.034	0.790	+0.109	+0.079
0.550	+0.086	-0.019	0.800	+0.093	+0.005
0.560	+0.087	+0.060	0.810	+0.116	+0.050
0.570	+0.056	-0.003	0.820	+0.099	+0.081
0.580	+0.087	-0.002	0.830	+0.091	+0.040
0.590	+0.068	+0.098	0.840	+0.106	+0.094
0.600	+0.047	+0.060	0.850	+0.113	+0.144
0.610	+0.096	+0.038	0.860	+0.099	+0.099
0.620	+0.099	+0.126	0.870	+0.122	+0.120
0.630	+0.103	+0.148	0.880	+0.141	+0.178
0.640	+0.125	+0.090	0.890	+0.127	+0.133
0.650	+0.178	+0.204	0.900	+0.163	+0.132
0.660	+0.185	+0.180	0.910	+0.214	+0.208
0.670	+0.230	+0.080	0.920	+0.210	+0.222
0.680	+0.298	+0.058	0.930	+0.272	+0.196
0.690	+0.276	+0.051	0.940	+0.369	+0.253
0.700	+0.233	-0.051	0.950	+0.482	+0.202
0.710	+0.218	-0.055	0.960	+0.437	+0.060
0.720	+0.173	+0.022	0.970	+0.456	-0.020
0.730	+0.136	-0.001	0.980	+0.389	-0.037
0.740	+0.124	-0.046	0.990	+0.307	-0.123
			1.000	+0.206	-0.129

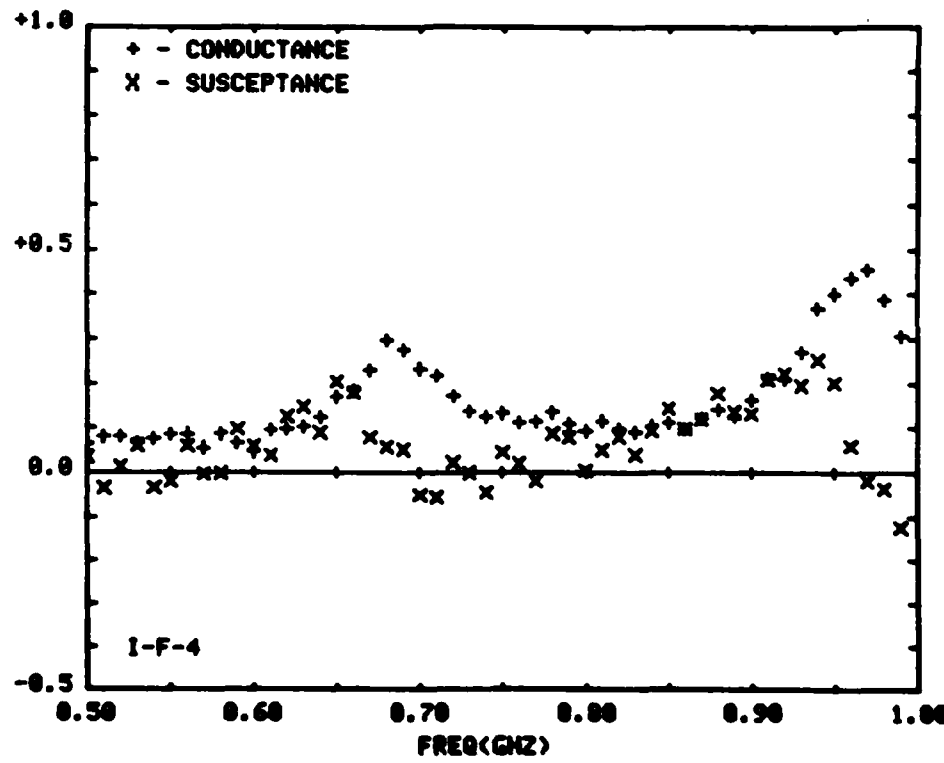


FIGURE 4-46

Aperture Admittance of Sleeve Monopole
Antenna Above Salt Water (I-F-4)

FREQ. (GHZ)	G1	B1	FREQ. (GHZ)	G1	B1
0.500	+0.065	+0.026	0.750	+0.367	+0.392
0.510	+0.092	-0.017	0.760	+0.405	+0.326
0.520	+0.098	+0.008	0.770	+0.503	+0.272
0.530	+0.078	+0.071	0.780	+0.611	+0.315
0.540	+0.087	-0.041	0.790	+0.595	+0.209
0.550	+0.098	+0.002	0.800	+0.634	+0.051
0.560	+0.098	+0.076	0.810	+0.675	0.000
0.570	+0.068	+0.019	0.820	+0.601	-0.039
0.580	+0.105	+0.017	0.830	+0.543	-0.175
0.590	+0.099	+0.093	0.840	+0.527	-0.291
0.600	+0.059	+0.077	0.850	+0.458	-0.137
0.610	+0.108	+0.058	0.860	+0.380	-0.203
0.620	+0.099	+0.147	0.870	+0.379	-0.257
0.630	+0.103	+0.133	0.880	+0.356	-0.185
0.640	+0.109	+0.103	0.890	+0.386	-0.298
0.650	+0.129	+0.197	0.900	+0.294	-0.227
0.660	+0.123	+0.199	0.910	+0.309	-0.168
0.670	+0.125	+0.123	0.920	+0.268	-0.172
0.680	+0.157	+0.197	0.930	+0.236	-0.185
0.690	+0.143	+0.217	0.940	+0.248	-0.133
0.700	+0.159	+0.178	0.950	+0.214	-0.106
0.710	+0.211	+0.241	0.960	+0.195	-0.151
0.720	+0.211	+0.327	0.970	+0.200	-0.113
0.730	+0.242	+0.302	0.980	+0.194	-0.058
0.740	+0.303	+0.320	0.990	+0.181	-0.105
			1.000	+0.193	-0.116

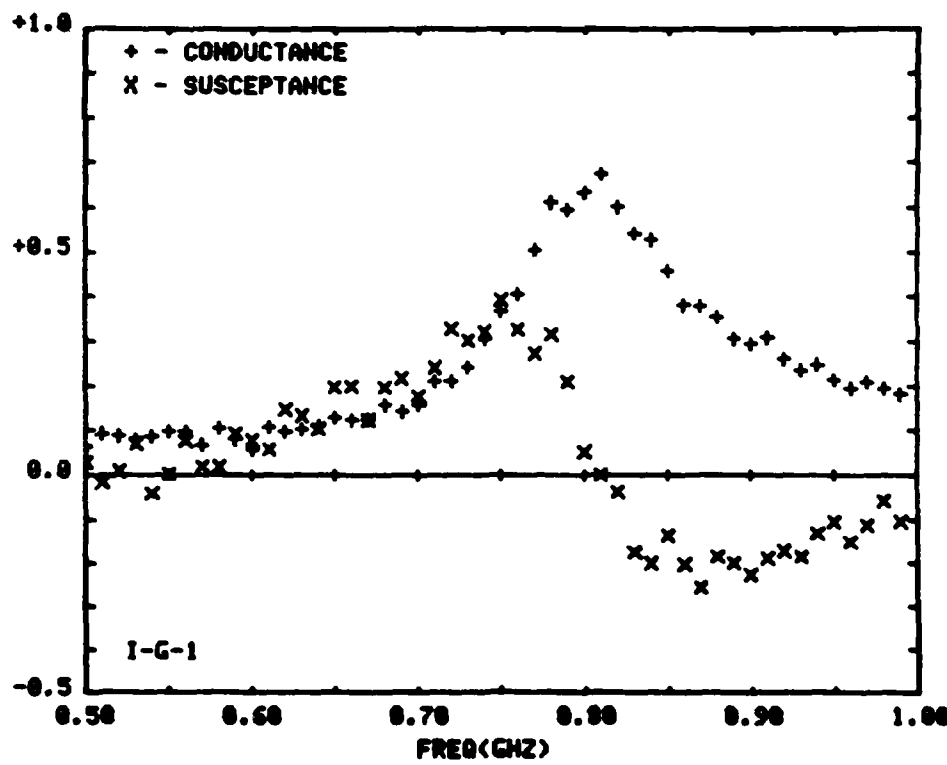


FIGURE 4-47

Aperture Admittance of Sleeve Monopole
Antenna Above Salt Water (I-G-1)

FREQ. (GHZ)	G1	B1	FREQ. (GHZ)	G1	B1
0.500	+0.049	+0.050	0.750	+0.110	+0.075
0.510	+0.075	-0.022	0.760	+0.102	+0.039
0.520	+0.070	-0.004	0.770	+0.110	-0.003
0.530	+0.061	+0.060	0.780	+0.130	+0.096
0.540	+0.076	-0.031	0.790	+0.103	+0.058
0.550	+0.086	-0.016	0.800	+0.093	-0.008
0.560	+0.093	+0.057	0.810	+0.116	+0.036
0.570	+0.067	+0.001	0.820	+0.099	+0.057
0.580	+0.099	-0.089	0.830	+0.091	-0.012
0.590	+0.087	+0.068	0.840	+0.100	+0.038
0.600	+0.075	+0.049	0.850	+0.102	+0.106
0.610	+0.124	+0.019	0.860	+0.086	+0.051
0.620	+0.128	+0.090	0.870	+0.100	+0.053
0.630	+0.133	+0.066	0.880	+0.118	+0.076
0.640	+0.143	+0.006	0.890	+0.092	+0.045
0.650	+0.163	+0.064	0.900	+0.114	+0.035
0.660	+0.146	+0.053	0.910	+0.128	+0.063
0.670	+0.137	-0.045	0.920	+0.115	+0.061
0.680	+0.150	-0.014	0.930	+0.121	+0.056
0.690	+0.124	+0.030	0.940	+0.137	+0.114
0.700	+0.113	-0.030	0.950	+0.114	+0.122
0.710	+0.129	-0.029	0.960	+0.117	+0.069
0.720	+0.109	+0.047	0.970	+0.149	+0.123
0.730	+0.095	+0.018	0.980	+0.152	+0.154
0.740	+0.101	-0.007	0.990	+0.150	+0.182
			1.000	+0.184	+0.186

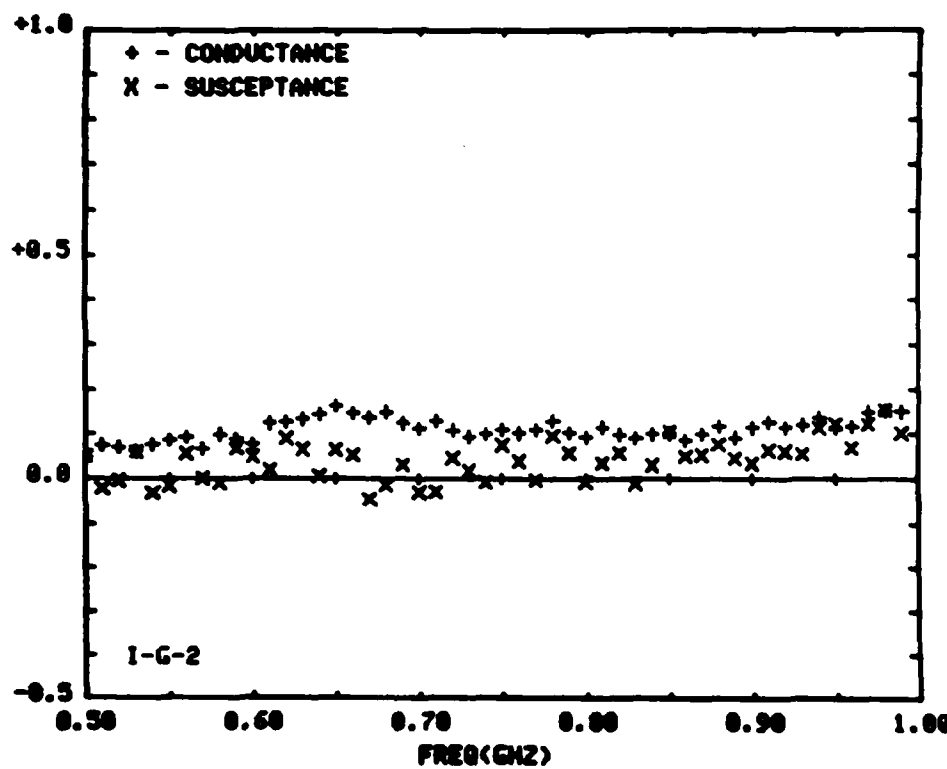


FIGURE 4-48

Aperture Admittance of Sleeve Monopole
Antenna Above Salt Water (I-G-2)

FREQ. (GHZ)	G1	B1	FREQ. (GHZ)	G1	B1
0.500	+0.838	+0.879	0.750	+0.887	+0.197
0.510	+0.863	+0.884	0.760	+0.884	+0.158
0.520	+0.864	+0.826	0.770	+0.895	+0.128
0.530	+0.856	+0.882	0.780	+0.123	+0.232
0.540	+0.866	-0.915	0.790	+0.100	+0.192
0.550	+0.874	-0.882	0.800	+0.098	+0.142
0.560	+0.875	+0.871	0.810	+0.129	+0.207
0.570	+0.845	+0.887	0.820	+0.110	+0.226
0.580	+0.876	-0.884	0.830	+0.120	+0.184
0.590	+0.849	+0.869	0.840	+0.147	+0.241
0.600	+0.827	+0.849	0.850	+0.161	+0.308
0.610	+0.874	+0.821	0.860	+0.171	+0.264
0.620	+0.863	+0.101	0.870	+0.235	+0.300
0.630	+0.866	+0.109	0.880	+0.267	+0.331
0.640	+0.867	+0.047	0.890	+0.293	+0.294
0.650	+0.889	+0.125	0.900	+0.402	+0.287
0.660	+0.875	+0.122	0.910	+0.489	+0.314
0.670	+0.871	+0.035	0.920	+0.499	+0.215
0.680	+0.890	+0.090	0.930	+0.569	+0.889
0.690	+0.872	+0.121	0.940	+0.590	+0.841
0.700	+0.869	+0.067	0.950	+0.502	-0.825
0.710	+0.888	+0.101	0.960	+0.430	-0.137
0.720	+0.866	+0.156	0.970	+0.401	-0.143
0.730	+0.867	+0.128	0.980	+0.330	-0.890
0.740	+0.874	+0.117	0.990	+0.276	-0.142
			1.000	+0.272	-0.156

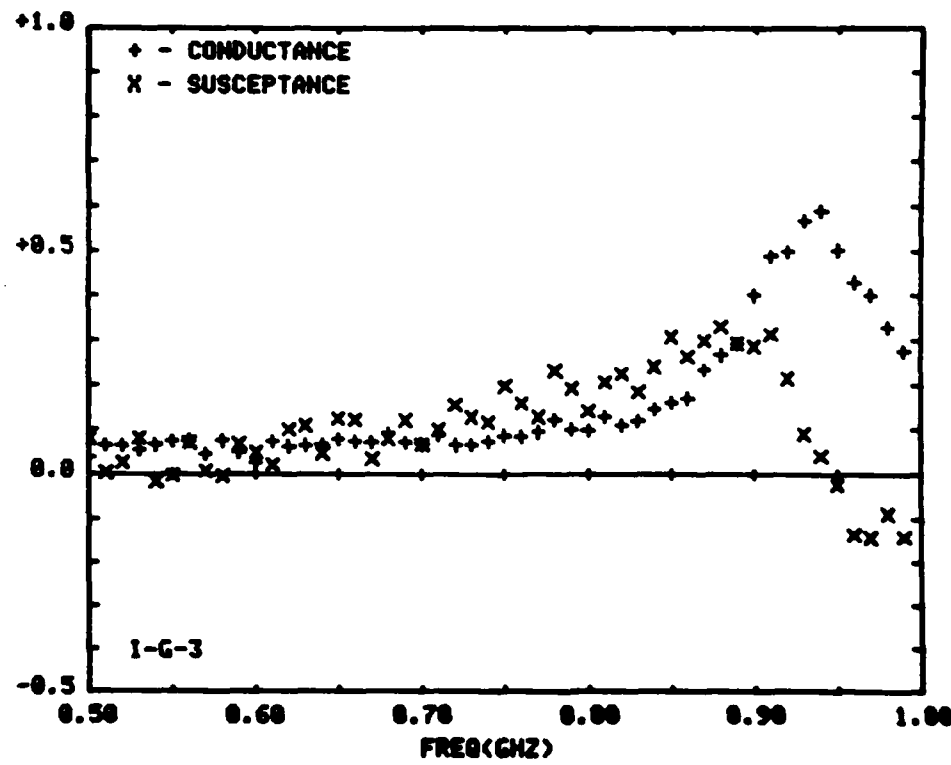


FIGURE 4-49

Aperture Admittance of Sleeve Monopole
Antenna Above Salt Water (I-G-3)

FREQ. (GHZ)	G1	B1	FREQ. (GHZ)	G1	B1
0.500	+0.865	+0.825	0.750	+0.145	+0.852
0.510	+0.893	-0.845	0.760	+0.123	+0.826
0.520	+0.879	+0.803	0.770	+0.126	-0.813
0.530	+0.867	+0.870	0.780	+0.142	+0.897
0.540	+0.876	-0.845	0.790	+0.109	+0.864
0.550	+0.886	-0.803	0.800	+0.099	+0.889
0.560	+0.887	+0.875	0.810	+0.122	+0.856
0.570	+0.857	+0.814	0.820	+0.104	+0.886
0.580	+0.897	-0.815	0.830	+0.091	+0.822
0.590	+0.861	+0.887	0.840	+0.112	+0.877
0.600	+0.841	+0.874	0.850	+0.113	+0.153
0.610	+0.897	+0.853	0.860	+0.099	+0.184
0.620	+0.893	+0.140	0.870	+0.121	+0.898
0.630	+0.894	+0.135	0.880	+0.135	+0.158
0.640	+0.114	+0.100	0.890	+0.122	+0.131
0.650	+0.152	+0.196	0.900	+0.158	+0.140
0.660	+0.164	+0.200	0.910	+0.196	+0.184
0.670	+0.204	+0.108	0.920	+0.184	+0.196
0.680	+0.284	+0.129	0.930	+0.243	+0.201
0.690	+0.286	+0.893	0.940	+0.320	+0.276
0.700	+0.265	-0.829	0.950	+0.352	+0.248
0.710	+0.258	-0.854	0.960	+0.412	+0.114
0.720	+0.202	+0.813	0.970	+0.473	+0.862
0.730	+0.155	-0.818	0.980	+0.421	+0.817
0.740	+0.148	-0.840	0.990	+0.342	-0.894
			1.000	+0.323	-0.132

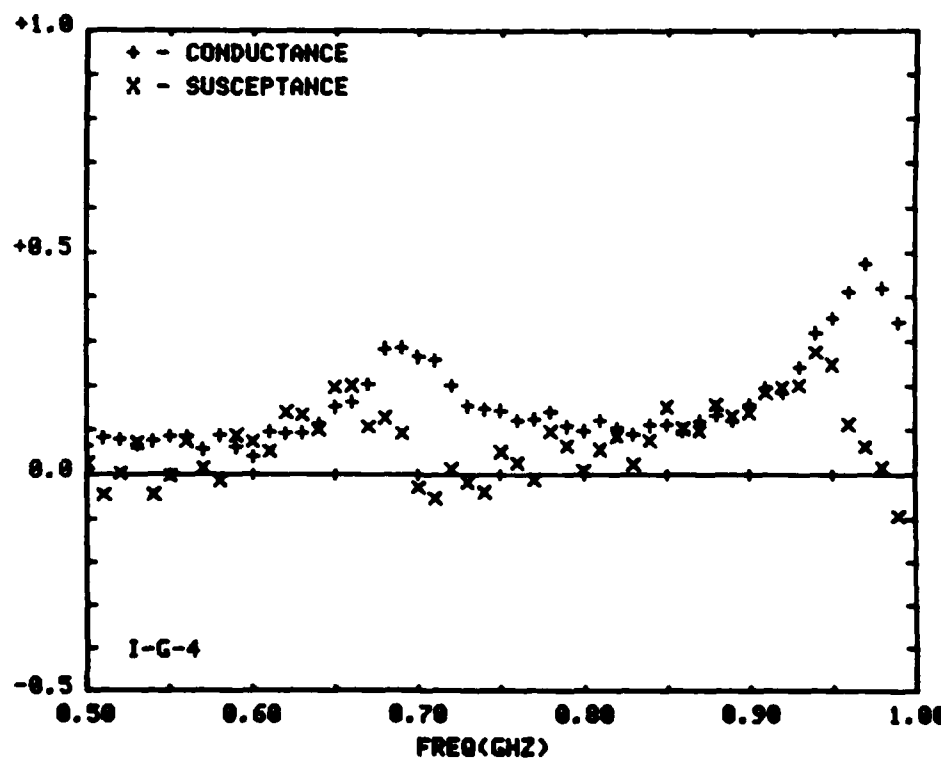


FIGURE 4-50

Aperture Admittance of Sleeve Monopole
Antenna Above Salt Water (I-G-4)

FREQ. (GHZ)	G1	B1	FREQ. (GHZ)	G1	B1
0.500	+0.067	+0.061	0.750	+0.246	+0.310
0.510	+0.098	+0.028	0.760	+0.303	+0.334
0.520	+0.100	+0.028	0.770	+0.347	+0.353
0.530	+0.097	+0.018	0.780	+0.415	+0.342
0.540	+0.101	+0.037	0.790	+0.476	+0.305
0.550	+0.103	+0.011	0.800	+0.553	+0.297
0.560	+0.118	+0.005	0.810	+0.683	+0.258
0.570	+0.105	+0.043	0.820	+0.633	+0.154
0.580	+0.103	+0.079	0.830	+0.644	+0.069
0.590	+0.088	+0.098	0.840	+0.683	+0.003
0.600	+0.082	+0.090	0.850	+0.541	-0.057
0.610	+0.104	+0.101	0.860	+0.503	-0.123
0.620	+0.101	+0.151	0.870	+0.457	-0.146
0.630	+0.110	+0.135	0.880	+0.405	-0.185
0.640	+0.119	+0.138	0.890	+0.383	-0.192
0.650	+0.119	+0.140	0.900	+0.357	-0.174
0.660	+0.129	+0.133	0.910	+0.320	-0.161
0.670	+0.131	+0.152	0.920	+0.296	-0.143
0.680	+0.134	+0.165	0.930	+0.277	-0.150
0.690	+0.137	+0.194	0.940	+0.246	-0.096
0.700	+0.149	+0.231	0.950	+0.218	-0.093
0.710	+0.168	+0.284	0.960	+0.224	-0.093
0.720	+0.162	+0.303	0.970	+0.200	-0.049
0.730	+0.190	+0.295	0.980	+0.189	-0.056
0.740	+0.211	+0.304	0.990	+0.198	-0.035
			1.000	+0.195	-0.043

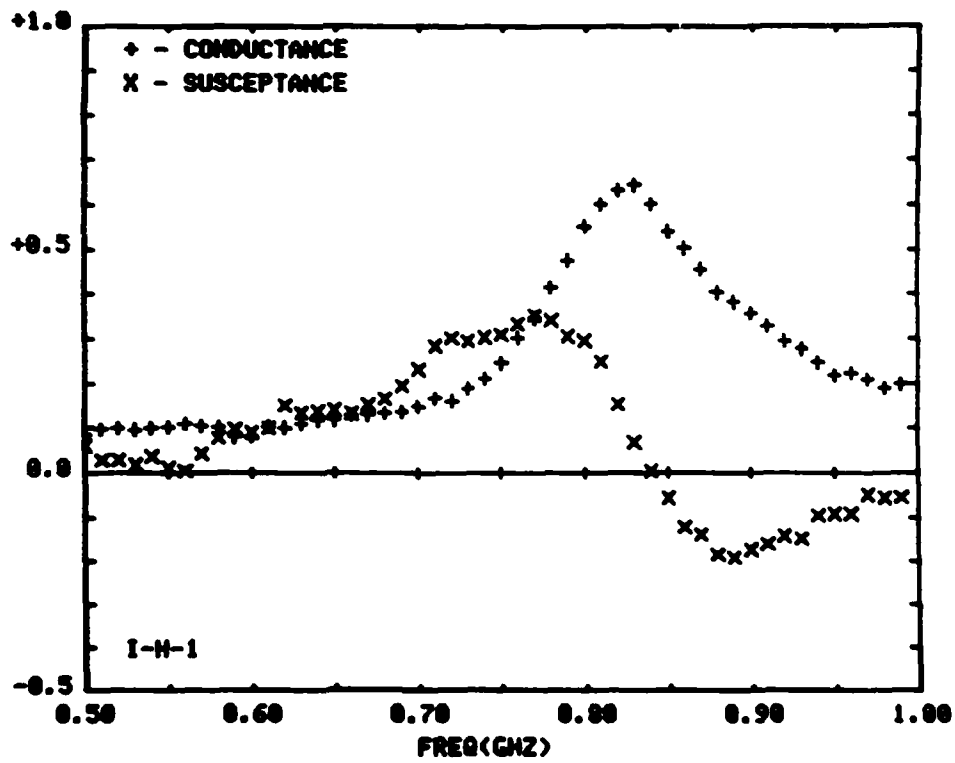


FIGURE 4-51

Aperture Admittance of Sleeve Monopole
Antenna Above Tap Water (I-H-1)

FREQ. (GHZ)	G1	B1	FREQ. (GHZ)	G1	B1
0.500	+0.062	+0.042	0.750	+0.124	+0.002
0.510	+0.075	+0.036	0.760	+0.124	+0.014
0.520	+0.081	+0.031	0.770	+0.123	+0.017
0.530	+0.085	+0.017	0.780	+0.131	+0.002
0.540	+0.082	+0.015	0.790	+0.121	+0.016
0.550	+0.086	+0.011	0.800	+0.118	+0.019
0.560	+0.096	-0.023	0.810	+0.115	+0.019
0.570	+0.094	+0.045	0.820	+0.098	+0.024
0.580	+0.094	+0.048	0.830	+0.115	+0.042
0.590	+0.081	+0.067	0.840	+0.112	+0.061
0.600	+0.089	+0.085	0.850	+0.095	+0.076
0.610	+0.115	+0.098	0.860	+0.102	+0.058
0.620	+0.129	+0.116	0.870	+0.113	+0.062
0.630	+0.154	+0.095	0.880	+0.102	+0.035
0.640	+0.183	+0.101	0.890	+0.117	+0.032
0.650	+0.198	+0.078	0.900	+0.122	+0.032
0.660	+0.203	+0.030	0.910	+0.121	+0.036
0.670	+0.205	+0.011	0.920	+0.112	+0.002
0.680	+0.194	-0.038	0.930	+0.112	+0.043
0.690	+0.178	-0.019	0.940	+0.098	+0.008
0.700	+0.163	-0.005	0.950	+0.089	+0.005
0.710	+0.151	+0.023	0.960	+0.106	+0.076
0.720	+0.128	+0.030	0.970	+0.104	+0.116
0.730	+0.120	+0.006	0.980	+0.106	+0.097
0.740	+0.122	+0.023	0.990	+0.120	+0.099
			1.000	+0.128	+0.106

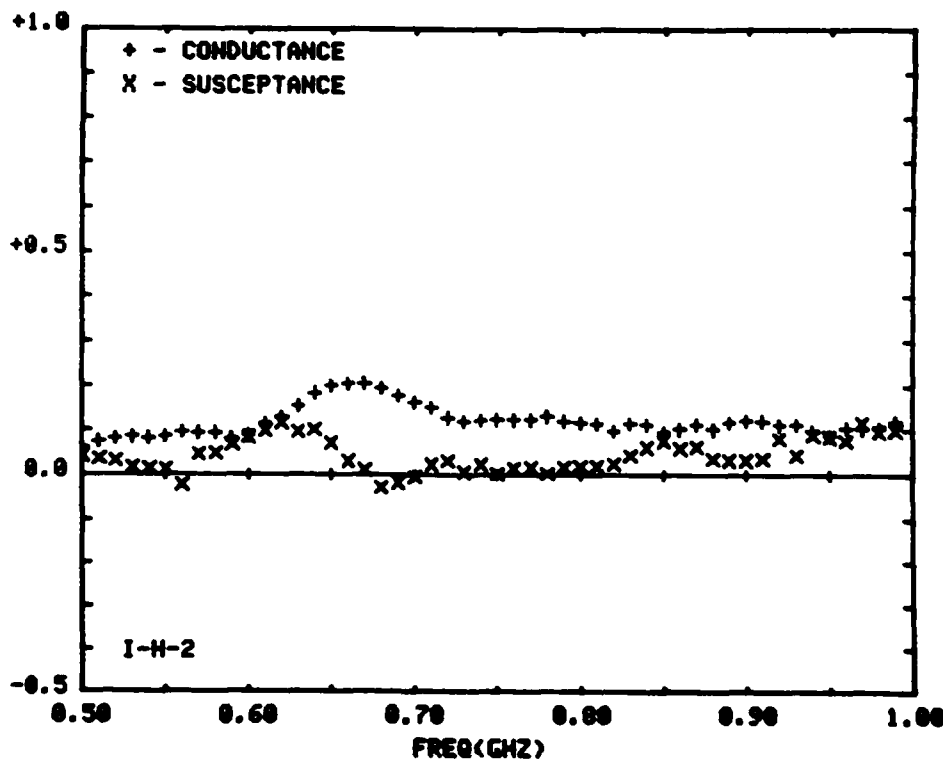


FIGURE 4-52

Aperture Admittance of Sleeve Monopole
Antenna Above Tap Water (I-H-2)

FREQ. (GHZ)	G1	B1	FREQ. (GHZ)	G1	B1
0.500	+0.058	+0.071	0.750	+0.095	+0.144
0.510	+0.070	+0.062	0.760	+0.097	+0.141
0.520	+0.076	+0.055	0.770	+0.104	+0.147
0.530	+0.080	+0.036	0.780	+0.113	+0.133
0.540	+0.077	+0.033	0.790	+0.108	+0.159
0.550	+0.081	+0.024	0.800	+0.111	+0.189
0.560	+0.086	+0.008	0.810	+0.106	+0.181
0.570	+0.083	+0.052	0.820	+0.097	+0.189
0.580	+0.080	+0.051	0.830	+0.120	+0.215
0.590	+0.062	+0.062	0.840	+0.133	+0.245
0.600	+0.057	+0.076	0.850	+0.133	+0.288
0.610	+0.074	+0.084	0.860	+0.156	+0.265
0.620	+0.078	+0.125	0.870	+0.177	+0.285
0.630	+0.084	+0.089	0.880	+0.189	+0.270
0.640	+0.089	+0.102	0.890	+0.236	+0.284
0.650	+0.085	+0.087	0.900	+0.290	+0.333
0.660	+0.092	+0.074	0.910	+0.338	+0.309
0.670	+0.087	+0.085	0.920	+0.418	+0.324
0.680	+0.094	+0.089	0.930	+0.482	+0.273
0.690	+0.089	+0.079	0.940	+0.527	+0.294
0.700	+0.084	+0.107	0.950	+0.526	+0.080
0.710	+0.092	+0.142	0.960	+0.484	-0.021
0.720	+0.076	+0.147	0.970	+0.417	-0.049
0.730	+0.077	+0.131	0.980	+0.355	-0.007
0.740	+0.085	+0.147	0.990	+0.315	-0.098
			1.000	+0.281	-0.091

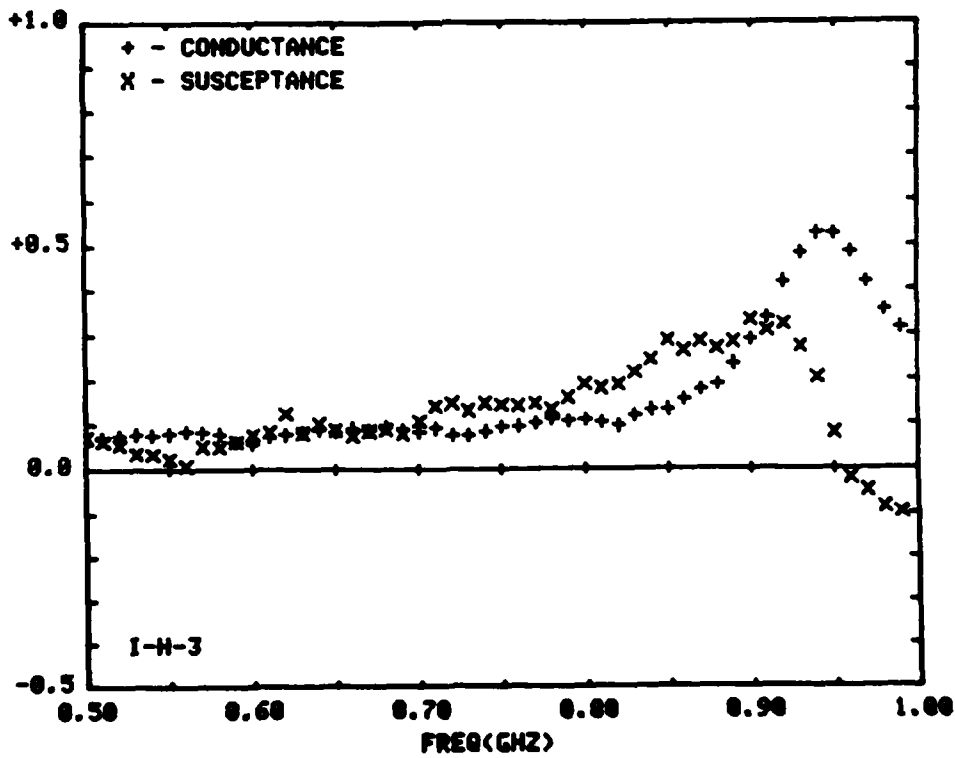


FIGURE 4-53

Aperture Admittance of Sleeve Monopole
Antenna Above Tap Water (I-H-3)

FREQ. (GHZ)	G1	B1	FREQ. (GHZ)	G1	B1
0.500	+0.097	+0.011	0.750	+0.141	-0.030
0.510	+0.092	+0.013	0.760	+0.139	+0.001
0.520	+0.092	+0.019	0.770	+0.129	+0.023
0.530	+0.102	-0.029	0.780	+0.131	-0.005
0.540	+0.094	+0.021	0.790	+0.127	+0.021
0.550	+0.092	+0.011	0.800	+0.118	+0.045
0.560	+0.106	-0.042	0.810	+0.108	+0.036
0.570	+0.100	+0.050	0.820	+0.097	+0.043
0.580	+0.086	+0.057	0.830	+0.116	+0.087
0.590	+0.081	+0.047	0.840	+0.107	+0.101
0.600	+0.082	+0.084	0.850	+0.096	+0.111
0.610	+0.088	+0.087	0.860	+0.112	+0.122
0.620	+0.097	+0.107	0.870	+0.111	+0.126
0.630	+0.114	+0.105	0.880	+0.107	+0.094
0.640	+0.125	+0.151	0.890	+0.131	+0.119
0.650	+0.135	+0.138	0.900	+0.137	+0.131
0.660	+0.169	+0.129	0.910	+0.143	+0.134
0.670	+0.190	+0.167	0.920	+0.162	+0.207
0.680	+0.237	+0.149	0.930	+0.170	+0.196
0.690	+0.293	+0.091	0.940	+0.195	+0.245
0.700	+0.309	+0.059	0.950	+0.249	+0.255
0.710	+0.263	+0.027	0.960	+0.324	+0.237
0.720	+0.212	-0.910	0.970	+0.388	+0.225
0.730	+0.183	-0.022	0.980	+0.430	+0.000
0.740	+0.151	+0.006	0.990	+0.409	-0.003
			1.000	+0.348	-0.051

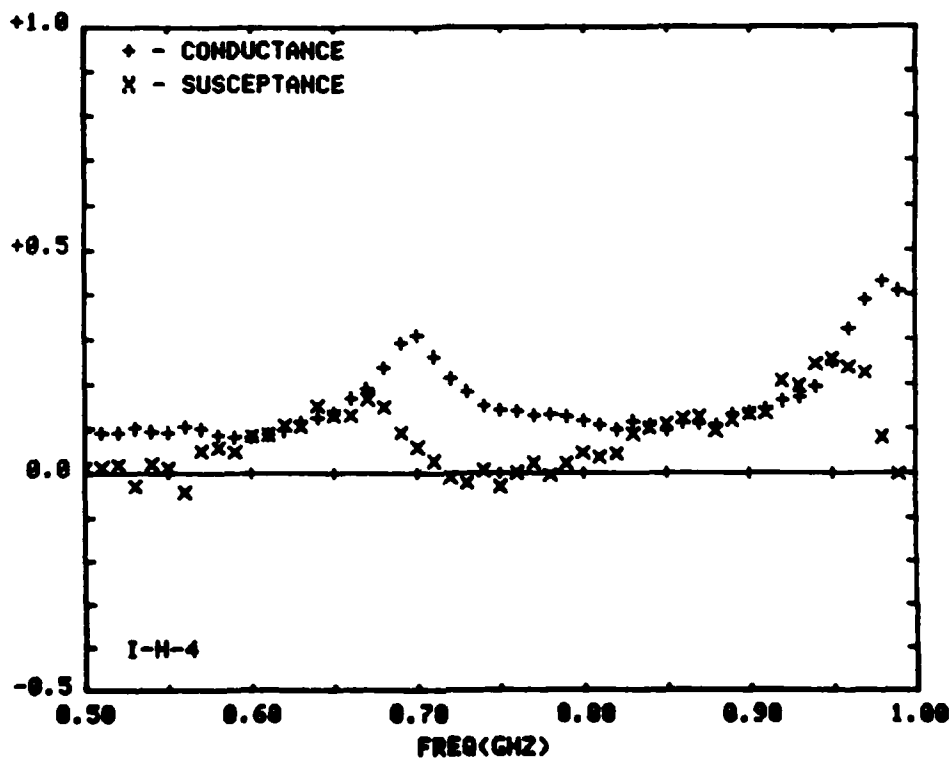


FIGURE 4-54

Aperture Admittance of Sleeve Monopole
Antenna Above Tap Water (I-H-4)

FREQ. (GHZ)	G1	B1	FREQ. (GHZ)	G1	B1
0.500	+0.862	+0.385	0.750	+0.412	+0.658
0.510	+0.868	+0.376	0.760	+0.436	+0.628
0.520	+0.877	+0.365	0.770	+0.461	+0.593
0.530	+0.882	+0.401	0.780	+0.529	+0.667
0.540	+0.889	+0.339	0.790	+0.559	+0.647
0.550	+0.105	+0.364	0.800	+0.566	+0.622
0.560	+0.104	+0.415	0.810	+0.634	+0.694
0.570	+0.109	+0.418	0.820	+0.658	+0.668
0.580	+0.115	+0.432	0.830	+0.676	+0.628
0.590	+0.117	+0.495	0.840	+0.720	+0.619
0.600	+0.111	+0.485	0.850	+0.754	+0.585
0.610	+0.134	+0.465	0.860	+0.750	+0.585
0.620	+0.148	+0.526	0.870	+0.889	+0.476
0.630	+0.153	+0.488	0.880	+0.859	+0.438
0.640	+0.180	+0.485	0.890	+0.860	+0.390
0.650	+0.204	+0.548	0.900	+0.889	+0.355
0.660	+0.211	+0.556	0.910	+0.924	+0.347
0.670	+0.211	+0.589	0.920	+0.921	+0.301
0.680	+0.231	+0.567	0.930	+0.909	+0.275
0.690	+0.242	+0.607	0.940	+0.913	+0.252
0.700	+0.267	+0.595	0.950	+0.889	+0.296
0.710	+0.294	+0.611	0.960	+0.856	+0.150
0.720	+0.319	+0.673	0.970	+0.838	+0.108
0.730	+0.342	+0.655	0.980	+0.825	+0.062
0.740	+0.373	+0.627	0.990	+0.814	+0.012
			1.000	+0.800	-0.014

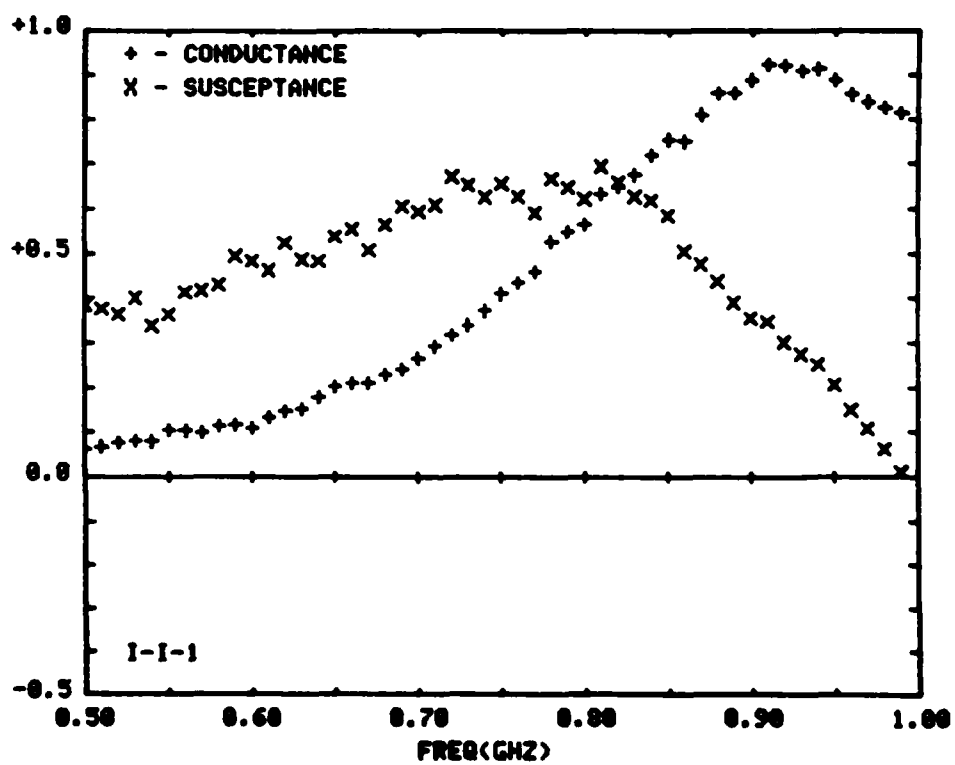


FIGURE 4-55

Aperture Admittance of Sleeve Monopole
Antenna Above Tap Water (I-I-1)

FREQ. (GHZ)	G1	B1	FREQ. (GHZ)	G1	B1
0.500	+0.184	+0.415	0.750	+0.751	+0.318
0.510	+0.186	+0.387	0.760	+0.752	+0.247
0.520	+0.133	+0.412	0.770	+0.768	+0.183
0.530	+0.131	+0.427	0.780	+0.782	+0.166
0.540	+0.144	+0.393	0.790	+0.788	+0.127
0.550	+0.171	+0.427	0.800	+0.765	+0.082
0.560	+0.183	+0.450	0.810	+0.756	+0.076
0.570	+0.195	+0.481	0.820	+0.727	+0.068
0.580	+0.216	+0.458	0.830	+0.696	+0.014
0.590	+0.238	+0.565	0.840	+0.662	-0.011
0.600	+0.247	+0.558	0.850	+0.627	-0.088
0.610	+0.283	+0.530	0.860	+0.602	-0.068
0.620	+0.322	+0.584	0.870	+0.586	-0.097
0.630	+0.341	+0.539	0.880	+0.569	-0.090
0.640	+0.375	+0.516	0.890	+0.568	-0.128
0.650	+0.448	+0.571	0.900	+0.561	-0.153
0.660	+0.466	+0.563	0.910	+0.543	-0.139
0.670	+0.491	+0.508	0.920	+0.525	-0.114
0.680	+0.542	+0.546	0.930	+0.501	-0.125
0.690	+0.570	+0.525	0.940	+0.472	-0.091
0.700	+0.598	+0.495	0.950	+0.450	-0.089
0.710	+0.649	+0.486	0.960	+0.424	-0.125
0.720	+0.693	+0.484	0.970	+0.409	-0.106
0.730	+0.702	+0.429	0.980	+0.390	-0.096
0.740	+0.713	+0.352	0.990	+0.382	-0.124
			1.000	+0.384	-0.137

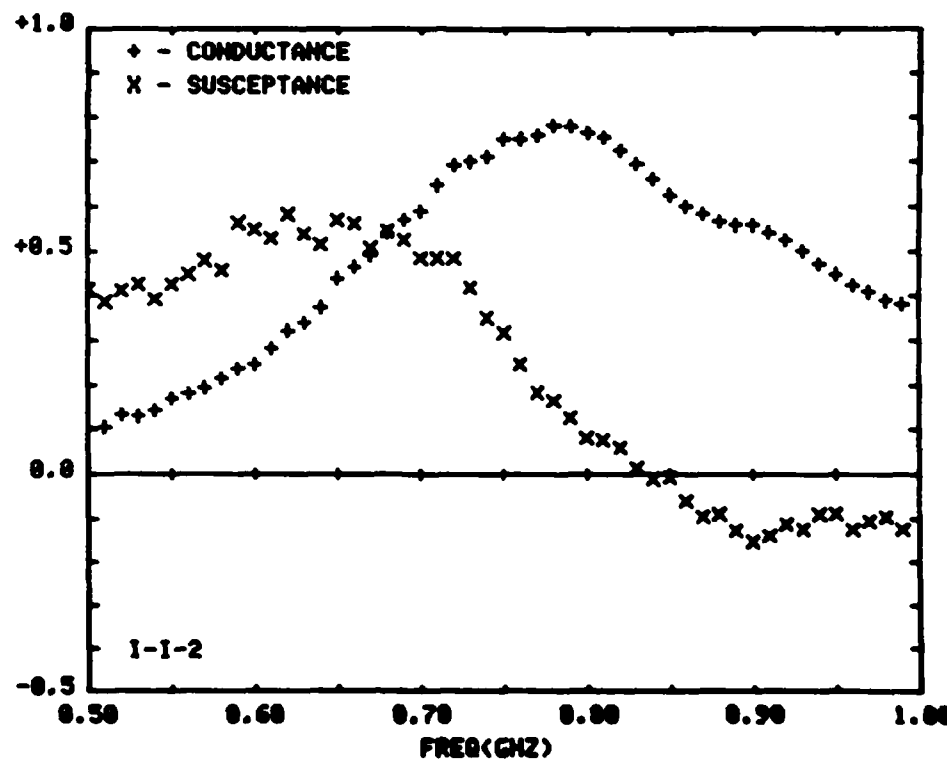


FIGURE 4-56

Aperture Admittance of Sleeve Monopole
Antenna Above Tap Water (I-I-2)

FREQ. (GHZ)	G1	B1	FREQ. (GHZ)	G1	B1
0.500	+0.182	+0.456	0.750	+0.446	-0.864
0.510	+0.213	+0.428	0.760	+0.424	-0.886
0.520	+0.236	+0.437	0.770	+0.416	-0.129
0.530	+0.274	+0.462	0.780	+0.405	-0.897
0.540	+0.296	+0.425	0.790	+0.395	-0.883
0.550	+0.340	+0.423	0.800	+0.373	-0.184
0.560	+0.387	+0.470	0.810	+0.356	-0.106
0.570	+0.420	+0.461	0.820	+0.336	-0.062
0.580	+0.454	+0.435	0.830	+0.317	-0.070
0.590	+0.516	+0.483	0.840	+0.298	-0.065
0.600	+0.518	+0.416	0.850	+0.276	-0.007
0.610	+0.541	+0.347	0.860	+0.263	-0.070
0.620	+0.593	+0.363	0.870	+0.259	-0.088
0.630	+0.597	+0.286	0.880	+0.260	-0.042
0.640	+0.611	+0.222	0.890	+0.253	-0.076
0.650	+0.631	+0.195	0.900	+0.268	-0.100
0.660	+0.640	+0.153	0.910	+0.252	-0.067
0.670	+0.619	+0.065	0.920	+0.256	-0.041
0.680	+0.624	+0.058	0.930	+0.237	-0.045
0.690	+0.597	+0.042	0.940	+0.229	+0.001
0.700	+0.577	+0.003	0.950	+0.214	+0.005
0.710	+0.548	-0.012	0.960	+0.203	-0.032
0.720	+0.518	+0.014	0.970	+0.201	0.000
0.730	+0.482	-0.011	0.980	+0.199	+0.012
0.740	+0.464	-0.068	0.990	+0.198	-0.016
			1.000	+0.205	-0.023

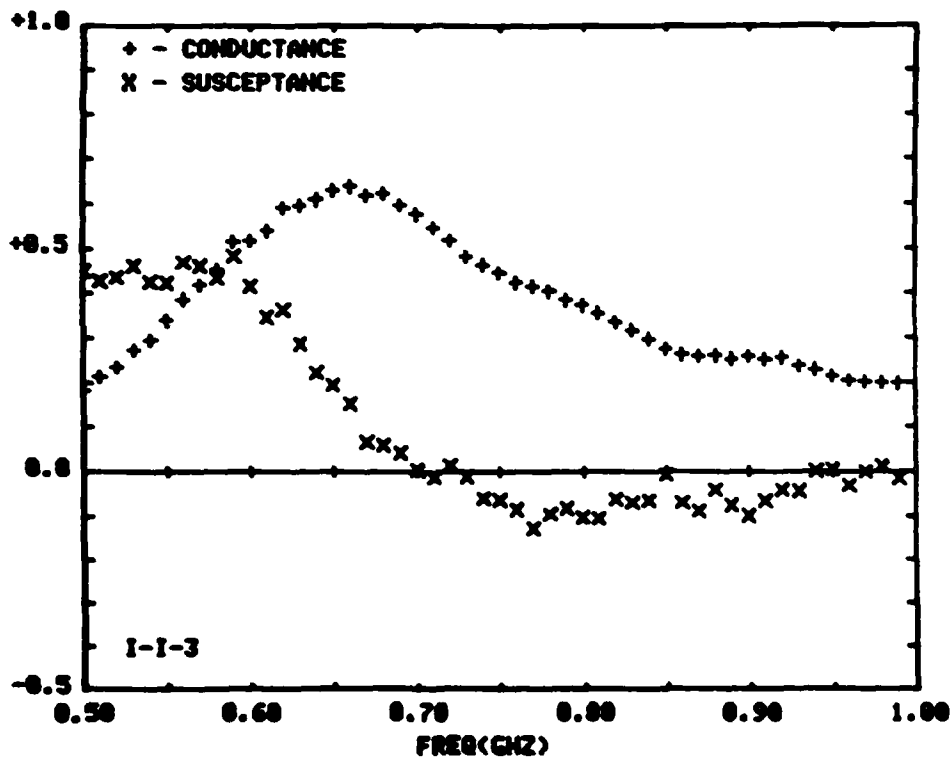


FIGURE 4-57

Aperture Admittance of Sleeve Monopole
Antenna Above Tap Water (I-I-3)

FREQ. (GHZ)	G1	B1	FREQ. (GHZ)	G1	B1
0.500	+0.432	+0.173	0.750	+0.134	+0.007
0.510	+0.402	+0.109	0.760	+0.124	+0.042
0.520	+0.408	+0.058	0.770	+0.131	+0.008
0.530	+0.379	+0.067	0.780	+0.142	+0.054
0.540	+0.371	-0.023	0.790	+0.128	+0.000
0.550	+0.350	-0.032	0.800	+0.122	+0.058
0.560	+0.339	+0.006	0.810	+0.119	+0.065
0.570	+0.296	-0.019	0.820	+0.108	+0.100
0.580	+0.295	-0.052	0.830	+0.102	+0.105
0.590	+0.259	+0.012	0.840	+0.107	+0.115
0.600	+0.247	+0.006	0.850	+0.102	+0.164
0.610	+0.232	-0.016	0.860	+0.095	+0.181
0.620	+0.218	+0.025	0.870	+0.102	+0.085
0.630	+0.209	+0.006	0.880	+0.102	+0.139
0.640	+0.193	-0.012	0.890	+0.103	+0.097
0.650	+0.195	+0.003	0.900	+0.117	+0.087
0.660	+0.189	+0.021	0.910	+0.118	+0.116
0.670	+0.177	-0.032	0.920	+0.106	+0.140
0.680	+0.184	-0.006	0.930	+0.099	+0.143
0.690	+0.166	+0.010	0.940	+0.090	+0.167
0.700	+0.154	+0.006	0.950	+0.086	+0.183
0.710	+0.156	+0.019	0.960	+0.083	+0.158
0.720	+0.140	+0.009	0.970	+0.091	+0.189
0.730	+0.130	+0.005	0.980	+0.092	+0.170
0.740	+0.127	+0.047	0.990	+0.098	+0.143
			1.000	+0.111	+0.169

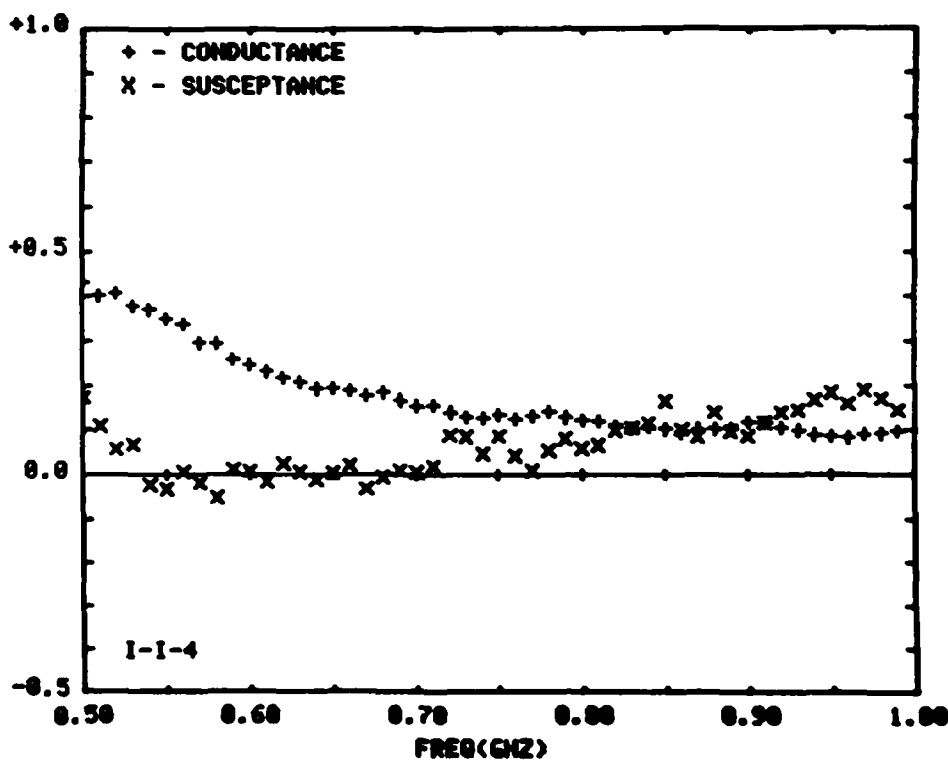


FIGURE 4-58

Aperture Admittance of Sleeve Monopole
Antenna Above Tap Water (I-I-4)

FREQ. (GHZ)	G1	B1	FREQ. (GHZ)	G1	B1
0.500	+0.873	+0.116	0.750	+0.953	+0.255
0.510	+0.876	+0.066	0.760	+0.962	+0.236
0.520	+0.872	+0.067	0.770	+0.977	+0.282
0.530	+0.873	+0.108	0.780	+0.987	+0.264
0.540	+0.870	+0.065	0.790	+0.977	+0.293
0.550	+0.883	+0.052	0.800	+0.972	+0.252
0.560	+0.882	+0.106	0.810	+0.969	+0.300
0.570	+0.862	+0.124	0.820	+0.963	+0.326
0.580	+0.869	+0.101	0.830	+0.965	+0.338
0.590	+0.856	+0.178	0.840	+0.974	+0.361
0.600	+0.844	+0.166	0.850	+0.979	+0.376
0.610	+0.854	+0.131	0.860	+0.987	+0.346
0.620	+0.857	+0.172	0.870	+0.104	+0.339
0.630	+0.858	+0.177	0.880	+0.105	+0.407
0.640	+0.861	+0.166	0.890	+0.113	+0.349
0.650	+0.872	+0.189	0.900	+0.128	+0.338
0.660	+0.861	+0.182	0.910	+0.134	+0.417
0.670	+0.856	+0.129	0.920	+0.143	+0.458
0.680	+0.867	+0.148	0.930	+0.145	+0.441
0.690	+0.851	+0.192	0.940	+0.162	+0.511
0.700	+0.850	+0.195	0.950	+0.175	+0.528
0.710	+0.856	+0.213	0.960	+0.197	+0.506
0.720	+0.845	+0.277	0.970	+0.232	+0.536
0.730	+0.848	+0.277	0.980	+0.253	+0.531
0.740	+0.851	+0.212	0.990	+0.302	+0.505
			1.000	+0.361	+0.570

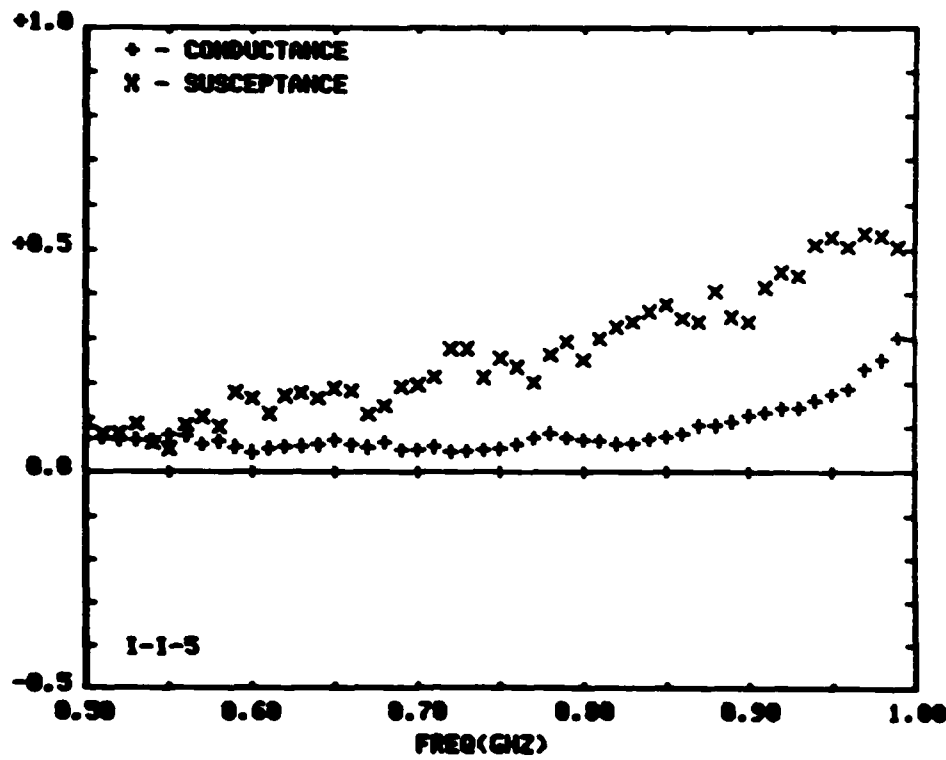


FIGURE 4-59

Aperture Admittance of Sleeve Monopole
Antenna Above Tap Water (I-I-5)

FREQ. (GHZ)	G1	B1	FREQ. (GHZ)	G1	B1
0.500	+0.034	+0.296	0.750	+0.170	+0.070
0.510	+0.050	+0.274	0.760	+0.156	+0.054
0.520	+0.059	+0.276	0.770	+0.153	+0.026
0.530	+0.059	+0.324	0.780	+0.154	+0.070
0.540	+0.070	+0.267	0.790	+0.134	+0.094
0.550	+0.089	+0.292	0.800	+0.123	+0.086
0.560	+0.103	+0.359	0.810	+0.114	+0.122
0.570	+0.108	+0.361	0.820	+0.101	+0.163
0.580	+0.139	+0.397	0.830	+0.091	+0.148
0.590	+0.175	+0.467	0.840	+0.091	+0.170
0.600	+0.197	+0.453	0.850	+0.086	+0.221
0.610	+0.268	+0.440	0.860	+0.081	+0.190
0.620	+0.340	+0.473	0.870	+0.094	+0.186
0.630	+0.403	+0.433	0.880	+0.092	+0.226
0.640	+0.466	+0.317	0.890	+0.093	+0.194
0.650	+0.510	+0.277	0.900	+0.102	+0.182
0.660	+0.517	+0.175	0.910	+0.105	+0.251
0.670	+0.484	+0.066	0.920	+0.094	+0.262
0.680	+0.439	+0.015	0.930	+0.095	+0.273
0.690	+0.383	+0.032	0.940	+0.091	+0.343
0.700	+0.318	+0.003	0.950	+0.086	+0.372
0.710	+0.285	-0.016	0.960	+0.092	+0.317
0.720	+0.237	+0.055	0.970	+0.119	+0.377
0.730	+0.205	+0.053	0.980	+0.132	+0.393
0.740	+0.184	+0.014	0.990	+0.149	+0.371
			1.000	+0.187	+0.446

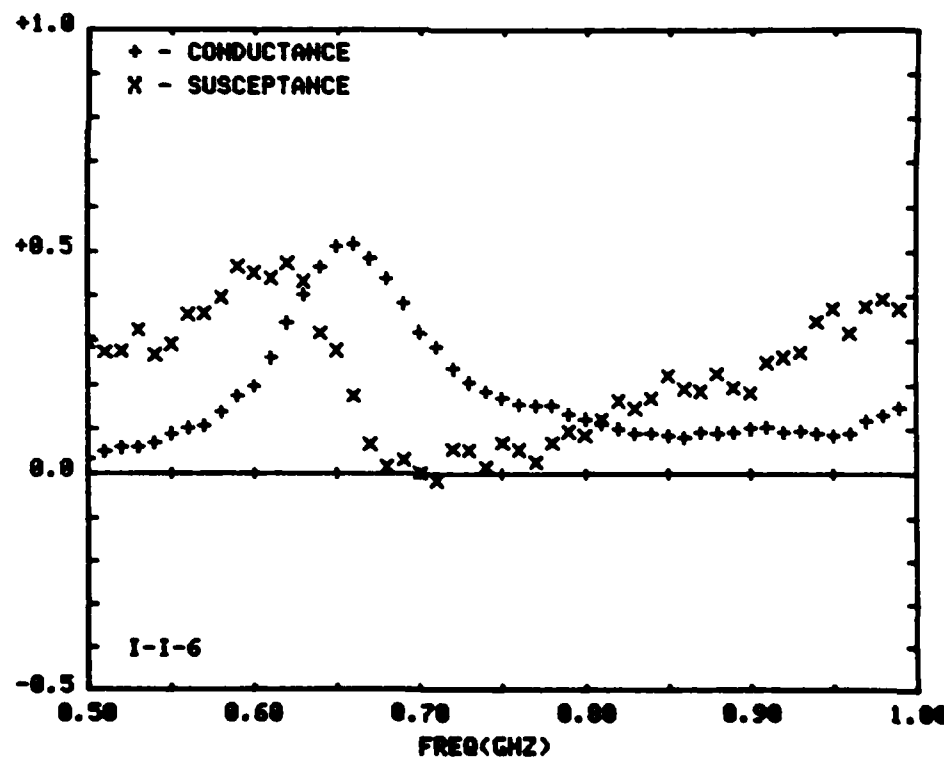


FIGURE 4-60

Aperture Admittance of Sleeve Monopole
Antenna Above Tap Water (I-I-6)

FREQ. (GHZ)	G	B	FREQ. (GHZ)	G	B
0.500	+0.029	-0.102	0.750	+0.061	+0.198
0.510	+0.033	-0.079	0.760	+0.079	+0.215
0.520	+0.028	-0.066	0.770	+0.094	+0.248
0.530	+0.024	-0.075	0.780	+0.109	+0.305
0.540	+0.028	-0.055	0.790	+0.130	+0.343
0.550	+0.028	-0.045	0.800	+0.162	+0.401
0.560	+0.029	-0.032	0.810	+0.208	+0.472
0.570	+0.031	-0.014	0.820	+0.269	+0.547
0.580	+0.037	+0.013	0.830	+0.361	+0.616
0.590	+0.033	+0.031	0.840	+0.511	+0.683
0.600	+0.037	+0.053	0.850	+0.743	+0.696
0.610	+0.031	+0.059	0.860	+1.048	+0.605
0.620	+0.033	+0.079	0.870	+1.309	+0.263
0.630	+0.031	+0.080	0.880	+1.332	-0.209
0.640	+0.031	+0.089	0.890	+1.076	-0.520
0.650	+0.036	+0.090	0.900	+0.773	-0.640
0.660	+0.030	+0.102	0.910	+0.552	-0.601
0.670	+0.034	+0.104	0.920	+0.410	-0.562
0.680	+0.034	+0.117	0.930	+0.315	-0.508
0.690	+0.034	+0.122	0.940	+0.254	-0.468
0.700	+0.033	+0.131	0.950	+0.208	-0.424
0.710	+0.046	+0.139	0.960	+0.174	-0.400
0.720	+0.043	+0.156	0.970	+0.152	-0.367
0.730	+0.050	+0.156	0.980	+0.129	-0.359
0.740	+0.053	+0.180	0.990	+0.115	-0.334
			1.000	+0.102	-0.310

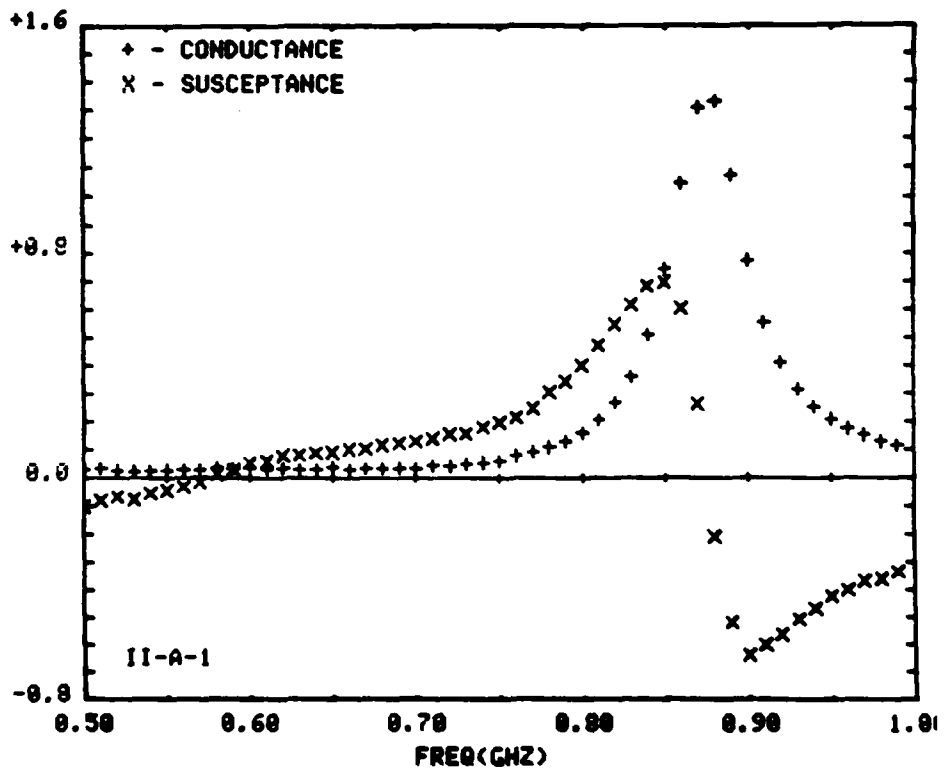


FIGURE 4-61

Aperture Admittance of Coax-Fed Wire Monopole
Antenna Above Tap Water (II-A-1)

ANTENNA APERTURE ADMITTANCE (NORMALIZED)

FREQ. (GHZ)	G	B	FREQ. (GHZ)	G	B
0.500	+0.025	-0.066	0.750	+0.067	+0.202
0.510	+0.032	-0.039	0.760	+0.079	+0.221
0.520	+0.024	-0.033	0.770	+0.101	+0.264
0.530	+0.019	-0.038	0.780	+0.116	+0.312
0.540	+0.028	-0.022	0.790	+0.137	+0.350
0.550	+0.027	-0.013	0.800	+0.177	+0.412
0.560	+0.028	-0.003	0.810	+0.232	+0.487
0.570	+0.029	+0.020	0.820	+0.315	+0.554
0.580	+0.037	+0.038	0.830	+0.448	+0.614
0.590	+0.033	+0.055	0.840	+0.668	+0.627
0.600	+0.042	+0.079	0.850	+0.891	+0.516
0.610	+0.031	+0.091	0.860	+1.122	+0.201
0.620	+0.036	+0.097	0.870	+1.048	-0.133
0.630	+0.037	+0.099	0.880	+0.957	-0.406
0.640	+0.031	+0.106	0.890	+0.653	-0.439
0.650	+0.042	+0.107	0.900	+0.473	-0.448
0.660	+0.029	+0.120	0.910	+0.383	-0.382
0.670	+0.034	+0.121	0.920	+0.296	-0.373
0.680	+0.034	+0.129	0.930	+0.260	-0.332
0.690	+0.034	+0.134	0.940	+0.212	-0.312
0.700	+0.039	+0.140	0.950	+0.197	-0.280
0.710	+0.047	+0.148	0.960	+0.162	-0.272
0.720	+0.048	+0.164	0.970	+0.153	-0.247
0.730	+0.053	+0.165	0.980	+0.132	-0.252
0.740	+0.055	+0.184	0.990	+0.132	-0.233
			1.000	+0.121	-0.220

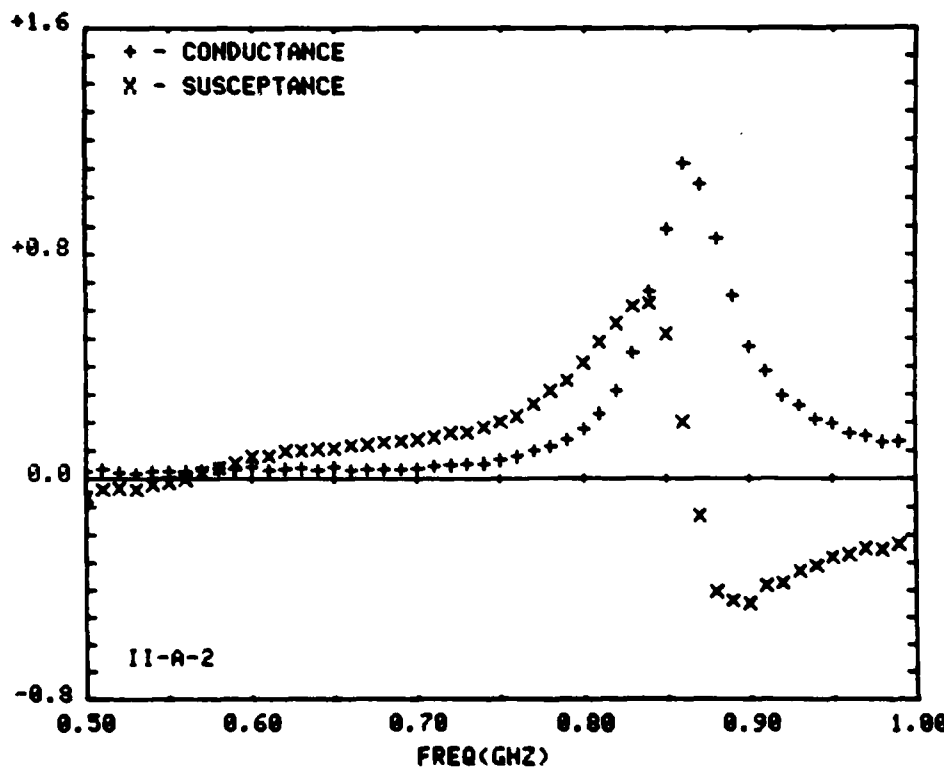


FIGURE 4-62

Aperture Admittance of Coax-Fed Wire Monopole
Antenna Above Tap Water (II-A-2)

FREQ. (GHZ)	G	B	FREQ. (GHZ)	G	B
0.500	+0.043	-0.047	0.750	+0.089	+0.165
0.510	+0.050	-0.027	0.760	+0.107	+0.211
0.520	+0.041	-0.020	0.770	+0.128	+0.237
0.530	+0.036	-0.028	0.780	+0.143	+0.274
0.540	+0.045	-0.013	0.790	+0.178	+0.304
0.550	+0.044	-0.003	0.800	+0.206	+0.347
0.560	+0.045	+0.006	0.810	+0.254	+0.400
0.570	+0.049	+0.025	0.820	+0.316	+0.433
0.580	+0.053	+0.046	0.830	+0.415	+0.467
0.590	+0.050	+0.061	0.840	+0.535	+0.440
0.600	+0.059	+0.087	0.850	+0.664	+0.396
0.610	+0.048	+0.097	0.860	+0.769	+0.217
0.620	+0.053	+0.101	0.870	+0.799	+0.084
0.630	+0.054	+0.104	0.880	+0.730	-0.119
0.640	+0.047	+0.107	0.890	+0.667	-0.201
0.650	+0.059	+0.111	0.900	+0.533	-0.266
0.660	+0.052	+0.117	0.910	+0.476	-0.275
0.670	+0.056	+0.117	0.920	+0.377	-0.279
0.680	+0.056	+0.127	0.930	+0.352	-0.273
0.690	+0.056	+0.130	0.940	+0.287	-0.263
0.700	+0.056	+0.137	0.950	+0.275	-0.255
0.710	+0.069	+0.138	0.960	+0.230	-0.245
0.720	+0.071	+0.153	0.970	+0.224	-0.239
0.730	+0.075	+0.154	0.980	+0.191	-0.240
0.740	+0.083	+0.170	0.990	+0.193	-0.234
			1.000	+0.174	-0.219

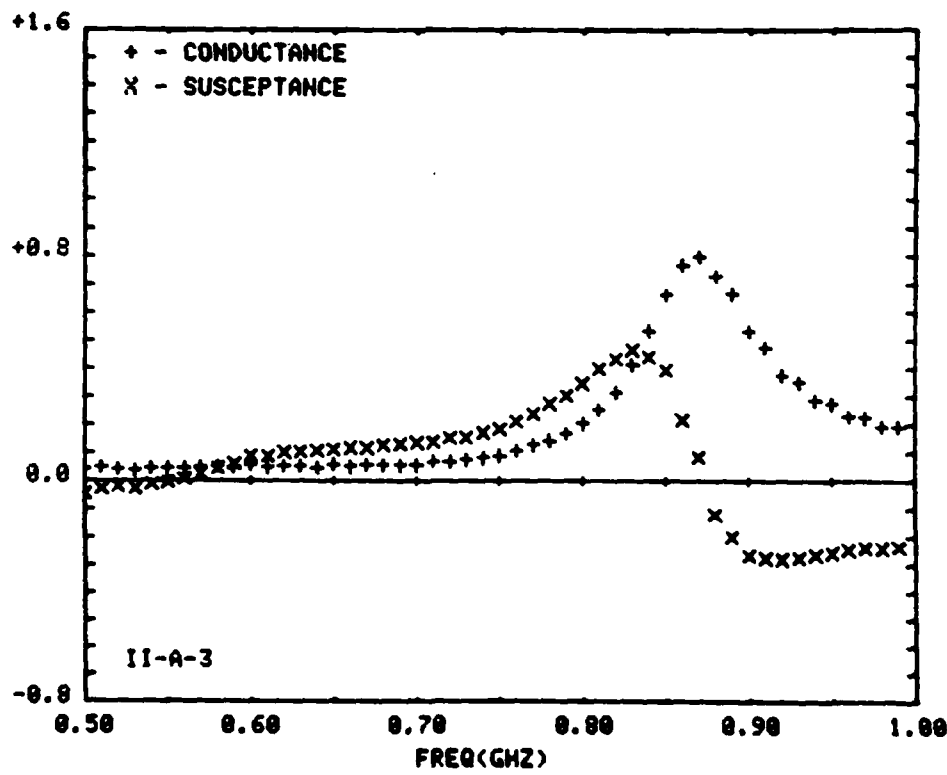


FIGURE 4-63

Aperture Admittance of Coax-Fed Wire Monopole
Antenna Above Tap Water (II-A-3)

ANTENNA APERTURE ADMITTANCE (NORMALIZED)

FREQ. (GHZ)	G	B	FREQ. (GHZ)	G	B
0.500	+0.069	-0.067	0.750	+0.060	+0.174
0.510	+0.072	-0.050	0.760	+0.072	+0.193
0.520	+0.064	-0.048	0.770	+0.086	+0.223
0.530	+0.059	-0.055	0.780	+0.101	+0.275
0.540	+0.059	-0.036	0.790	+0.127	+0.306
0.550	+0.062	-0.032	0.800	+0.150	+0.355
0.560	+0.057	-0.021	0.810	+0.191	+0.415
0.570	+0.059	-0.003	0.820	+0.245	+0.473
0.580	+0.060	+0.016	0.830	+0.339	+0.525
0.590	+0.056	+0.033	0.840	+0.463	+0.562
0.600	+0.059	+0.056	0.850	+0.625	+0.543
0.610	+0.048	+0.062	0.860	+0.820	+0.436
0.620	+0.053	+0.073	0.870	+0.963	+0.216
0.630	+0.049	+0.076	0.880	+0.964	-0.060
0.640	+0.042	+0.081	0.890	+0.844	-0.271
0.650	+0.048	+0.086	0.900	+0.664	-0.363
0.660	+0.041	+0.097	0.910	+0.530	-0.378
0.670	+0.043	+0.095	0.920	+0.422	-0.384
0.680	+0.039	+0.109	0.930	+0.346	-0.355
0.690	+0.039	+0.111	0.940	+0.292	-0.335
0.700	+0.039	+0.118	0.950	+0.248	-0.313
0.710	+0.046	+0.126	0.960	+0.218	-0.294
0.720	+0.042	+0.138	0.970	+0.193	-0.278
0.730	+0.052	+0.145	0.980	+0.171	-0.278
0.740	+0.054	+0.160	0.990	+0.159	-0.268
			1.000	+0.146	-0.243

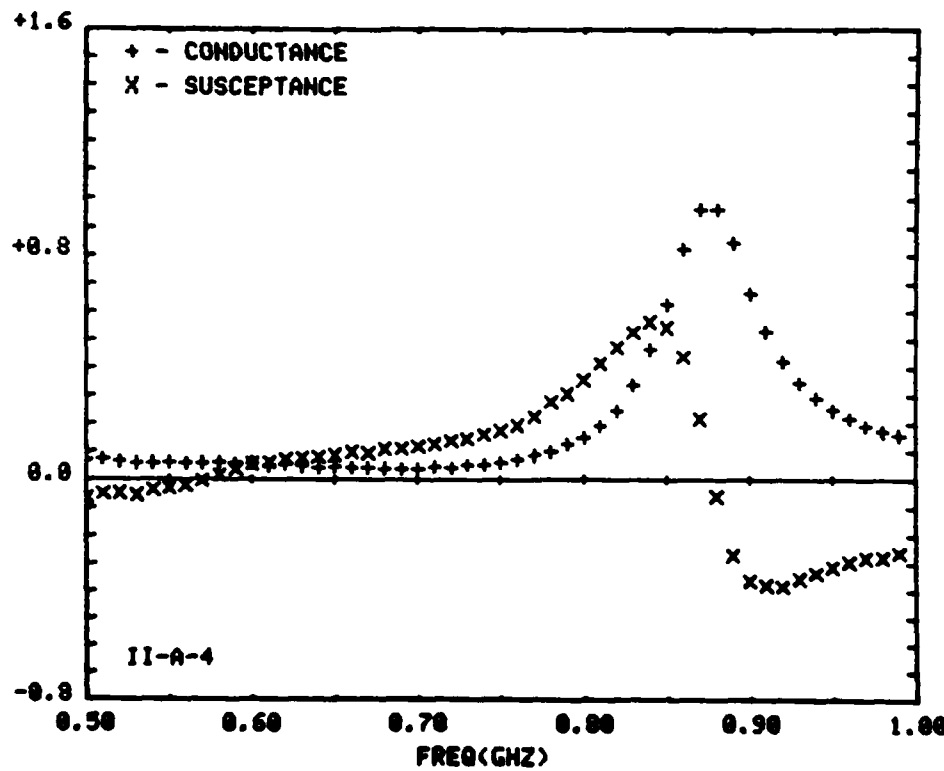


FIGURE 4-64

Aperture Admittance of Coax-Fed Wire Monopole
Antenna Above Tap Water (II-A-4)

FREQ. (GHZ)	G	B	FREQ. (GHZ)	G	B
0.500	+0.044	-0.007	0.600	+0.110	+0.196
0.510	+0.050	+0.002	0.610	+0.110	+0.213
0.520	+0.049	+0.005	0.620	+0.110	+0.239
0.530	+0.034	+0.005	0.630	+0.122	+0.256
0.540	+0.031	+0.015	0.640	+0.134	+0.277
0.550	+0.042	+0.022	0.650	+0.141	+0.284
0.560	+0.048	+0.035	0.660	+0.158	+0.296
0.570	+0.050	+0.050	0.670	+0.170	+0.307
0.580	+0.057	+0.068	0.680	+0.176	+0.321
0.590	+0.055	+0.077	0.690	+0.184	+0.327
0.600	+0.054	+0.088	0.700	+0.199	+0.345
0.610	+0.042	+0.103	0.710	+0.215	+0.365
0.620	+0.047	+0.113	0.720	+0.251	+0.365
0.630	+0.049	+0.116	0.730	+0.293	+0.382
0.640	+0.053	+0.123	0.740	+0.328	+0.386
0.650	+0.064	+0.118	0.750	+0.356	+0.379
0.660	+0.058	+0.110	0.760	+0.398	+0.401
0.670	+0.056	+0.122	0.770	+0.451	+0.395
0.680	+0.050	+0.114	0.780	+0.511	+0.385
0.690	+0.056	+0.121	0.790	+0.574	+0.363
0.700	+0.055	+0.118	0.800	+0.655	+0.328
0.710	+0.062	+0.126	0.810	+0.731	+0.283
0.720	+0.069	+0.118	0.820	+0.778	+0.226
0.730	+0.068	+0.113	0.830	+0.832	+0.159
0.740	+0.074	+0.112	0.840	+0.877	+0.069
0.750	+0.070	+0.123	0.850	+0.886	-0.044
0.760	+0.077	+0.123	0.860	+0.866	-0.142
0.770	+0.084	+0.143	0.870	+0.817	-0.232
0.780	+0.094	+0.169	0.880	+0.758	-0.305
0.790	+0.096	+0.183	0.890	+0.687	-0.344
			1.000	+0.634	-0.368

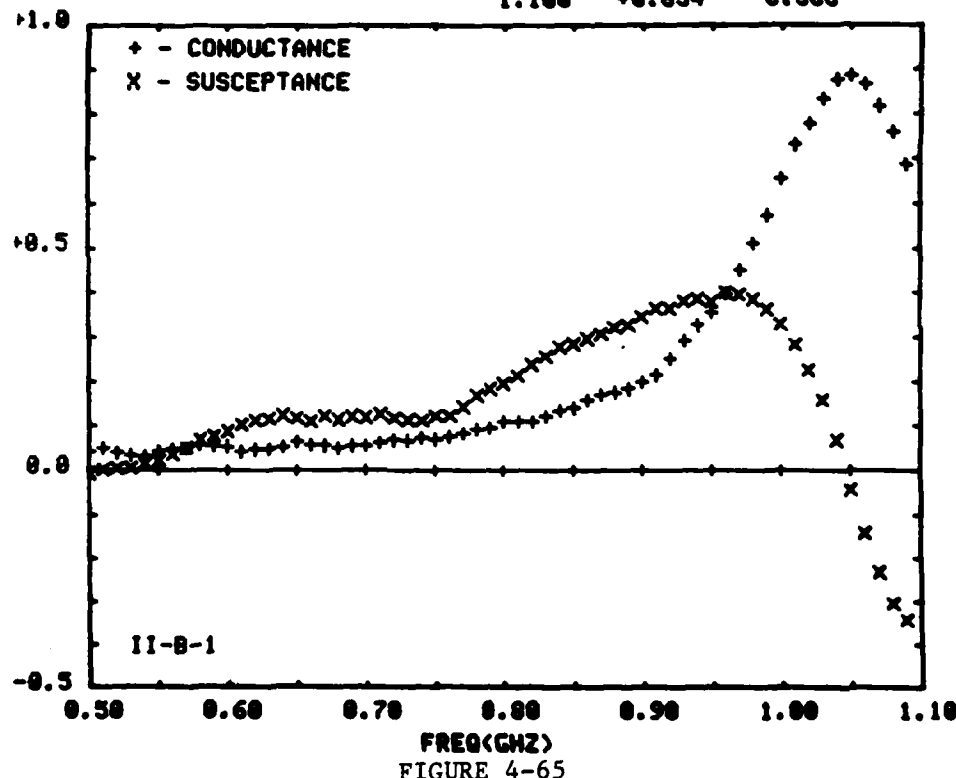


FIGURE 4-65

Aperture Admittance of Coax-Fed Bent Wire Antenna
With Open End Immersed in Tap Water (II-B-1)

FREQ. (GHZ)	G	B	FREQ. (GHZ)	G	B
0.500	+0.050	+0.126	0.800	+0.321	-0.245
0.510	+0.063	+0.142	0.810	+0.297	-0.228
0.520	+0.057	+0.144	0.820	+0.272	-0.213
0.530	+0.055	+0.151	0.830	+0.251	-0.205
0.540	+0.055	+0.165	0.840	+0.228	-0.199
0.550	+0.064	+0.188	0.850	+0.207	-0.193
0.560	+0.070	+0.214	0.860	+0.182	-0.173
0.570	+0.082	+0.238	0.870	+0.170	-0.157
0.580	+0.098	+0.265	0.880	+0.152	-0.136
0.590	+0.116	+0.287	0.890	+0.146	-0.132
0.600	+0.145	+0.298	0.900	+0.137	-0.121
0.610	+0.151	+0.299	0.910	+0.121	-0.113
0.620	+0.164	+0.306	0.920	+0.122	-0.120
0.630	+0.172	+0.318	0.930	+0.120	-0.107
0.640	+0.192	+0.350	0.940	+0.115	-0.106
0.650	+0.226	+0.374	0.950	+0.108	-0.117
0.660	+0.272	+0.398	0.960	+0.095	-0.098
0.670	+0.341	+0.414	0.970	+0.099	-0.105
0.680	+0.424	+0.387	0.980	+0.090	-0.109
0.690	+0.503	+0.334	0.990	+0.089	-0.186
0.700	+0.544	+0.254	1.000	+0.092	-0.093
0.710	+0.568	+0.194	1.010	+0.096	-0.087
0.720	+0.585	+0.136	1.020	+0.100	-0.078
0.730	+0.617	+0.084	1.030	+0.099	-0.062
0.740	+0.647	-0.008	1.040	+0.095	-0.047
0.750	+0.636	-0.111	1.050	+0.084	-0.047
0.760	+0.582	-0.210	1.060	+0.090	-0.017
0.770	+0.496	-0.258	1.070	+0.088	-0.013
0.780	+0.417	-0.267	1.080	+0.093	-0.005
0.790	+0.361	-0.260	1.090	+0.099	+0.020
			1.100	+0.098	+0.032

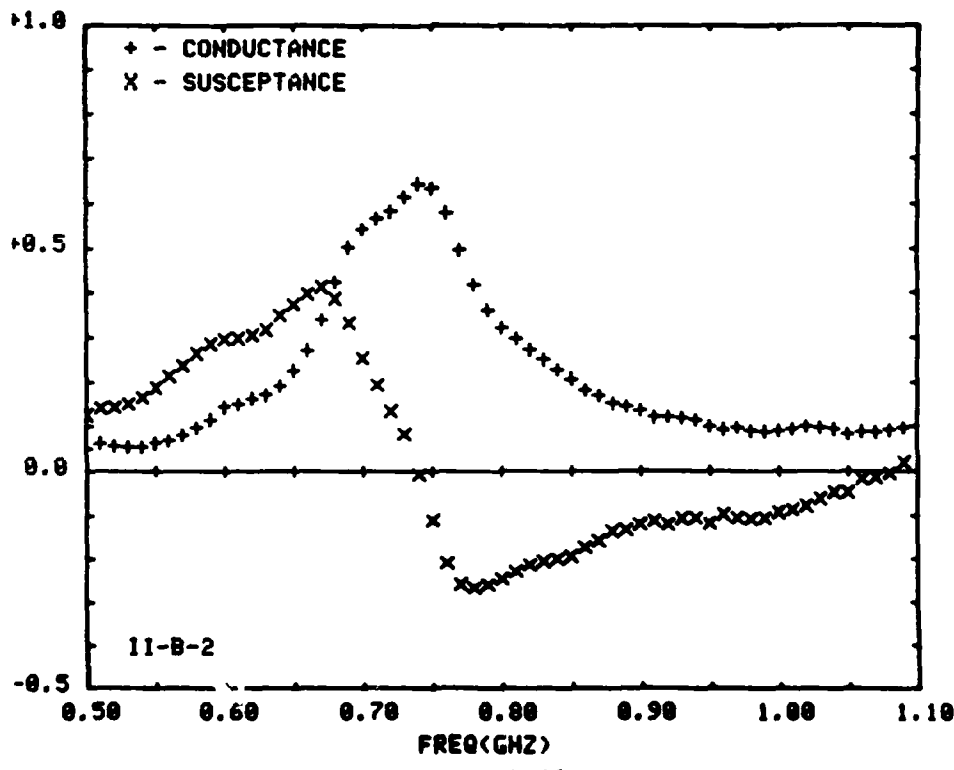


FIGURE 4-66

Aperture Admittance of Coax-Fed Bent Wire Antenna
With Open End Immersed in Tap Water (II-B-2)

FREQ. (GHZ)	G	B	FREQ. (GHZ)	G	B
0.500	+0.375	+0.359	0.800	+0.084	-0.001
0.510	+0.443	+0.291	0.810	+0.084	+0.015
0.520	+0.473	+0.216	0.820	+0.079	+0.035
0.530	+0.461	+0.158	0.830	+0.087	+0.047
0.540	+0.471	+0.148	0.840	+0.086	+0.062
0.550	+0.496	+0.118	0.850	+0.084	+0.066
0.560	+0.544	+0.068	0.860	+0.090	+0.080
0.570	+0.564	-0.016	0.870	+0.091	+0.097
0.580	+0.551	-0.127	0.880	+0.086	+0.102
0.590	+0.465	-0.203	0.890	+0.086	+0.097
0.600	+0.382	-0.220	0.900	+0.093	+0.103
0.610	+0.299	-0.217	0.910	+0.084	+0.111
0.620	+0.246	-0.195	0.920	+0.091	+0.108
0.630	+0.209	-0.173	0.930	+0.095	+0.123
0.640	+0.182	-0.142	0.940	+0.102	+0.129
0.650	+0.159	-0.125	0.950	+0.094	+0.127
0.660	+0.147	-0.110	0.960	+0.102	+0.150
0.670	+0.136	-0.084	0.970	+0.111	+0.159
0.680	+0.123	-0.077	0.980	+0.119	+0.167
0.690	+0.122	-0.068	0.990	+0.142	+0.178
0.700	+0.116	-0.065	1.000	+0.168	+0.205
0.710	+0.114	-0.058	1.010	+0.201	+0.225
0.720	+0.114	-0.061	1.020	+0.237	+0.242
0.730	+0.108	-0.064	1.030	+0.281	+0.269
0.740	+0.103	-0.062	1.040	+0.345	+0.288
0.750	+0.093	-0.056	1.050	+0.391	+0.280
0.760	+0.090	-0.054	1.060	+0.468	+0.279
0.770	+0.084	-0.041	1.070	+0.525	+0.236
0.780	+0.089	-0.027	1.080	+0.584	+0.168
0.790	+0.082	-0.013	1.090	+0.601	+0.090
			1.100	+0.611	+0.009

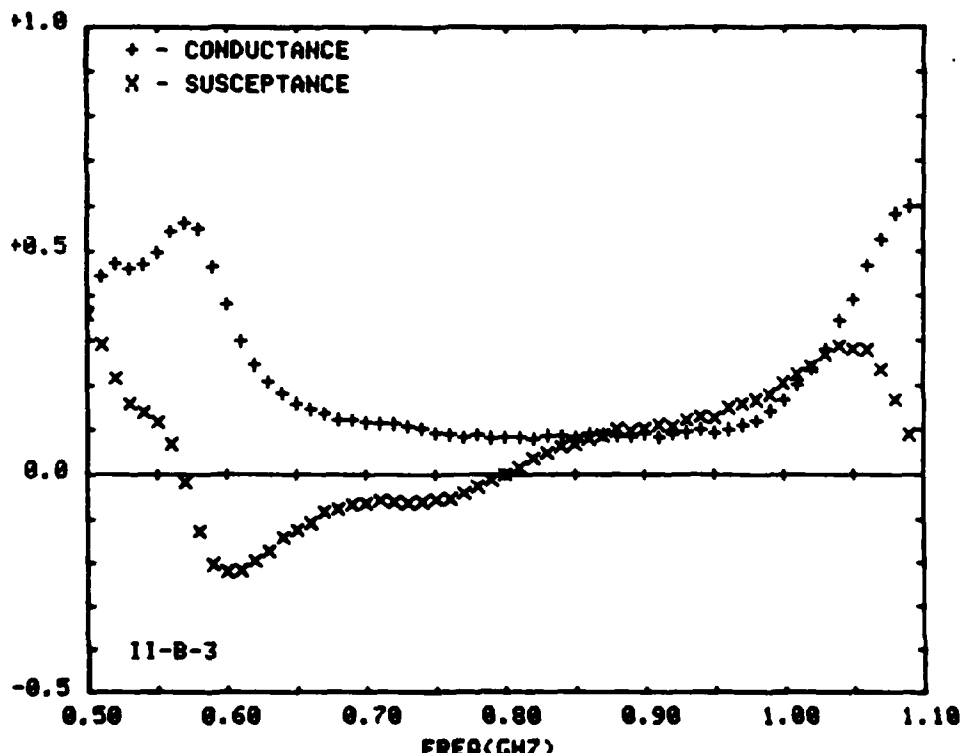


FIGURE 4-67

Aperture Admittance of Coax-Fed Bent Wire Antenna
With Open End Immersed in Tap Water (II-B-3)

FREQ. (GHZ)	G	B	FREQ. (GHZ)	G	B
0.500	+0.104	+0.228	0.800	+0.068	+0.842
0.510	+0.127	+0.281	0.810	+0.069	+0.869
0.520	+0.157	+0.308	0.820	+0.063	+0.888
0.530	+0.199	+0.343	0.830	+0.072	+0.108
0.540	+0.260	+0.378	0.840	+0.076	+0.132
0.550	+0.357	+0.415	0.850	+0.073	+0.141
0.560	+0.506	+0.419	0.860	+0.078	+0.162
0.570	+0.658	+0.345	0.870	+0.086	+0.179
0.580	+0.781	+0.129	0.880	+0.094	+0.206
0.590	+0.738	-0.129	0.890	+0.101	+0.215
0.600	+0.585	-0.272	0.900	+0.118	+0.241
0.610	+0.424	-0.303	0.910	+0.135	+0.265
0.620	+0.316	-0.290	0.920	+0.174	+0.282
0.630	+0.240	-0.244	0.930	+0.221	+0.314
0.640	+0.193	-0.202	0.940	+0.282	+0.332
0.650	+0.157	-0.173	0.950	+0.356	+0.331
0.660	+0.138	-0.150	0.960	+0.469	+0.328
0.670	+0.115	-0.115	0.970	+0.588	+0.242
0.680	+0.097	-0.193	0.980	+0.682	+0.116
0.690	+0.090	-0.086	0.990	+0.703	-0.061
0.700	+0.078	-0.078	1.000	+0.636	-0.210
0.710	+0.078	-0.059	1.010	+0.537	-0.309
0.720	+0.070	-0.055	1.020	+0.423	-0.318
0.730	+0.065	-0.045	1.030	+0.341	-0.315
0.740	+0.065	-0.038	1.040	+0.277	-0.285
0.750	+0.061	-0.025	1.050	+0.215	-0.264
0.760	+0.063	-0.020	1.060	+0.191	-0.221
0.770	+0.057	-0.004	1.070	+0.167	-0.199
0.780	+0.065	+0.013	1.080	+0.155	-0.161
0.790	+0.061	+0.033	1.090	+0.138	-0.148
			1.100	+0.126	-0.110

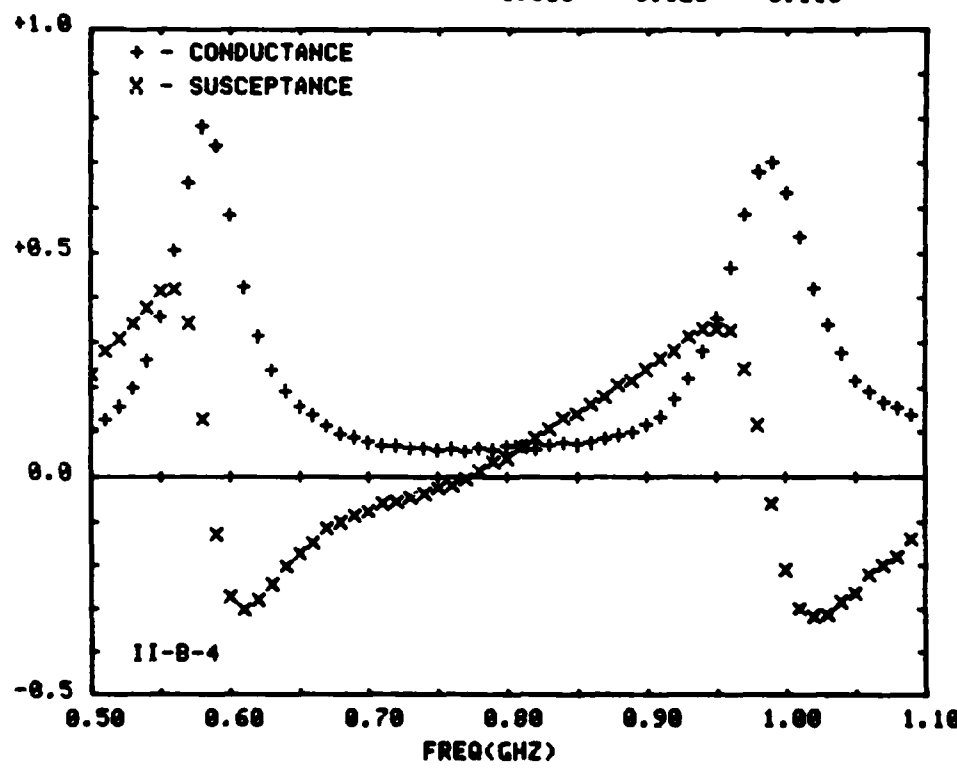


FIGURE 4-68

Aperture Admittance of Coax-Fed Bent Wire Antenna
Above Tap Water (II-B-4)

FREQ. (GHZ)	G1	B1	FREQ. (GHZ)	G1	B1
0.250	+0.934	+4.809	0.300	+5.891	-1.106
0.260	+1.899	+5.274	0.310	+4.874	-0.936
0.270	+1.567	+5.737	0.320	+4.635	-0.784
0.280	+2.186	+6.098	0.330	+4.494	-0.664
0.290	+2.497	+6.253	0.340	+4.241	-0.668
0.300	+3.160	+6.307	0.350	+4.137	-0.636
0.310	+3.894	+6.015	0.360	+3.777	-0.684
0.320	+3.974	+7.193	0.370	+3.465	-1.005
0.330	+4.996	+6.959	0.380	+3.448	-0.940
0.340	+5.821	+7.052	0.390	+3.415	-0.723
0.350	+6.867	+6.318	0.400	+3.351	-0.537
0.360	+6.360	+5.489	0.410	+3.416	-0.420
0.370	+6.879	+4.191	0.420	+3.469	-0.383
0.380	+7.673	+3.325	0.430	+3.295	-0.278
0.390	+8.814	+2.443	0.440	+3.347	-0.247
0.400	+7.837	+1.334	0.450	+3.244	-0.251
0.410	+8.810	-0.019	0.460	+3.241	-0.199
0.420	+7.594	-0.651	0.470	+3.176	-0.176
0.430	+7.421	-1.754	0.480	+3.174	-0.219
0.440	+6.685	-1.738	0.490	+3.179	-0.269
0.450	+6.449	-1.865	0.500	+3.121	-0.249
0.460	+6.206	-1.825	0.510	+3.096	-0.290
0.470	+5.719	-1.695	0.520	+3.008	-0.265
0.480	+5.448	-1.477	0.530	+2.978	-0.207
0.490	+5.205	-1.273	0.540	+2.966	-0.167
			0.550	+2.918	-0.091

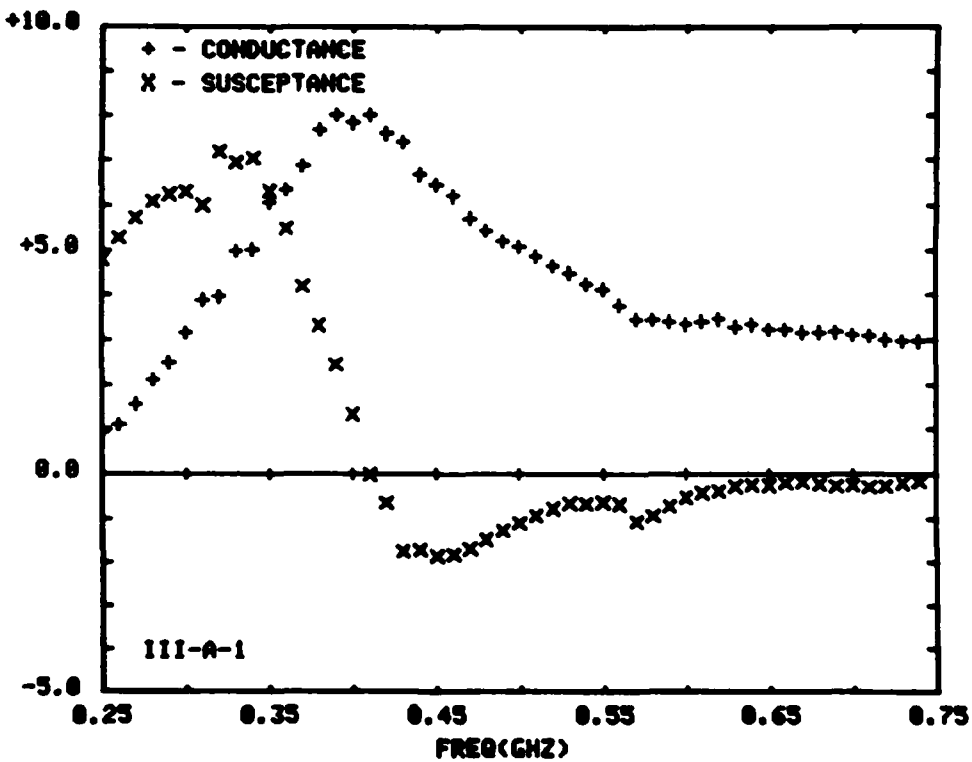


FIGURE 4-69

Aperture Admittance of Cylindrical Coax-Fed Monopole
Antenna Immersed in Water
(III-A-1)

FREQ(GHZ)	EPS-R	SIGMA(SI/M)	LINEAR REGRESSION	
			EPS-R	SIGMA(SI/M)
0.500	81.6	1.229E-001	81.3	1.040E-001
0.525	81.7	1.239E-001	81.3	1.143E-001
0.550	81.6	1.289E-001	81.4	1.246E-001
0.575	81.3	1.359E-001	81.4	1.350E-001
0.600	81.1	1.419E-001	81.4	1.453E-001
0.625	80.7	1.529E-001	81.4	1.556E-001
0.650	80.6	1.621E-001	81.4	1.659E-001
0.675	81.0	1.676E-001	81.4	1.763E-001
0.700	81.4	1.753E-001	81.5	1.866E-001
0.725	81.9	1.924E-001	81.5	1.969E-001
0.750	82.1	1.981E-001	81.5	2.072E-001
0.775	81.9	2.089E-001	81.5	2.176E-001
0.800	81.8	2.219E-001	81.5	2.279E-001
0.825	81.8	2.346E-001	81.6	2.382E-001
0.850	81.6	2.471E-001	81.6	2.485E-001
0.875	81.7	2.622E-001	81.6	2.589E-001
0.900	81.8	2.706E-001	81.6	2.692E-001
0.925	81.7	2.848E-001	81.6	2.795E-001
0.950	81.7	2.916E-001	81.7	2.898E-001
0.975	81.5	3.122E-001	81.7	3.002E-001
1.000	81.2	3.173E-001	81.7	3.105E-001

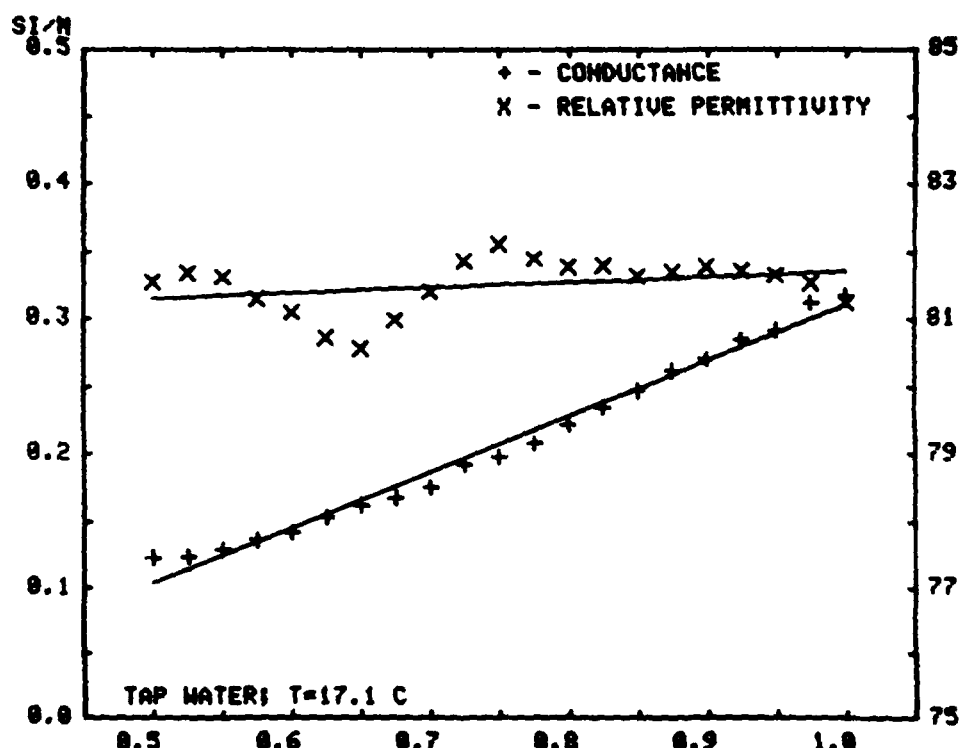


FIGURE 4-70

Effective Conductivity and Relative Permittivity of Tap Water
Used in Configuration I, Series A Experiments

FREQ(GHZ)	EPS-R	SIGMA(SI/M)	LINEAR REGRESSION	
			EPS-R	SIGMA(SI/M)
0.500	79.6	1.445E+000	78.3	1.420E+000
0.525	79.8	1.447E+000	78.3	1.430E+000
0.550	79.6	1.449E+000	78.2	1.441E+000
0.575	77.7	1.444E+000	78.2	1.451E+000
0.600	76.9	1.450E+000	78.2	1.462E+000
0.625	77.4	1.461E+000	78.2	1.472E+000
0.650	77.6	1.474E+000	78.2	1.483E+000
0.675	79.1	1.487E+000	78.2	1.493E+000
0.700	79.1	1.500E+000	78.1	1.504E+000
0.725	78.0	1.511E+000	78.1	1.514E+000
0.750	77.9	1.516E+000	78.1	1.525E+000
0.775	77.9	1.521E+000	78.1	1.535E+000
0.800	78.0	1.537E+000	78.1	1.545E+000
0.825	78.1	1.553E+000	78.1	1.556E+000
0.850	78.3	1.568E+000	78.1	1.566E+000
0.875	78.8	1.582E+000	78.0	1.577E+000
0.900	78.8	1.597E+000	78.0	1.587E+000
0.925	78.6	1.605E+000	78.0	1.598E+000
0.950	78.2	1.618E+000	78.0	1.608E+000
0.975	77.7	1.621E+000	78.0	1.619E+000
1.000	77.3	1.630E+000	78.0	1.629E+000

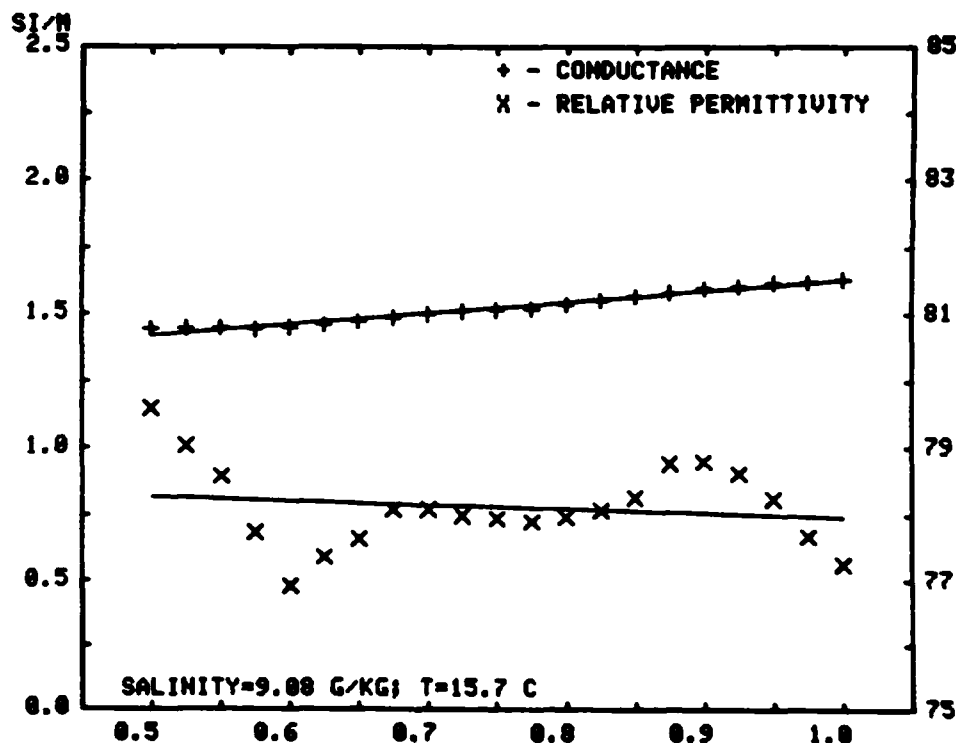


FIGURE 4-71

Effective Conductivity and Relative Permittivity of Salt Water
Used in Configuration I, Series C Experiments

FREQ(GHZ)	EPS-R	SIGMA(SI/M)	LINEAR REGRESSION EPS-R	SIGMA(SI/M)
0.500	78.5	1.146E+000	78.7	1.138E+000
0.525	78.5	1.154E+000	78.7	1.148E+000
0.550	78.8	1.164E+000	78.7	1.159E+000
0.575	79.0	1.174E+000	78.7	1.170E+000
0.600	79.0	1.181E+000	78.7	1.180E+000
0.625	78.8	1.194E+000	78.7	1.191E+000
0.650	78.7	1.199E+000	78.7	1.202E+000
0.675	78.3	1.203E+000	78.7	1.212E+000
0.700	78.1	1.212E+000	78.8	1.223E+000
0.725	78.4	1.221E+000	78.8	1.234E+000
0.750	78.8	1.236E+000	78.8	1.244E+000
0.775	79.1	1.257E+000	78.8	1.255E+000
0.800	79.4	1.269E+000	78.8	1.266E+000
0.825	79.3	1.275E+000	78.8	1.276E+000
0.850	79.1	1.287E+000	78.9	1.287E+000
0.875	78.8	1.293E+000	78.9	1.298E+000
0.900	78.7	1.307E+000	78.9	1.308E+000
0.925	78.6	1.317E+000	78.9	1.319E+000
0.950	78.9	1.332E+000	78.9	1.330E+000
0.975	78.9	1.347E+000	78.9	1.341E+000
1.000	78.8	1.362E+000	78.9	1.351E+000

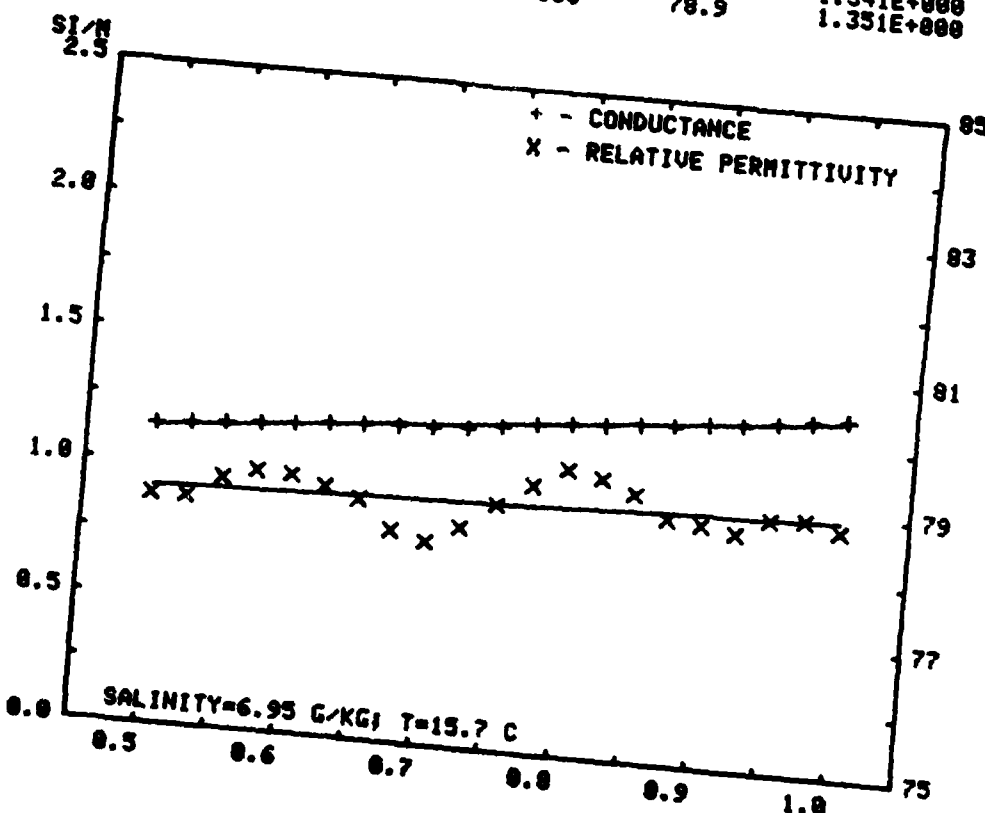


FIGURE 4-72
Effective Conductivity and Relative Permittivity of Salt Water
Used in Configuration I, Series D Experiments

FREQ(GHZ)	EPS-R	SIGMA(SI/M)	LINEAR REGRESSION EPS-R	SIGMA(SI/M)
0.500	81.0	2.231E-001	80.7	2.158E-001
0.525	80.9	2.373E-001	80.7	2.258E-001
0.550	80.9	2.422E-001	80.7	2.357E-001
0.575	80.8	2.496E-001	80.7	2.457E-001
0.600	80.7	2.545E-001	80.7	2.556E-001
0.625	80.2	2.638E-001	80.7	2.656E-001
0.650	80.3	2.719E-001	80.7	2.756E-001
0.675	80.4	2.803E-001	80.7	2.855E-001
0.700	80.4	2.911E-001	80.7	2.955E-001
0.725	80.7	2.968E-001	80.7	3.055E-001
0.750	80.8	3.099E-001	80.7	3.154E-001
0.775	80.7	3.218E-001	80.6	3.254E-001
0.800	80.7	3.298E-001	80.6	3.354E-001
0.825	80.6	3.372E-001	80.6	3.453E-001
0.850	80.6	3.509E-001	80.6	3.553E-001
0.875	80.6	3.590E-001	80.6	3.652E-001
0.900	80.8	3.733E-001	80.6	3.752E-001
0.925	80.8	3.888E-001	80.6	3.852E-001
0.950	80.8	3.981E-001	80.6	3.951E-001
0.975	80.3	4.190E-001	80.6	4.051E-001
1.000	80.2	4.264E-001	80.6	4.151E-001

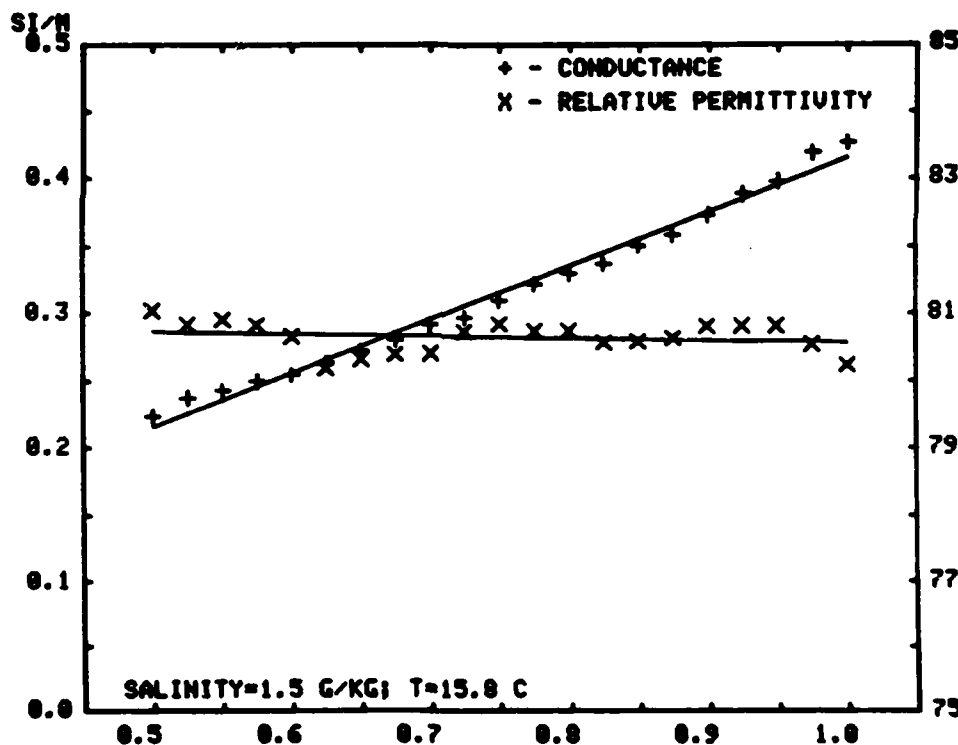


FIGURE 4-73

Effective Conductivity and Relative Permittivity of Salt Water
Used in Configuration I, Series E Experiments

FREQ(GHZ)	EPS-R	SIGMA(SIG/M)	LINEAR REGRESSION	
			EPS-R	SIGMA(SIG/M)
0.500	78.9	1.570E+000	78.1	1.553E+000
0.525	78.6	1.576E+000	78.2	1.564E+000
0.550	78.3	1.578E+000	78.2	1.574E+000
0.575	77.9	1.581E+000	78.2	1.584E+000
0.600	77.5	1.588E+000	78.2	1.594E+000
0.625	77.4	1.594E+000	78.2	1.604E+000
0.650	77.7	1.603E+000	78.2	1.615E+000
0.675	78.2	1.623E+000	78.2	1.625E+000
0.700	78.5	1.638E+000	78.3	1.635E+000
0.725	78.4	1.647E+000	78.3	1.645E+000
0.750	78.0	1.650E+000	78.3	1.656E+000
0.775	78.0	1.650E+000	78.3	1.666E+000
0.800	78.0	1.667E+000	78.3	1.676E+000
0.825	78.3	1.680E+000	78.3	1.686E+000
0.850	78.7	1.693E+000	78.3	1.697E+000
0.875	79.6	1.716E+000	78.4	1.707E+000
0.900	79.4	1.727E+000	78.4	1.717E+000
0.925	78.8	1.728E+000	78.4	1.727E+000
0.950	78.5	1.749E+000	78.4	1.739E+000
0.975	77.9	1.756E+000	78.4	1.748E+000
1.000	77.4	1.754E+000	78.4	1.758E+000

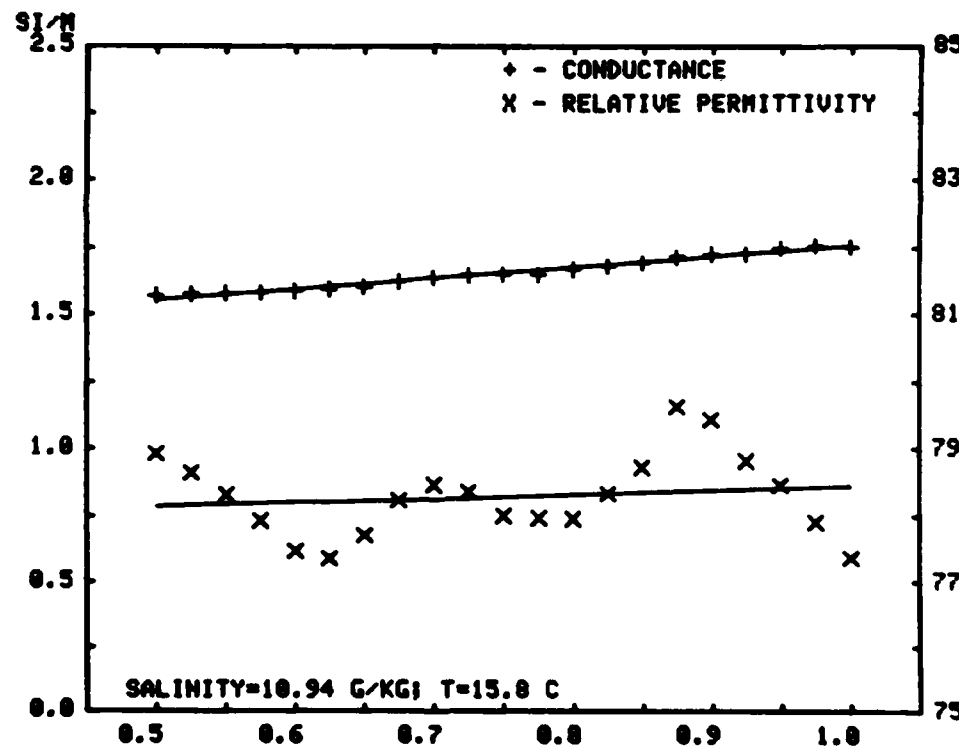


FIGURE 4-74

Effective Conductivity and Relative Permittivity of Salt Water
Used in Configuration I, Series F Experiments

FREQ(GHZ)	EPS-R	SIGMA(SI/M)	LINEAR REGRESSION	
			EPS-R	SIGMA(SI/M)
0.500	78.9	1.263E+000	78.3	1.249E+000
0.525	78.9	1.277E+000	78.3	1.259E+000
0.550	78.6	1.278E+000	78.3	1.269E+000
0.575	78.1	1.281E+000	78.3	1.288E+000
0.600	77.6	1.287E+000	78.3	1.298E+000
0.625	77.2	1.289E+000	78.3	1.301E+000
0.650	77.6	1.294E+000	78.3	1.311E+000
0.675	78.1	1.314E+000	78.3	1.321E+000
0.700	78.5	1.328E+000	78.4	1.332E+000
0.725	78.8	1.348E+000	78.4	1.342E+000
0.750	78.8	1.354E+000	78.4	1.352E+000
0.775	78.7	1.355E+000	78.4	1.363E+000
0.800	78.3	1.362E+000	78.4	1.373E+000
0.825	78.9	1.371E+000	78.4	1.384E+000
0.850	78.2	1.386E+000	78.4	1.394E+000
0.875	78.5	1.403E+000	78.5	1.404E+000
0.900	78.9	1.420E+000	78.5	1.415E+000
0.925	79.8	1.437E+000	78.5	1.425E+000
0.950	78.9	1.449E+000	78.5	1.435E+000
0.975	78.4	1.455E+000	78.5	1.446E+000
1.000	78.9	1.457E+000	79.5	1.456E+000

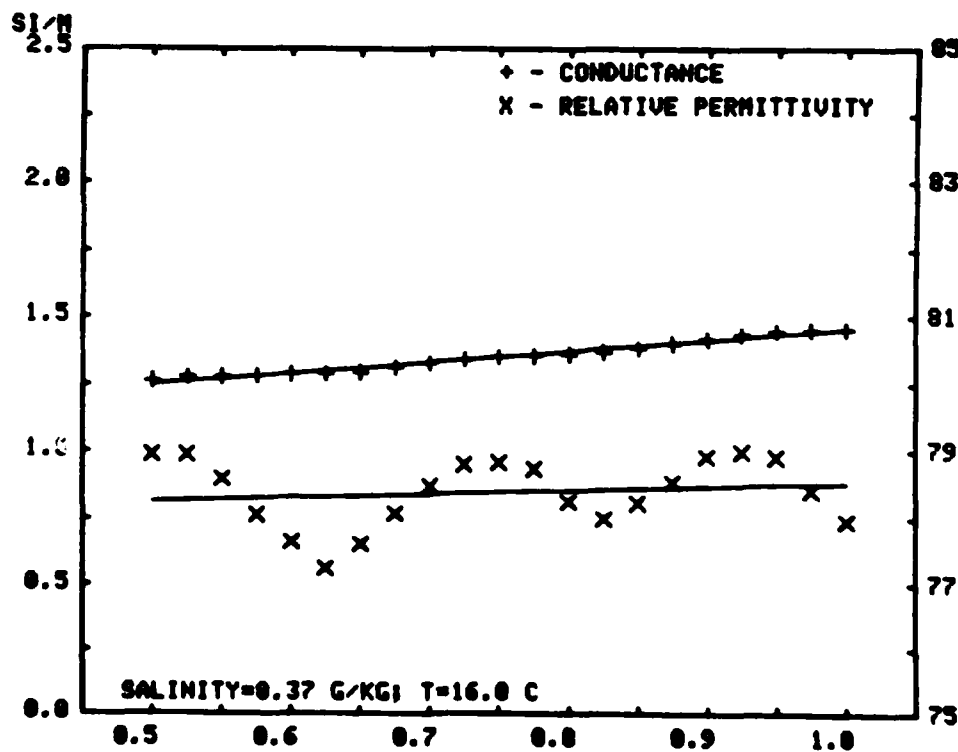


FIGURE 4-75

Effective Conductivity and Relative Permittivity of Salt Water
Used in Configuration I, Series G Experiments

FREQ(GHZ)	EPS-R	SIGMA(SI/M)	LINEAR REGRESSION	
			EPS-R	SIGMA(SI/M)
0.500	81.4	1.329E-001	81.8	1.181E-001
0.525	81.7	1.357E-001	81.8	1.275E-001
0.550	81.5	1.433E-001	81.8	1.370E-001
0.575	81.1	1.502E-001	80.9	1.464E-001
0.600	80.5	1.499E-001	80.9	1.539E-001
0.625	80.1	1.600E-001	80.9	1.653E-001
0.650	79.8	1.639E-001	80.9	1.748E-001
0.675	80.2	1.815E-001	80.9	1.842E-001
0.700	80.8	1.901E-001	80.8	1.937E-001
0.725	81.0	1.999E-001	80.8	2.031E-001
0.750	81.1	2.070E-001	80.8	2.126E-001
0.775	81.0	2.182E-001	80.8	2.220E-001
0.800	80.7	2.273E-001	80.7	2.315E-001
0.825	80.8	2.319E-001	80.7	2.409E-001
0.850	80.6	2.462E-001	80.7	2.504E-001
0.875	80.9	2.604E-001	80.7	2.598E-001
0.900	80.8	2.689E-001	80.7	2.693E-001
0.925	80.8	2.865E-001	80.6	2.787E-001
0.950	80.8	2.908E-001	80.6	2.882E-001
0.975	80.6	3.058E-001	80.6	2.977E-001
1.000	80.4	3.151E-001	80.6	3.071E-001

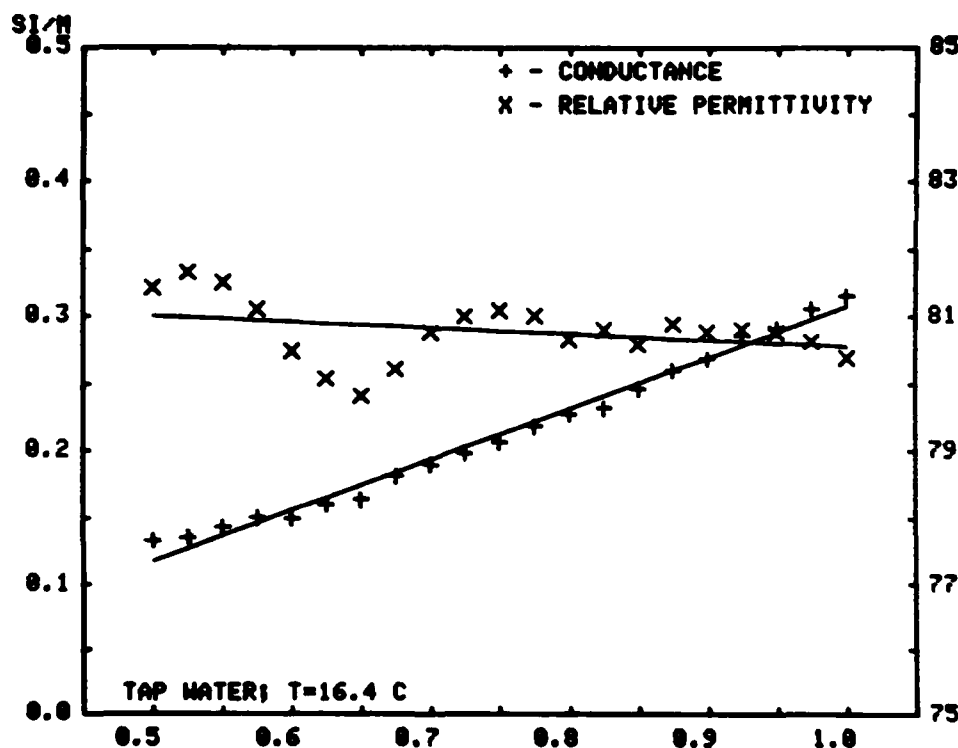


FIGURE 4-76

Effective Conductivity and Relative Permittivity of Tap Water
Used in Configuration I, Series H Experiments

FREQ(GHZ)	EPS-R	SIGMA(SI/M)	LINEAR REGRESSION	
			EPS-R	SIGMA(SI/M)
0.500	81.5	1.281E-001	81.1	1.281E-001
0.525	81.7	1.360E-001	81.1	1.294E-001
0.550	81.6	1.409E-001	81.1	1.387E-001
0.575	81.2	1.472E-001	81.0	1.480E-001
0.600	80.7	1.478E-001	81.0	1.373E-001
0.625	80.1	1.647E-001	81.0	1.666E-001
0.650	80.0	1.692E-001	81.0	1.759E-001
0.675	80.4	1.845E-001	80.9	1.851E-001
0.700	80.7	1.911E-001	80.9	1.944E-001
0.725	81.0	1.992E-001	80.9	2.037E-001
0.750	81.2	2.128E-001	80.9	2.130E-001
0.775	81.1	2.212E-001	80.8	2.223E-001
0.800	80.8	2.327E-001	80.8	2.316E-001
0.825	80.9	2.459E-001	80.8	2.409E-001
0.850	80.7	2.492E-001	80.8	2.501E-001
0.875	80.9	2.639E-001	80.7	2.594E-001
0.900	80.9	2.717E-001	80.7	2.687E-001
0.925	80.7	2.836E-001	80.7	2.780E-001
0.950	80.8	2.791E-001	80.6	2.873E-001
0.975	80.6	3.006E-001	80.6	2.966E-001
1.000	80.0	3.040E-001	80.6	3.059E-001

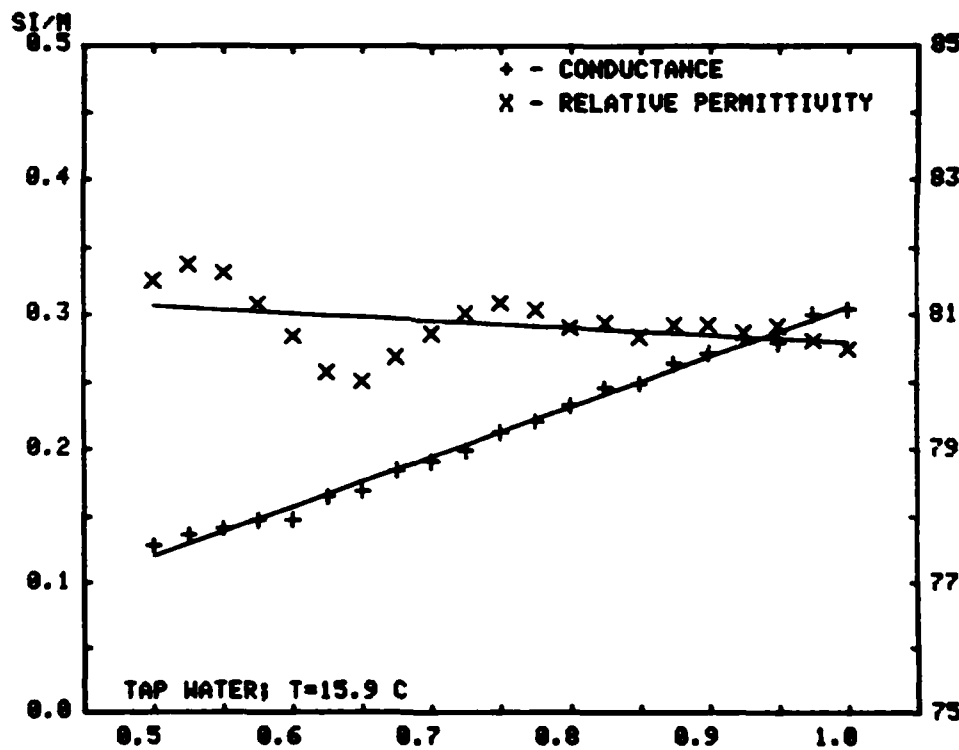


FIGURE 4-77

Effective Conductivity and Relative Permittivity of Tap Water
Used in Configuration I, Series I Experiments

APPENDICES

Appendix A

MEASUREMENT OF THE ELECTROMAGNETIC CONSTITUTIVE PROPERTIES OF WATER

The purpose of this appendix is to outline the theoretical basis for the technique used to determine the electromagnetic constitutive properties of water. The attenuation and phase shift of an electric field propagating in a water-filled waveguide was measured at several positions along the propagation (z) axis of the waveguide. The wavenumber (k_z) was derived from these measurements, and the electromagnetic constitutive properties were calculated from k_z .

For a waveguide operating in a TE (or TEM) mode, and in which there is no reflected wave, the electric field at any position on the propagation axis is

$$E(z) = E_t(x,y)e^{-jk_z z} , \quad (1)$$

where $E_t(x,y)$ is the transverse field at $z = 0$ and is independent of z . The intrinsic wavenumber (k) for a lossy medium like water is given by

$$k = \omega[\mu(\epsilon - j\sigma/\omega)]^{1/2} . \quad (2)$$

Since k_z is dependent upon k , k_z is complex and may be expressed as

$$k_z = \beta - j\alpha , \quad (3)$$

and $E(z)$ may be expressed as

$$E(z) = E_t(x,y)e^{-\alpha z} e^{-j\beta z} . \quad (4)$$

If the magnitude and phase angle of the electric field is measured at any reference position (z_0), then

$$\ln \frac{|E(z_0)|}{|E_t(x,y)|} = -\alpha z_0 , \quad (5)$$

and

$$\Phi(z_0) = -\beta z_0 , \quad (6)$$

where $\Phi(z_0)$ is the phase angle of the electric field at z_0 . The magnitude and phase angle of the electric field measured at any position (z) is related to that measured at the reference position by

$$\ln \frac{|E(z_0)|}{|E(z)|} = \alpha(z-z_0) . \quad (7)$$

and

$$\Phi(z_0) - \Phi(z) = \beta(z-z_0) . \quad (8)$$

The wavenumber (k_z) may be obtained by solving (7) and (8) for α and β and substituting the solutions into (3). Relative permittivity (ϵ_r) and effective conductivity (σ) may then be computed from (2) and the relationship between k and k_z for the particular waveguide configuration.

For a coaxial waveguide, $k_z = k$, and hence from (2) and (3)

$$\epsilon_r = \frac{\beta^2 - \alpha^2}{\omega^2 \mu \epsilon_0} , \quad (9)$$

and

$$\sigma = 2\alpha\beta/(\omega\mu) . \quad (10)$$

For a rectangular waveguide operating in dominant (TE_{01}) mode,

$$k_z = [k^2 - (\pi/b)^2]^{1/2} , \quad (11)$$

where b is the width of the broad wall of the waveguide. From (2) and (3), for the rectangular waveguide

$$\epsilon_r = \frac{\beta^2 - \alpha^2 + (\pi/b)^2}{\omega^2 \mu \epsilon_0} . \quad (12)$$

and conductivity is calculated as in (10).

Field magnitudes and phase angles were measured at several (5 to 9) positions along the waveguide propagation axis for each frequency of interest. Linear regression with respect to z was performed on the values obtained for α and β before solving for ϵ_r and σ . Since ϵ_r and σ are known to be smooth, slowly-varying functions of frequency, linear regression of ϵ_r and σ with respect to frequency was performed over narrow frequency bands (less than 1 octave) in order to provide more useful results.

Appendix B

DERIVATION OF ANTENNA APERTURE ADMITTANCE

It is usually not possible to make a direct measurement of aperture admittance (Y) for a microwave antenna. Typical instrumentation permits measurement of reflection coefficient (Γ) at the antenna driving point connector. The driving point connector serves as access port to a transmission line which terminates at the antenna aperture. The purpose of this appendix is to formulate the relationship between Y and Γ .

If the electrical length ($k\ell$) for the transmission line is known, then from the general transmission line equations [18]

$$Y(\ell) = Z_0^{-1} \frac{1 - \Gamma(0)e^{j2k\ell}}{1 + \Gamma(0)e^{j2k\ell}}, \quad (1)$$

where Z_0 is the characteristic impedance of the transmission line. In practice, k is often not known and establishing the exact length (ℓ) may be difficult. It is desirable, then, that any method for deriving $Y(\ell)$ from $\Gamma(0)$ not depend upon $k\ell$.

REFERENCE SHORT METHOD

One method for deriving Y from Γ involves use of a device herein called a "reference short." A reference short is constructed from a transmission line and connector identical to that used with the antenna

under consideration. A high-quality short circuit is formed at the position where the aperture plane exists in the antenna (Figure B-1). Reflection coefficient (Γ_s) measured at the connector of the reference short can be used with Γ to derive Y independent of $k\ell$. From the general transmission line equations,

$$\Gamma(0) = \Gamma(\ell)e^{-j2k\ell} , \quad (2)$$

where $\Gamma(\ell)$ is the reflection coefficient measured at the antenna aperture plane (if that were possible). If the aperture is replaced with a short circuit, as is done in the reference short method, then

$$\Gamma_s(\ell) = -1 ,$$

and (2) becomes

$$\Gamma_s(0) = -e^{-j2k\ell} . \quad (3)$$

Substitution of (3) into (1) yields

$$Y(\ell) = Z_o^{-1} \frac{\Gamma_s(0) + \Gamma(0)}{\Gamma_s(0) - \Gamma(0)} , \quad (4)$$

which relates Y to driving point reflection coefficients, but eliminates dependence upon $k\ell$.

In the foregoing derivation, $Y(\ell)$ depends in part upon Z_o so that the result is not entirely independent of transmission line characteristics. In low-loss coaxial waveguide, Z_o is independent of frequency and depends only upon waveguide geometry and constitutive properties of the dielectric. Experience has shown that in high-quality waveguide, the specified Z_o is maintained very well by the manufacturer.

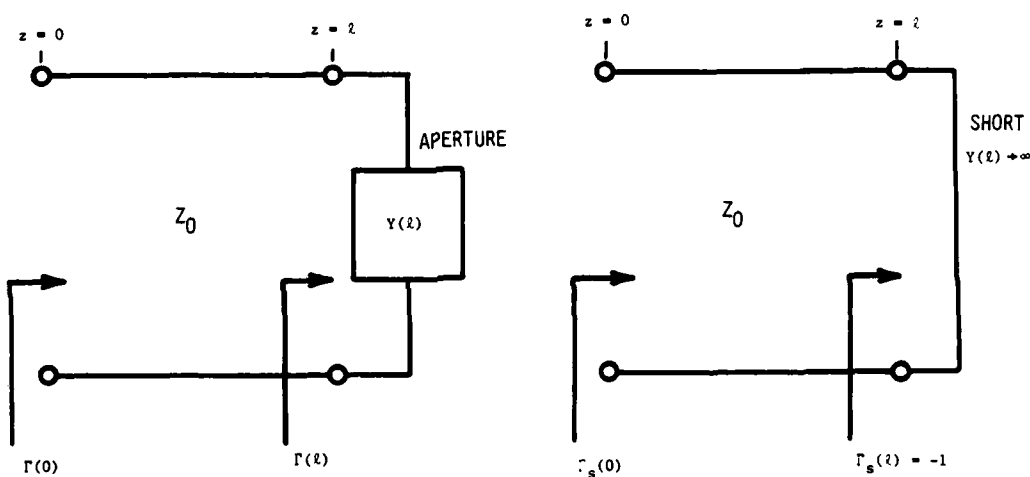


FIGURE B-1

Model for Deriving Aperture Admittance
From Reflection Coefficient

EFFECT OF A DIELECTRIC BEAD IN THE TRANSMISSION LINE

The monopole antenna used in the Series III procedures was constructed from a section of air-filled coaxial waveguide. A 1-cm bead of Teflon was placed at the antenna aperture to center and support the center conductor and to prevent water from entering the transmission line. This Teflon bead alters the characteristic impedance of the transmission line where it displaces the air dielectric and determines the characteristic impedance of the antenna aperture. The "reference short" method for deriving antenna aperture admittance from driving point reflection coefficient must be modified to accomodate the presence of the bead.

A model of the antenna and the reference short, each of which is of identical length ($\ell_1 + \ell_2$), and each of which contains an identical Teflon bead, can be seen in Figure B-2. The measured antenna and reference short driving point reflection coefficients, $\Gamma(0)$ and $\Gamma_s(0)$, respectively, can be referred to the air-Teflon interface ($z = \ell_1$) and thence to the antenna aperture ($z = \ell_1 + \ell_2$), so that

$$\Gamma(\ell_1 + \ell_2) = \frac{Z_{01}^{(1+A)} - Z_{02}^{(1-A)}}{Z_{01}^{(1+A)} + Z_{02}^{(1-A)}} , \quad (5)$$

and

$$\Gamma_s(\ell_1 + \ell_2) = \frac{Z_{01}^{(1+B)} - Z_{02}^{(1-B)}}{Z_{01}^{(1+B)} + Z_{02}^{(1-B)}} , \quad (5a)$$

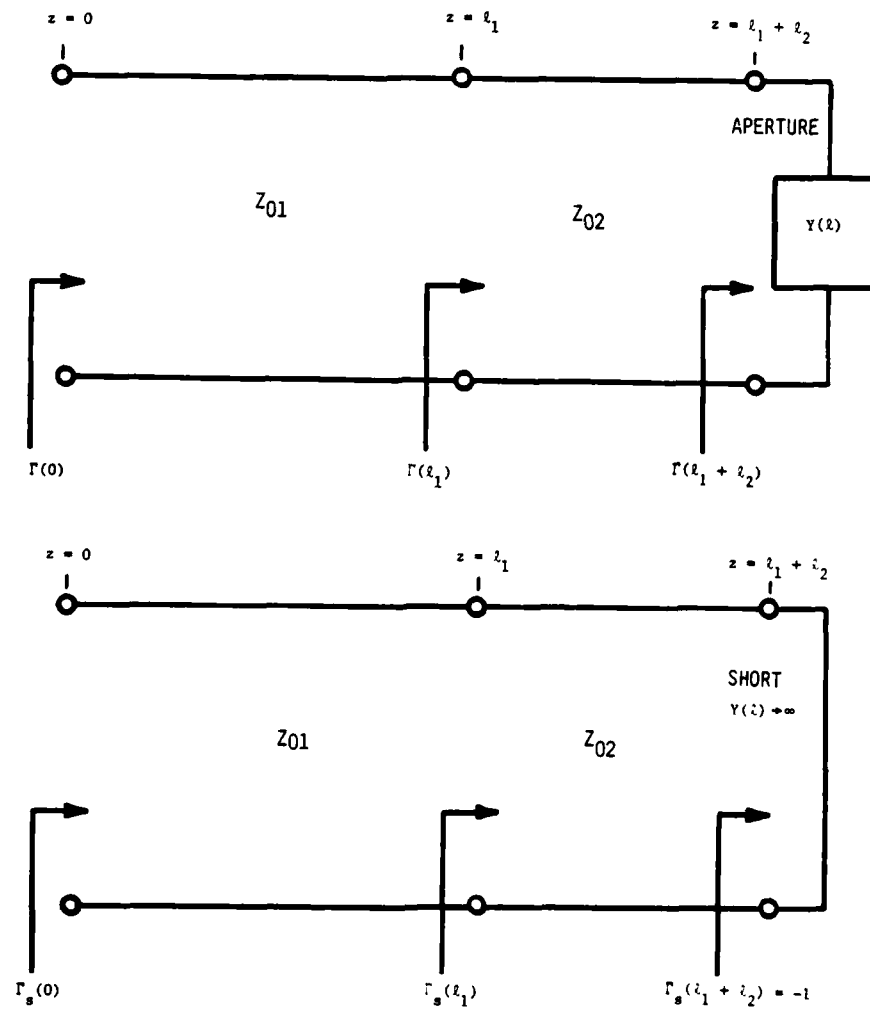


FIGURE B-2

Model for Deriving Aperture Admittance From Reflection Coefficient with Dielectric Bead in Feed Line

where $A = \Gamma(0)e^{j2k_1\ell_1}$ and $B = \Gamma_s(0)e^{j2k_1\ell_1}$.

Z_{01} and Z_{02} are characteristic impedance of section 1 and section 2 respectively. Since $\Gamma_s(\ell_1 + \ell_2) = -1$, (5a) can be solved to obtain

$$e^{j2k_1\ell_1} = \frac{Z_{02} \tan(k_2\ell_2) + j Z_{01}}{Z_{02} \tan(k_2\ell_2) - j Z_{01}} \Gamma_s(0)^{-1}. \quad (6)$$

The antenna aperture admittance is

$$Y(\ell_1 + \ell_2) = Z_{02}^{-1} \frac{1 - \Gamma(\ell_1 + \ell_2)}{1 + \Gamma(\ell_1 + \ell_2)}. \quad (7)$$

When (6) is combined with (5) and (7), then

$$Y(\ell_1 + \ell_2) = Z_{02}^{-1} \frac{Z_{01}Z_{02}[1 + \tan^2(k_2\ell_2)]C - j(Z_{01}^2 - Z_{02}^2)\tan(k_2\ell_2)}{Z_{02}^2 \tan^2(k_2\ell_2) + Z_{01}^2}, \quad (8)$$

where $C = (\Gamma_s(0) + \Gamma(0))/(\Gamma_s(0) - \Gamma(0))$. If $\ell_2 = 0$, then (8) reduces to (4), so that the same data reduction program, with proper branching, may be used for all antennas.

In order to eliminate both $k_1\ell_1$ and $k_2\ell_2$ from the derivation of antenna aperture admittance, it would be necessary to obtain reflection coefficient data from another reference short of length ℓ_1 and without a dielectric bead. Since ℓ_2 was small, and Teflon is relatively lossless and has well-known electromagnetic constitutive properties, $k_2\ell_2$ was computed for $\ell_2 = 1$ cm and $\epsilon_r = 2.1$ at each frequency, and entered into (8) along with Z_{01} as follows:

$$k_2\ell_2 = 2\pi f \epsilon_r^{1/2}/c$$

$$Z_{02} = Z_{01}/\epsilon_r^{1/2}$$

PROCEDURES

Reference shorts were constructed and used in the Series II and III experiments which involved monopole-above-ground-plane configurations. The transmission line leading from driving point to antenna aperture was relatively short (~ 5 cm), and the aperture plane was transverse to the propagation axis of the transmission line, which made construction of the reference shorts inexpensive and simple. The sleeve monopole used in Series I experiments presented a somewhat different situation. First, the transmission line (or sleeve) from driving point to aperture (source gap) was approximately 90 cm in length, which would have made construction of reference shorts for each of the three antennas a relatively expensive undertaking. Second, the aperture plane for this type of antenna is not transverse to the propagation axis of the transmission line (see Figure 2-8), which would make establishment of a short circuit more difficult. To economize on construction, and to provide what is believed to be a more appropriate short circuit, a brass collar was clamped around the gap to short circuit the source gap. Γ_s was measured with the collar in place and the results applied in (4), as in the Series II experiments. The finite width of the source gap introduces an unknown error into this procedure because this width adds length to the transmission line and the air in the gap alters the characteristic admittance at the gap. This error has been neglected because the source gaps are so small (~ 0.5 mm) relative to sleeve length.

All of the foregoing procedures assume that the connector at the driving point is lossless and is an ideal match to the transmission line. The antennas and reference shorts were all examined with a time-domain reflectometer (TDR), and the results of this examination appear to validate this assumption.

DATA REDUCTION

Data reduction and the graphical display of the results were accomplished "on board" the semi-automatic network analyzer with the computer-controller.

Appendix C

COMPUTATIONS RELATED TO THE DESIGN OF THE SLOTTED COAXIAL WAVEGUIDE

A slotted coaxial waveguide apparatus was constructed for use in measuring the electromagnetic constitutive properties of water. This appendix presents the criteria used in selection of diametric dimensions for the waveguide and derives the resulting characteristic impedances for the various sections of the waveguide.

DIAMETRIC DIMENSIONS

The diametric dimensions of a coaxial waveguide determine its characteristic impedance in the TEM mode of operation and its ability to support propagation of higher order (than TEM) modes. The three objectives in this design, listed in order of importance, were (1) to suppress higher order modes below 1 GHz in the water-filled section, (2) to achieve sufficient separation between center and outer conductors so that the E-field probe would not seriously perturb the E-field, and (3) to achieve a 50-ohm characteristic impedance in the air-filled section. The final design was a compromise between these objectives and the availability of brass rod and tubing of standard diameters.

Reference [19] suggests that suppression of higher order modes in a coaxial waveguide can be achieved by restricting waveguide circumference at mean diameter to the desired limiting wavelength. This is expressed as

$$\lambda_c \geq \pi(a+b) , \quad (1)$$

where $2a$ is the outer diameter of the center conductor, $2b$ is the inner diameter of the outer conductor (Figure C-1), and f_c is the cutoff frequency of the next higher order mode (TE_{11}). The minimum separation between the center and outer conductors was considered to be 0.4 cm, or about 3 times the minimum practical probe length of 0.05 inch (0.125 cm). Thus

$$(b-a) \geq 0.4\text{cm} . \quad (2)$$

The characteristic impedance of a coaxial waveguide with low-loss dielectric is determined by the approximation

$$Z_0 \approx \frac{\eta_0}{2\pi} \epsilon_r^{-\frac{1}{2}} \ln(b/a) , \quad (3)$$

where η_0 is free-space intrinsic impedance and ϵ_r is relative permittivity of the dielectric. The derivation of this approximation and its applicability to this waveguide is considered in the next section of this appendix.

Since the air-filled section of the waveguide is electrically smaller in cross-section than the water-filled section, a design which ensures suppression of higher-order modes in the water-filled section will also ensure suppression of these modes in the air-filled section. From (1), the TE_{11} mode will be cut off below approximately 1 GHz for

$$a+b \approx 1.1\text{cm} . \quad (4)$$

In the air-filled section, a characteristic impedance of 50 ohms requires (from (3)) that

$$b/a \approx 2.3 . \quad (5)$$

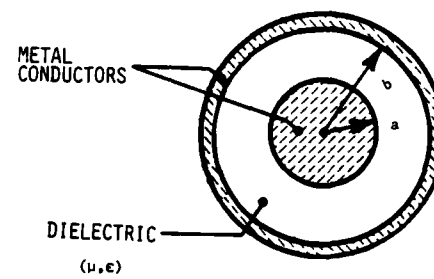


FIGURE C-1
Cross-Section of Coaxial Waveguide

When (2) and (4) are combined,

$$a \approx 0.35\text{cm} (0.14 \text{ inch})$$

and

$$b \approx 0.75\text{cm} (0.30 \text{ inch}) .$$

The standard brass stock with nearest to these dimensions was 0.250-inch OD rod (center conductor) and 0.650-inch ID (0.750-inch OD) tubing (conductor). With these materials, separation between the conductors is 0.51 cm, and $b/a \approx 2.6$, for which $Z_0 \approx 57.3$ ohms for the air-filled section of the waveguide.

A more careful examination of the propagation characteristics of a coaxial waveguide indicates that the cutoff frequency for the TE_{mn} mode is determined by the mth root of the transcendental equation

$$J'_n(k_\rho a)N'_n(k_\rho b) - J'_n(k_\rho b)N'_n(k_\rho a) = 0 , \quad (6)$$

where $k^2 = k_z^2 - k^2$. J_n and N_n are Bessel functions of the first and second kind, respectively, and k and k_z are open-space and axial waveguide propagation constants, respectively. A convenient plot of the roots of (6) in terms of $\lambda_c/2b$ as a function of b/a may be found in reference [19]. From this plot, the TE_{11} mode will indeed be suppressed below approximately 1 GHz in this waveguide.

CHARACTERISTIC IMPEDANCE

The characteristic impedance (Z_0) for coaxial waveguides operating in the TEM mode is [20]

$$Z_0 \approx \frac{1}{2\pi} (\mu/\epsilon)^{\frac{1}{2}} \ln(b/a) , \quad (7)$$

where $\hat{\epsilon}$ is the complex permittivity of the dielectric. The permeability of all materials used in this waveguide (brass, air, Teflon and water) is μ_0 , and (7) may be written as

$$Z_0 \approx \frac{\eta_0}{2\pi} [\epsilon_r (1 - j \tan |\delta_d|)]^{-\frac{1}{2}} \ln(b/a), \quad (8)$$

where $\tan |\delta_d|$ is the dielectric loss tangent. For the air-filled and the Teflon filled sections of the waveguide, $\tan |\delta_d| \approx 0$, and (8) reduces to (3). The conductivity (σ) of tap water at 16° Celcius is $\sim 10^{-1}$ Si/m in the frequency band 0.5 – 1.0 GHz, and the loss tangent is $\sim 10^{-2}$. As the computations below indicate, tap water may be considered as low-loss dielectric in determining characteristic impedance of the waveguide. When approximately 10 grams of salt (NaCl) is added per kilogram of water, increases to ~ 1 Si/m, and the loss tangent increases to $\sim 10^{-1}$, and as the computations indicate, the characteristic impedance of the waveguide becomes complex and must be computed from (8). From (3) and (8), the following results are obtained:

$$\text{Air Section} - Z_0 \approx 57.3 \Omega$$

$$\text{Teflon Section} - Z_0 \approx 39.6 \Omega$$

$$\text{Water Section} - Z_0 \approx 6.37 (1 + j 0.03) \approx 6.37 \Omega$$

(Tap water; $\sigma_d = 0.15$ Si/m, $\epsilon_r = 81$, $f = 0.6$ GHz)

$$- Z_0 \approx 6.41(0.91 + j0.25) \approx (5.85 + j 1.60) \Omega$$

(Salt water; $S \approx 10$ g/kg, $\sigma_d = 1.60$ Si/m, $\epsilon_r = 80$,

$f = 0.6$ GHz)

The water-filled section of the waveguide was terminated with an array of three 20-ohm, 0.125-watt, resistors connected between the center conductor and the outer conductor. This termination provides a

d-c resistance of approximately 6 ohms and serves as an added precaution against the existence of a standing wave in the water-filled section of the waveguide.

REFERENCES

1. A. Banos. Dipole Radiation in the Presence of a Conducting Half-Space. New York: Pergamon, 1966.
2. R. W. P. King and G. S. Smith. Antennas in Matter. Cambridge, MA: The MIT Press, 1981.
3. R. M. Sorbello, R. W. P. King, et al., "The Horizontal-Wire Antenna Over a Dissipative Half-Space: Generalized Formula and Measurements," IEEE Transactions on Antennas and Propagation, Vol. AP-25, No. 6, November, 1977, pp. 850-854.
4. M. Siegel and R. W. P. King, "Radiation from Linear Antennas in a Dissipative Half-Space," IEEE Transactions on Antennas and Propagation, Vol. AP-19, No. 4, July, 1971, pp. 477-485.
5. C. M. Butler, et al., "Experimental Investigation of a Wire Antenna Above a Lossy Medium," University of Mississippi, University, MS, Final Report (Contract N66001-81-Q-0210RS) to Naval Ocean Systems Center, San Diego, CA, September, 1981.
6. Victor L. Streeter and E. Benjamin Wylie, Fluid Mechanics (Sixth Edition). New York: McGraw-Hill, 1975, pp. 18-20.
7. "Semi-Automatic Measurements Using the 8410B Microwave Network Analyzer and the 9825A Desk-Top Calculator." Hewlett-Packard Application Note 221. Palo Alto, CA: Hewlett-Packard, October, 1977.
8. John C. Stapleton, "Translation of the Hewlett-Packard 11863A Semi-Automatic Network Analyzer Program for Use with the Textronix (sic) 4051 Graphic System." University of Kentucky Technical Note 80-1. Lexington: University of Kentucky, April, 1980.
9. Notes from a Short Course on Fundamentals of Numerical Solution Methods in Electromagnetics. University of Mississippi, March, 1982, pp. 5-54 - 5-91.
10. C. M. Butler and M. G. Harrison, "Analysis of the Sleeve Monopole Antenna," Proceedings of the 9th Annual (1971) IEEE Region III Convention, Charlottesville, VA, April 1971, pp. 303-308.
11. R. F. Harrington, Time-Harmonic Electromagnetic Fields, New York: McGraw-Hill, 1961, p. 94.
12. C. M. Butler and K. A. Michalski, "The Ground Stake Antenna", University of Mississippi, 1983 (to be published).
13. J. D. Kraus, Antennas, New York: McGraw-Hill, 1950, pp. 276-278.

14. A. J. Julian, J. C. Logan and J. W. Rockway, "MININEC: A Mini-Numerical Electromagnetics Code," Technical Document 516, Naval Ocean Systems Center, San Diego, CA, September, 1982.
15. C. M. Butler, K. A. Michalski and S. Filipovic, "Analysis of Coax-Fed Monopole", University of Mississippi, 1983 (to be published).
16. C. M. Butler, et al., "Experimental Investigation of a Monopole in a Lossy Medium," University of Mississippi, University, MS, Final Report (Contract N66001-81-M-5991) to Naval Ocean Systems Center, San Diego, CA, September, 1981.
17. J. Baumgartner, "A Program to Calculate the Real Effective Permittivity and the Real Effective Conductivity of Seawater as a Function of Temperature, Salinity, and Frequency," Naval Ocean Systems Center, San Diego, CA, August, 1982 (private communication).
18. Edward C. Jordan and Keith G. Balmain, Electromagnetic Waves and Radiating Systems (Second Edition). Edgewood Cliffs, NJ: Prentice-Hall, 1968, pp. 215-235.
19. Theodore Moreno. Microwave Transmission Design Data. New York: Dover, 1958, pp. 69-72.
20. Carl T. A. Johnk. Engineering Electromagnetic Fields and Waves. New York: John Wiley and Sons, 1975, pp. 498-510.

END

FILMED

B&W

DTIC